# PAIRWISE COMPARISONS OF SHRUB CHANGE ACROSS ALPINE CLIMATES SHOW HETEROGENEOUS RESPONSE TO TEMPERATURE IN DALL'S SHEEP RANGE

By

Mark Melham

A Thesis Submitted in Partial Fulfillment of the Requirements

for the Degree of

Master of Science

In

Natural Resource Management

University of Alaska Fairbanks

December 2019

APPROVED:

Dave Valentine, Committee Co-Chair
Santosh Panda, Committee Co-Chair
Todd Brinkman, Committee Member
Dave Valentine, Department Chair
*Dept. of Natural Resources & Environment*
Kinchel Doerner, Dean
*College of Natural Science & Mathematics*
Mike Castellini, *Dean of the Graduate School*

## Abstract

Encroachment of woody vegetation into alpine and high latitude systems complicates resource use for specialist wildlife species. We converted Landsat imagery to maps of percent shrub cover in alpine areas of Dall's sheep (*Ovis dalli dalli*) range. We then compared percent cover to interpolated climate data to infer drivers of shrub change between the 1980s and 2010s and determine if that change is occurring at different rates in climatically distinct alpine areas. We identified areas spatially interconnected by their mean July temperature intervals and compared their rates of shrub change, finding net rates of shrub growth were higher at temperatures notably above shrub growing season minimums. Along a climatic gradient, high precipitation areas had highest net shrub change, Arctic areas followed, while alpine areas of interior Alaska and the cold Arctic showed the least amount of net shrub change at these higher temperatures. Despite the requirement of higher temperatures for shrub growth, temperature and net shrub change displayed different relationships across the range wide climatic gradient. In areas of rapid climate warming, such as the Arctic and cold Arctic, the linear correlation between shrub change and temperature was highest. In the high precipitation areas where temperatures have been largely above growing season minimums during the study period, precipitation had the strongest linear correlation with shrub change. High latitude studies on shrub change focus primarily on expansion in the Arctic, where increased greening trends are linked to higher rates of warming. We provide the broadest climatic examination of shrub change and its drivers in Alaska and suggest shrub expansion 1) occurs more broadly than just in areas of notable climate warming and 2) is dependent on different environmental factors based on regional climate. The implications for Dall's sheep are complicated and further research is necessary to understand their adaptive capacity in response to this widespread vegetative shift.

## Table of Contents

## List of Figures

## List of Tables

## Definitions

Above-ground Biomass: All vegetative biomass located above the ground; differentiated here between plant and shrub

Acquisition Date: The date represented by satellite imagery data

Alpine Zone: Mountain range or partial mountain range comprising individual alpine units within the area of interest

Analyzable: All known cloud contaminants removed, allowing high likelihood of true values to be representative

Band: Layer of an image that contains a single value per-pixel and generally comprises one type of electromagnetic energy or lights per multi-band satellite image

Bilinear Interpolation: Uses a weighted average of the four nearest cell centers to construct values of new pixels within continuous raster data

Boreal: Relating to or characteristic of the cold climatic zone south of the Arctic dominated be dense spruce and birch stands

Cirrus-free: Containing no cirrus clouds within a pixel based on visual examination and use of screening bands to detect and eliminate cirrus clouds from pixels

Clear-sky: Containing neither cloud, nor cloud-shadow in the pixel based on USGS algorithms

Climate Class: Multiple mountain ranges that exhibit similar climatic characteristics in terms of growing season temperature, winter temperature, and precipitation

Climatic Variable: Refers to 30-year change or modern values for July temperature, modern length of growing season, modern annual precipitation, or modern winter temperature

Color-infrared composite: Manipulated imagery that displays non-visible near-infrared light as part of an RGB color composite, used heavily in broadscale vegetative research

Growth Classes: Groups of pixels representative of different classes of growing conditions for shrubs based on their July temperature minimums

Interpolation: Method of constructing new data points within the range of a discrete set of known data points

Landsat: Longest running program for acquisition of satellite imagery of the earth with a pixel resolution of 30 meters

Operational Land Imager: Sensor used for satellite imagery in the most recent iteration of Landsat satellites

Pixel: Base unit of an image or band, that when totaled allows inference of visual data and when analyzed allows inference of numerical data

Resampling: Resizing an image by reducing or increasing its number of pixels

Resolution: Size of pixels comprising their encompassing image

Scene-pair: Combination of Landsat OLI and Landsat TM scenes that share the same spatial constraint over two time periods allowing inference into climate change

Shrub Dominance: The ratio, in percent, of shrub above-ground biomass to plant above-ground biomass measured by kg / $m^2$

Shrub Variable: Refers to either change in percent shrub dominance or modern percent shrub dominance

Temperature Connectivity: Refers to interconnected spatial areas with identical temperature value; any discontinuity results in a separate and independent group.

Thematic Mapper: Sensor used for satellite imagery of Landsat satellites between 1982 – 2013 that is most commonly used for climate studies and inference

## Acknowledgements

I thank my committee for their continued support and effort given to this project. I am grateful to my co-chair Dr. Santosh Panda for providing the necessary expertise in remote sensing that maximizes the value of our approach, to co-chair Dr. David Valentine for providing overarching guidance on the project and inherent academic challenges, and Dr. Todd Brinkman for being a voice of reason from start to finish. I also thank all project collaborators, notably Dr. Laura Prugh of the University of Washington, Mathew Sorum and Kumi Rattenbury of the National Park Service, and Maxwell Newton, Hannah Gerrish, and Cascade Galasso-Irish for their work in the field.

I thank my brother and father for their unconditional support. And I thank Kristen for helping me find perspective during this project.

Primary funding was provided by the Arctic-Boreal Vulnerability Experiment of the National Aeronautics and Space Administration, through the grant NNX15AU21A to Dr. Prugh. Completion funding was provided through the Graduate School at the University of Alaska Fairbanks. Additional support was provided by Gates of the Arctic National Park and Preserve, the Geological Society of America, AmeriCorps, and the Undergraduate Research & Scholarly Activity program within the University of Alaska Fairbanks.

# 1 Introduction

## 1.1 Warming Climate and Woody Vegetation

Climate warming at high latitudes is altering vegetative productivity (Verbyla 2008; Beck and Goetz 2011). Using satellite-derived indices of vegetative productivity, Verbyla (2008) found decreases in productivity in the boreal regions of Alaska occurring between 1982 and 2003. In the same time frame, he identified areas of increasing productivity in the Arctic, though smaller areas within the region showed contrasting trends (i.e. the greening is not universal nor homogenous within the Arctic). Beck and Goetz (2011) executed a similar study on the circumpolar north, finding trends of increasing productivity at Arctic latitudes and decreasing productivity in boreal zones from 1982 to 2008. Moreover, they found the increases in productivity were extending spatially (i.e. more area is becoming more productive, not solely increased production in the same area). Ju and Masek (2016) provide the most recent broad-scale greening study, using higher-resolution (30m) indices between 1984 and 2012 and found similar patterns of greening and browning across Alaska and Canada.

Higher-resolution studies contain evidence that shrub expansion in Alaska is part of the greening trend (Tape et al. 2006; Dial et al. 2007). From 1999 to 2002, Tape et al. (2006) recreated 202 aerial photos initially taken between 1945 and 1953. Comparing the spatial extents and coverage of shrubs over a roughly 50-year span, they were able to demonstrate increases in shrub extents in areas along the Arctic foothills and Brooks Range. Dial et al. (2007) used orthophotos from 1951 and 1996 to determine increases in woody vegetation (shrub, open woodland, and closed-canopy forest) along altitudinal gradients in the Kenai mountains. They found 4% increases in shrub cover per decade as well as 50m altitudinal increases in treeline (open woodland). However, timberline, the upper limit of closed-canopy forest, did not change during same time period. The findings led Dial et al. (2007) to identify alpine tundra as “the overwhelming entry state for new shrub[s].”

Plot-scale studies provide further evidence for shrub expansion (Elmendorf et al. 2012; Berner et al. 2018). Elmendorf et al. (2012) executed a global meta-analysis of plot studies that examined 158 plant communities at 46 locations across the tundra biome occurring between 1980 and 2010. They found increases in vascular plant growth in both canopy and maximum height. Growth of tall and low-growing shrubs increased in response to tundra summer warming. However, dwarf and evergreen shrubs did not exhibit a positive response to increased warming. Not all increases in vascular growth were associated with changes in shrub extent. For example, increases in herbaceous cover have been documented as a climatic response (Alatolo et al. 2016). While vascular growth responds positively to warming temperatures, additional factors can impact the type of vascular growth (e.g. shrub, herbaceous, etc.) that occurs in response to warming temperatures. Some of these factors include moisture regime and permafrost presence (Swanson 2015; Tape et al. 2016). Berner et al. (2018) provided direct links between the satellite-based greening trends and the increases in greening and shrubification by using published biomass data to develop a regression model predicting tundra above-ground biomass (AGB) across the North Slope as a function of Landsat-derived NDVI. Shrub AGB was positively and significantly correlated with Landsat-derived indices from the Beaufort coastal plain (2018). In areas of shrub-dominant communities, shrubs accounted for 53% of AGB; shrubs comprise anywhere from 8% to 39% of AGB in tussock and sedge communities.

Temperature increases play a prominent role in promoting shrub growth and expansion. (Hallinger et al. 2010; Hudson et al. 2011; Tape et al. 2012; Swanson 2015). Shrub height and leaf size increased significantly in response to artificial warming of +1.5 C° from 1992 to 2008 in open-top chambers (Hudson et al. 2011). Tape et al. (2012) sampled 26 expanding or stable shrub patches examining environment factors including thaw depth, soil temperature, soil moisture, and shrub growth. Results indicated expanding patches typically occur in areas with higher soil temperatures and deeper

active layers, and, in general, more resource-rich circumstances. Using dendrochronological measurements, they found summer and spring temperatures correspond positively to annual ring growth in expanding patches. In Arctic mountains and western foothills in Alaska, 10.5 - 12 C° is the limiting mean July temperature for tall shrub canopy (Swanson 2015). Temperature requirements vary by species (Table 1-1). Notably, the *Alnus* genus may not exhibit full canopy growth until 14-15 C°, though its lower temperature threshold for growth is much lower at 12.4 C°.

*Table 1-1: Lower temperature thresholds for various tall shrub species found in Alaska. Increasing temperatures in areas throughout Alaska will meet or exceed many of these thresholds over the next century. The asterisk denotes a higher temperature threshold (14-15 C°) is required for full canopy to occur.*

| Shrub Group | Lower Temp. Threshold |
|---|---|
| Diamondleaf Willow (*Salix pulchra*) | 10.5 C° |
| Birch genus (*Betula* sp.) | 11.1 C° |
| Richardson's Willow (*Salix richardsonii*) | 11.7 C° |
| Feltleaf Willow (*Salix alaxensis*) | 11.8 C° |
| Grayleaf Willow (*Salix glauca*) | 12.0 C° |
| Green Alder (*Alnus viridis*) | 12.4 C°* |

Soil and topographic factors influence the shrub growth response to a warming climate (Swanson 2015; Ackerman et al. 2017). Most of the Arctic mountains are close to the mean July temperature necessary for large canopies (≥ 10.5 C°), though current growth does not mirror temperatures evenly (Swanson 2015). Swanson examined 471 plots at 24 locations across northern and western Alaska, concluding tall shrubs species have lower limit temperature ranges of 10.5 to 12.4 C° and an increase in 2 C° July mean temperature would increase suitable areas for tall shrub species between 23 and 70%. However, Swanson notes soil pH and drainage could function as growth-limiting factors that could reduce expansion by more than half the susceptible area. Additional factors on the landscape, such as disturbance in the form of flooding or wildfire, would likely reduce soil acidity to a point viable for shrub growth. Wildfire especially functions as a benefactor to shrubs, as it can create

deeper soil thaw depth and improved drainage. Shrub expansion has occurred following tundra wildfires (Racine et al. 2004). Shifts in disturbance, like increases in wildfire, may increase soil pH, and facilitate greater shrub expansion in the wake of warming temperatures. In Arctic Alaska, Ackerman et al. (2018) documented a regionally coherent and robust response of Salix pulchra ring growth to June temperature, with local soil properties contributing minor influence on shrub growth. However, models from similar studies project increasing differences between shrub growth in mesic and dry sites due to factors like evapotranspiration (Ackerman et al. 2017).

Shrubs have their own impacts on the landscape; including warmer soil temperatures, enhanced nutrient cycling, reduced surface albedo, and shifts in snowpack depth (Sturm et al. 2005; Myers-Smith et al. 2011). Snowpack depth can increase as shrubs expand. Riparian corridors provide a barrier for windswept snow, enabling deeper snowpack. Increases in snowpack depth can impact the soil thermal regime by providing improved insulation from ambient air temperatures (Sturm et al. 2005; Ling and Zhang 2007), as well as impact wildlife winter movements (Pozzanghera et al. 2016; Mahoney et al. 2018) and forage availability for herbivores (Visscher et al. 2006).

Shrub impacts are part of positive feedback loops that further warm the climate. (Sturm et al. 2005; Chapin et al. 2005). Shrub abundance leads to substantial atmospheric heating caused by 1) reduced albedo facilitating a terrestrial increase in absorbed radiation and 2) increased atmospheric moisture content from evapotranspiration (Chapin et al. 2005; Swann et al. 2010). Reduced albedo has impacts like earlier snowmelt, warmer winter soil temperatures, and permafrost thaw (Sturm et al. 2005; Bonfils et al. 2012). These impacts are especially important as milder winters are associated with the global advance of treeline at elevations (Harsch et al. 2009). So woody vegetation may expand despite the cooling effects of its canopy on summer soil temperatures. As winter biological processes allow more below ground productivity, shrubs continue to expand (Sturm et al. 2001; Myers-Smith et al. 2011). Positive feedback loops involving shrub expansion are overviewed in Figure 1-1.

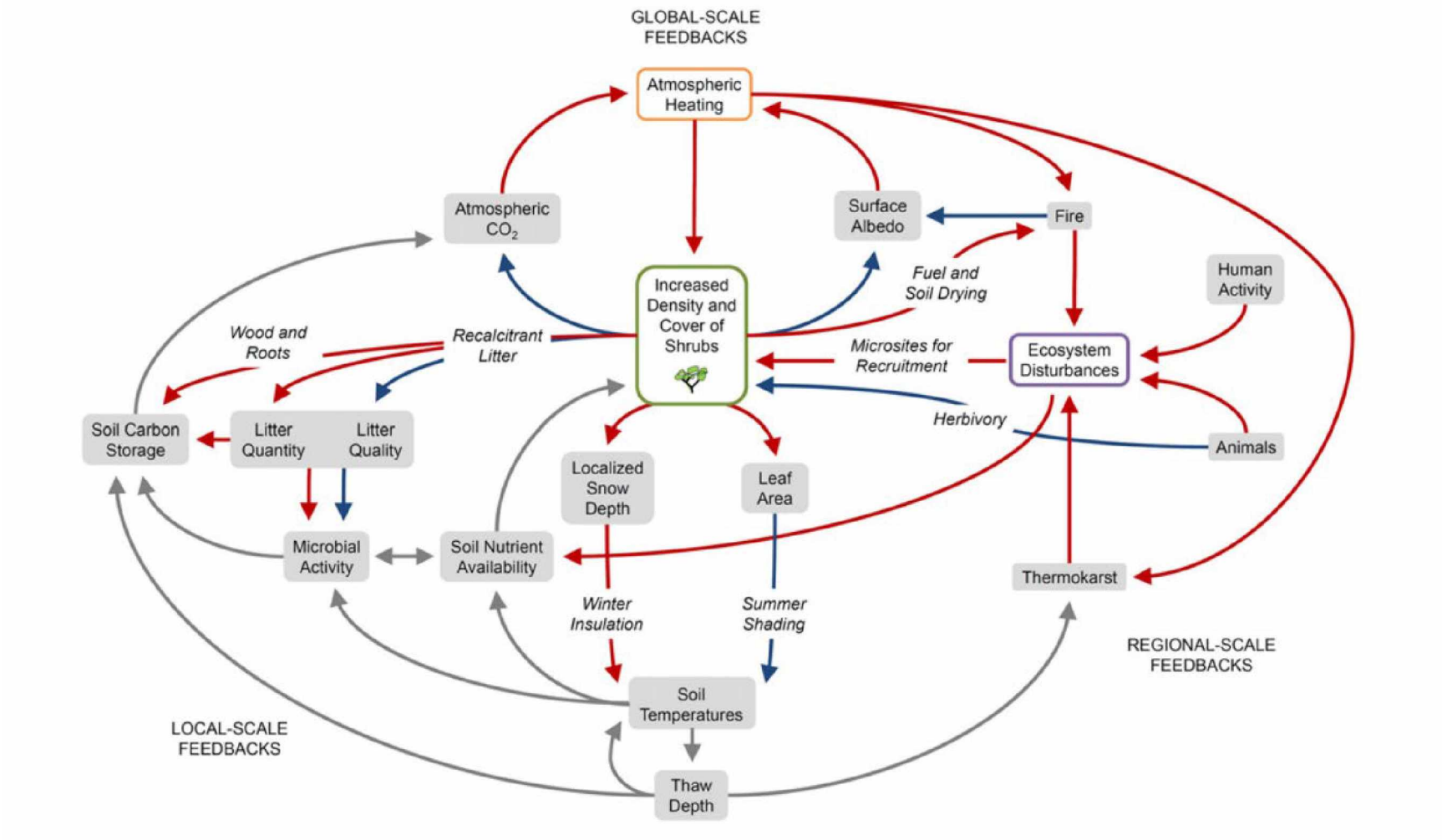


*Figure 1-1: Feedback loops involving shrubs (Myers-Smith et al. 2011). Red arrows indicate positive relationships, blue arrows indicate negative, grey arrows indicate as yet undetermined relationships.*

## 1.2 Wildlife Response to Vegetative Shifts

Encroachment of shrubs into alpine systems may negatively impact alpine specialists. Shrubby encroachment has different impacts, dependent on species' needs (Boelman et al. 2015; Wheeler and Hik 2014). Increased cover due to shrub infilling can lead to increased energy expenditure by prey species (Wheeler and Hik 2014). Using video recordings of foraging behavior in low and high shrub density environments, Wheeler and Hik (2014) found increases in density led to less efficient foraging (e.g. more effort directed to predation risk, less time allotted for foraging) in Arctic ground squirrels (*Spermophilus parryyii*). Tall shrub can alternatively function as a form of improved cover for prey species acclimated to the habitat type (Zhou et al. 2017). The impacts of tall shrubs on wildlife species are not limited to direct impacts (such as the increases in vigilance). Increased snow depths due to shrub expansion (Sturm et al. 2005) can restrict winter movements (Mahoney et al. 2018), and forage availability due habitat shifts (Dial et al. 2016) as well as provide increased habitat for predatory species (Marcot et al. 2015) or alternative prey species that boost predator populations (Arthur and Prugh 2010).

Shrub expansion could reduce Dall's sheep (*Ovis Dall'si Dall'si*) populations through increased predation and decreased forage availability. Lambs are vulnerable to predation, and therefore ewes typically forage in open areas near escape terrain (Rachlow and Bowyer 1998). With shrub expansion, hiding cover for vertebrate predators such as grizzly bears (*Ursus arctos*), wolves (*Canis lupus*), and coyotes (*Canis latrans*) could increase. In the Alaska Range, Arthur and Prugh (2010) found annual lamb survival rates as low as 15 percent, with coyotes and golden eagles (*Aquila chrysaetos*) accounting for over 75 percent of the mortality of radio-collared lambs. The expansion of shrubs might also lead to an increase in snowshoe hare (*Lepus americanus*) habitat which may maintain a higher population of coyotes since snowshoe hares are the primary food of coyotes (Arthur and Prugh 2010). There are at least 2 mechanisms that might lead to a decrease in Dall's sheep forage availability due to shrub

expansion. First, with shrub expansion there likely would be deeper snowpack in shrub patches leading to later spring plant phenology in areas of deep snowpack. For example, delayed plant phenology during a late spring corresponded with a 2-week delay in onset of parturition and thus reduction in time available for lamb growth, weaning, and acquisition of body reserves for ewes prior to the onset of plant senescence (Rachlow and Bowyer 1998). Second, with shrub expansion, open areas where Dall's sheep forage such as grasses and forbs first green up in the spring would be reduced (Dial et al. 2016) leading to increased foraging distance, greater risk of predation, and less efficient foraging (Rachlow and Bowyer 1998).

As with other alpine specialists, Dall's sheep have high levels of genetic diversity isolated by the mountain ranges across their distribution (Worley et al. 2004). These populations have higher genetic variability than other mountain ungulates largely due to isolation, geographical barriers, and, in some cases different management approaches (2004). The broad distribution of isolated Dall's sheep populations indicates that changes across climatic zones will vary and those impacts could imperil genetically distinct populations. These population differences make inferring contractions of their habitat important on a range-wide scale as contracting range in one climatic region could have impacts on a genetically distinct population.

The susceptibility of Dall's sheep to shrub encroachment is bolstered by basic biological parameters. As large ungulates tend to exist in populations close to carrying capacity (McCullough 1999), shrinking ecological boundaries could readily translate to shrinking populations for species with high dispersal reluctance, such as Dall's sheep. Logistical difficulties in studying Dall's sheep limit the consistency of high-resolution population assessments (Alaska Dept. of Fish and Game 2011; Jex et al. 2016), but there remain indications of declines in populations within distinct climatic ranges during our period of interest (Alaska Dept. of Fish and Game 2014). Understanding how climatic factors impact vegetation shifts in different climates could help identify areas to focus future research.

## 1.3 Applications of Multispectral Imagery to Quantifying Climate Change Impacts

Multispectral imagery displays electromagnetic radiation (Figure 1-2), including visible light, ultraviolet and infrared that can be converted into numerical indices for interpretation of environmental systems and their change (Melesse et al. 2007). Values are assigned to pixels in a digital image based on a designated range of bandwidths. Applications of these images vary by bandwidth range (Table 1-2).

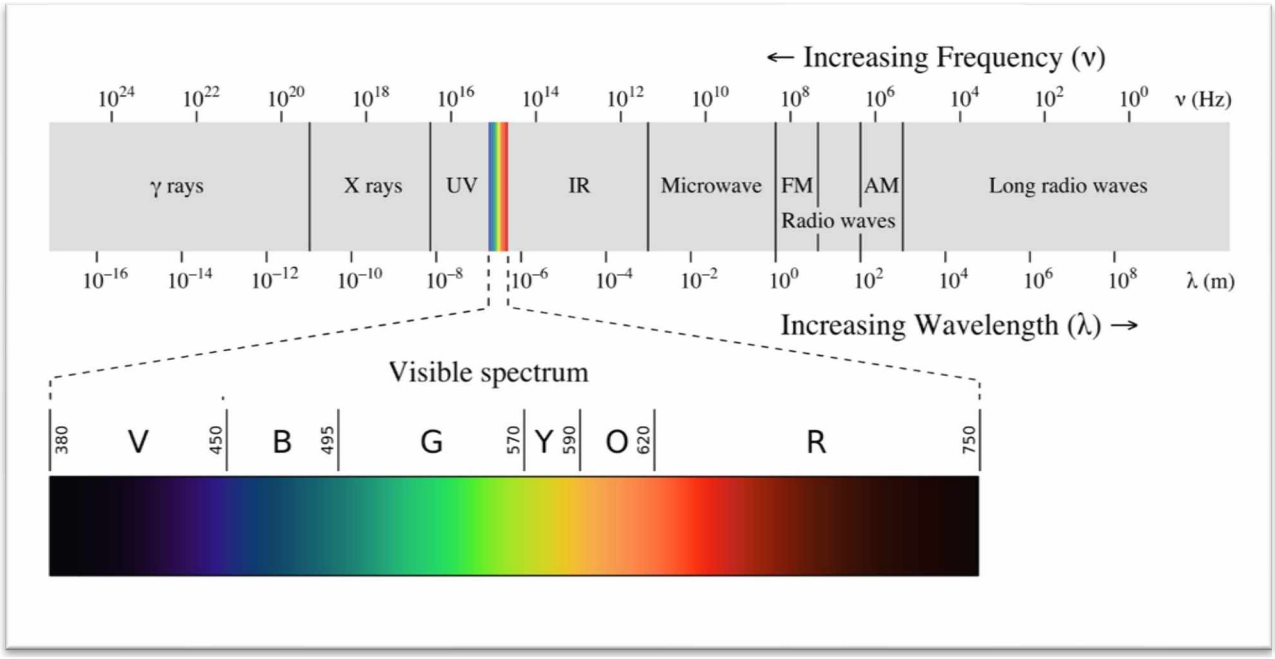


*Figure 1-2: Bands of electromagnetic radiation showing the frequency (ν) and wavelength (λ) ranges from γ rays to long radio waves (top) and the visible spectrum of energy (bottom). The visible spectrum is flanked by lower wavelength ultraviolet and high wavelength infrared. These are the most common elements of electromagnetic radiation to be used in remote sensing climate studies.*

The Landsat program (Table 1-2) uses substantially higher-resolution sensors (30 – 120m) and is one of the longest running satellite programs for earth observations from space (Irons et al. 2012) as imagery was first acquired in 1972. Landsat imagery has been used to calculate shrub biomass (Berner et al. 2018), infer shrub-albedo interactions (Juszak et al. 2014), and document warming-induced shrub expansion at high latitudes (Fraser et al. 2014).

The Landsat Multispectral Scanner System (MSS) launched with Landsat-1 at a general resolution of 60 meters (m) in 1972 and was carried in Landsat missions 1- 5. All MSS contained at least four bands: blue, green, red, and near-infrared. Landsat-3 MSS had an additional thermal infrared band (Chander et al. 2009). MSS has been used in comparisons with more recent Landsat sensors (Walker and Zenone 1988; Tømmervik et al. 2003). However, MSS pixel resolution (60m) is lower than all succeeding Landsat sensors (30m), which limits applications in studies due to limitations in cross-sensor comparison.

With improved resolution (30m) and additional bands (spatial data layers with numerical values representative of a specific type of light), the Thematic Mapper (TM) sensor carried in Landsat-4 and 5 missions offers the best historical reference for inferring long-term change, available over the 40-year period 1982 - 2012. As with MSS, the blue, red, and near-infrared bands of TM offered applications for bathymetric and vegetation inference. The additional bands, two short-wave infrared and one thermal infrared, enabled differentiation between moisture contents, geology, and thermal elements.

Errors in policy and planning limited the breadth of temporal and spatial continuity across the sensors following TM. Landsat-6 failed during launch (Irons et al. 2012). Images collected from the Enhanced Thematic Mapper + (ETM+) sensor used in the Landsat-7 mission contain spatial gaps within the data. These gaps can be filled, the scenes can be used for analysis, or a combination (Irons et al. 2012; Macander et al. 2017), though the spatial gaps prevent a relatively seamless comparison.

The Operational Land Imager (OLI) from the Landsat-8 mission offers an excellent modern tool for mapping environmental change. The images contain the same pixel size and comparable spatial coverage to TM allowing for analysis of environmental change over roughly a 30-year period. OLI contains all bands present in TM with additional bands that include panchromatic (collection of all visible wavelengths), a cirrus band for detecting non-visible clouds, and an additional thermal infrared band.

*Table 1-2: Landsat sensor characteristics: band number, name, type of electromagnetic radiation, wavelength documented, resolution (pixel size of image), and applications for the Landsat Program from mission 4 through mission 8. Mission 8 follows on the ensuing page.*

| **LANDSAT THEMATIC MAPPER** | | **MISSIONS 4&5** | **1982 - 1992; 1984 - 2012** | | |
|---|---|---|---|---|---|
| BAND NUMBER | Band Name | Type of Electromagnetic Radiation | Wavelength (µm) | Resolution (m) | Applications |
| **1** | Blue | Visible Blue | 0.45-0.52 | 30 | Bathymetry; differentiating soil and vegetation; differentiating between conifers and broadleaves |
| **2** | Green | Visible Green | 0.52-0.60 | 30 | Emphasizes peak vegetation |
| **3** | Red | Visible Red | 0.63-0.69 | 30 | Discriminates vegetation slopes |
| **4** | NIR | Near-Infrared | 0.76-0.90 | 30 | Emphasizes biomass content and shoreline |
| **5** | SWIR 1 | Short-wave Infrared | 1.55-1.75 | 30 | Discriminates moisture content from soil; penetrates thin clouds |
| **6** | Thermal | Thermal infrared (Long-wave) | 10.4-12.50 | 120* | Thermal mapping and estimating soil moisture |
| **7** | SWIR 2 | Short-wave Infrared | 2.08-2.35 | 30 | Hydrothermally altered rocks associated with mineral deposits |
| **LANDSAT ENHANCED THEMATIC MAPPER +** | | **MISSION 7** | **1999 - Present** | | |
| BAND NUMBER | Band Name | Type of Electromagnetic Radiation | Wavelength (µm) | Resolution (m) | Applications |
| **1** | Blue | Visible Blue | 0.45-0.52 | 30 | Bathymetry; differentiating soil and vegetation; differentiating between conifers and broadleaves |
| **2** | Green | Visible Green | 0.52-0.60 | 30 | Emphasizes peak vegetation |
| **3** | Red | Visible Red | 0.63-0.69 | 30 | Discriminates vegetation slopes |
| **4** | NIR | Near-Infrared | 0.77-0.90 | 30 | Emphasizes biomass content and shoreline |
| **5** | SWIR 1 | Short-wave Infrared | 1.55-1.75 | 30 | Discriminates moisture content from soil; penetrates thin clouds |
| **6** | Thermal | Thermal infrared (Long-wave) | 10.4-12.50 | 60* | Thermal mapping and estimating soil moisture |
| **7** | SWIR 2 | Short-wave Infrared | 2.08-2.35 | 30 | Hydrothermally altered rocks associated with mineral deposits |
| **8** | Panchromatic | Multiple Types | 0.52-0.90 | 15 | Improve image resolution |

*Table 1-2: Landsat sensor characteristics: band number, name , type of electromagnetic radiation, wavelength documented, resolution (pixel size of an image) and applications for the Landsat Program from mission 8*

| **LANDSAT OPERATIONAL LAND IMAGER** | **MISSION 8** | **2013 - Present** | | |
|---|---|---|---|---|
| BAND NUMBER | Band Name | Type of Electromagnetic Radiation | Wavelength (μm) | Resolution (m) | Applications |
| **1** | Coastal | | 0.43-0.45 | 30 | Coastal and aerosol studies |
| **2** | Blue | Visible Blue | 0.45-0.52 | 30 | Bathymetry; differentiating soil and vegetation; differentiating between conifers and broadleaves |
| **3** | Green | Visible Green | 0.52-0.60 | 30 | Emphasizes peak vegetation |
| **4** | Red | Visible Red | 0.63-0.69 | 30 | Discriminates vegetation slopes |
| **5** | NIR | Near-Infrared | 0.77-0.90 | 30 | Emphasizes biomass content and shoreline |
| **6** | SWIR 1 | Short-wave Infrared | 1.57-1.65 | 30 | Discriminates moisture content from soil; penetrates thin clouds |
| **7** | SWIR 2 | Short-wave Infrared | 2.11 - 2.29 | 30 | Hydrothermally altered rocks associated with mineral deposits |
| **8** | Panchromatic | Multiple Types | 0.50-0.68 | 15 | Improve image resolution |
| **9** | Cirrus | Short-wave Infrared | 1.36-1.38 | 30 | Detection of cirrus cloud (non-visible) contamination |
| **10** | TIRS 1 | Thermal infrared (Long-wave) | 10.60-11.19 | 100 | Thermal mapping and estimating soil moisture |
| **11** | TIRS 2 | Thermal infrared (Long-wave) | 11.5-12.51 | 100 | Thermal mapping and estimating soil moisture |

Spatial resolution can limit inference of environmental change (Ju and Masek 2012). Many of the studies using sensors with larger pixels (e.g. AVHRR, MODIS) show broadscale changes across large areas but are unable to demonstrate heterogenous differences on a landscape scale. The large swath and relatively high resolution of Landsat pixels offer the ability to map environmental change in large areas at a resolution that can infer climatic and spatial heterogeneity (Ju and Masek 2016; Fraser et al. 2014).

The Normalized Difference Vegetation Index (NDVI; Equation 1) provides a numerical index that corresponds to vegetative productivity based on spectral reflectance of vegetation types (Knipling 1970; Peñuelas and Filella 1998). Chlorophyll absorbs visible light for use in photosynthesis. Red light is the absorbed visible light used to determine NDVI. Leaf cell structure helps directs reflectance of near-infrared light (Weier and Herring 2000). Calculating a normalized ratio of the red and near-infrared reflectance allows inference into vegetative type and productivity.

Normalized Difference Vegetation Index =

(Near Infrared – Red) / (Near Infrared + Red)

Equation 1: *The formula for Normalized Difference Vegetation Index (NDVI) that can be used to create a numerical index that corresponds to vegetation type and productivity. This formula is typical in remote sensing studies to determine vegetative properties across the landscape that are difficult to execute physically on the landscape.*

NDVI has been used commonly in prior studies examining broadscale high latitude vegetation changes (Song et al. 2001). There are other multispectral indices used for vegetative analysis, but NDVI is arguably the most prevalent (2001). Studies include examining browning and greening trends (Verbyla 2008; Ju and Masek 2016), calculating shrub biomass on the Beaufort coastal plain (Berner et al.2018), capturing variation in peak tall shrub canopy in Arctic foothills (Boelman et al. 2011). The imagery used to calculate NDVI varies in resolution. Lower resolution satellites include the Advanced Very High Resolution Radiometer (AVHRR), which has 1.1 km pixels at nadir, and Moderate Resolution Imaging

Spectroradiometer (MODIS), which ranges in pixel size from 250 to 1000m. Both satellites have been used to document broadscale changes in productivity at high latitudes (Parent and Verbyla 2010; Ju and Masek 2016).

By calculating NDVI in Landsat-8 OLI and Landsat-4/5 TM, changes in vegetative distributions over time, such as tall shrub, can be mapped by isolating the appropriate index values. The distributions of NDVI pixels with these values can be used to infer 1) shrub extent and 2) areas of change. The large spatial and temporal coverage offers the ability to find cloud-free scenes with similar dates of acquisition in order to provide respectable levels of data continuity and pixel sample sizes. We investigate this vegetative shift in high-latitude alpine systems using the applications of Landsat multispectral imagery.

## 1.4 Research Questions and Expectations

Research on shrub expansion has been primarily focused on localized regions, such as the Arctic coastal plain, in controlled study areas (e.g. open top chambers), and at lower elevations (e.g. Arctic riparian corridors). We executed a study that examines shrub expansion across multiple climatic gradients across Alaska's alpine systems to determine if different rates of shrub expansion are occurring and how these rates are related to regional climatic factors. We focused on lower temperature limits of shrubs as a primary factor in their multidecadal change. We ask:

1. What is percent shrub dominance in alpine areas of Dall's sheep range and what has the change in percent shrub dominance been over a roughly 30-year period?
2. Is shrub expansion predominantly in a zone of 10-12 degrees of mean July temperature and how do rates of shrub expansion differ among a regional climatic gradient ranging from cold arctic mountains, arctic mountains, high precipitation mountains, warmest/driest interior mountains?

We expected shrub increases would be evident throughout the study area with expansion highest in areas with mean July temperatures between 10.5 and 12 C°. At higher temperatures, we expected density thresholds would limit shrub expansion. Variation in mean July temperature ranges between alpine climate classes will drive the relationship of areal percent shrub dominance between climate classes: highest in warm, interior mountains, moderate in cool, maritime climates, and lowest in Arctic and cold Arctic mountains.

# 2 Methods

## 2.1 Area of Interest & Environment

The area of interest includes 18 Alaskan alpine zones where Dall's sheep occur (Figure 2-1; van de Kerk et al. 2018a). These zones comprise approximately 454,941.5 $km^2$ and cover 12 level III ecological regions (ecoregions) delineated by the United States Geological Survey (Gallant et al. 1995). Primary ecoregions (from north to south) include Arctic Foothills (33,658.$km^2$; 7.4% of study area), Interior Highlands (71,516.6 $km^2$; 15.7%), Alaska Range (107,688.0 $km^2$; 23.2%), Wrangell and St. Elias Mountains (24,316.7 $km^2$; 5.3%), and Pacific Coastal Mountains (42,289.5 $km^2$; 9.3%).

Climate has warmed throughout Alaska. Increases to mean annual temperature, derived from 25 weather stations between 1949 and 1998, have been highest in the dry interior mountain ranges, with moderate increases in the northwestern regions, and the smallest changes in the southern regions (Stafford et al. 2000). Increases in seasonal temperatures mirror annual temperature change in spatial distribution, though magnitude of change in mean temperature varies by season. Winter and spring mean temperature increases are highest. For example, mean annual temperature change is highest in the interior mountains at 2.2 C°, and its mean winter temperature change is 4.5 C°. Temperature increase in mean spring temperature is second highest at 3.0 C°. Summer warming is modest (0.5 to 1.5 C° across study region), and temperatures in fall are the only decreasing seasonal temperatures across the study region.

This pattern of temperature increase has resulted in longer growing seasons (Sharratt 1991, Tucker et al. 2001). The satellite-derived Normalized Difference Vegetation Index (NDVI) has been used to infer changes in high-latitude growing season and shows an average 3.4-day earlier onset of growing season (Tucker et al. 2001) over the 1980s and 1990s, with high interannual variability in growing season length.

The northernmost portions of the study area receive the lowest annual precipitation (200mm) and the southernmost portions receiving more the 1000mm of precipitation annually (Stafford et al. 2000). The interior region has annual precipitation ranging from 200 to 400mm. In all but the southernmost portions of the study region precipitation ranges from 600 to 1000mm annually. Excluding the Arctic coastal plain, statewide precipitation has increased over the last half of the 20$^{th}$ century, most notably in western Alaska (Stafford et al. 2000).

The study areas were restricted to Alaskan Dall's sheep range (van de Kerk et al. 2018a; Figure 2-1; Table 2-1). Using data from the 2011 National Landcover Classification Database (NLCD), we removed known forests from consideration for analysis. We used the boundaries of those layers as an estimate of treeline across the study area and removed those habitats from each alpine zone to limit our study to alpine regions (Figure 2-1). We then applied published elevation minimums (2018a; Table 2-1) to these "treeless" areas to 1) identify areas of similar alpine habitats and 2) help remove false positives from our alpine pixels.

We grouped the 18 alpine zones into 4 climate classes: Arctic mountains, cold Arctic mountains, interior mountains and high precipitation mountains based on temperature and precipitation characteristics: two environmental drivers of tall shrub growth and expansion.

### 2.1.1 Arctic Mountains

The southern Brooks Range comprises nearly the entire northern width of Alaska, covering approximately 122,530.8 km$^2$ of low shrub, tundra, and, at higher elevations, alpine sparse vegetation and barren ground (Swanson 2015). Its primary ecoregion is the Brooks Range, though it also includes portions of Arctic Foothills in the west and interior highland and lowlands at its southernmost extensions.

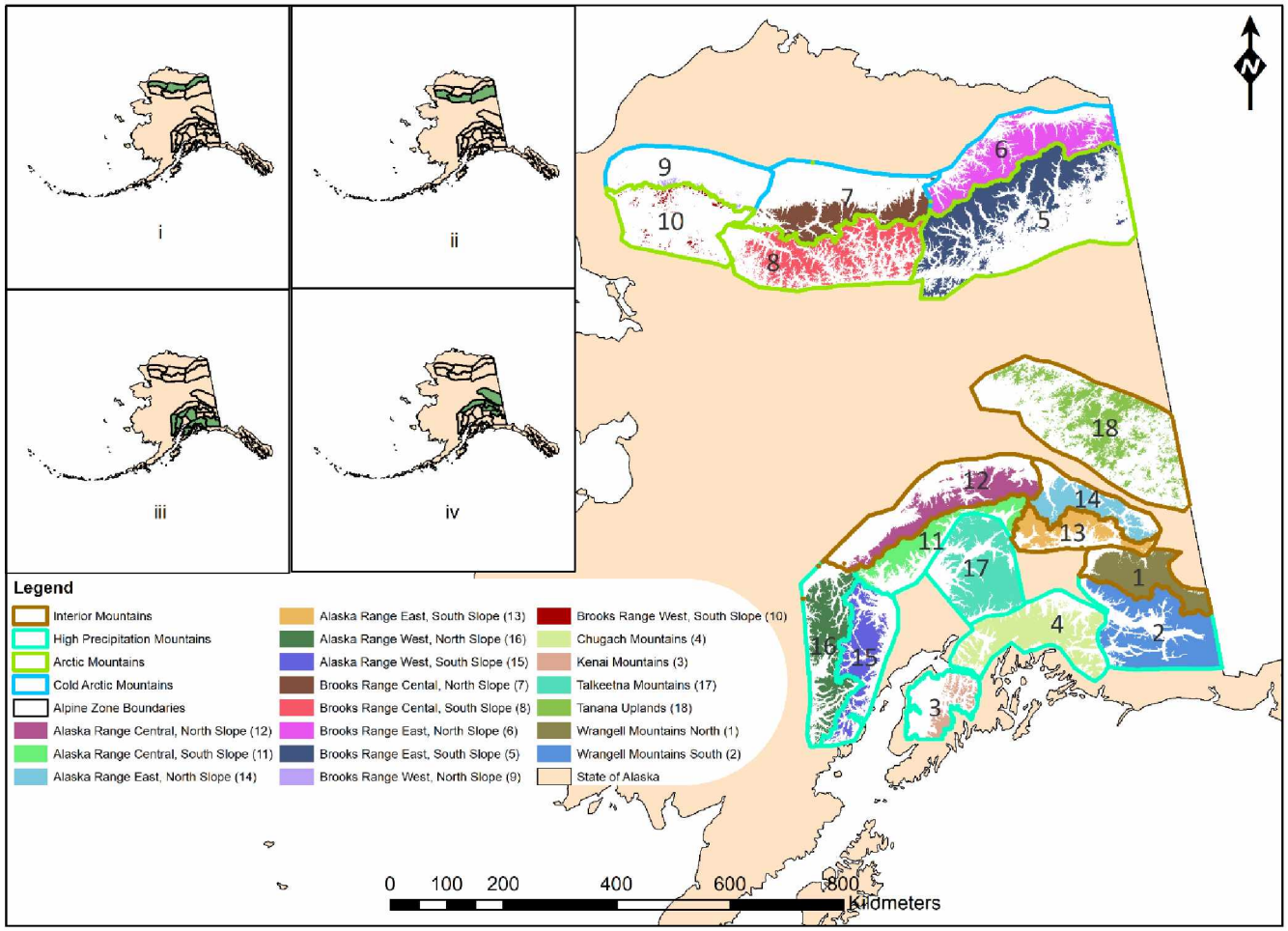


*Figure 2-1:* The area of interest, depicting the 18 alpine zones across the state of Alaska (right) with regional alpine climate classes shown by different colored outlines (top, left). The alpine climate classes include (1) Cold Arctic mountains lacking a latitudinal treeline in the Tundra biome; (2) Arctic mountains that approach the Arctic-Boreal transition zone; (3) high snowpack mountains in the Boreal biome; (4) interior mountains in the Boreal biome. Alpine areas included in this study: (1) Alaska Range East, South Slope; (2) Alaska Range East, North Slope; (3) Alaska Range Central, South Slope; (4) Alaska Range Central, North Slope; (5) Alaska Range West, South Slope; (6) Alaska Range West, North Slope; (7) Brooks Range East, South Slope; (8) Brooks Range East, North Slope; (9) Brooks Range Central, South Slope; (10) Brooks Range Central, North Slope; (11) Brooks Range West, South Slope; (12) Brooks Range West, North Slope; (13) Chugach Mountains; (14) Kenai Mountains; (15) Talkeetna Mountains; (16) Tanana Uplands; ; (17)Wrangell Mountains North; (18)Wrangell Mountains South.

*Table 2-1: The elevation minimums, maximums, ranges, and means for the 18 alpine zones being examined, including Dall's sheep elevation thresholds. To eliminate calculation of non-shrub woody vegetation, we removed deciduous, coniferous, and mixed forests based on NLCD classifications. Using the National Elevation Dataset as reference, we used published Dall's sheep elevation thresholds for all alpine zones (van de Kerk et al. 2018a). Upper elevation limits were implicit by examining only vegetated pixels.*

| Alpine Zone Name | Min. (m) | Max. (m) | Range (m.) | Elevation Threshold for Dall's Sheep (m) |
|---|---|---|---|---|
| Alaska Range Central, North Slope | 191.9 | 6197.2 | 6005.3 | 901.2 |
| Alaska Range Central, South Slope | 53.9 | 6152.6 | 6098.7 | 1114.3 |
| Alaska Range East, North Slope | 320.9 | 3871.7 | 3550.8 | 1161.2 |
| Alaska Range East, South Slope | 595.7 | 3095.9 | 2500.2 | 1053.9 |
| Alaska Range West, North Slope | 26.7 | 2997.3 | 2970.6 | 985.3 |
| Alaska Range West, South Slope | 6.2 | 3495.7 | 3489.5 | 902.3 |
| Brooks Range Central, North Slope | 158.8 | 2359.1 | 2200.3 | 788.7 |
| Brooks Range Central, South Slope | 43.6 | 2520.7 | 2477.0 | 831.7 |
| Brooks Range East, North Slope | 70.1 | 2747.6 | 2677.5 | 970.6 |
| Brooks Range East, South Slope | 200.7 | 2536.3 | 2335.6 | 819.9 |
| Brooks Range West, North Slope | 143.2 | 1476.2 | 1333.0 | 535.4 |
| Brooks Range West, South Slope | 69.4 | 1524.4 | 1454.9 | 496.4 |
| Chugach Mountains | 7.4 | 4008.7 | 4001.3 | 1153.4 |
| Kenai Mountains | 6.6 | 2028.3 | 2021.7 | 521.4 |
| Talkeetna Mountains | 89.7 | 5006.2 | 4480.7 | 1354.1 |
| Tanana Uplands | 145.2 | 5035.8 | 5018.7 | 818.6 |
| Wrangell Mountains North | 525.5 | 2693.4 | 2603.7 | 535.4 |
| Wrangell Mountains South | 17.1 | 1991.2 | 1846.0 | 496.4 |

The harsh climate combined with heavily erodible and shallow soils results in generally sparse vegetation as elevation increases, leading vegetation to be primarily in valleys and lower hillslopes (Gallant et al. 1995). Dwarf shrub communities dominate the drier sites, and sedges dominate areas of mesic herbaceous cover.

Spruce and birch forest occur at the lower latitudes forming the latitudinal treeline, while shrub species extend northward beyond the Brooks Range and out to the Arctic Coastal Plane. *Alnus* species extend most prominently northward from latitudinal treeline, thinning into *Salix* and *Betula* species as latitude increases. Tall shrubs are most evident on smaller scales in riparian areas (Swanson 2015).

Summer temperature data were obtained from the weather station in Anaktuvuk Pass. Growing season temperatures averages between 3 and 16 C°, with temperatures reaching 0 C° or below in almost all months. Annual precipitation is 280mm and most of that (160mm) occurs as snow (Gallant et al. 1995)

The alpine zones occurring in the Arctic climate class are: Brooks Range east, south slope; Brooks Range central, south slope; and Brooks Range west, south slope. Analysis of SNAP temperature data for 2000-2009 (Table 2-2) reveals mean July temperature ranges from 5.1 to 17.9 C° with average mean July temperature hovering around the lower temperature thresholds for shrub growth (~12 – 14 C°) (Gallant et al. 1995).

### 2.1.2 Cold Arctic Mountains

The northern Brooks Range is primarily arctic and alpine tundra, with alpine barrens and sparse vegetation at higher elevations (Swanson 2015). It encompasses the Arctic Foothills and Brooks Range ecoregions (Gallant et al. 1995). On a landscape scale, the primary difference between the Cold Arctic and Arctic climate classes is a lack of a treeline in the former. Tall shrubs are visibly on the landscape, generally occurring along alluvial plains and riparian corridors along hill slopes (Swanson 2015).

Alpine zones in the cold Arctic climate class include: Brooks Range east, north slope; Brooks Range central, north slope; and Brooks Range west, north slope. Mean July temperatures between 2000 – 2009 ranged from 4.8 – 14.9 C across these alpine zones (Scenarios Network for Alaska and Arctic Planning), with average mean July temperatures just reaching the lower threshold for tall shrub growth (10.5 – 13.3 C°) (Gallant et al. 1995).

### 2.1.3 Interior Mountains

The interior mountains are characterized by a continental climate with very dry cold winters and comparatively warm growing seasons (Gallant et al. 1995). Lower elevations sustain dense coniferous forests dominated by black spruce (*Picea mariana*) and white spruce (*Picea glauca*) with open woodland stands of deciduous species. Higher elevations are dominated by dwarf scrub communities (ericaceous and mountain-aven dominated) with the highest elevations being barren of vegetation (1995).

The more extreme elevations of the interior mountains include the ecoregions Alaska Range and Wrangell Mountains, both of which are defined by steep, rugged mountains and similar vegetative distributions. Both ecoregions contain glacial systems, though lower elevation glaciers are more common in the Wrangell Mountains ecoregion.

Analysis of satellite imagery reveals recent browning trends through much of the interior climate class (Verbyla 2008; Parent and Verbyla 2010) in vegetated areas, e.g. interior highlands. The cause of the browning is undetermined, but potential causes include wildfire and insect infestations.

Mean annual temperatures average -3.3 C° and mean July temperatures range from -12.9 C° at the highest elevations to 18.2 C° in lower elevations, which is the highest maximum mean July temperature of any of the climate classes (Scenarios Network for Alaska and Arctic Planning). Mean annual precipitation across the alpine zones is 636.3 mm between 2000 -2009.

Alpine zones included in this climate class include Tanana Uplands, Alaska Range East (north and south slopes), Alaska Range Central (north slope only), and the North Wrangell Mountains.

### 2.1.4 High Precipitation Mountains

These mountains are characterized by a transitional climate (between maritime and continental) that has moderate winters, cool summers and the highest relative annual precipitation within the study region (Gallant et al. 1995). The primary ecoregions encompassed include Pacific Coastal Mountains and Alaska Range. The climate class is heavily glaciated, including ice fields and relatively barren vegetation at high elevations. At lower elevations, glacial recession offers suitable soil for successional vegetation types such as shrubs. Lower elevation vegetation may include spruce-dominated forests and broadleaf forests dominated by quaking aspen (*Populus tremuloides*) and balsam poplar (*Populus balsamifera*) as well as scrub thickets dominated by alder and willow species (Gallant et al. 1995).

Mean annual temperature averages -2.4 C° across alpine zones and this class has the lowest average mean July temperature for 2000 – 2009 at 10.8 C°. Mean annual precipitation is both the highest and most variable. Mean annual precipitation between 2000-2009 is 1634.5mm.

Alpine zones included in this climate class are the Chugach Mountains, Kenai Mountains, Alaska range West (north and south Slopes), Alaska Range Central (south slope), Talkeetna Mountains and southern Wrangell Mountains.

*Table 2-2: Mean annual temperature (C°) and mean July temperature (C°) based on 10-year averages for all alpine zones within the area of interest. All temperatures derived from decadal averages for the period 2000-2009 available from the Scenarios Network for Alaska and Arctic Planning.*

| | Mean Annual Temperature (C°) | | | Mean July Temperature (C°) | | |
|---|---|---|---|---|---|---|
| Name | Min. | Max | Mean | Min | Max | Mean |
| **Alaska Range Central, North Slope** | -20.7 | 0.0 | -2.8 | -12.9 | 18.2 | 12.5 |
| **Alaska Range Central, South Slope** | -20.6 | 3.2 | -3.2 | -12.6 | 17.7 | 11.0 |
| **Alaska Range East, North Slope** | -10.3 | -0.2 | -3.9 | 1.9 | 17.3 | 11.5 |
| **Alaska Range East, South Slope** | -7.8 | -0.2 | -3.2 | 4.9 | 17.3 | 12.1 |
| **Alaska Range West, North Slope** | -6.9 | 2.7 | -2.6 | 5.5 | 17.1 | 11.1 |
| **Alaska Range West, South Slope** | -10.3 | 4.1 | -1.2 | 1.0 | 17.0 | 11.3 |
| **Brooks Range Central, North Slope** | -11.7 | -6.4 | -9.0 | 6.7 | 14.9 | 12.3 |
| **Brooks Range Central, South Slope** | -11.1 | -3.7 | -7.5 | 7.4 | 16.7 | 12.8 |
| **Brooks Range East, North Slope** | -13.3 | -6.0 | -9.2 | 4.8 | 14.5 | 10.5 |
| **Brooks Range East, South Slope** | -13.3 | -2.9 | -7.0 | 5.1 | 17.9 | 13.2 |
| **Brooks Range West, North Slope** | -10.2 | -6.4 | -8.5 | 10.7 | 14.3 | 13.3 |
| **Brooks Range West, South Slope** | -8.9 | -4.2 | -6.8 | 11.6 | 16.5 | 14.5 |
| **Chugach Mountains** | -10.7 | 4.8 | -2.3 | 1.1 | 15.7 | 10.0 |
| **Kenai Mountains** | -0.5 | 5.6 | 3.0 | 9.7 | 16.6 | 13.7 |
| **North Wrangell Mountains** | -17.4 | 0.0 | -5.8 | -8.6 | 16.5 | 7.6 |
| **South Wrangell Mountains** | -17.1 | 2.7 | -4.1 | -8.1 | 15.4 | 9.1 |
| **Talkeetna Mountains** | -7.0 | 3.5 | -2.8 | 6.7 | 17.7 | 11.9 |
| **Tanana Uplands** | -5.5 | 0.1 | -2.4 | 9.4 | 17.9 | 14.5 |

## 2.2 Sourcing Landsat Imagery

We sourced Landsat-8 Operational Land Imagery (OLI) scenes dating from the modern era (defined as 2013 – 2018; hereafter referred to as modern) and Landsat 4-5 Thematic Mapper (TM) scenes dating from the historic era (defined as 1984 – 1989; hereafter referred to as historic) occurring within July and containing 70% or greater cloud-free pixels. If multiple scenes were available for the same area of coverage, we selected the scene with the least amount of cloud cover and used the availability of historic TM scenes to determine which modern OLI scenes to use. If the historic TM scene had more cloud-free pixels than its modern OLI counterpart we would select it for analysis. If the historic TM had less cloud-free pixels than its modern OLI counterpart, we were likely to exclude it. Table 2-3 overviews all scene-pairs with 70% or greater cloud-free pixels according to the United States Geological Survey (USGS).

We prioritized scenes with July acquisition dates as mid-July NDVI is most representative of shrub canopy (Boelman et al. 2015) and previous studies using Landsat data to examine greening trends center their acquisition dates around July (Raynolds et al. 2013; Frost et al. 2014). Additionally, the July data helps account for anomalous weather events, such as late springs, that could impact early summer July (Jia et al. 2004).

*Table 2-3: July Landsat scenes by alpine zone. Path, row, acquisition dates, analyzable area (km²), total area of scene overlap with area of interest (km²), and percentage of analyzable area are provided. Bolded rows indicate areas that had sufficient analyzable percentage (70%) after accounting for contamination. None refers to Landsat scenes that lacked sufficient analyzable coverage after accounting for contamination, had errors with calibrating reflectance, or negligible total coverage*

| Path | Row | Historic Date TM Landsat | Modern Date OLI Landsat | Analyzable Area (km²) | Total (km²) | Analyzable Percentage |
|---|---|---|---|---|---|---|
| **Kenai Mountains** | | | | | | |
| **67** | **18** | **1986-July-28** | **2013-July-22** | **1389.2** | **1939.2** | **71.6** |
| 69 | 18 | 1989-July-10 | 2018-July-18 | 1337.6 | 9444.0 | 14.2 |
| 69 | 17 | 1989-July-10 | 2018-July-2 | 2088.7 | 3358.8 | 62.2 |
| **Chugach Mountains** | | | | | | |
| 66 | 18 | 1987-July-24 | 2014-July-2 | 512.7 | 737.9 | 69.5 |
| **67** | **18** | **1986-July-28** | **2013-July-22** | **554.7** | **760.5** | **72.9** |
| 69 | 17 | 1989-July-10 | 2018-July-2 | 786.4 | 4784.4 | 16.4 |
| **Wrangell Mountains South** | | | | | | |
| None | | | | | | |
| **Wrangell Mountains North** | | | | | | |
| 65 | 16 | 1986-July-30 | 2018-July-22 | 1491.7 | 8042.3 | 18.5 |
| **Talkeetna Mountains** | | | | | | |
| 69 | 17 | 1989-July-10 | 2018-July-2 | 606.2 | 3935.2 | 15.4 |
| **Alaska Range East, North Slope** | | | | | | |
| 65 | 16 | 1986-July-30 | 2018-July-22 | 2456.9 | 5708.3 | 43.0 |
| 67 | 15 | 1986-July-28 | 2018-July-4 | 1837.1 | 5297.7 | 34.7 |
| **Alaska Range East, South Slope** | | | | | | |
| 65 | 16 | 1986-July-30 | 2018-July-22 | 2191.1 | 4303.7 | 50.9 |
| **Alaska Range Central, North Slope** | | | | | | |
| 67 | 15 | 1986-July-28 | 2018-July-4 | 1236.7 | 2578.9 | 48.0 |
| **Alaska Range Central, South Slope** | | | | | | |
| 69 | 17 | 1989-July-10 | 2018-July-2 | 301.1 | 545.1 | 55.2 |
| **Alaska Range West, North Slope** | | | | | | |
| None | | | | | | |
| **Alaska Range West, South Slope** | | | | | | |
| 69 | 17 | 1989-July-10 | 2018-July-2 | 475.0 | 1826.3 | 26.0 |
| 69 | 18 | 1989-July-10 | 2018-July-18 | 0.0 | 775 | 0.0 |
| **Brooks Range Central, North Slope** | | | | | | |
| 75 | 11 | 1986-July-4 | 2013-July-14 | 971.3 | 1443.3 | 67.3 |
| **75** | **12** | **1986-July-4** | **2016-July-22** | **15981.2** | **20666.8** | **77.3** |
| **75** | **13** | **1986-July-5** | **2015-July-4** | **271.1** | **386.1** | **70.2** |
| **Brooks Range Central, South Slope** | | | | | | |
| 75 | 12 | 1986-July-4 | 2016-July-22 | 2477.1 | 8795.2 | 28.2 |
| **75** | **13** | **1986-July-5** | **2015-July-4** | **11111.3** | **13355.3** | **83.2** |
| **Brooks Range East, North Slope** | | | | | | |
| 68 | 11 | 1986-July-3 | 2013-July-13 | 4166.7 | 6293.9 | 66.2 |
| **Brooks Range East, South Slope** | | | | | | |
| 66 | 12 | 1986-July-29 | 2013-July-15 | 777.9 | 2912.7 | 26.7 |
| 66 | 13 | 1989-July-29 | 2013-July-15 | 2400.1 | 3535.5 | 67.9 |
| **68** | **11** | **1986-July-3** | **2013-July-13** | **188.7** | **202.9** | **93.0** |
| **Brooks Range West, North Slope** | | | | | | |
| None | | | | | | |
| **Brooks Range West, South Slope** | | | | | | |
| None | | | | | | |
| **Tanana Uplands** | | | | | | |
| **65** | **16** | **1986-July-30** | **2018-July-22** | **4949.0** | **6188.7** | **80.0** |
| 67 | 15 | 1986-July-28 | 2018-July-4 | 8706.0 | 18437.3 | 47.2 |

## 2.3 Cloud Contamination, Sensor Normalization and Calculating Spectral Indices

With our imagery selected, we processed the historic TM and modern OLI scenes prior to determining shrub extent and expansion (Figure 2-2). These steps include:

1. Calibrating reflectance of selected bands (red and near-infrared)
2. Identifying cloudless areas in both eras and eliminating atmospheric contamination
3. Executing radiometric correction of the modern OLI scene to the historic TM scene
    i. Calculating Normalized Difference Vegetation Index (NDVI) for both eras
    ii. Identifying water and rock (consistent across eras) using NDVI
    iii. Extracting red and near-infrared values to rock and water
    iv. Regressing historic red and near-infrared values as products of modern red and near-infrared values, respectively
    v. Recalculating the modern red and near-infrared values using the linear equation from each regression
    vi. Recalculating a normalized modern NDVI
4. Identifying vegetated areas using the historic NDVI and modern normalized NDVI
5. Applying local Dall's sheep elevation minimums for summer range

The normalized difference vegetation index (NDVI) is the index used to calculate percent shrub dominance. It is computed from processed modern OLI and historic TM red and near-infrared bands. To process these bands for the NDVI calculation, we first used ENVI 5.5.1 (API version 3.3) to calibrate reflectance of the red and near-infrared bands (spatial data layers that contain single numerical values within each pixel representative of a specific type of light/electromagnetic radiation) for modern OLI (bands 4 and 5 respectively) and historic TM (bands 3 and 4 respectively). Calibration is useful for limiting atmospheric impacts on spectral bands and the indices that use those bands, such as

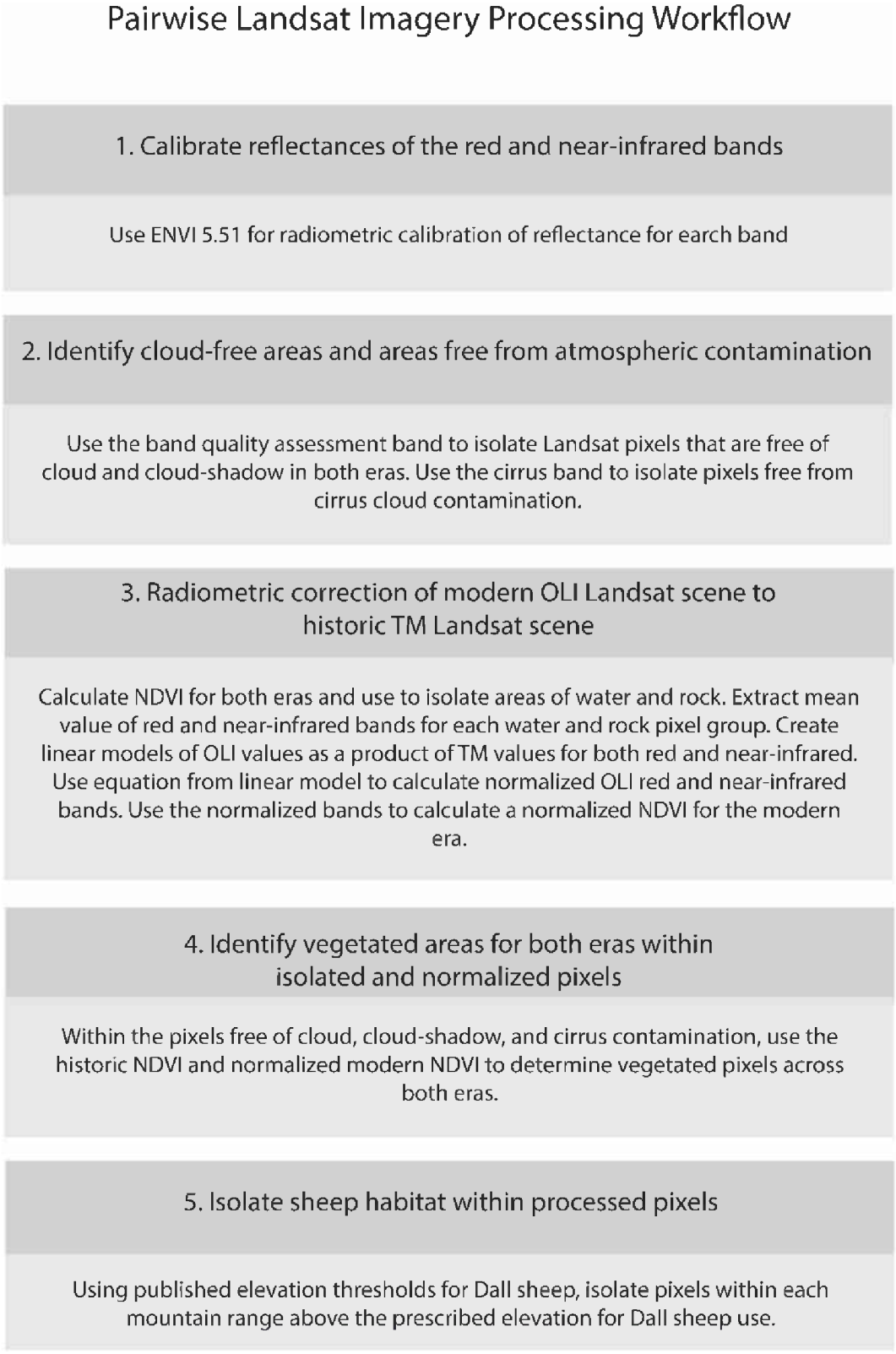


*Figure 2-2: Processing workflow to prepare Landsat OLI and TM imagery for NDVI calculation and subsequent conversion into percent shrub dominance.*

NDVI, which is the most widely used vegetation index applied in remote sensing studies (Song et al. 2000). Using these calibrated bands, we isolate completely cloud-free areas that could be used for analysis via NDVI.

Low cloud cover scenes (<30%) still require isolation of cloudless areas, meaning free from both cloud and cloud impacts such as shadows (hereafter clear sky pixels). The quality assessment band (BQA) included in all TM and OLI imagery provides numerical values for pixels that indicate the likelihood the pixel contains cloud or is impacted by cloud (e.g. within a cloud shadow) (Irons et al. 2012). Using the BQA for each era, we isolated areas of clear sky pixels for both the historic TM and modern OLI areas. We masked (removed from consideration) all BQA pixels that were not clear sky for both eras (Figure 2-3).

Cirrus clouds are minimally visible clouds that can scatter radiances of red and near-infrared bands, thus impacting index values based on these bands, such as NDVI (Gao and Li 2000). Modern OLI scenes contain a cirrus band (detects cirrus clouds and assigns pixels a numerical value based on likelihood of cirrus cloud), whereas historic TM scenes lack such a band that can help isolate cirrus-free pixels. To account for this absence, we prioritized historic TM scenes with low cloud contamination over modern OLI scenes. Most scenes used for analysis have cloud cover between 10 and 15%. The acceptable portion (pixels within the northcentral Brooks Range alpine zone) of the modern OLI scene at path 75 row 12 contained relatively high cloud cover (22.7%). We inspected the clear sky pixels modern OLI scene for cirrus cloud contamination by visually assessing cirrus extent in the Cirrus band and isolating all cirrus-free pixels (Figure 2-4). We then combined these pixels with the historic TM clear sky pixels so that the remaining area contained pixels that were both clear sky across eras and cirrus-free (hereafter analyzable pixels; Figure 2-5).

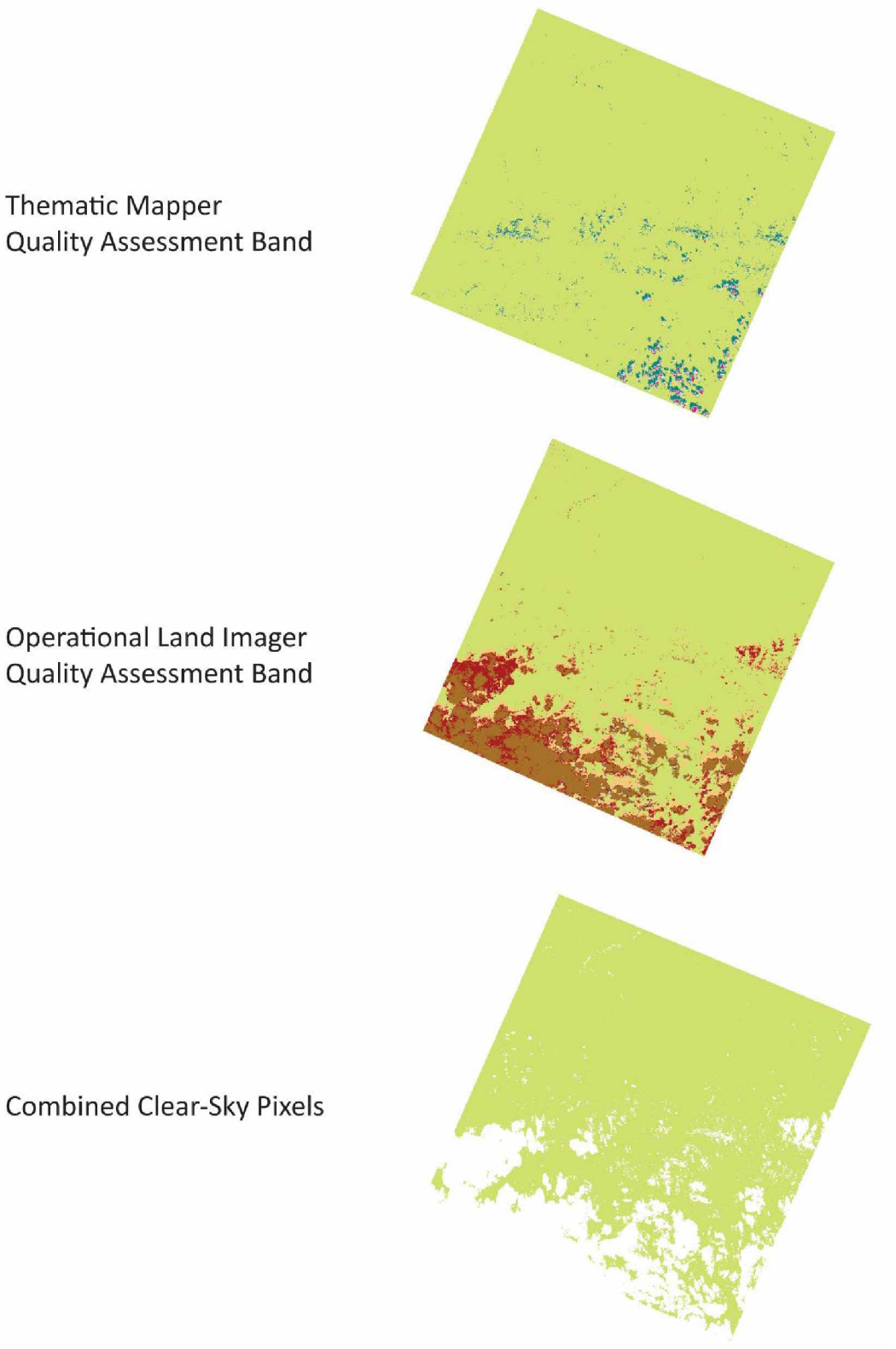


*Figure 2-3: Quality Assessment Bands (BQA) for a 1986 Thematic Mapper scene (top), 2016 Operational Land Imager scene (middle) and all clear sky pixel areas consistent across the modern and historic eras at Path 75 Row 12. All light green colors indicate clear sky pixels. The contaminated areas (cloud likely, cloud shadow likely, etc.).are pictured in alternative colors.*

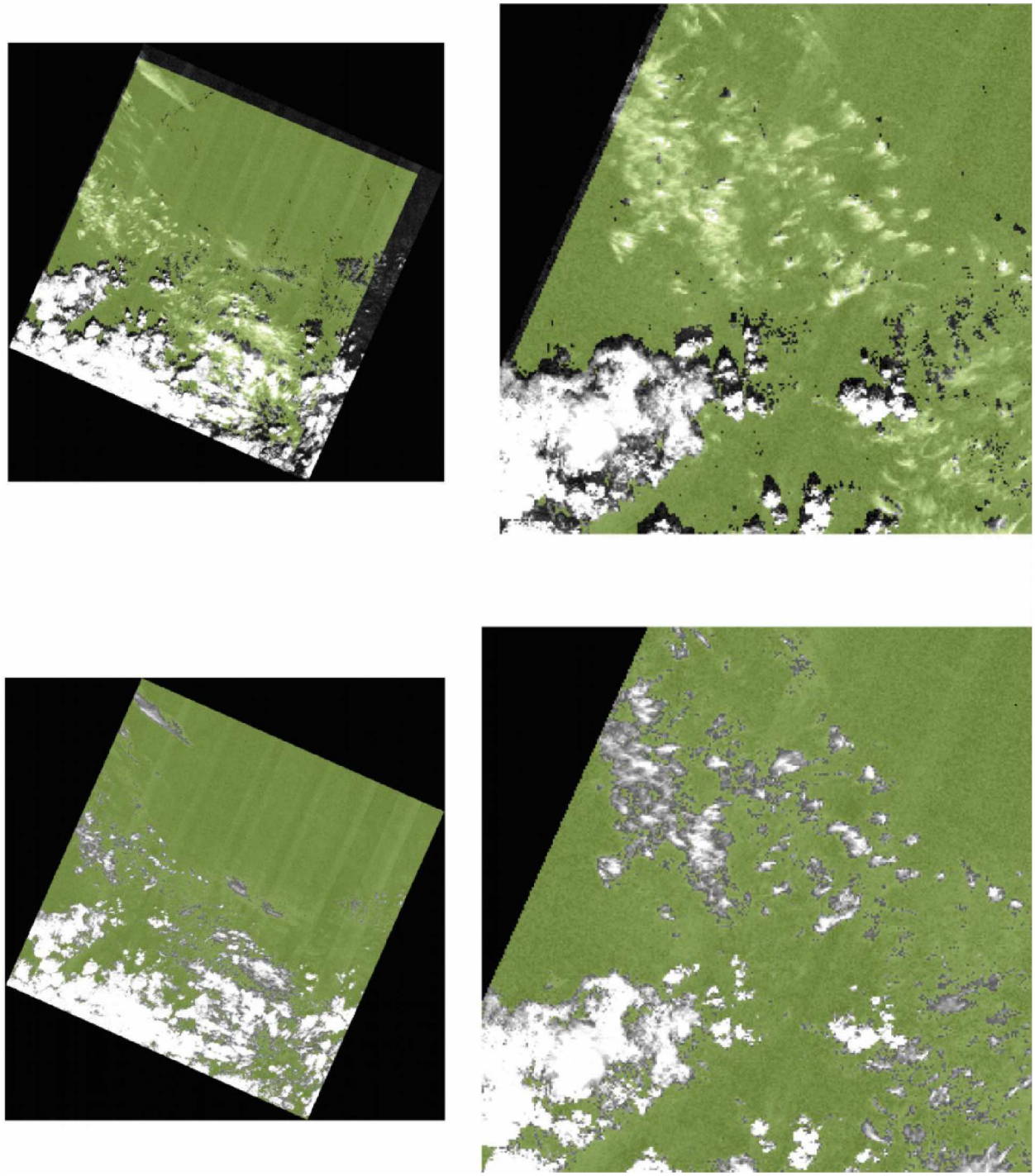

*Figure 2-4: Masks based on cloud contamination (green) developed using different methods: BQA and visually delineated Cirrus. BQA clear sky pixels for both eras displayed in top images and the cirrus-free pixels displayed in bottom images. The black and white image is Path 75 Row 12 cirrus band (band 9). Note that cloud shadows are removed in the BQA clear sky pixels though some cirrus pixels are included in the study area. The cirrus-free pixels exclude most of the cirrus pixels but still incorporate areas with cloud shadow. Combining the two into a set of clear sky cirrus-free pixels provides the lowest possible atmospheric contamination from a cloudy scene. These two methods of cloud removal were combined to isolate a set of clear sky and cirrus-free pixels usable for analysis (analyzable pixels).*

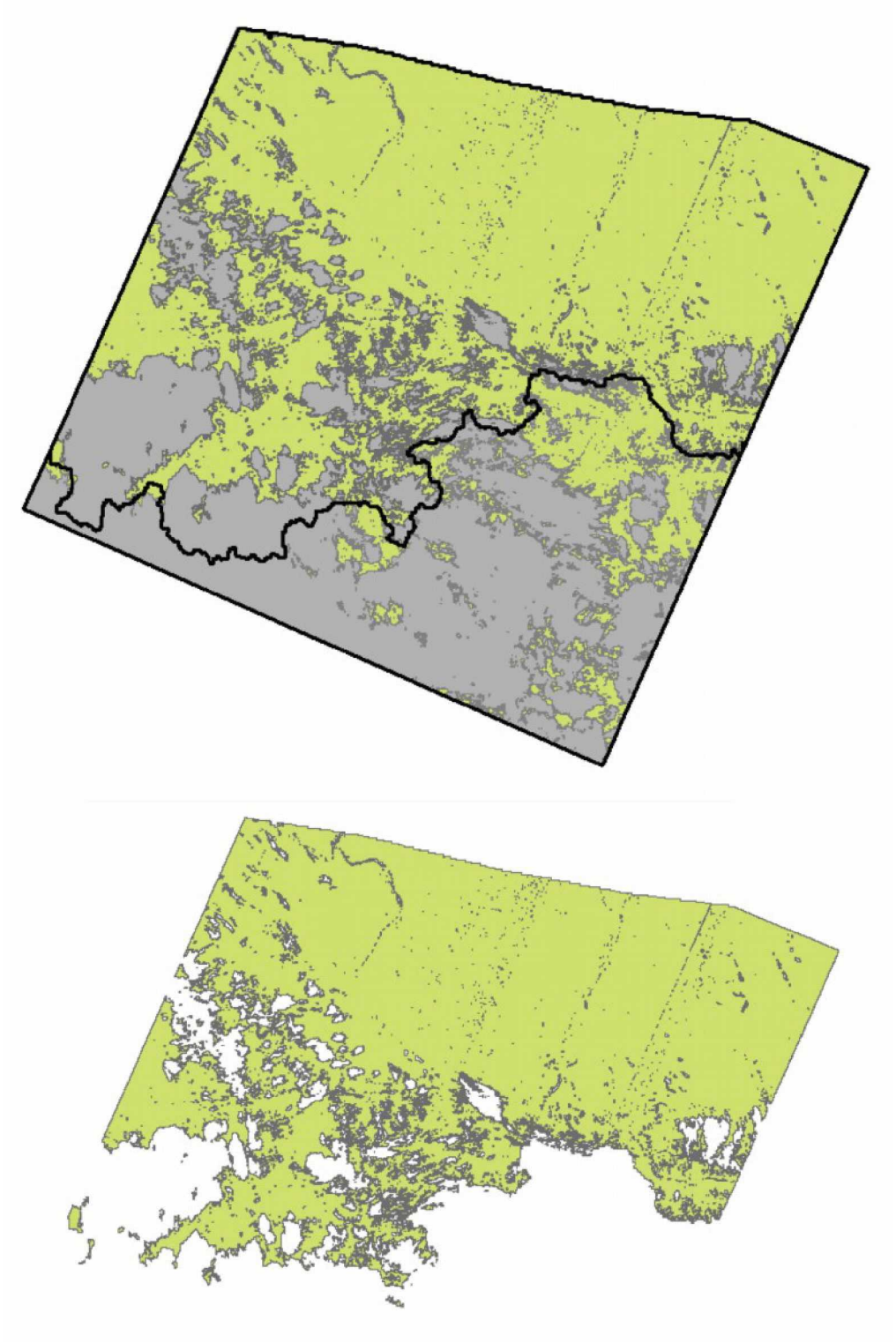

*Figure 2-5: Analyzable areas (green) of Path 75 Row 12 over total coverage of the Landsat scene (grey) separated by black boundary lines into the climate classes covered: cold Arctic and Arctic. The analyzable percentage of Path 75 Row 12 in the cold Arctic climate was an acceptable rate (77.3%, and 15,981.2 km), However analyzable percentage in the Arctic climate was below the acceptable 70% rate (28.2% and 2,477.1 km) and was removed from the study. The area used for the study is pictured at bottom.*

If analyzable pixels represented less than 70% total available coverage within a climate class, we removed that area from consideration (to coincide with the 30% cloud cover threshold set during the sourcing process). For example, Path 75 Row 12 has spatial coverage in two climate classes: Arctic and Cold Arctic. The cloud contamination in the Arctic portion of that scene exceeded 30% (n = 71.8%), meaning only 28.2% of the study area contained analyzable pixels. However, the Cold Arctic portion maintained the acceptable standard of cloud cover below 30% (n = 22.7%). We removed the Arctic portion of that scene from consideration due to substantial cloud contamination but kept the Cold Arctic portion for our analysis (Figure 2-5).

Glaciers can impact BQAs due to similar reflectance of ice and cloud, and therefore must be accounted for when isolating analyzable pixels from cloud-contaminated ones. We manually checked all scenes in the high precipitation climate class with color infrared composites to determine if cloud-contaminated pixels contained false positives (i.e. clear-sky pixels of glaciers). When glaciers resulted in cloud contamination false positives, we corrected the issue by combining BQA clear-sky pixels with polygons of glaciers from Global Land Ice Measurements from Space (GLIMS) available from the National Snow and Ice Data Center. If necessary, we isolated the cirrus-free pixels within that area to determine percent cloud cover. Figure 2-6 shows our study area that contains sufficient analyzable pixels for calculating percent shrub dominance, with the total pixel coverage by Landsat scenes in the inset.

We used radiometric correction methods defined by Chen et al. (2005) and utilized by other Landsat-based vegetation change studies (Olthof et al. 2008; Raynolds et al. 2013) to develop equations that normalized the modern OLI spectral values for the near-infrared and red bands to their historic TM counterparts.

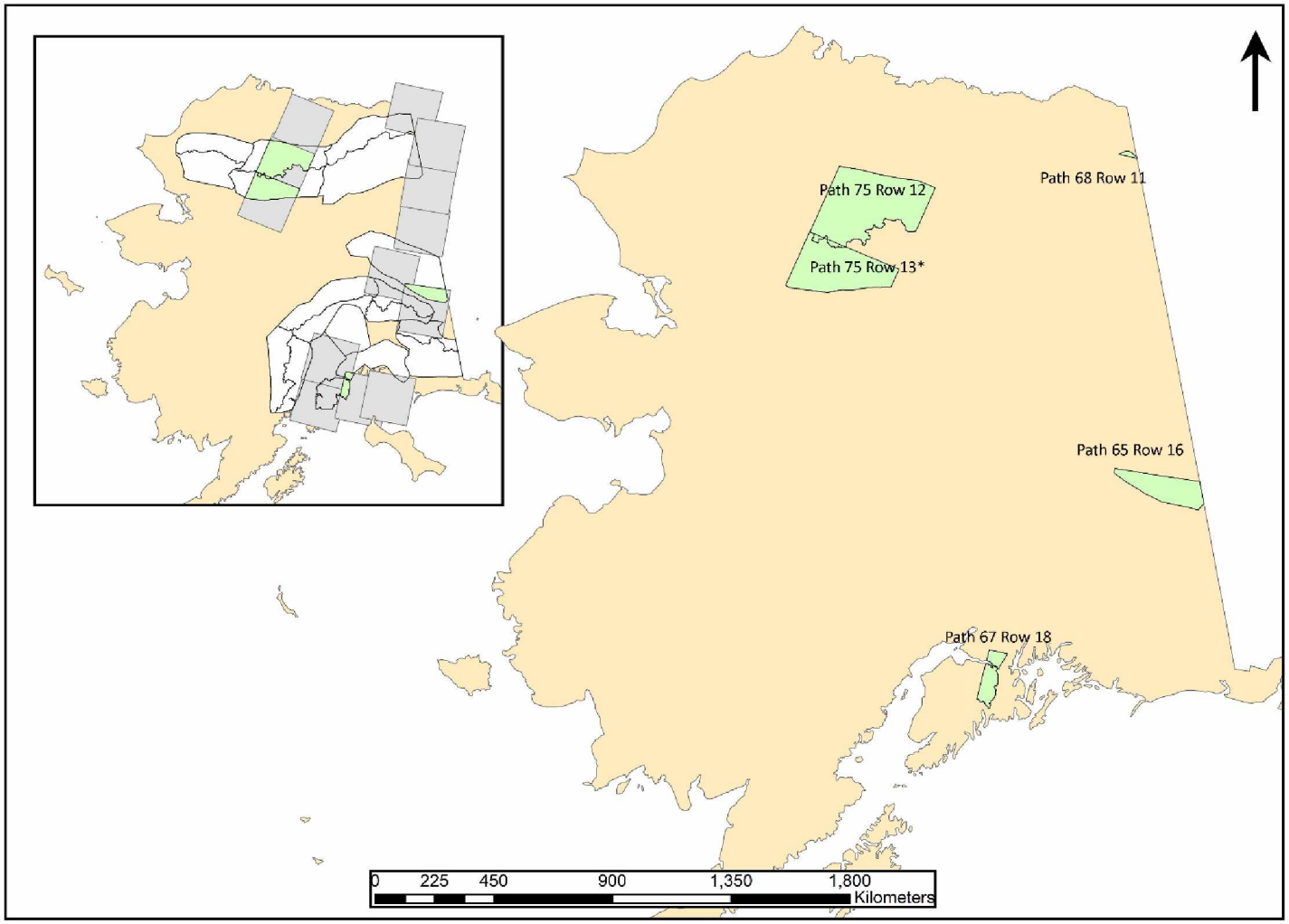


*Figure 2-6: Map of the study area depicted in green polygons with their associated Landsat path and row as labels. The asterisk by Path 75 Row 13 indicates that scene spans two climate classes, each analyzed separately. The inset map shows the available Landsat data with July acquisition dates that were removed after analyzing them for cloud contamination.*

With clear-sky and cirrus-free pixels identified, we determined areas of water bodies and exposed sediment (e.g. rocks, bare soil) for use in calibrating spectral values between sensors. We calculated a historic NDVI and initial, non-normalized modern NDVI and isolated all pixels that contained a value less than 0.2. These pixel groups were assumed to be water bodies and areas of exposed sediment (Figure 2-7), consistent with prior research (Verbyla 2018). Water is considered an invariant feature because it contains lower and more stable reflectance features than other surfaces (Chen et al. 2005). Bare lands (e.g. rocks) typically display the brightest invariant pixels and their reflectance is less influenced by phenology (2005). Using values from these types of surfaces to normalize spectral values across sensors offers a range of values that are not confounded by long-term (multi-year) or short-term (seasonal) temporal changes.

We extracted the summary statistics of the red and near-infrared band values for each era to by the individual, contiguous areas of rock and water. We removed any singular areas of water and rock with pixels areas between 1800 and 9000 $m^2$, dependent on sample size available. For example, in the Cold Arctic climate class alpine barrens dominate (Swanson 2015) so there was extensive representation of exposed sediment pixels as well as water pixels to normalize values across sensors. However, in the heavily vegetated and glaciated areas there was less overall water and exposed sediments pixel groupings with which to correct. We used a smaller pixel area threshold depending on available pixels. We calculated linear regressions using the historic red and near-infrared values as products of the modern red and near-infrared values, respectively (Figure 2-8.).

After extracting all values, we further limited chance of error from landcover change (e.g. alluvial plain to shrub) by setting a maximum standard deviation. For example, in path 75 row 12 we removed groups with standard deviations exceeding 0.05 for any of the eras and bands. To account for this across all scene pairs, minimum parameters (such as minimum acceptable standard deviation of

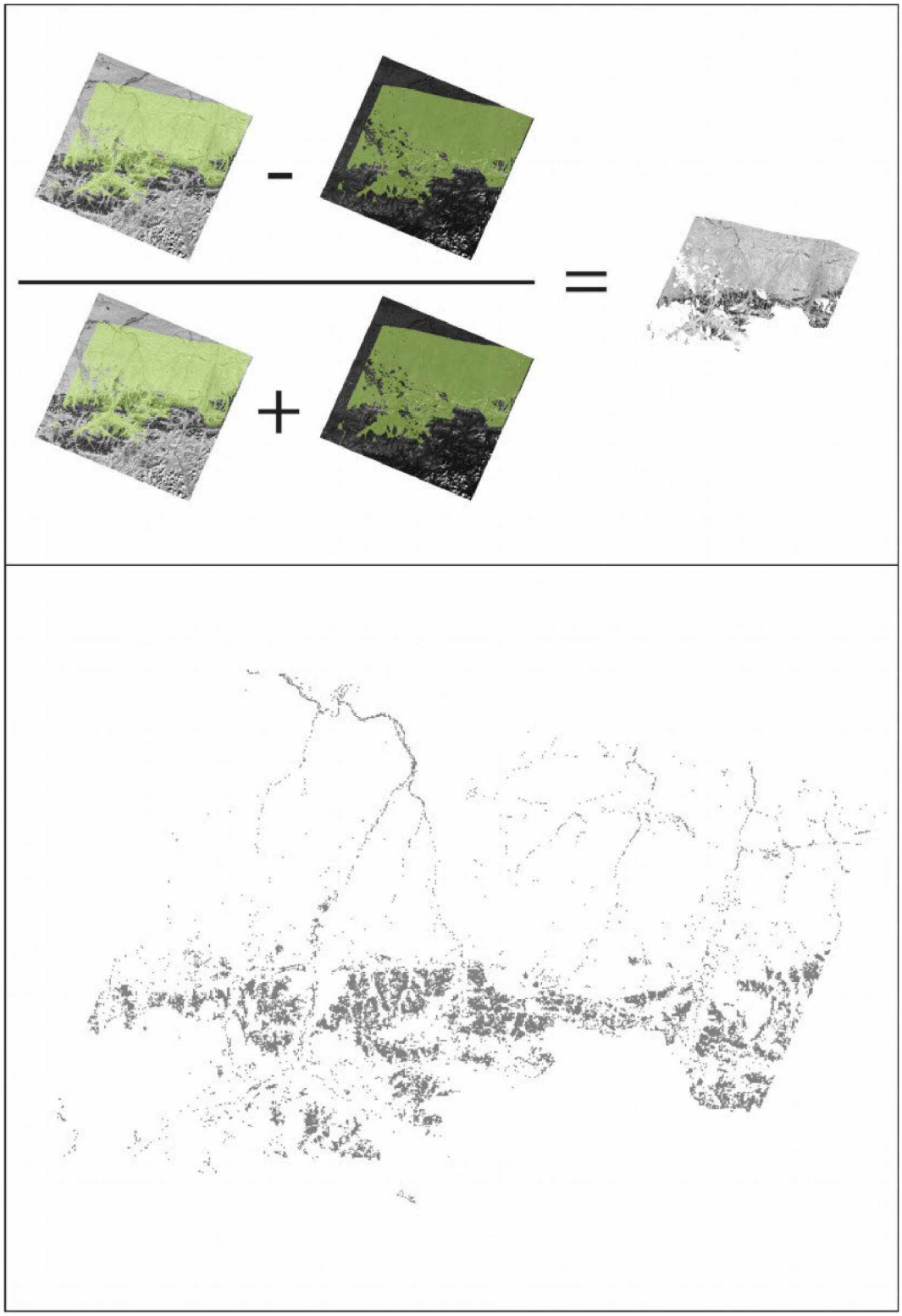

*Figure 2-7: The equation for NDVI visualized using Landsat TM red and near-infrared bands (grey and white images) covered by a mask of analyzable pixels for Path 75 Row 12 (top) and areas of rock and water identified using NDVI (bottom). Vegetated pixels should have a value >= 0.2 (Verbyla 2018). By removing all vegetated pixels we selected water and exposed sediment areas. Areas of change between eras were accounted for by removing pixels > 0.2 in either era.*

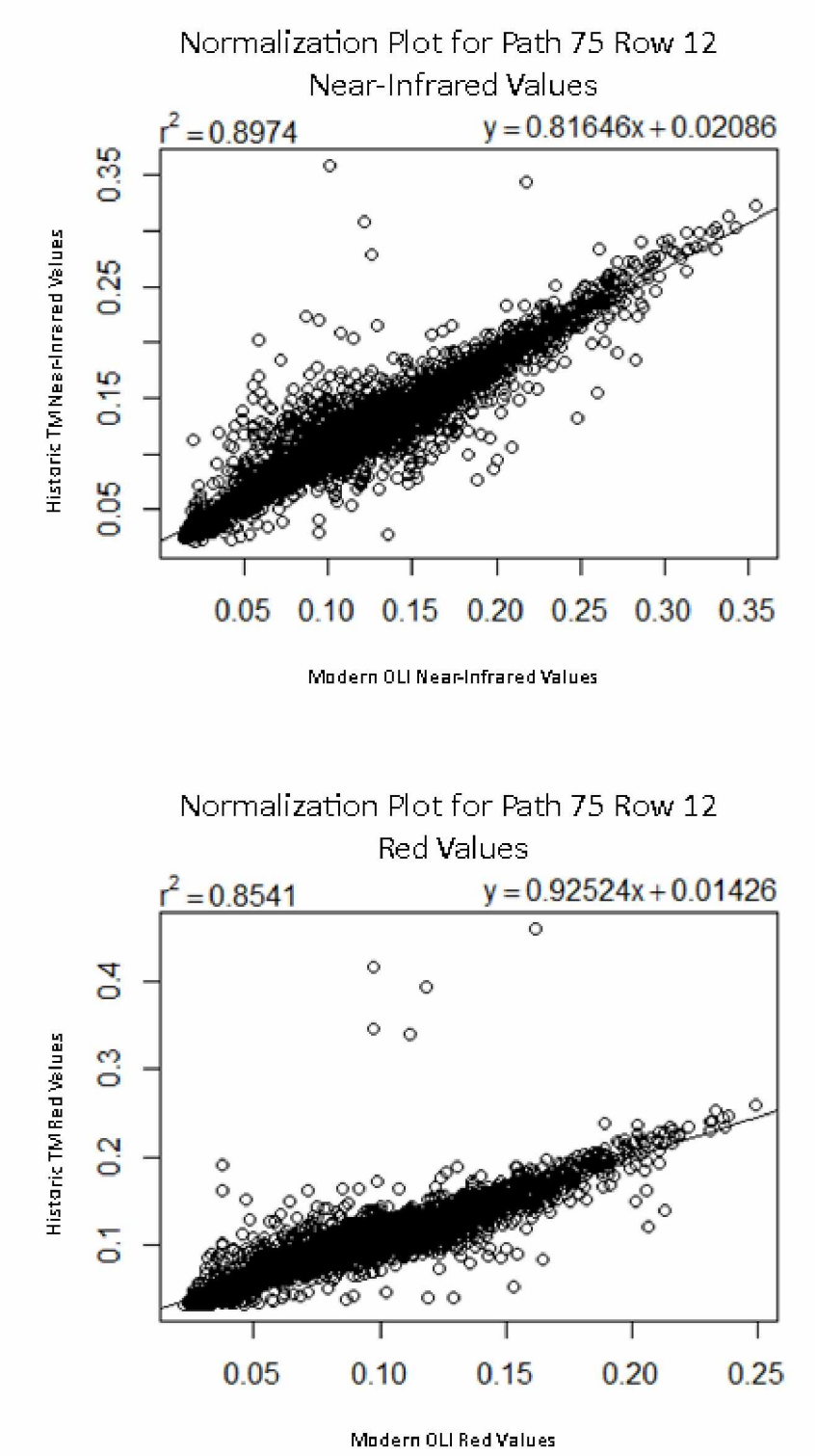


*Figure 2-8: Scatterplots of the near-infrared (top) and red (bottom) values for rock and water areas across both eras of Path 75 Row 12. The historic value for each band is on the y-axis and the modern value for each band is on the x-axis. The equation from each plot is used to normalize the modern OLI band to the historic TM band.*

mean red values for rock and water) varied by scene pairs (e.g. all standard deviations used in path 75 row 12 were < 0.05, while standard deviations used in path 75 row 13 were 0.04).

Reflectance values across glaciers can vary due to factors such as glacial recession. As glaciers recede, sediment is exposed. Due to this confounding issue, we eliminated glaciers from consideration when developing linear equations to normalize values across sensors.

Across all scene pairs, we attempted to minimize variance created by small pixel counts and large standard deviations of the mean spectral values. Large standard deviations could indicate areas where some pixels represented surface change rather than sensor difference (e.g. vegetative growth in pockets of a large alluvial fan). To limit this variance, we set a minimum area per rock or water "group" by scene and minimum standard deviation for each era and band also by scene (Table 2-4)

We then used the equations from the slope of each regression to normalize the modern OLI values for the red and near-infrared bands to the historic TM values (acquired with a TM sensor). After normalizing modern NDVI in this way, we reran the NDVI calculation for the modern era (Eq. 1). We then used raster calculator to subtract the historic NDVI values from the normalized modern NDVI values to determine change in NDVI within the period of interest. Using these layers, we isolated all vegetated areas (defined as NDVI > 0.2) and relegated our study to these pixels only.

$$NDVI_{Norm} = (Near\text{-}Infrared_{Norm} - Red_{Norm}) / (Infrared_{Norm} + Red_{Norm})$$

where $Near\text{-}Infrared_{Norm} = \alpha_1(Near\text{-}Infrared) + \beta_1$

and $Red_{Norm} = \alpha_2(Near\text{-}Infrared) + \beta_2$

*Equation 2: Normalized Difference Vegetation Index after normalizing the red and near-infrared Landaat-8 OLI values to the Landsat-4/5 TM values, enabling more accurate vegetation comparisons across sensors and time.*

*Table 2-4: Normalization parameters using (Chen et al. 2005) correction methods to correct Landsat OLI pixels to Landsat TM for each scene-pair to be analyzed. All correction equations were based on single-variate linear relationships: y = αx + β, where parameters are provided. Minimum sample size is the minimum size necessary for a group of pixels to be incorporated in the analysis*

| Class | Path | Row | Normalization Parameters | | | | Minimum Sample Size ($m^2$) | Maximum Standard Deviation | |
|---|---|---|---|---|---|---|---|---|---|
| | | | Red | | Near-Infrared | | | | |
| | | | α | β | α | β | | Red | Near-Infrared |
| **Arctic** | 68 | 11 | 0.88574 | 0.02519 | 0.76987 | 0.03585 | 2700 | 0.04 | 0.04 |
| **Arctic** | 75 | 13 | 1.05644 | 0.00236 | 0.93929 | 0.00112 | 9000 | 0.04 | 0.04 |
| **Cold Arctic** | 75 | 12 | 0.92524 | 0.01426 | 0.81646 | 0.02086 | 9000 | 0.05 | 0.05 |
| **Cold Arctic** | 75 | 13 | 1.05644 | 0.00236 | 0.93929 | 0.00112 | 9000 | 0.04 | 0.04 |
| **High Precipitation** | 67 | 18 | 0.81863 | 0.06009 | 0.74931 | 0.07917 | 4500 | 0.05 | 0.05 |
| **High Precipitation** | 67 | 18 | 0.81863 | 0.06009 | 0.74931 | 0.07917 | 4500 | 0.05 | 0.05 |
| **Interior Mountains** | 65 | 16 | 0.54851 | 0.05911 | 0.68725 | 0.07481 | 1800 | 0.05 | 0.05 |

## 2.4 Determining Tall Shrub Dominance and Extracting Climate Data

In order to determine percent shrub dominance in Dall's sheep range and its change over a roughly 30-year interval (answering research question one), we needed to convert the normalized NDVI values to percent shrub dominance values. To do this, we used existing shrub cover maps to define the equation that transforms NDVI values to percent shrub dominance. Recent percent shrub cover maps (Macander et al. 2015; Berner et al. 2018) provide accurate in-depth projections of shrub cover and intersect portions of our high latitude study areas. Using the most recent and extensive tall shrub map overlapping in our study area (Figure 2-9; Berner et al. 2018), we extracted modern normalized mean NDVI values (available from the path 75 row 12 modern OLI scene) corresponding to percent shrub

dominance values (Figure 2-9). We determined the logarithmic relationship between percent shrub dominance and modern OLI NDVI values. Using this equation, we generated rasters representative of shrub dominance in scene-pairs comprising our study areas. Equipped with historic and modern maps of percent shrub dominance we calculated shrub change across time and compared change between different climate classes.

Gridded climate interpolation data were available, offering a better alternative to the highly dispersed and locally-limited permanent weather stations within the study areas. We sourced 771-m resolution climate research unit (CRU) time series 3.10 (TS31; Harris et al. 2014) gridded climate data available for the periods 1980 – 1989 and 2000 – 2009 from the Scenarios Network for Alaska and Arctic Planning. Variables included decadal mean July temperature, decadal mean length of growing season (LOGS), decadal mean annual precipitation, and decadal mean winter temperature. We executed a bilinear resampling of all SNAP climate data to the native resolution of the Landsat-derived shrub pixels (30m). For all variables, we generated their delta by subtracting the historic values from the modern.

We generated a 30-m digital elevation model from 60-m tiles sourced from the national elevation dataset (NED) using a bilinear resampling. We then executed the Slope and Aspect tools in ArcGIS to derive terrain statistics to compare with shrub change.

To explore relationships with climatic and terrain variables we classified each variable at natural breaks and extracted mean shrub change and mean modern percent shrub dominance as an exploratory analysis designed to identify variables with possible causal relationships to shrub dominance and change. We plotted single-variate plots for all variables within all scene-pairs to and generated pairwise comparisons to check for collinearity (see Appendix).

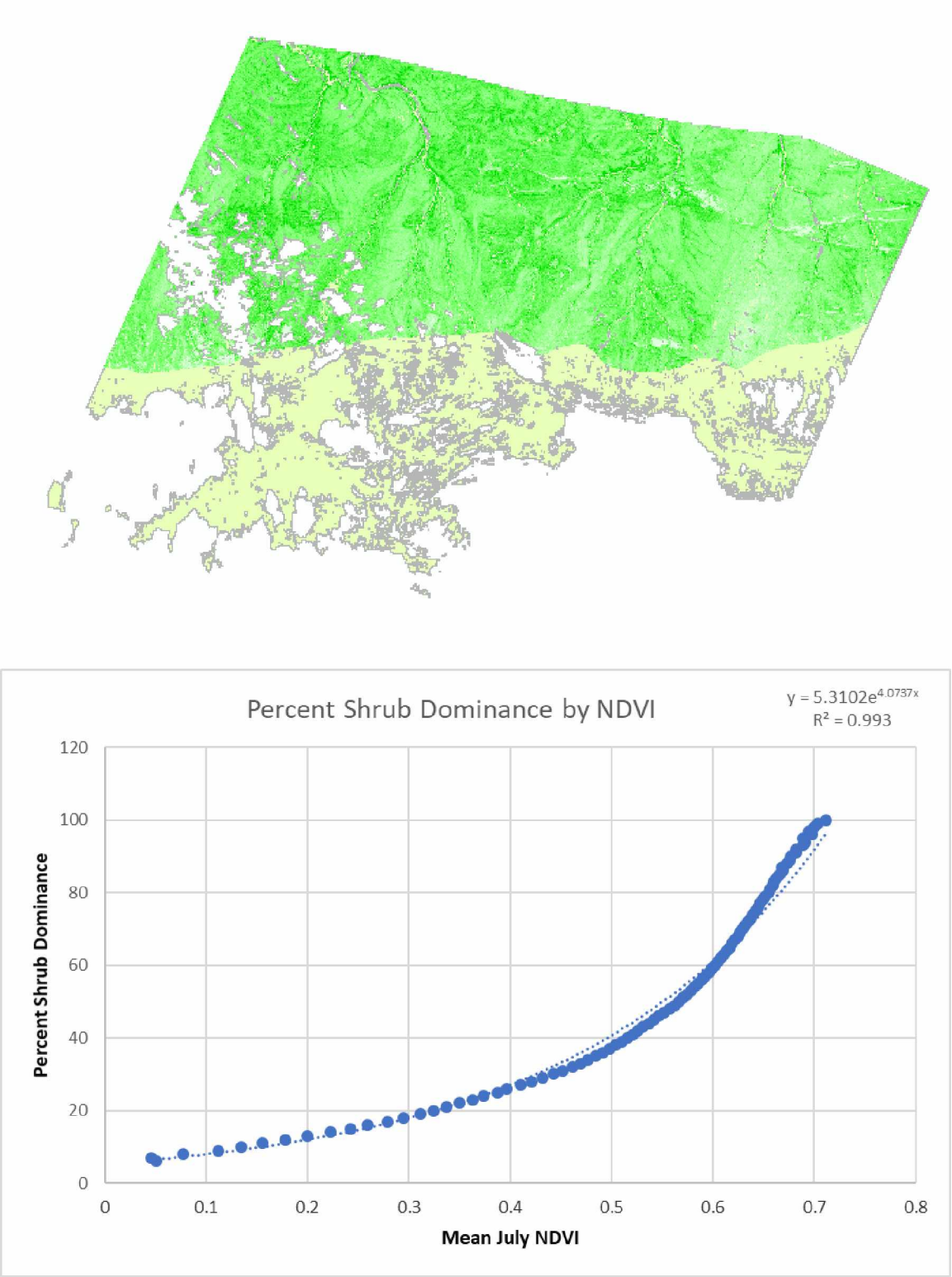


*Figure 2-9: The most recent percent shrub dominance map (Berner et al. 2018) overlaid analyzable pixels for path 75 row 12 (top) and a scatterplot showing percent shrub dominance as a function of mean modern normalized NDVI derived from the analyzable pixels (bottom). The logarithmic equation used to calculate percent shrub dominance across the study area is displayed in the top right corner of the plot.*

## 2.5 Determining Growth Class and Climate Class with Highest Shrub Expansion Rates

We extracted all (resampled) mean July temperature pixels within each scene-pair. For each scene-pair, we defined three classes of shrub growth facility: below growth limits (below 10.5 C°, Figure 2-10, blue), at growth limits (between 10.5 C° and 12 C°, green) and above growth limits (above 12 C°, red). We then executed the Region Group tool in ArcMap 10.6.1 to organize groups of high growth areas into isolated pixel groups for extracting means of change in percent shrub dominance. We extracted those means for each growth class in each scene-pair. We then executed a one-way ANoVA, using R version 3.5.1, to examine the difference in shrub change between growth classes as well as between climate classes within a specific growth class. If we found significant results ($\alpha = 0.05$), we executed Tukey multiple comparison of means to determine differences between classifications.

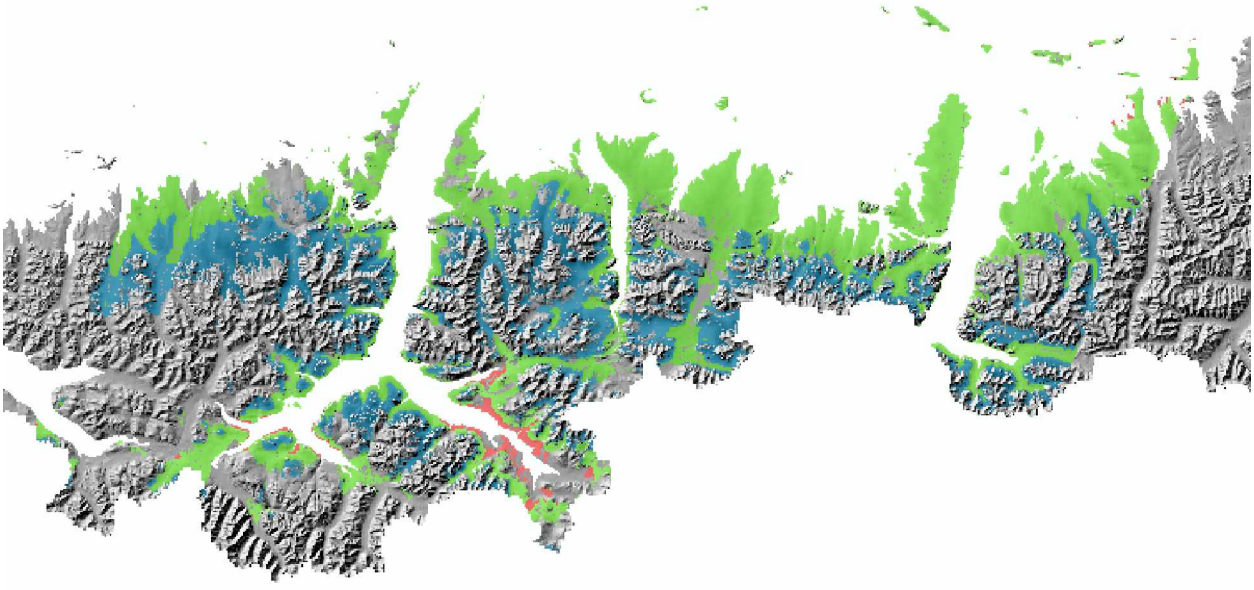

*Figure 2-10: Map of the cold Arctic pixels for path 75 row 12 that show the spatial distribution of growth classes based on shrub temperature limits. These classes include below growth limits (<10.5 C°, blue), at growth limits (between 10.5 C° and 12 C°, green), and above growth limits (>12.5 C°, red). Means of shrub change were extracted to pixel groups within each temperature class and tested to determine if differences between shrub change existed between classes.*

To explore temperature's effect, we examined the linear relationship between temperature intervals (value = 0.1 C°) and shrub change. To limit error, we excluded temperature intervals that contained less than 50 pixels within scene-pair. We then plotted the linear relationship of change in shrub dominance as a product of temperature above 12 C° for each scene-pair in the above limits growth class. We also looked at the linear relationship between shrub change and temperature within the at limits growth class for the cold Arctic climate in order to explore differences in growth rates between climate classes.

# 3 Results

## 3.1 Overview

Most of the analyzable pixels for the cold Arctic and Arctic climate classes occurred in the central Brooks Range (north and south slopes), though a small pocket of pixels on the eastern boundary of the southern Brooks was also analyzable. Most pixels contained between 20 and 50% shrub dominance. The Arctic climate class had even coverage of percent shrub dominance at the lower classes (10, 20, 30, & 40%), before decreasing at 50 or 60% depending on scene-pair. The most common percent dominance class in the cold Arctic climate was 50%. Values above and below tapered off evenly.

The analyzable pixels for the interior climate class occurred explicitly in the Tanana Uplands in eastern interior Alaska. The interior climate class had more variability in distribution of its percent shrub dominance. The most common percentage class was 50% but a steep drop-off occurs at values above. Additionally, there is more coverage of 20% shrub dominance than 30%. The interior climate class had the highest number of pixels reflecting negative shrub change (i.e. shrub loss). While all climate classes experienced shrub loss, the interior experienced it more dramatically with most common rates of loss occurring between 10 and 20%.

Analyzable pixels for high precipitation climate class occurred in the northeastern Kenai mountains and southwestern Chugach mountains. However, the high elevation threshold for the Chugach mountains (n = 1153.4 m) eliminated most analyzable pixels from consideration. Percent shrub dominance was consistently high across percent classes of all climate classes, with high numbers of pixels representing higher percent shrub classes, including 100%.

The lowest mean shrub dominance for the modern era was in path 68 row 11 of the Arctic climate class (n = 29.6%), though high percent shrub dominance was evident in the Arctic in path 73 row 13 (n =

45.8%) in the central Brooks Range. The highest mean shrub dominance (n = 48.9% occurred in path 67 row 18 of the high precipitation climate class.

Across all climate classes, shrub loss was limited in comparison with shrub expansion. The cold Arctic and Arctic climate classes experienced the least amount of loss, followed by the high precipitation climate class, and the interior climate class, which had the highest amount of shrub loss.

*Table 3-1: Summary statistics of percent shrub dominance for the historic and modern eras and the change between them for all scene-pairs. All scene-pairs and climate classes show overall net increases in shrub dominance. Increases appear relatively consistent across all scene pairs and climate classes though the ranges differ substantially.*

| Zone | Path | Row | Historic | | | | Modern | | | | Change | | |
|---|---|---|---|---|---|---|---|---|---|---|---|---|---|
| | | | Acquisition Date | Mean (%) | Std. Dev. (%) | Range (%) | Acquisition Date | Mean (%) | Std. Dev. (%) | Range (%) | Mean (%) | Std. Dev. (%) | Range (%) |
| **Cold Arctic** | 75 | 12 | 1986-July-4 | 34.3 | 12.5 | 0.8 - 99.3 | 2016-July-22 | 41.1 | 14.1 | 0.8-99.9 | 6.8 | 7.8 | -74.4 – 78.9 |
| **Cold Arctic** | 75 | 13 | 1986-July-5 | 30.8 | 13 | 12.0-85.5 | 2015-July-4 | 38.8 | 17.2 | 12.0-99.2 | 8.1 | 7.0 | -47.5 - 45.7 |
| **Arctic** | 75 | 13 | 1986-July-5 | 39.3 | 20.1 | 12.0-100.0 | 2015-July-4 | 45.8 | 21.4 | 12.0 - 100.0 | 6.4 | 7.8 | -95.2 - 99.0 |
| **Arctic** | 68 | 11 | 1986-July-3 | 23.9 | 9.5 | 4.4-76.2 | 2013-July-13 | 29.6 | 13.3 | 6.0 - 96.8 | 5.8 | 5.7 | -38.6 - 67.5 |
| **Interior** | 65 | 16 | 1986-July-30 | 31.3 | 8.6 | 6.8-88.5 | 2018-July-22 | 37.4 | 12.3 | 7.5-88.3 | 6.1 | 12.9 | -54.1 - 55.6 |
| **High Precipitation** | 67 | 18 | 1986-July-28 | 42.7 | 22.4 | 3.2 - 99.8 | 2013-July-22 | 48.9 | 24.1 | 4.0 - 100.0 | 6.3 | 9.5 | -54.0 - 67.4 |

## 3.2 Percent Shrub Dominance and Change Over Time

### 3.2.1 Cold Arctic Climate Class

The Landsat scene-pair at path 75 row 12 contained 77.3% uncontaminated pixels for projecting percent shrub dominance across eras. Modern percent shrub dominance ranged from 0.4 to 100.0% slightly above the historic range of percent shrub dominance (n = 0.2 – 99.9%). Modern mean shrub dominance was 41.1%, up from the 34.3% average from 1986. Change in percent shrub dominance had a large range (n = -74.4% to 78.9%; Figure 3-1) relative to other scene-pairs. Most positive change (i.e. shrub expansion) appeared to occur at the northern latitudes of the Brooks Range where the northern foothills transition to the coastal plain. Most of the negative change (i.e. shrub loss) appeared to occur in rugged (higher elevation, higher slope) portions of the range. Average change for the entire set of pixels was 6.8%. Modern percent shrub dominance mirrored the spatial distributions of shrub change with highest percent dominance in the coastal plain and lower percent shrub dominance in the southern mountainous regions (Figure 3-2).

Shrub change occurred most commonly between 0 and 10%, followed by 10 and 20% (Figure 3-3). Values either below or above this range were rare. Values of shrub dominance were most common between 40 and 50%, followed by 30 and 40% and 50 and 60%. Pixels with value between 0 and 30% showed increasing volume the larger the value. Pixels with a value above 60% were relatively rare, and very rare above 70%.

The Landsat scene-pair at path 75 row 13 contained 70.2% uncontaminated cold Arctic pixels (271.1 $km^2$) for projecting percent shrub dominance across eras. Modern percent shrub dominance ranged from 12.2 to 99.2% above the historic range of percent shrub dominance of 12.0 to 85.5%. 2015 mean shrub dominance was 38.8% up from 30.8% in 1986. Change in percent shrub dominance had a moderate range (n = - 47.5 to 45.7%; Figure. 3-4) relative other scene pairs, however, it had the highest

average change at 8.1%. Most of the positive change (i.e. shrub expansion) appeared to occur at the lower elevations near the continental divide of the Brooks Range. Most of the negative change (i.e. shrub loss) appeared to occur in patches. Modern percent shrub dominance appeared highest in the areas furthest from the continental divide and in areas of lower elevation (Figure 3-5)

Shrub change most commonly occurred between 0 and 10%, followed by 10 and 20% (Figure 3-6). Values either below or above this range were rare. Shrub dominance values were most common between 0 and 60%. Values above 60% were relatively rare, showing a precipitous drop in volume at this threshold.

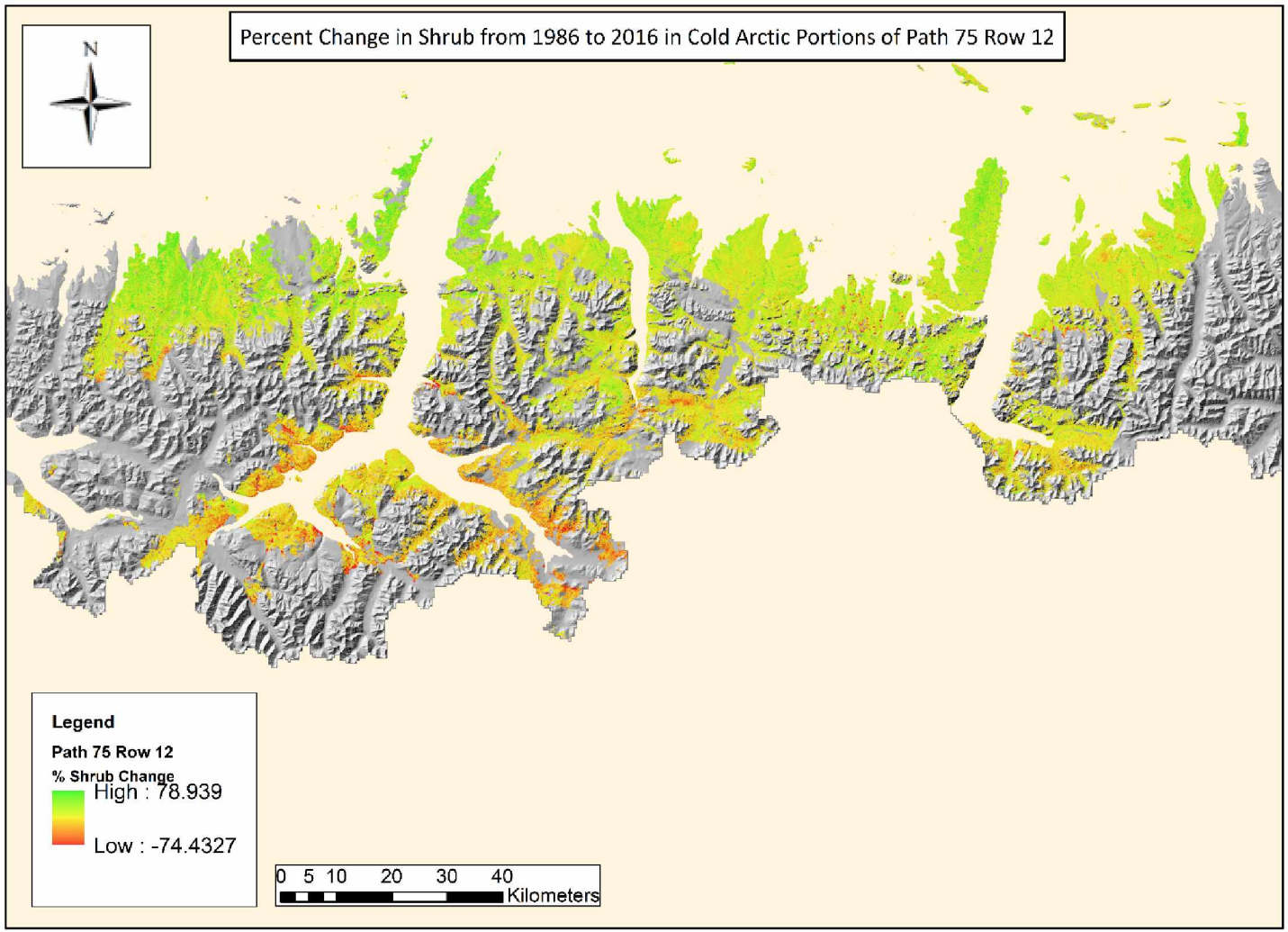


*Figure 3-1: Map of the change in shrub percent dominance based on the logarithmic relationship between NDVI and percent shrub dominance derived from a Landsat-8 scene acquired July 22nd, 2016 and a Landsat 5 scene acquired July 4th, 1986 for Path 75 row 12. Darker green areas show high increases percent shrub dominance compared to red pixels showing large decreases.*

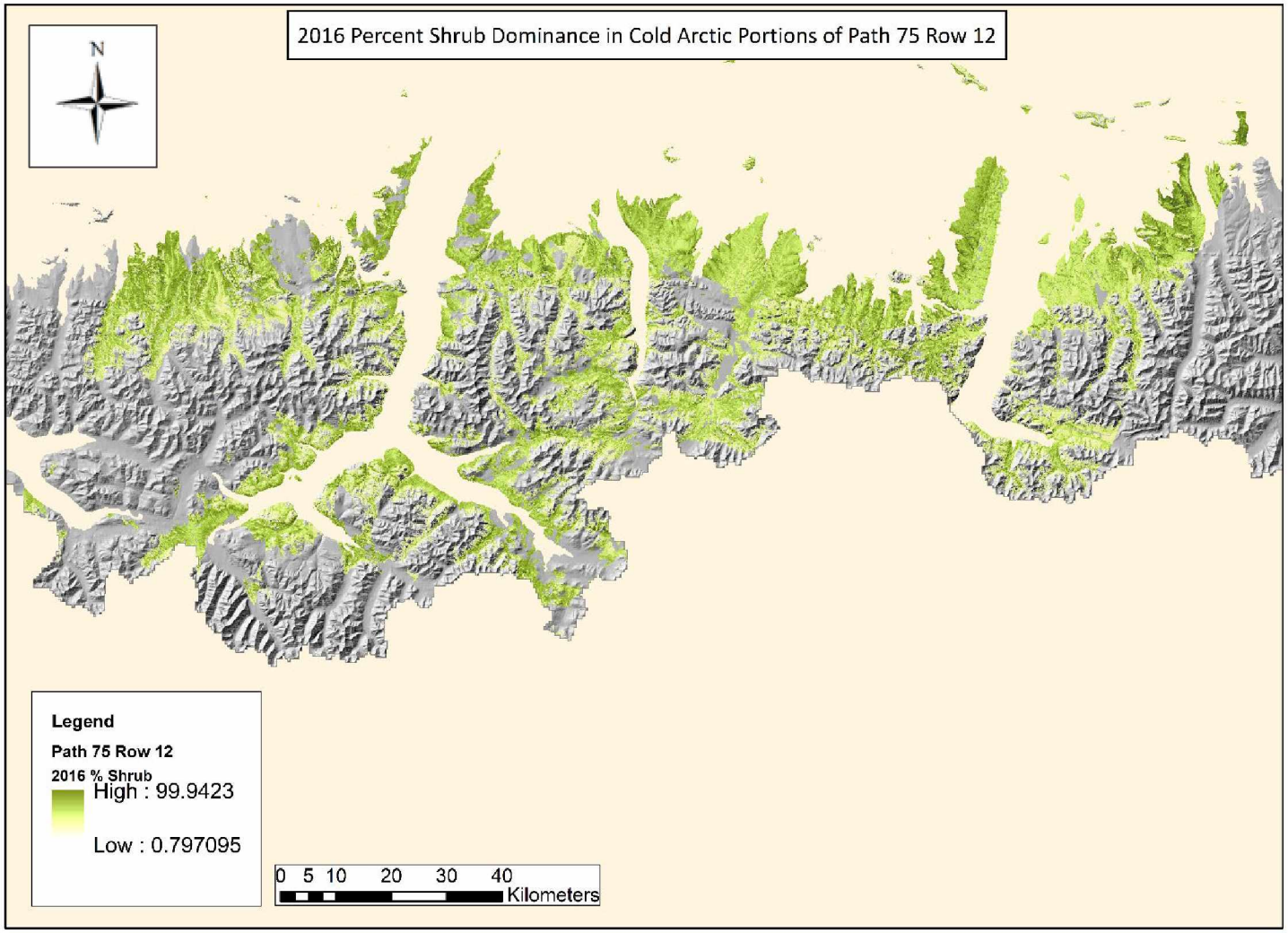


*Figure 3-2: Map of modern shrub percent dominance based on the logarithmic relationship between NDVI and percent shrub dominance derived from a Landsat-8 scene acquired July 22nd, 2016 for path 75 row 12. Darker green areas show high percent shrub dominance compared to light green and yellow.*

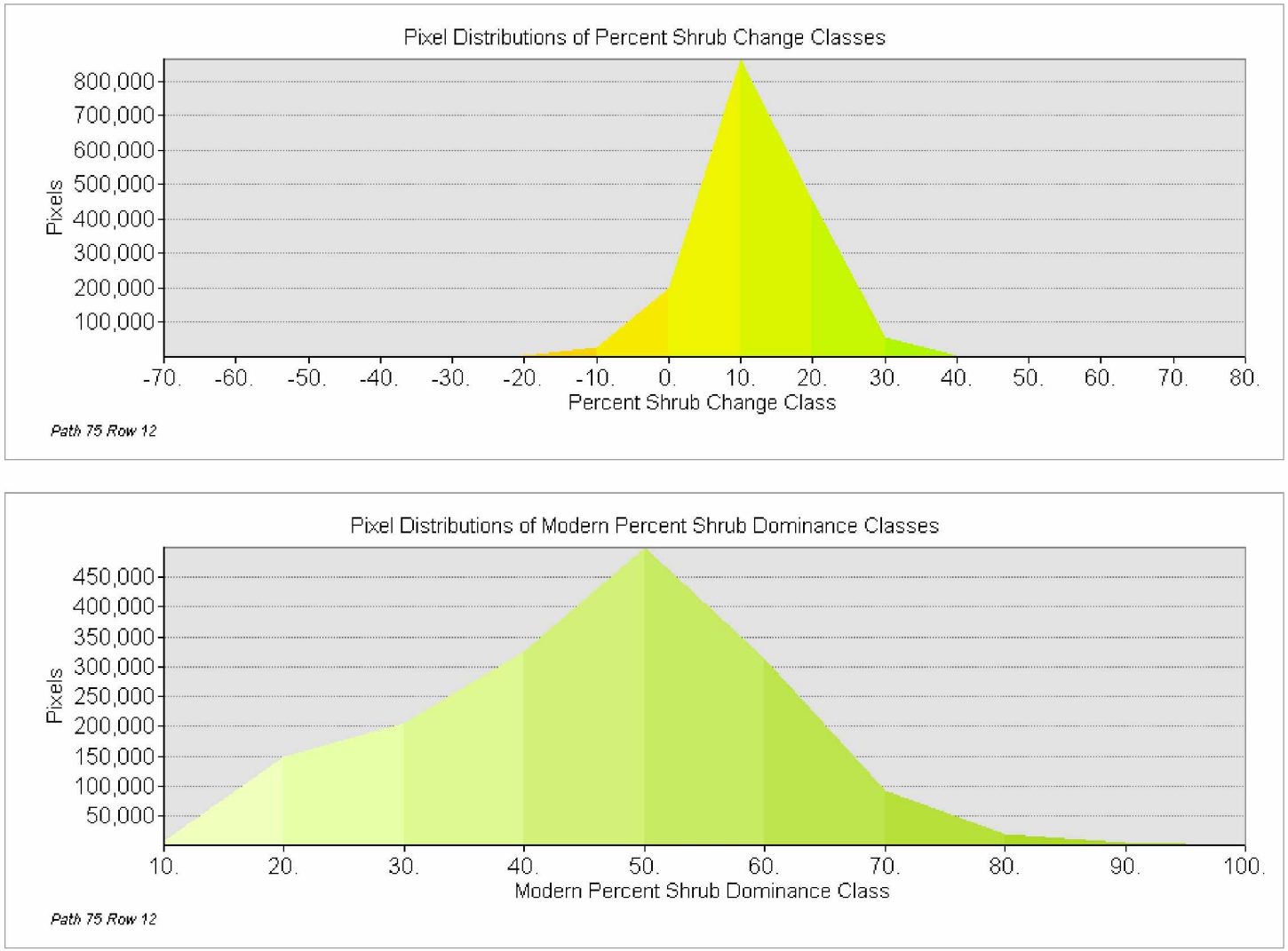


*Figure 3-3: Area plots of percent shrub change classes (bottom) and percent shrub dominance (top) for path 75 row 12 of the cold Arctic climate class. Pixel distribution of percent shrub dominance shows percent dominance between 30 and 60% are the most common cover classes. Pixel distribution for percent shrub change classes show most increases occurred between 0 and 10%.*

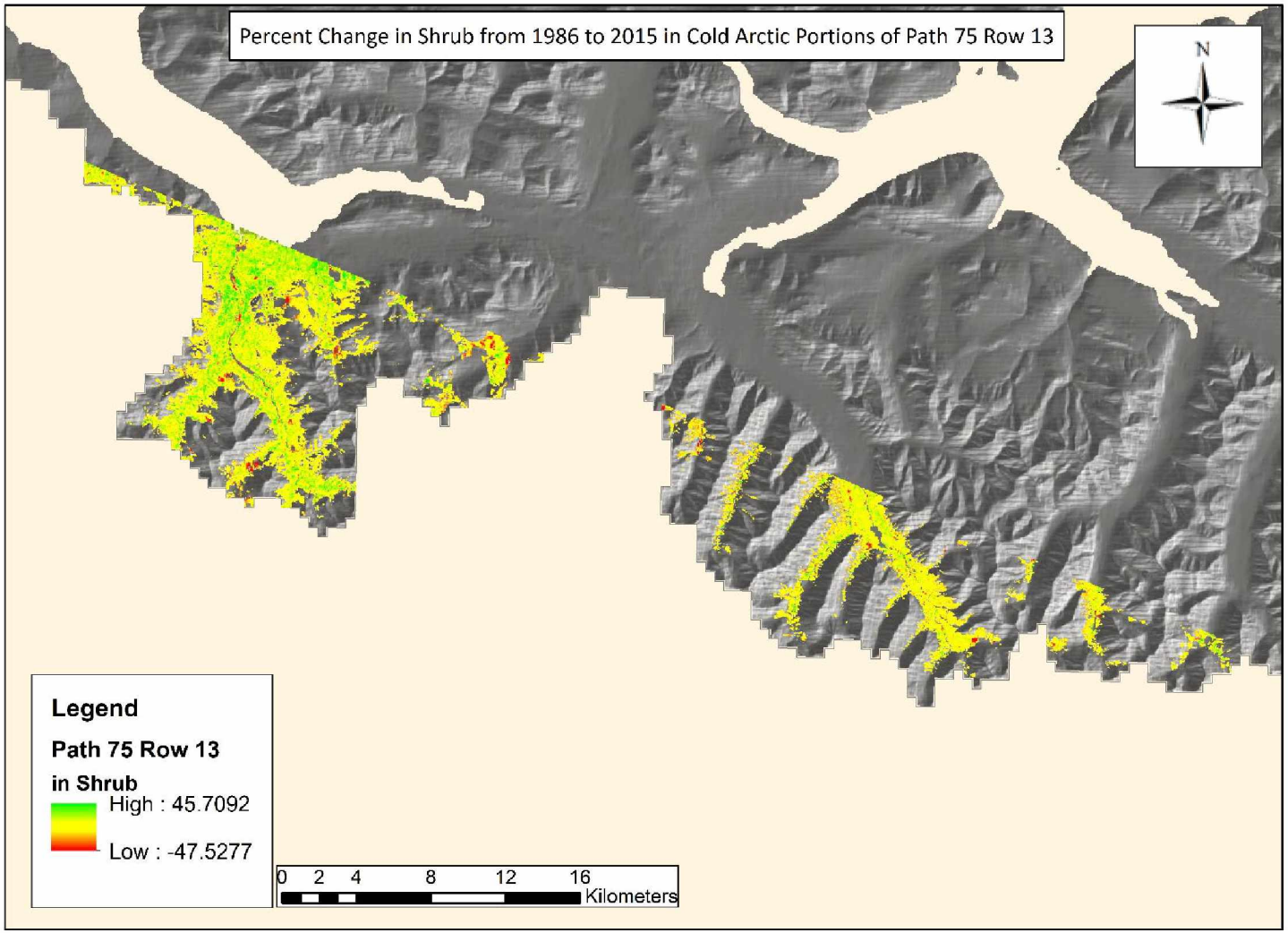


*Figure 3-4: Map of the change in shrub percent dominance based on the logarithmic relationship between NDVI and percent shrub dominance derived from a Landsat-8 scene acquired July 4th, 2015 and a Landsat 5 scene acquired July 4th, 1986 for path 75 row 13. Darker green areas show high increases percent shrub dominance compared to red pixels showing large decreases.*

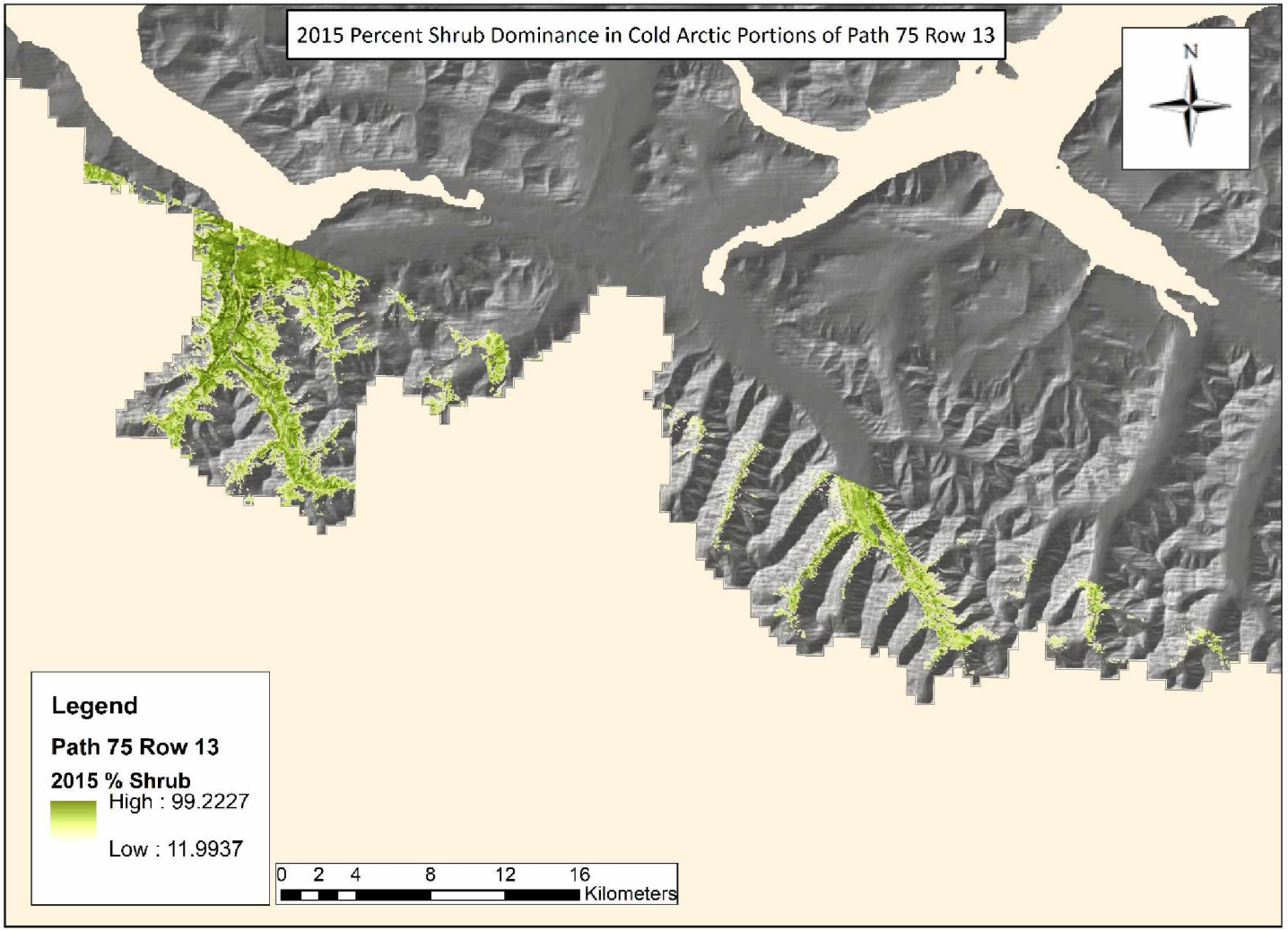


*Figure 3-5: Map of modern shrub percent dominance based on the logarithmic relationship between NDVI and percent shrub dominance derived from a Landsat-8 scene acquired July 4th, 2015 for path 75 row 13. Darker green areas show high percent shrub dominance compared to light green and yellow.*

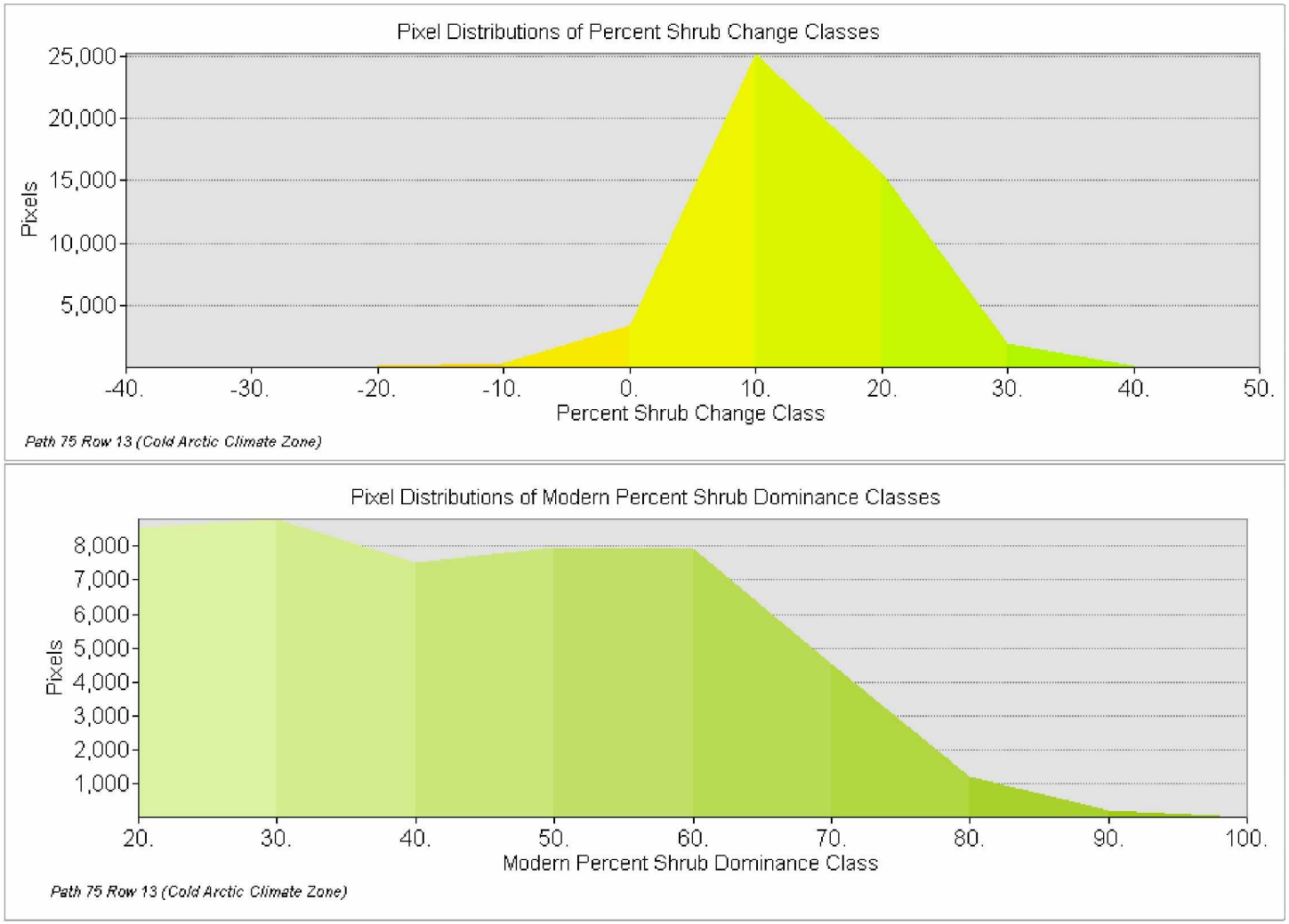


*Figure 3-6: Area plots of percent shrub change classes (top) percent shrub dominance (bottom) for path 75 row 13 of the cold Arctic climate class. Pixel distribution of percent shrub dominance shows percent dominance classes most common between 20 and 60%. Pixel distribution for percent shrub change classes show most increases occurred between 0 and 10%.*

### 3.2.2 Arctic Climate Class

The Landsat scene-pair at path 75 row 13 contained 83.2% uncontaminated Arctic pixels (11,111.3 $km^2$) for projecting percent shrub dominance across eras. Modern percent shrub dominance ranged from 12.0 to 100.0% the same as the historic range of percent shrub dominance of 12.0 to 100.0%. Despite containing the same ranges, their averages (n = 45.8% and 39.3%, respectively) differed. Change in percent shrub dominance had a large range (n = - 95.2 to 99.0%; Figure 3-7), though its average (n = 6.4%) was consistent with other scene-pairs. Most of the positive change (i.e. shrub expansion) appeared to occur at the lower elevations near the surrounding southern foothills of the Brooks Range. Most of the negative change (i.e. shrub loss) appeared to occur in the northeast portions near the continental divide. Modern percent shrub dominance appeared highest in both the southern foothills and the lower elevation portions of the higher latitude mountains near broad corridors (Figure 3-8).

Shrub change most commonly occurred between 0 and 10% (Figure 3-9). Values either below or above this range were rare, with the ranges 10 to 20% and 0 to -10% showing the next highest volumes. Shrub dominance values were most common between 0 and 60%. Values above 60% showed a continuous and stable decline to in volume as value approached 100%.

Path 68 row 11 contained 93.0% uncontaminated Arctic pixels (188.7 $km^2$) for projecting percent shrub dominance across eras. Change in percent shrub dominance had a moderate and mostly positive range (n = -38.6 to 67.5%; Figure 3-10). Despite the mostly positive range of change in percent shrub dominance, shrub loss was widely distributed throughout the lower elevation portions of this area. The average change (n = 5.8%) was the lowest among all scene-pairs and contained widespread areas of shrub loss. Positive change appeared to occur in pockets with no discernible terrain-based influences, excluding lower elevation. Modern percent shrub dominance ranged from 7.5 to 88.3% (Figure 3-11)

and averaged 29.6% (Table 3-1), up from the historic range of percent shrub dominance of 4.4% to 76.2% and average of 23.9%. Modern percent shrub dominance had a relatively even distribution of moderate values of percent shrub dominance with the maximums and minimums of the range appearing to occur in small pockets or thin corridors.

Shrub change most commonly occurred between 0 and 10% (Figure 3-12). Values either below or above this range were rare, with the ranges 10 to 20% and 0 to -10% had the next highest volumes. Shrub dominance values were most common between 10 and 50%. Values above 50% showed a precipitous decline in volume.

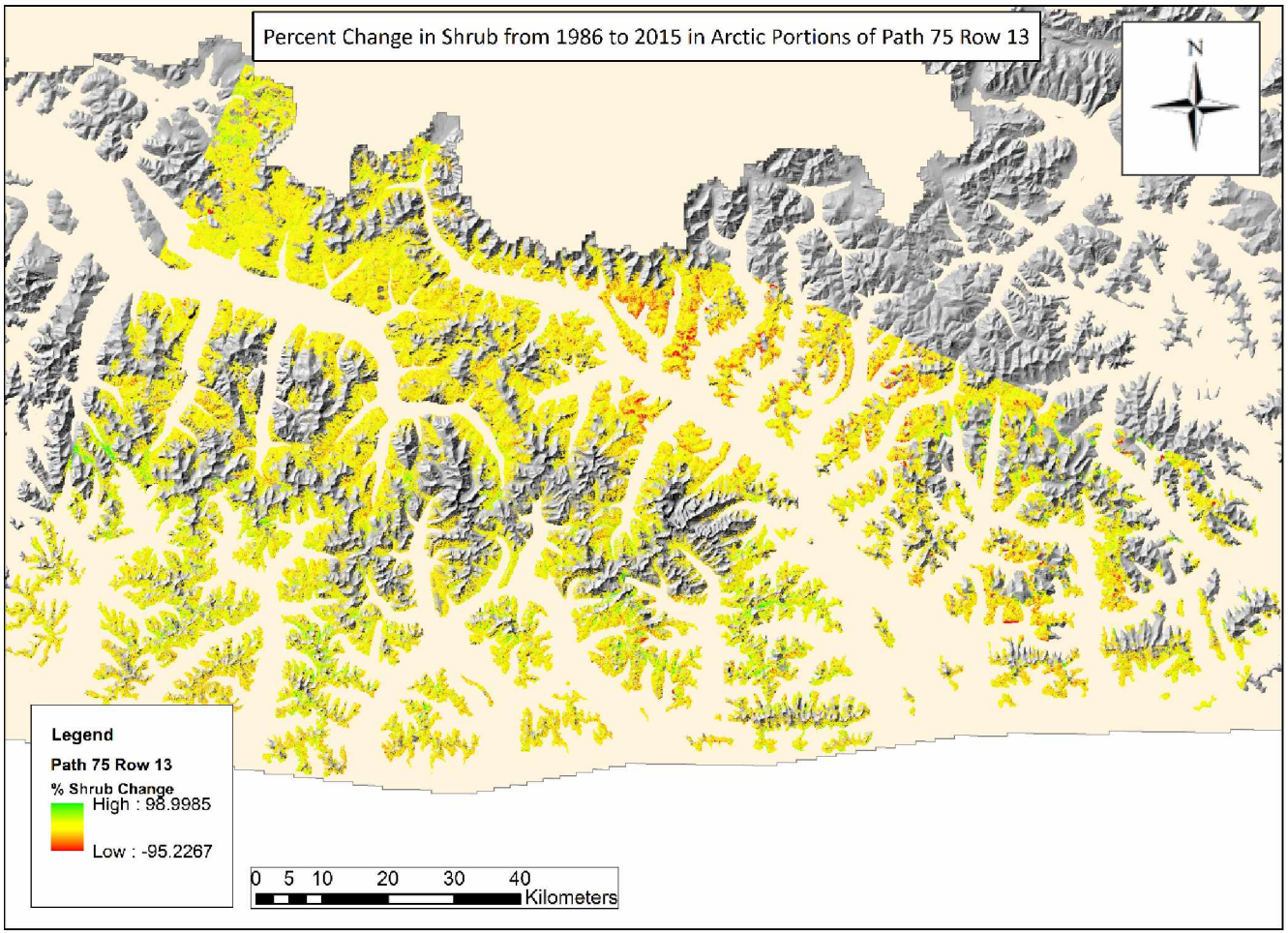


*Figure 3-7: Map of the change in shrub percent dominance based on the logarithmic relationship between NDVI and percent shrub dominance derived from a Landsat-8 scene acquired July 4th, 2015 and a Landsat 5 scene acquired July 4th, 1986 for Arctic pixels in path 75 row 13. Darker green areas show high increases percent shrub dominance compared to red pixels showing large decreases.*

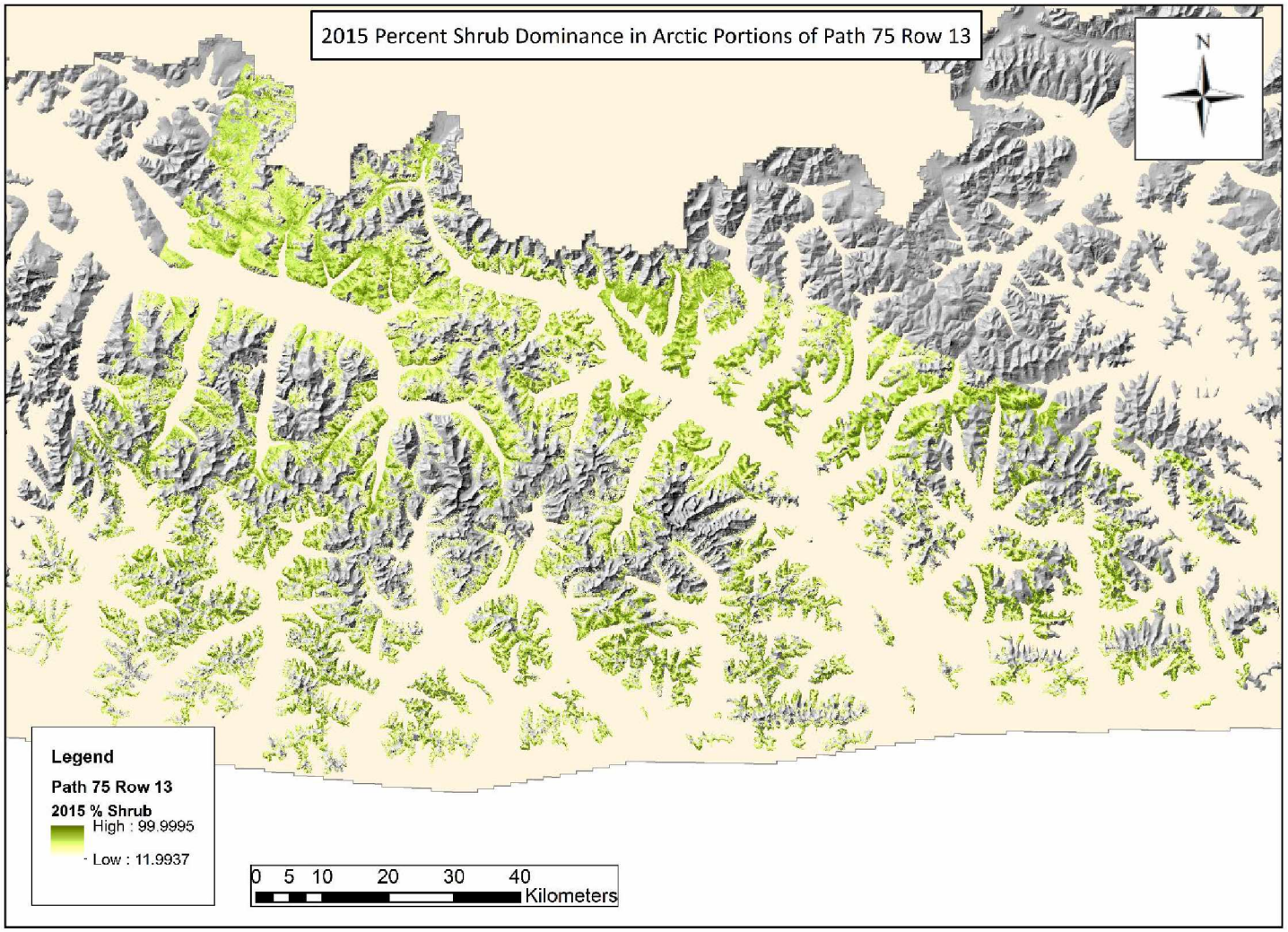


*Figure 3-8: Map of modern shrub percent dominance based on the logarithmic relationship between NDVI and percent shrub dominance derived from a Landsat-8 scene acquired July 4th, 2015 for path 75 row 13 of the Arctic climate class. Darker green areas show high percent shrub dominance compared to light green and yellow.*

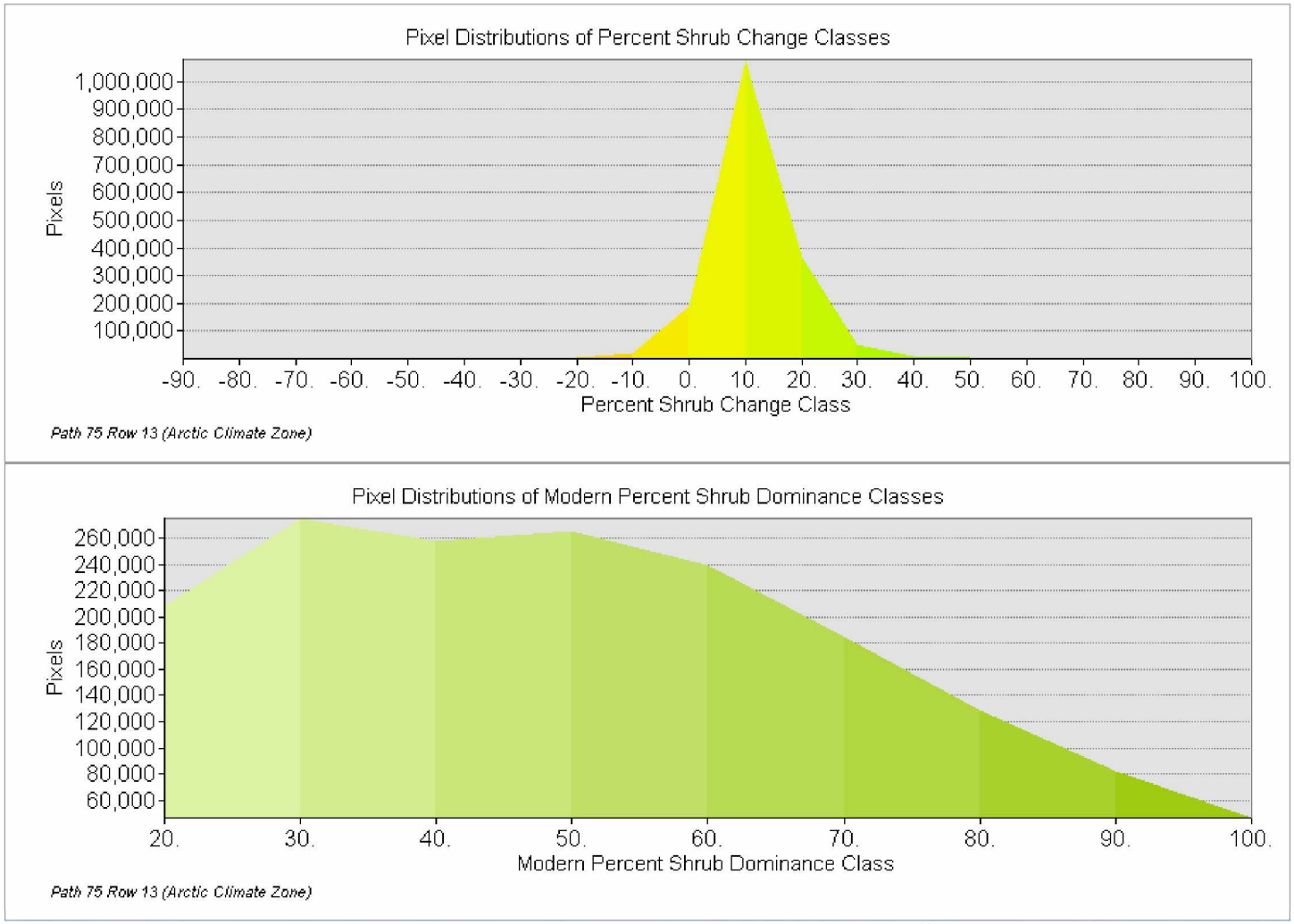


*Figure 3-9: Area plots of percent shrub change classes (top) and percent shrub dominance (bottom) for path 75 row 13 of the Arctic climate class. Pixel distribution of percent shrub dominance shows percent dominance classes most common between 20 and 70%. Pixel distribution for percent shrub change classes show most increases occurred between 0 and 10%.*

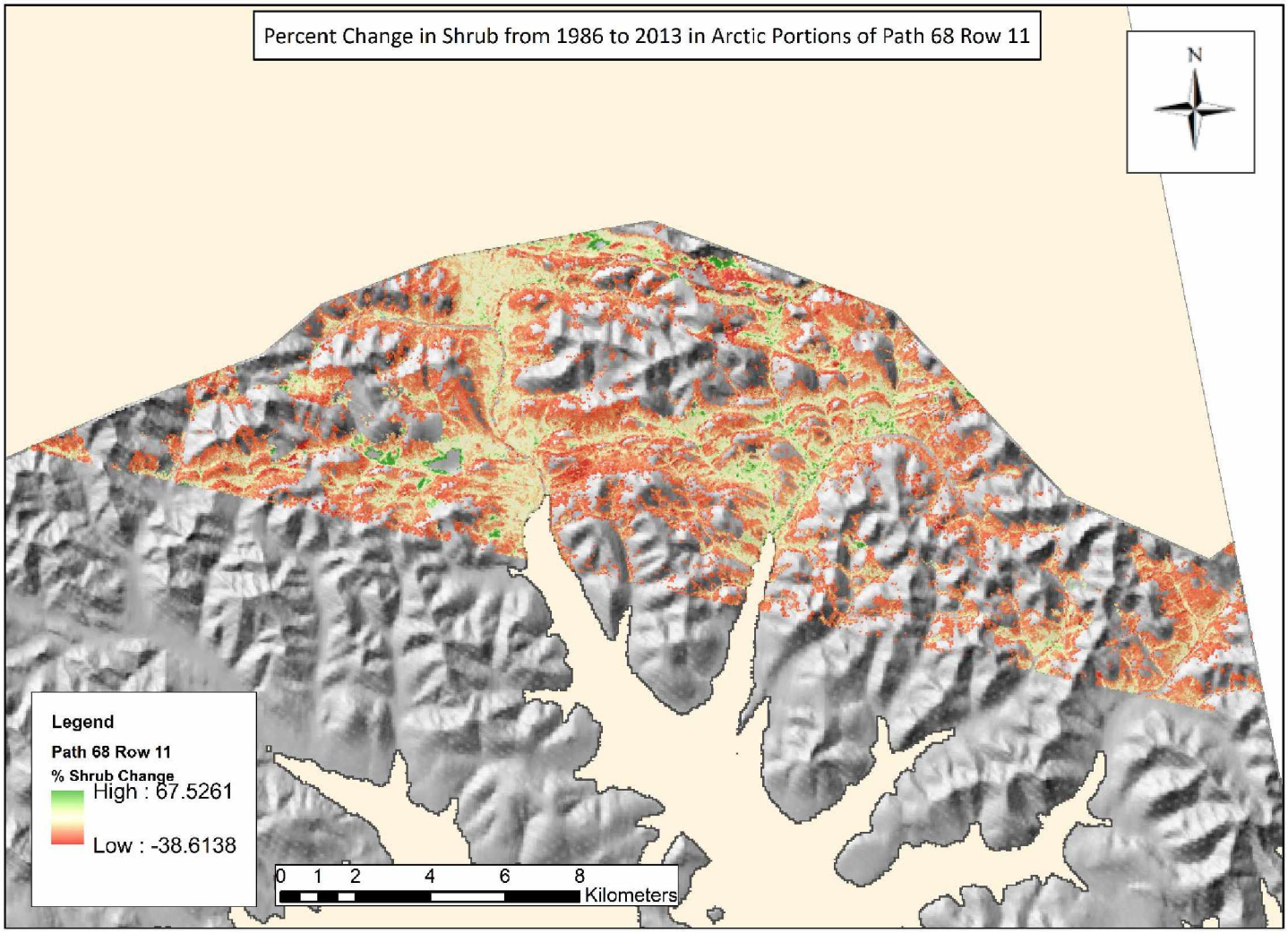


*Figure 3-10: Map of the change in shrub percent dominance based on the logarithmic relationship between NDVI and percent shrub dominance derived from a Landsat-8 scene acquired July 13th, 2013 and a Landsat 5 scene acquired July 3rd, 1986 for Arctic pixels in path 68 row 11. Darker green areas show high increases percent shrub dominance compared to red pixels showing large decreases*

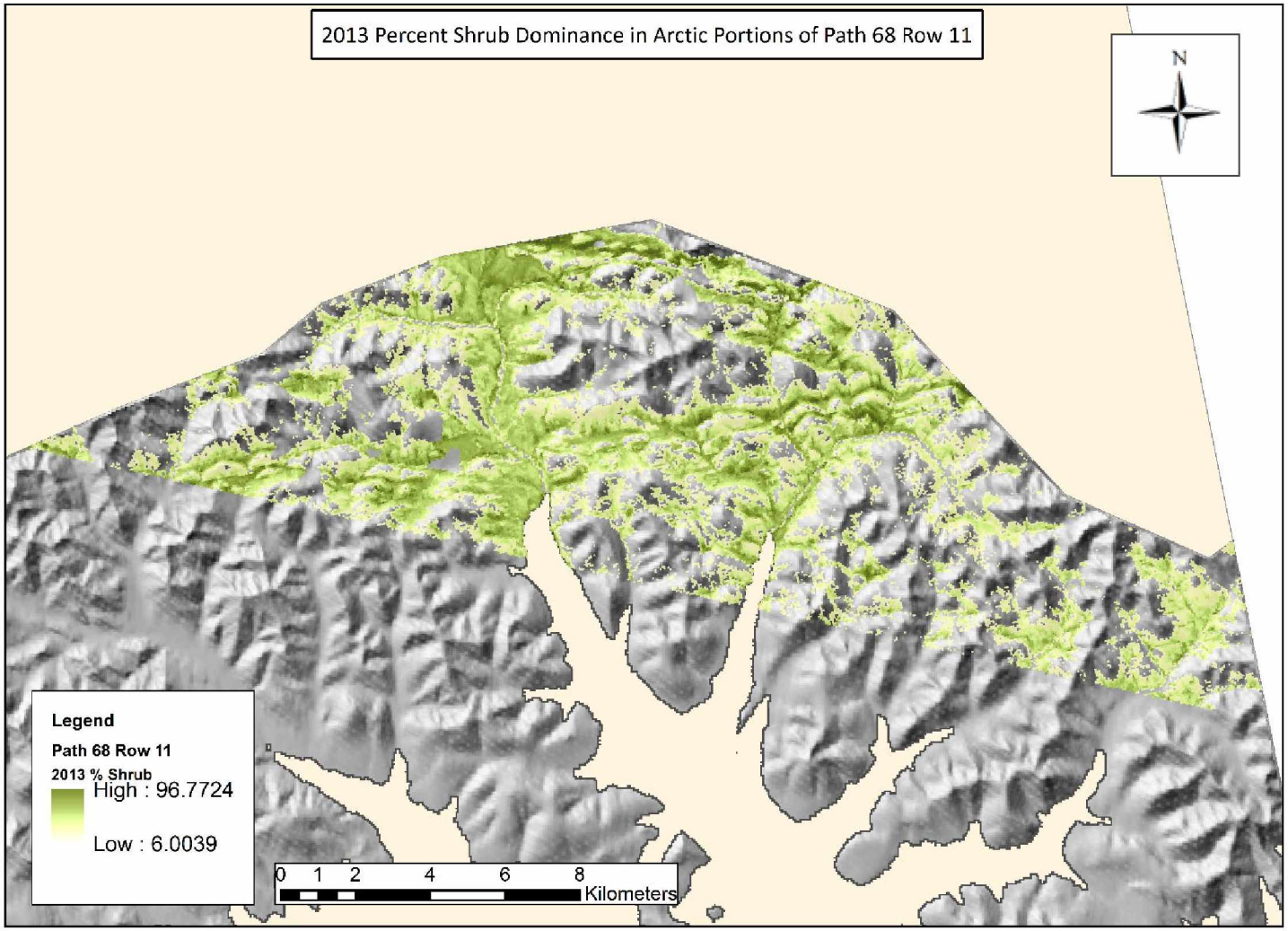


*Figure 3-11: Map of modern shrub percent dominance based on the logarithmic relationship between NDVI and percent shrub dominance derived from a Landsat-8 scene acquired July 13th, 2013 for path 68 row 11. Darker green areas show high percent shrub dominance compared to light green and yellow.*

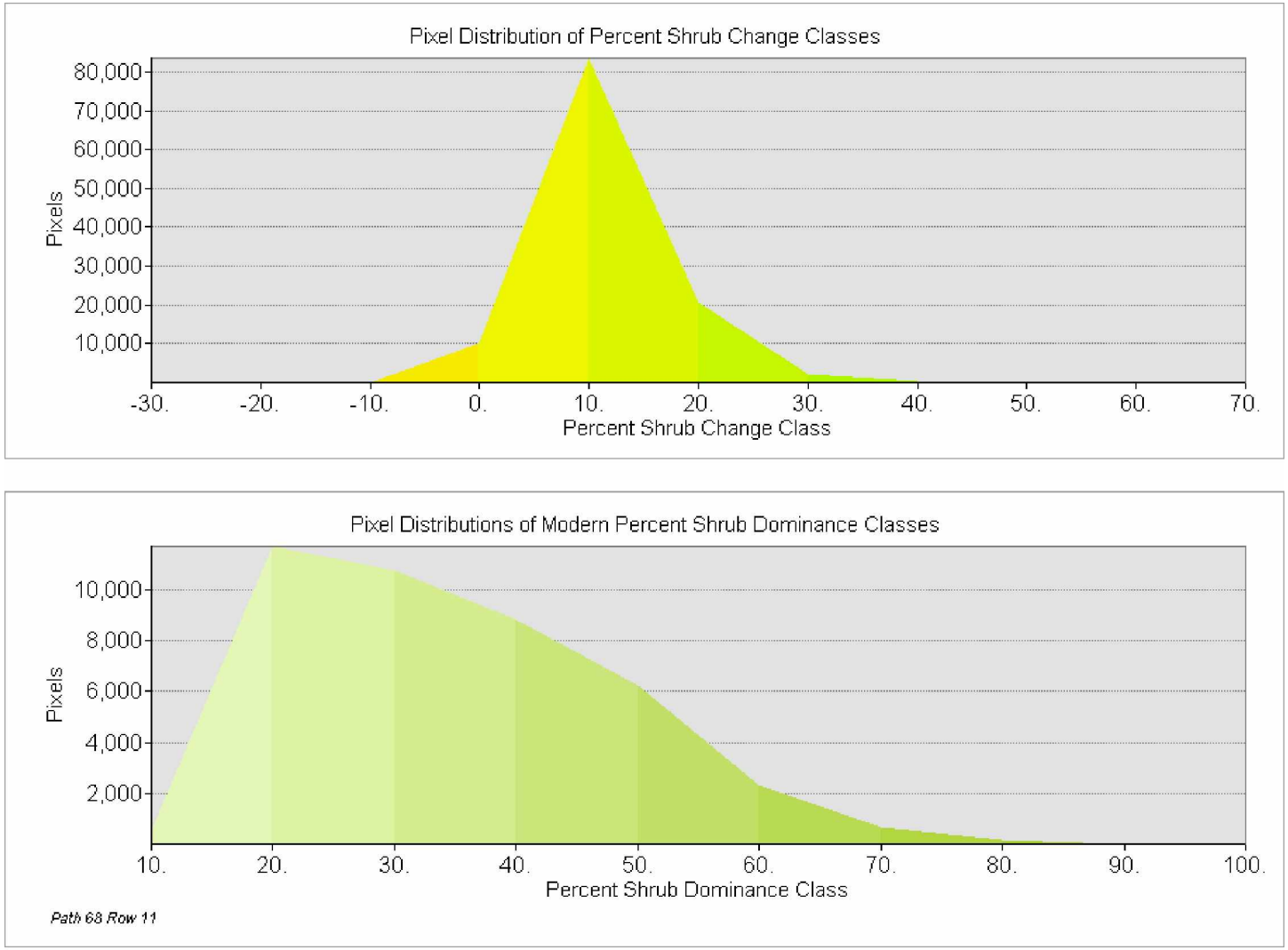


*Figure 3-12: Area plots of percent shrub change classes (top) and percent shrub dominance (bottom) for path 68 row 11 of the Arctic climate class. Pixel distribution of percent shrub dominance shows percent dominance classes most common between 20 and 50%. Pixel distribution for percent shrub change classes show most increases occurred between 0 and 10%.*

### 3.2.3 Interior Climate Class

The Landsat scene-pair at path 65 row 16 contained 80.0% uncontaminated interior pixels (4949.0 $km^2$) for projecting percent shrub dominance across eras in the Tanana Uplands alpine zone. It is the only section of the scene-pair that met the 70% threshold to be included in the analysis (other overlapping alpine zones were too contaminated for analysis). Change in percent shrub dominance had a moderate range (n = -54.1 to 55.6%; Figure 3-13) and averaged 6.1%, the second lowest among all scene-pairs. Change in percent shrub dominance appeared to occur in large patches and on a less graduated scale when compared to the other climate classes. The negative change appeared highest in the northern pockets, though some southerly portions experienced it as well. Modern percent shrub dominance ranged from 6.8 to 88.5% (Figure 3-14) and averaged 37.4% (Table 3-1). Historic percent shrub dominance ranged from 7.5 to 88.3% and averaged 31.3%. Modern percent shrub dominance mirrored the distribution of change in percent shrub dominance. Areas of shrub loss had lower shrub dominance; areas of shrub growth had higher percent shrub dominance.

Shrub change occurred most commonly between 10 and 20%, with a precipitous drop in values above (Figure 3-15). The interior climate class had the broadest distribution of shrub loss pixel values and highest relative volume of shrub loss to shrub gain, though gain was still overwhelmingly higher. Shrub dominance values were variable. Values between 30 and 60% were the most common, though values between 0 and 10% were also common.

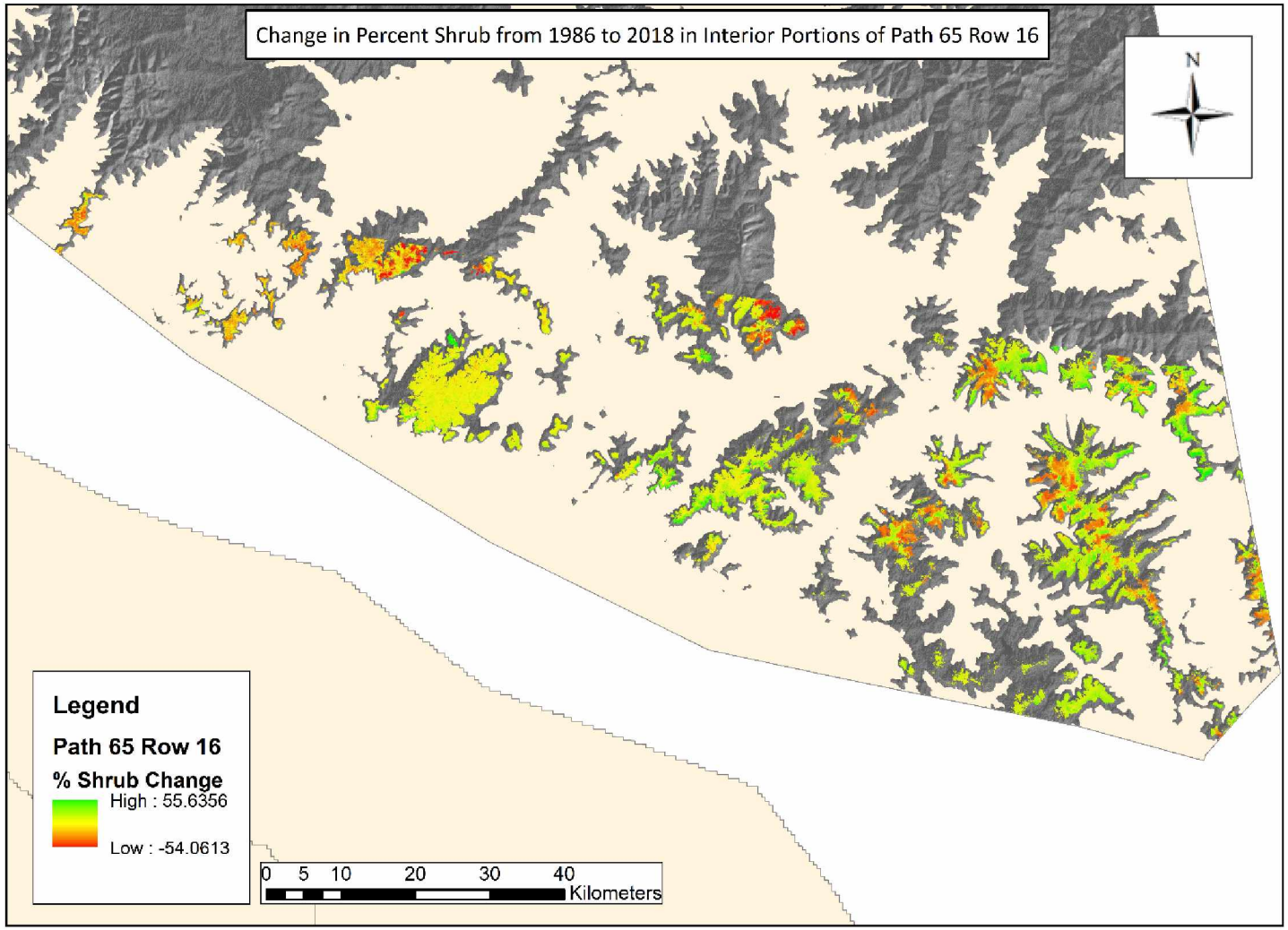


*Figure 3-13: Map of the change in shrub percent dominance based on the logarithmic relationship between NDVI and percent shrub dominance derived from a Landsat-8 scene acquired July 22nd, 2018 and a Landsat 5 scene acquired July 30th, 1986 for Arctic pixels in path 68 row 11. Darker green areas show high increases percent shrub dominance compared to red pixels showing large decreases*

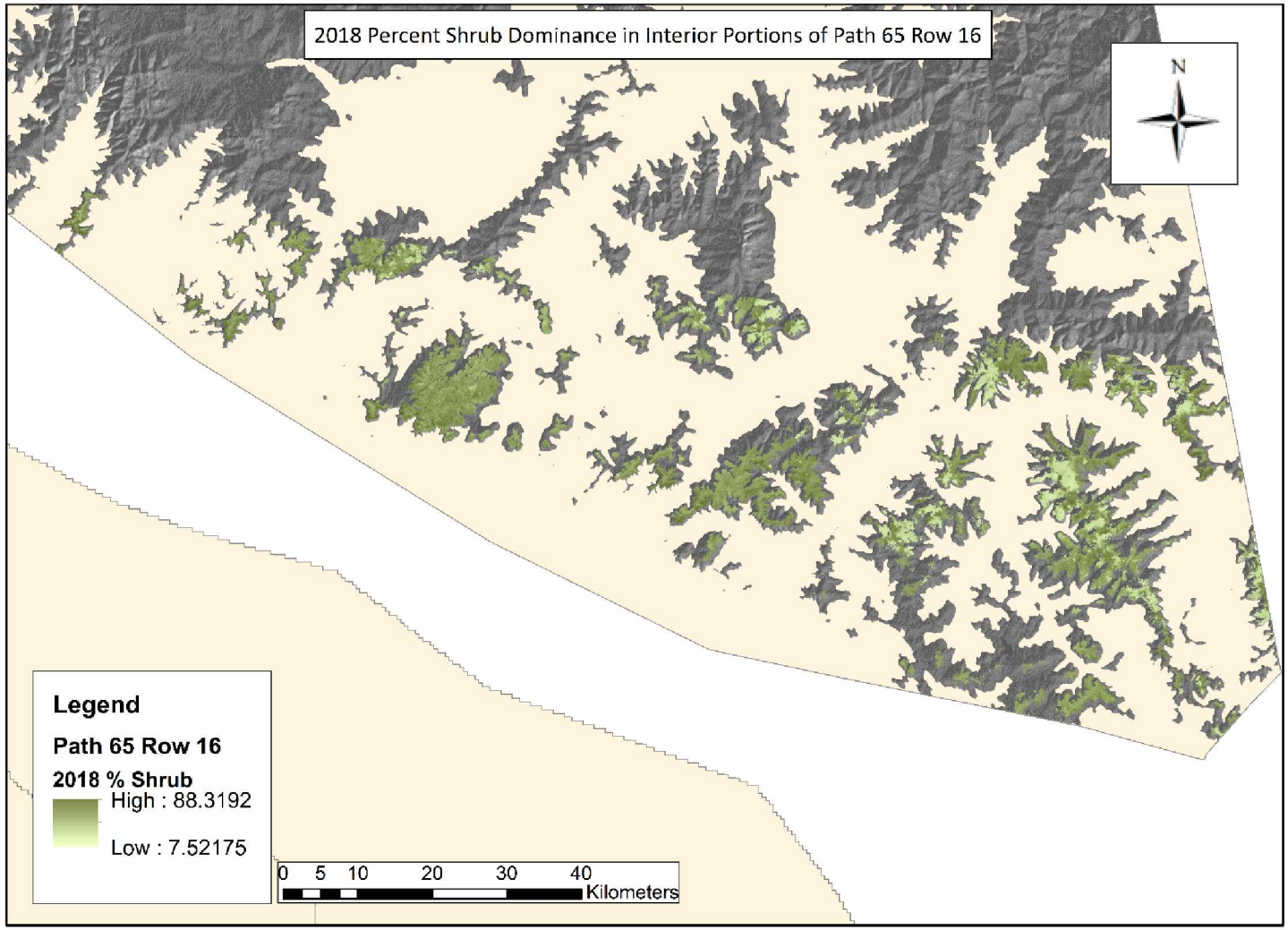


*Figure 3-14: Map of modern shrub percent dominance based on the logarithmic relationship between NDVI and percent shrub dominance derived from a Landsat-8 scene acquired July 22nd, 2018 for path 66 row 16. Darker green areas show high percent shrub dominance compared to light green.*

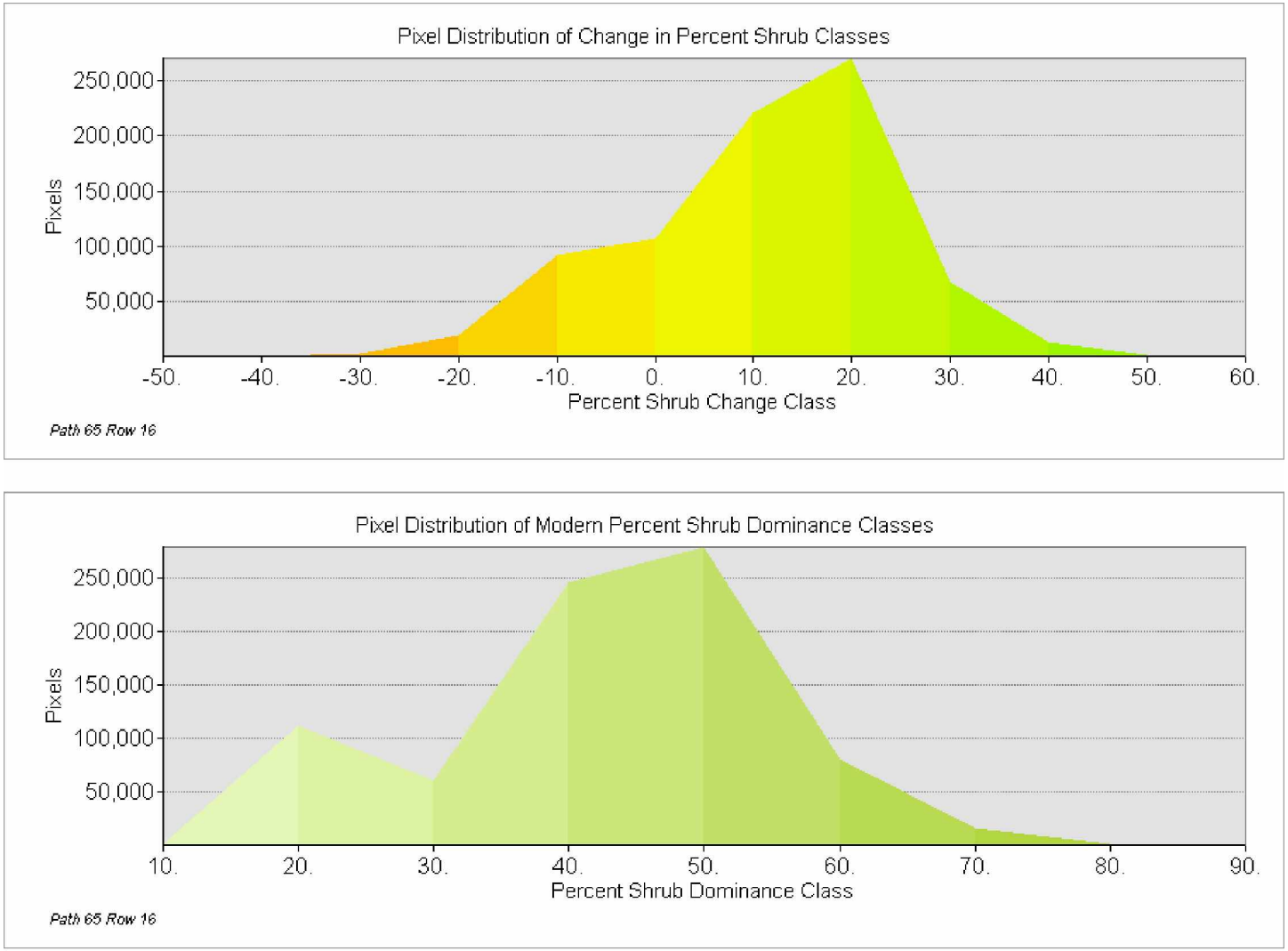


*Figure 3-15: Area plots of percent shrub change classes (top) and percent shrub dominance (bottom) for path 65 row 16 of the interior climate class. Pixel distribution of percent shrub dominance shows percent dominance classes most common between 20 and 50%. Pixel distribution for percent shrub change classes show most increases occurred between 0 and 10%*

### 3.2.4 High Precipitation Climate Class

The Landsat scene-pair at path 67 row 18 contained 71.6% (1389.2 $km^2$) and 72.9% (554.7 $km^2$) uncontaminated pixels in the Kenai and Chugach mountains, respectively, for projecting percent shrub dominance across eras. Change in percent shrub dominance had a moderate to large range (n = -54.0% to 67.4%; Figure 3-16). Most of the positive change (i.e. shrub expansion) appeared to occur in the eastern portions of the peninsula, closer to the ocean. Most of the negative change (i.e. shrub loss) appeared to occur in the western and more insulated portions of the peninsula. Modern percent shrub dominance ranged from 4.0 to 99.9% (Figure 3-17) slightly above the historic range of percent shrub dominance of 3.2 – 99.8%. Unlike in other climate classes, modern percent shrub dominance did not reflect the distributions of shrub change. Instead highest percent shrub dominance was evident consistently at lower elevations and lower at high elevations regardless of insulation or ocean proximity (Figure 3-17).

Shrub change occurred most commonly between 0 and 10% (Figure 3-18). Values either below or above this range were rare, with the ranges 10 and 20% and -10 and 0% showing the highest volumes. Shrub dominance values were relatively even across the range: between 10 and 100%, though the highest volume between 30 and 40%.

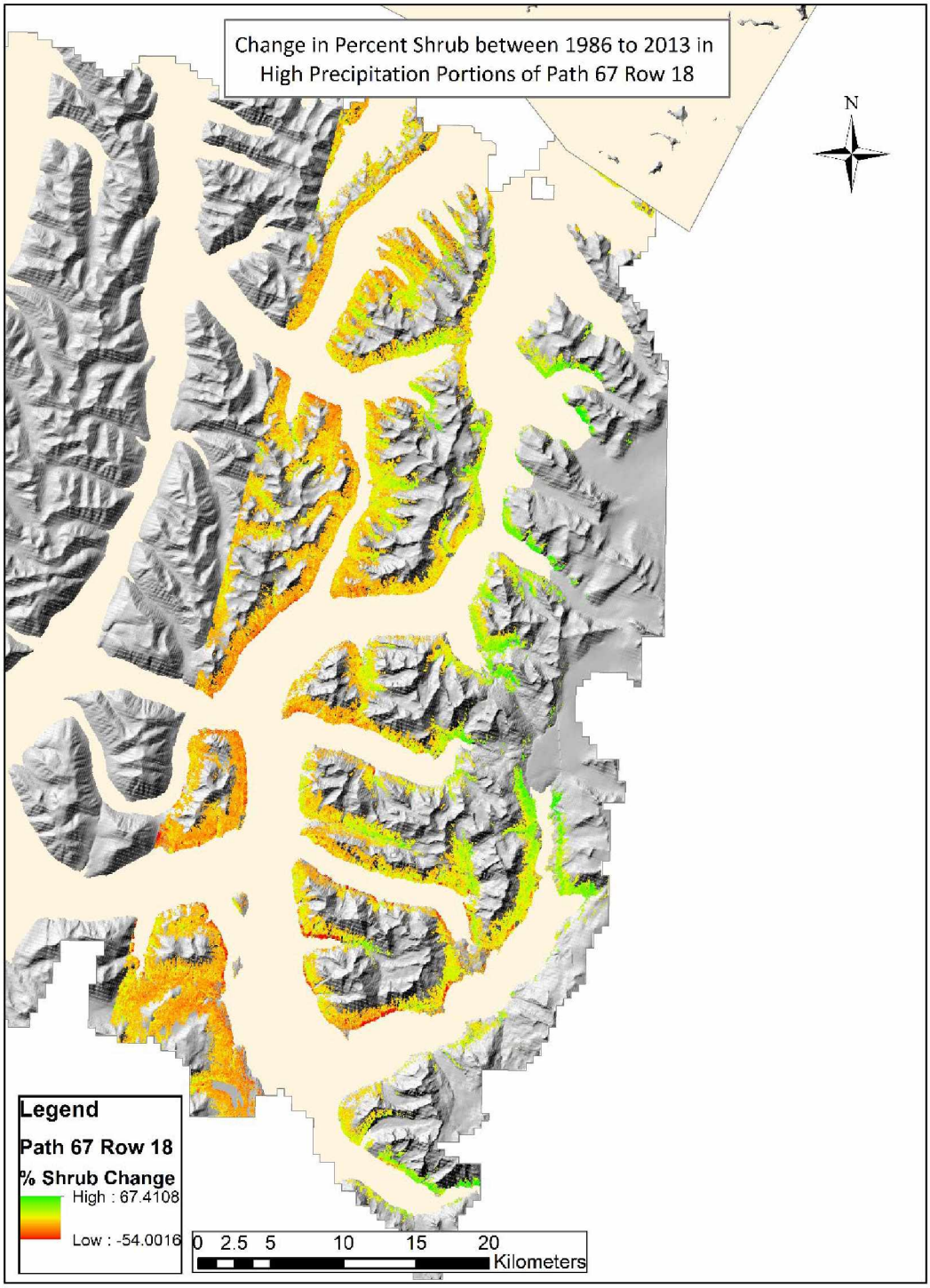


*Figure 3-16: Map of the change in shrub percent dominance based on the logarithmic relationship between NDVI and percent shrub dominance derived from a Landsat-8 scene acquired July 22nd, 2013 and a Landsat 5 scene acquired July 28th, 1986 for high precipitation pixels in path 67 row 18. Darker green areas show high increases percent shrub dominance compared to red pixels showing large decreases*

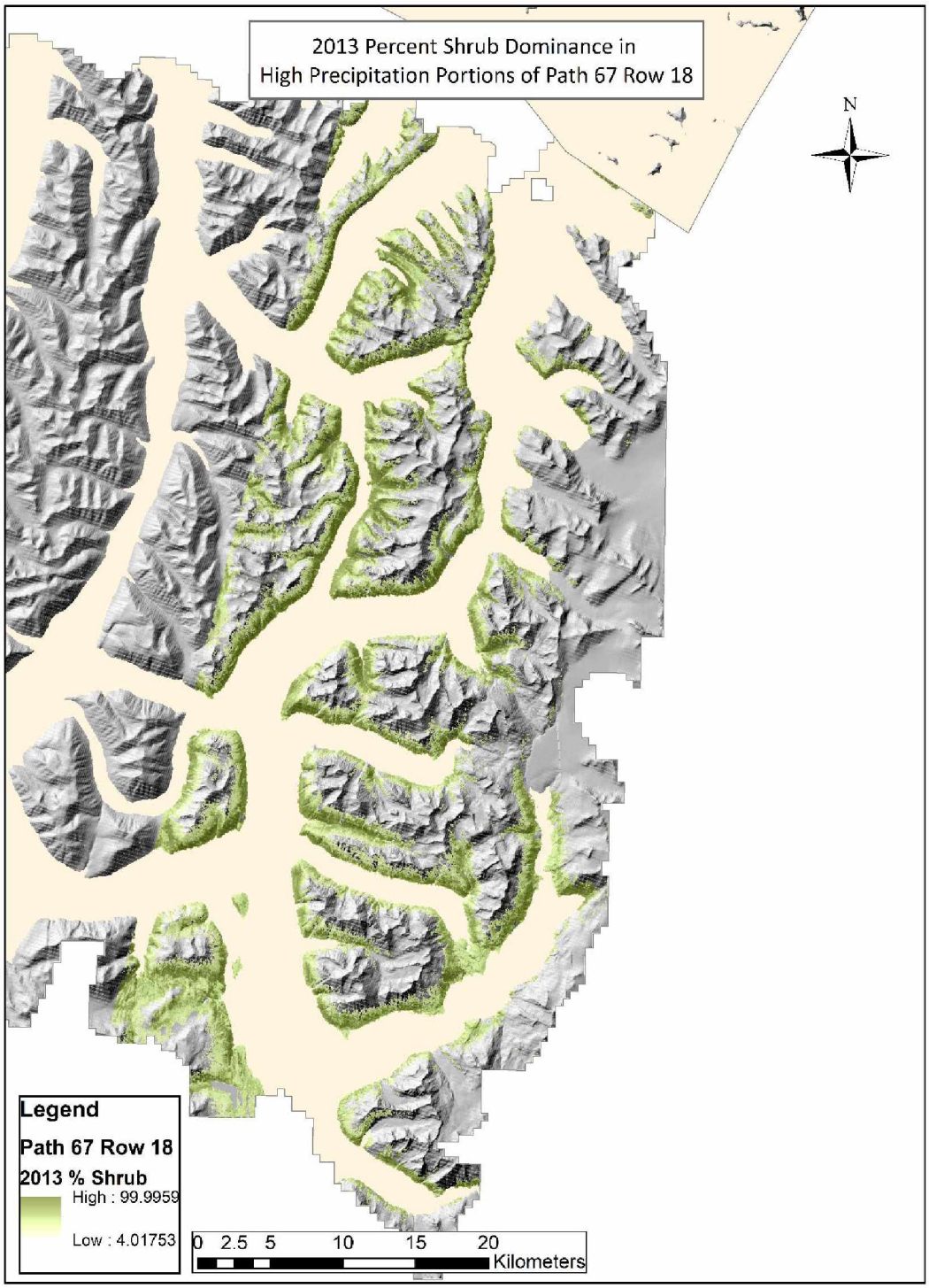


*Figure 3-17: : Map of modern shrub percent dominance based on the logarithmic relationship between NDVI and percent shrub dominance derived from a Landsat-8 scene acquired July 22nd, 2013 for path 67 row 18. Darker green areas show high percent shrub dominance compared to light green.*

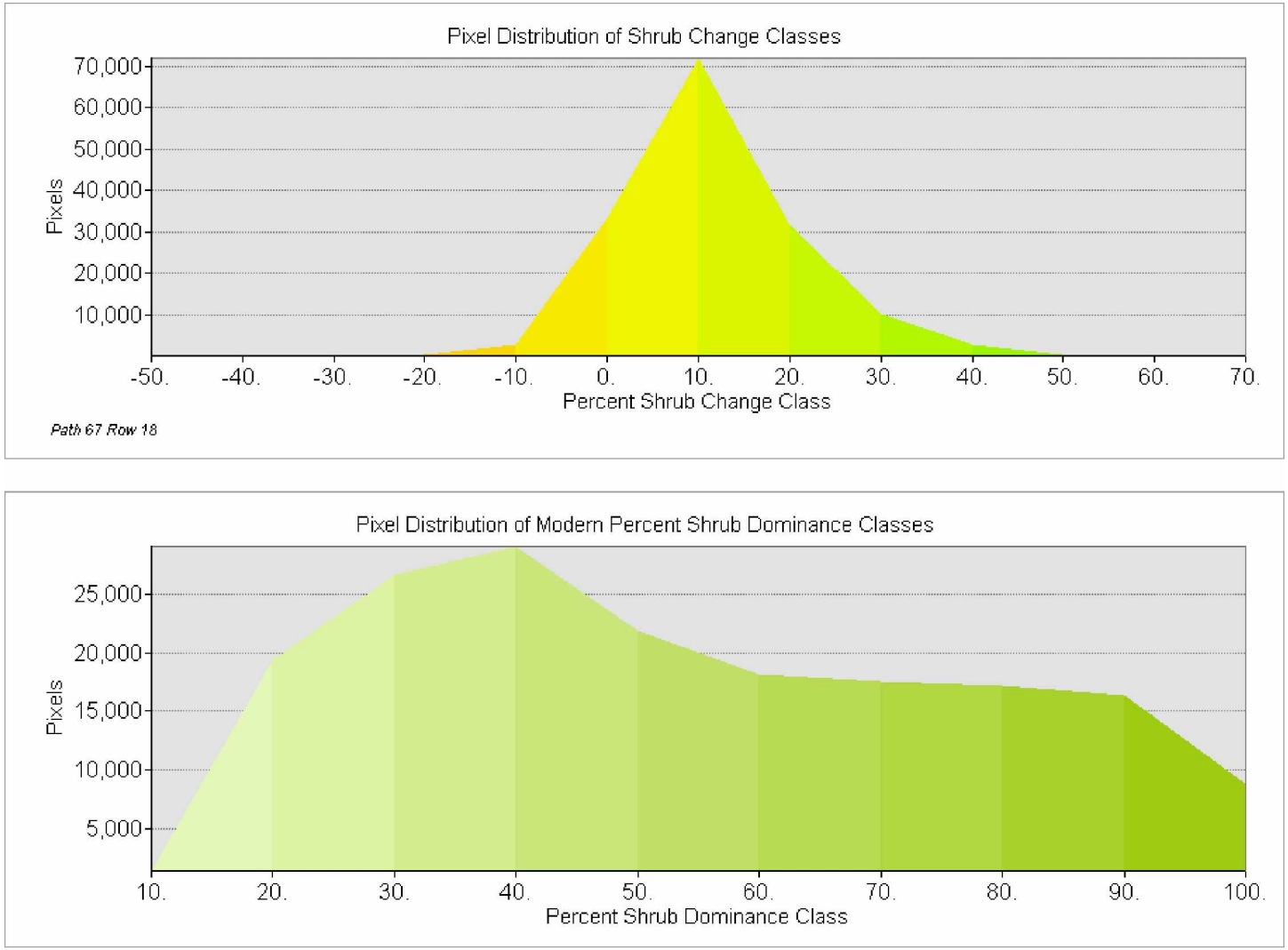


*Figure 3-18: Area plots of percent shrub change classes (top) and percent shrub dominance (bottom) for path 67 row 18 of the Arctic climate class. Pixel distribution of percent shrub dominance shows percent dominance classes most common between 20 and 50%, though classes with higher percent dominance taper off very slowly. The high precipitation climate class is the only area with high incidence of 100% shrub dominant pixels. Pixel distribution for percent shrub change classes show most increases occurred between 0 and 10%, that change classes at both 0% and 20% also had high incidence.*

## 3.3 Temperature as Shrub Change Driver Across Climate Classes

The change in mean July temperature during the period of interest (1980 – 2009, given the available data) was too low for the area of interest to indicate substantial increases in areas meeting minimum July growing temperatures. Therefore we used modern temperature (2000 -2009) to investigate the role of July minimum temperatures on shrub change. Figure 3-19 and 3-20 show the spatial distribution of growth classes by scene-pair: below shrub growth temperature limits (below limits; <10.5 C°), at shrub growth temperature limits (at limits; 10.5 C° – 12.0 C°), and above shrub growth temperature limits (above limits; >12.0 C° to 15.5 C°). An example of the individual pixel groups separated by temperature and connectivity within those growth classes is shown in Figure 3-21. All green pixel groups contain a value for modern July temperature to its tenth and mean shrub change.

The global means of shrub change throughout the study area in the growth classes are 5.89% in the below limits class, 7.35% in the at limits growth class, and 6.01% in the above limits growth class. Table 3-2 overviews means by growth class for each scene-pair and climate class. In the cold Arctic, the at limits growth class is most productive for shrubs. Many of the cold Arctic pixels in the above limits growth class show shrub loss. When comparing by scene-pair, results may be different. Cold Arctic pixels from Path 75 row 13 had the highest average shrub change (n = 10.94%) in the above limits growth class. This pattern of highest shrub change in the growth class with highest temperatures also occurred in the interior and high precipitation climate classes. However, the $r^2$ for shrub change and temperature was low (n = 0.00; Table 4-1) in the high precipitation climate class. The $r^2$ was higher for that relationship in the interior (n = 0.31). Further complicating, these relationships is low sample size. As an example, no temperatures in the interior met the below limits temperature requirements (n < 10.5 C°). In both the interior and high precipitation classes, temperatures are primarily above shrub temperature limits, so other climatic variables may drive shrub expansion and loss.

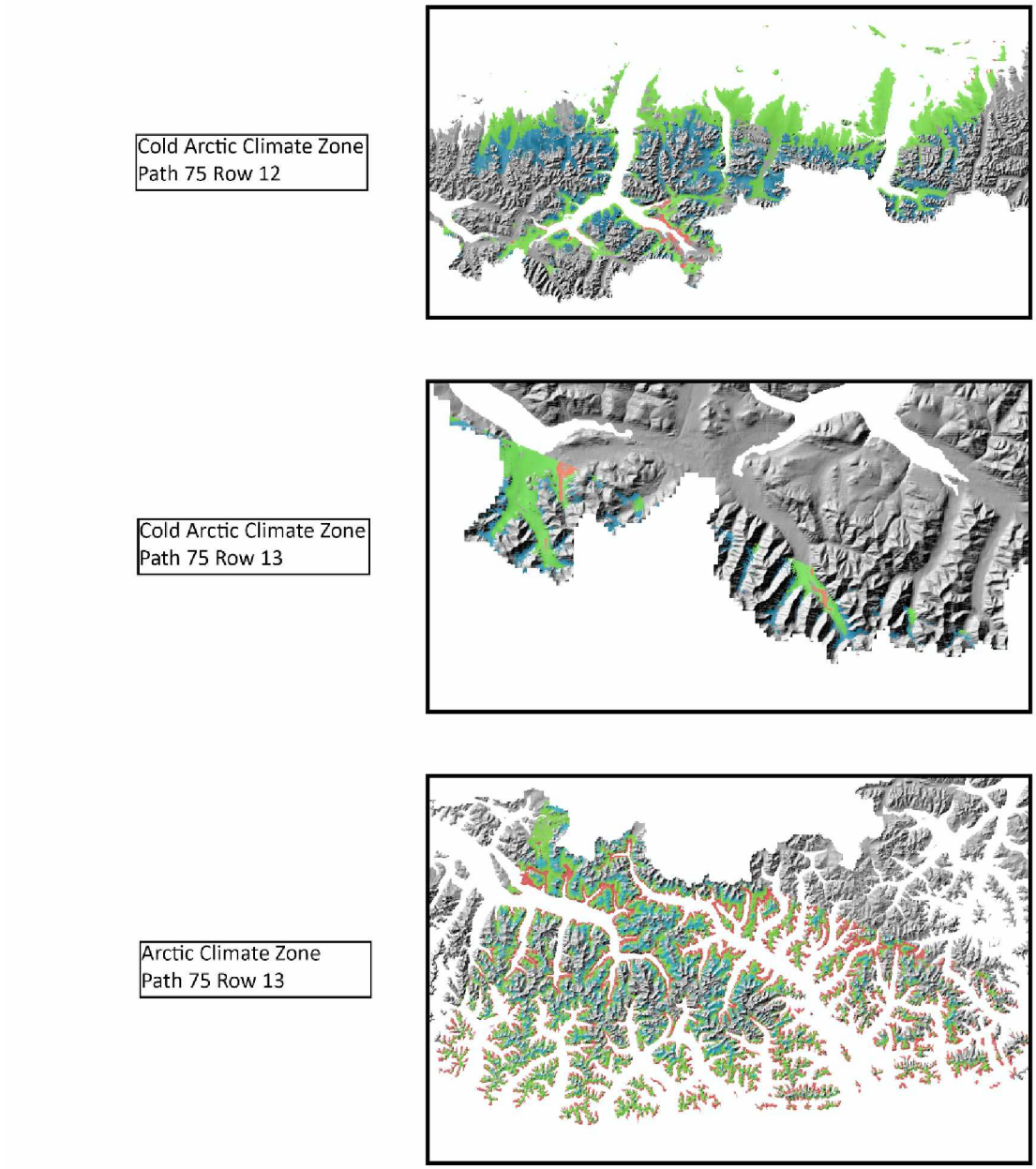


*Figure 3-19: Spatial distribution of modern growth classes by scene-pair for path 75 row 12 (top) and path 75 row 13 (middle) in the cold Arctic climate class and path 75 row 13 (bottom) in the Arctic climate class. Growth classes are below growing limits (under 10.5 C°; blue), at growing limits (10.5 C° - 12 C°; green), and above growing limits (above 12 C°; red).*

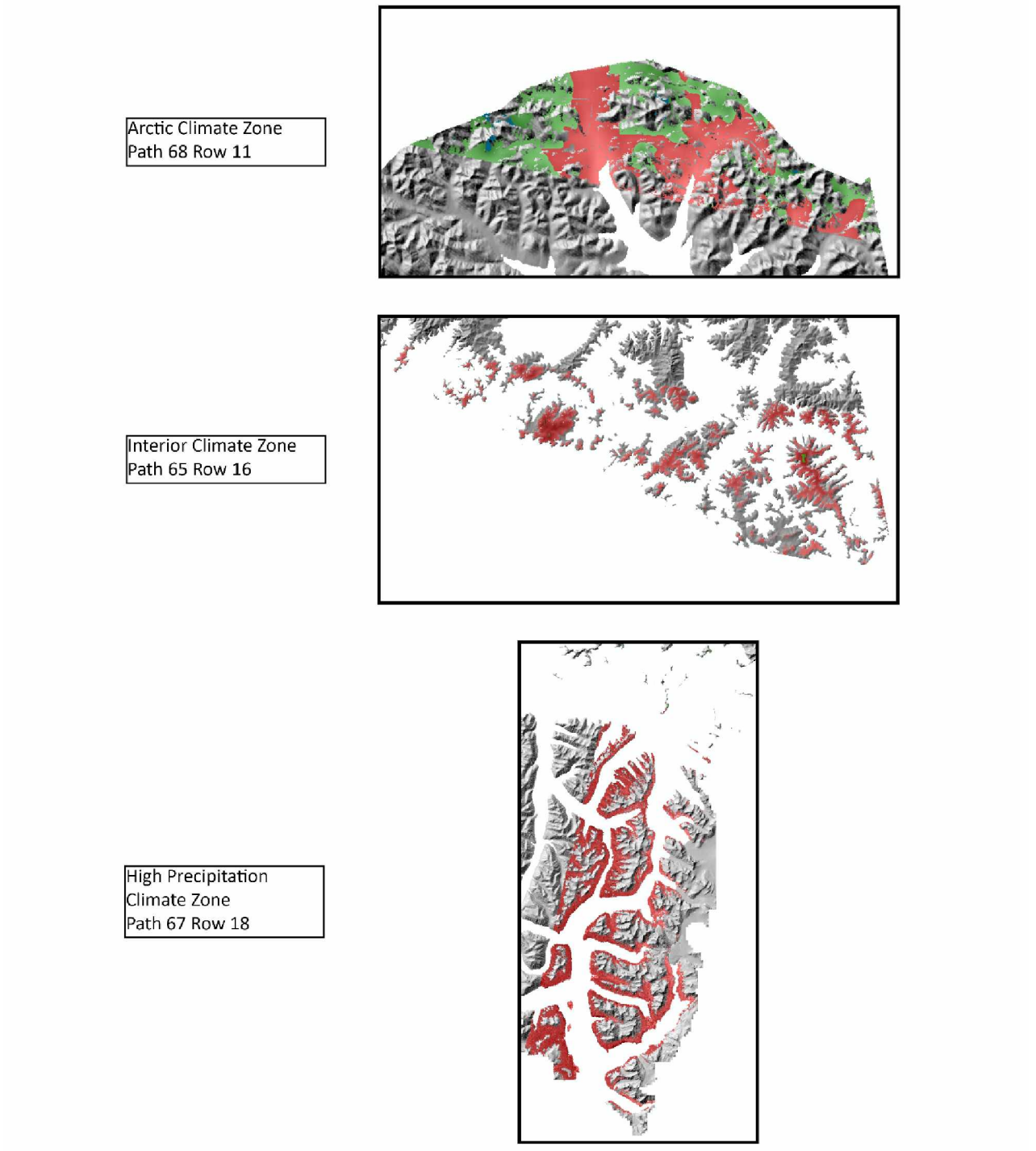


*Figure 3-20: Spatial distribution of modern growth classes for path 68 row 11 (top) of the Arctic climate class, path 65 row 16 (middle) in the interior climate class and path 67 row 18 (bottom) in the high precipitation climate class. Growth classes are below growing limits (under 10.5 C°; blue), at growing limits (10.5 C° - 12 C°; green), and above growing limits (above 12 C°; red).*

*Table 3-2: a) Summary statistics by growth class for each scene-pair (top) and b) by growth class for each climate class (bottom). The global means show highest shrub change in the cold Arctic, followed by the Arctic and High Precipitation classes, and lowest in the interior.*

| PATH ROW | CLIMATE CLASS | GROWTH CLASS | MEAN (%) | STD (%) | MIN (%) | MAX (%) |
|---|---|---|---|---|---|---|
| **7513** | Cold Arctic | Below Limits | 5.50 | 6.11 | -42.11 | 38.71 |
| | | At Limits | 9.84 | 6.78 | -37.26 | 45.71 |
| | | Above Limits | 10.94 | 7.05 | -28.08 | 40.50 |
| **7512** | Cold Arctic | Below Limits | 5.75 | 6.75 | -53.16 | 70.41 |
| | | At Limits | 7.88 | 8.07 | -74.43 | 78.94 |
| | | Above Limits | -1.81 | 7.33 | -51.97 | 39.17 |
| **7513** | Arctic | Below Limits | 6.23 | 6.30 | -67.70 | 87.86 |
| | | At Limits | 6.65 | 7.65 | -95.23 | 97.03 |
| | | Above Limits | 6.26 | 8.09 | -89.83 | 92.39 |
| **6811** | Arctic | Below Limits | 4.87 | 5.81 | -4.98 | 37.02 |
| | | At Limits | 4.96 | 5.72 | -31.01 | 67.12 |
| | | Above Limits | 6.79 | 5.55 | -22.20 | 45.70 |
| **6516** | Interior | Below Limits | n/a | n/a | n/a | n/a |
| | | At Limits | -3.17 | 8.96 | -27.35 | 26.83 |
| | | Above Limits | 6.17 | 12.88 | -52.14 | 55.64 |
| **6718** | High Precipitation | Below Limits | 5.47 | 3.97 | -4.16 | 29.89 |
| | | At Limits | 4.12 | 4.78 | -2.71 | 19.16 |
| | | Above Limits | 6.29 | 9.43 | -54.00 | 67.41 |

| CLIMATE | GROWTH CLASS | MEAN (%) | STD (%) | MIN (%) | MAX (%) |
|---|---|---|---|---|---|
| ARCTIC | Below Limits | 6.15 | 6.26 | -67.70 | 77.61 |
| | At Limits | 6.57 | 7.60 | -95.23 | 97.03 |
| | Above Limits | 6.26 | 8.02 | -89.83 | 88.76 |
| COLD ARCTIC | Below Limits | 5.75 | 6.73 | -53.16 | 70.41 |
| | At Limits | 7.93 | 8.05 | -74.43 | 78.94 |
| | Above Limits | -0.97 | 7.96 | -51.97 | 40.50 |
| INTERIOR | Below Limits | n/a | n/a | n/a | n/a |
| | At Limits | -3.17 | 8.96 | -27.35 | 26.83 |
| | Above Limits | 6.17 | 12.88 | -52.14 | 55.64 |
| HIGH PRECIPITATION | Below Limits | 5.47 | 3.97 | -4.16 | 29.89 |
| | At Limits | 4.12 | 4.78 | -2.71 | 19.16 |
| | Above Limits | 6.29 | 9.43 | -54.00 | 67.41 |

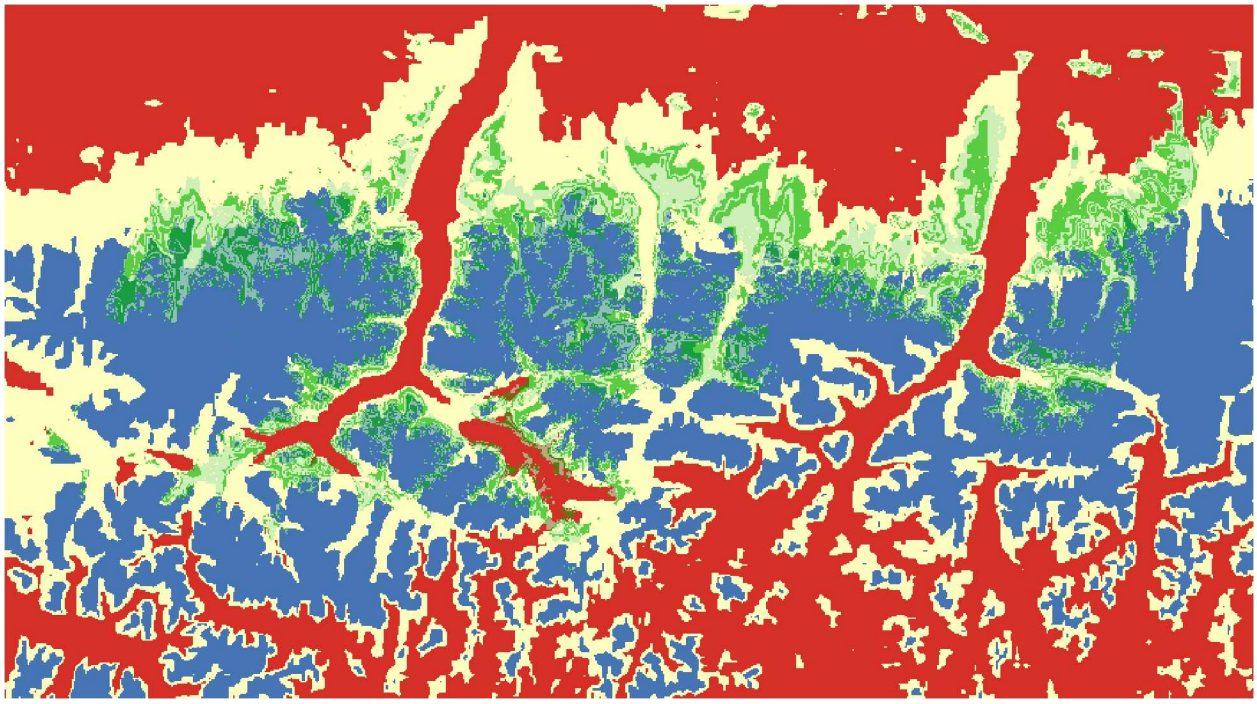

*Figure 3-21: Isolated pixel groups of temperature intervals overlaid growth classes for Path 75 Row 12 of the Cold Arctic climate class. Varying shades of green show groups of pixels based on connectivity and temperature, blue areas show the below limits growth class, white areas show the at limits growth class, and red areas show the above limits growth class.*

ANoVA testing global means of shrub change as the product of 1) growth classes or 2) climate classes were not significant ($\alpha = 0.05$). After accounting for temperature connectivity within our scene-pairs by isolating groups of interconnected pixels with the same temperature and extracting mean shrub change to those groups, the ANoVA was significant ($\alpha = 0.05$) for both models. The post-hoc Tukey multiple comparison of means revealed that percent shrub change is highest in the above limits growth class across the study area (Table 3-3). Across all climate classes, shrub change in the at limits growth class was 2.12% less, on average, than shrub change in the above limits growth class. The lower and upper limits of a 95% confidence interval for each comparison of means are provided in the adjoining columns. This finding is indicative of the study-wide pattern. Although exceptions exist, such as some cold Arctic areas in the above limits growth class, which had notable shrub loss but strong shrub growth at growth classes with lower temperatures (Table 3-2). Results of the Tukey multiple comparison of

means suggest that, in general, areas of low temperature that are warming to a temperature threshold high enough for shrub succession, do not experience the magnitude of shrub change that warmer areas do.

*Table 3-3: Results of a Tukey multiple comparison of means test determining difference between mean percent shrub change among pixel groups as a function of different shrub growth temperature classes (α = 0.05). Temperatures above the lower temperature growth thresholds (above limits) show the greatest change in percent shrub dominance.*

| | | | | *Mean Shrub Change ~ Growth Class* |
|---|---|---|---|---|
| **Pairwise Comparison: Growth Class A – Growth Class B** | **Difference In Means** | **Lower Limit (95% CI)** | **Upper Limit (95% CI)** | **Adjusted p-value** |
| At Limits - Above Limits | -2.12 | -2.36 | -1.88 | <0.001 |
| At Limits - Below Limits | 0.92 | 0.7 | 1.13 | <0.001 |
| Above Limits - Below Limits | 3.03 | 2.84 | 3.23 | <0.001 |

A Tukey multiple comparison of means testing shrub change as a product of climate classes revealed that shrub change quantified in this manner showed significant differences (α = 0.05) between climate classes in the rates of shrub change (Table 3-4).

*Table 3-4: Results of a Tukey multiple comparison of means test determining differences between means of percent shrub change among pixel groups as a function of different climate classes. Significant results (α = 0.05) show shrub change ranks in order of highest to lowest: 1) the high precipitation class 2) interior climate class 3) Arctic climate class and 4) cold Arctic climate class.*

| | | | | *Mean Shrub Change ~ Climate Class* |
|---|---|---|---|---|
| **Pairwise Comparison: Climate Class A - Climate Class B** | **Difference In Means** | **Lower Limit (95% CI)** | **Upper Limit (95% CI)** | **Adjusted p-value** |
| Cold Arctic - Arctic | -2.01 | -2.22 | -1.81 | <0.001 |
| Cold Arctic - Interior | -2.99 | -3.32 | -2.65 | <0.001 |
| Cold Arctic- High Precipitation | -5.21 | -5.75 | -4.68 | <0.001 |
| Arctic - Interior | -0.97 | -1.30 | -0.65 | <0.001 |
| Arctic - High Precipitation | -3.20 | -3.73 | -2.22 | <0.001 |
| Interior - High Precipitation | -2.23 | -2.82 | -1.64 | <0.001 |

In examining areas where shrub expansion is highest (i.e. above limits growth class), ANoVA testing shrub change as a product of climate class also had significant results (α = 0.05). The post-hoc Tukey multiple comparison of means test had significant results (α = 0.05, Table 3-5). Notably, shrub

expansion in the cold Arctic climate class was much lower than any other climate class. Shrub growth is highest in the cold Arctic in the "at limits" growth class, which may contribute to the large difference in shrub change rates when comparing rates across climates at warmer temperatures

*Table 3-5: Results of a Tukey multiple comparison of means test determining difference between mean percent shrub change in areas above shrub temperature limits as a product of their climate classes. Results are significant (α = 0.05) and indicate shrub change is highest in the high precipitation climate class and lowest in the cold Arctic, north of the Brooks Range.*

| | *Mean Shrub Change ~ Climate Class; Growth Class = Above Limits* | | | |
|---|---|---|---|---|
| **Pairwise Comparison: Climate Class A – Climate Class B** | **Difference In Means** | **Lower Limit (95% CI)** | **Upper Limit (95% CI)** | **Adjusted p-value** |
| Cold Arctic - Arctic | -6.36 | -7.9 | -4.81 | <0.001 |
| Cold Arctic - Interior | -5.58 | -7.14 | -4.02 | <0.001 |
| Cold Arctic - High Precipitation | -7.95 | -9.63 | -6.26 | <0.001 |
| Arctic - Interior | 0.77 | 0.22 | 1.32 | 0.002 |
| Arctic - High Precipitation | -1.59 | -2.42 | -0.75 | <0.001 |
| Interior - High Precipitation | -2.36 | -3.24 | -1.49 | <0.001 |

*Table 3-6: Results of a Tukey multiple comparison of means determining difference between mean percent shrub change in areas at shrub temperature limits as a product of their climate classes. Results are not significant (α = 0.05), excluding the relationship between cold Arctic and Arctic climate classes.*

| | *Mean Shrub Change ~ Climate Class; Growth Class = At Limits* | | | |
|---|---|---|---|---|
| **Pairwise Comparison: Climate Class A – Climate Class B** | Difference In Means | Lower Limit (95% CI) | Upper Limit (95% CI) | Adjusted p-value |
| Cold Arctic - Arctic | -1.35 | -1.8 | -0.9 | <0.001 |
| Cold Arctic - Interior | 0.24 | -8.27 | 8.75 | 1.000 |
| Cold Arctic - High Precipitation | -0.65 | -4.22 | 2.92 | 0.966 |
| Arctic - Interior | 1.59 | -6.91 | 10.1 | 0.963 |
| Arctic - High Precipitation | 0.7 | -2.85 | 4.26 | 0.957 |
| Interior - High Precipitation | -0.89 | -10.1 | 8.32 | 0.995 |

Testing means of shrub change as a product of climate class at shrub temperature limits (i.e. warm enough for growth to occur but not necessarily high enough for proliferation) showed no significant differences (α = 0.05) between climate classes excluding the cold Arctic and Arctic climate classes (Table 3-6).

# 4 Discussion

## 4.1 Temperature

A deeper examination of the relationship between shrub change and temperature is important to understand 1) if the impact to shrub change from temperature changes along a range of values increasing above growing minimums and 2) helps identify if additional factors play a role in shrub change. Single-variate plots of shrub change as a product of temperatures above 12 C° (Figure 4-1) show that the $r^2$ values differed substantially between climate classes. The relationship between temperature and shrub change was highest in the Arctic and cold Arctic. In the climate class where shrub change was highest, the high precipitation climate class, temperature appeared to have little to no relationship with shrub change. These differences indicate that additional climatic factors play a driving force in the differences in shrub expansion between regional climatic groups. We explored additional climatic variables between climate classes by addressing the climate classes with the strongest shrub change / temperature relationship, Arctic and cold Arctic first, and continued with the climate classes that have weaker shrub change-temperature relationships.

*Table 4-1: $R^2$ of linear models of shrub change as product of temperature intervals above 12 C°. Intervals higher than 12 C° had highest shrub change rates. Rates varied between climate classes. Differences in $r^2$ indicate additional climatic factors direct shrub change above 12 C°.*

| Zone | Path | Row | $r^2$ |
|---|---|---|---|
| **Cold Arctic** | 75 | 12 | 0.7741 |
| **Cold Arctic** | 75 | 13 | 0.8557 |
| **Arctic** | 75 | 13 | 0.5042 |
| **Arctic** | 68 | 11 | 0.6807 |
| **Interior** | 65 | 16 | 0.3079 |
| **High Precipitation** | 67 | 18 | 0.0005 |

## 4.2 Colder Growing Conditions: Arctic and Cold Arctic Climate Classes

### 4.2.1 Overview

The highest correlation of shrub change to temperature occurred in the Arctic and cold Arctic. This relationship has multiple causal possibilities: 1) temperature increases in the Arctic are more

pronounced than at lower latitudes (Myers-Smith and Hik 2018) and 2) temperatures in the Arctic are currently increasing above growing season minimums for shrubs (Swanson 2015) and will continue to do so (Swann et al. 2010). The Arctic and cold Arctic shared similar means for climatic variables such as lower July temperature, shorter length of growing season, lower levels of precipitation, and colder winter temperatures compared with the other climate classes. However, the Arctic climate class had a broader range of temperatures (more comparable to the ranges of the interior and high precipitation climate classes than the cold Arctic). When comparing single-variate relationships of shrub change with mean July temperature, mean length of growing season, mean annual precipitation, and mean winter temperature, the Arctic and cold Arctic displayed similar relationships. All Arctic and cold Arctic scenes displayed strong relationships with modern July temperature and modern length of growing season. The collinearity between these two variables was high, indicating that exploring the relationship between length of growing season and shrub would not generate substantial additional inference.

### 4.2.2 Negative Trend

Path 75 Row 12 displayed a negative linear relationship between shrub change and temperatures above 12 C°. This negative relationship required further investigation given the demonstrated relationship between temperature and shrub growth. The anomaly may be caused by an issue such as limited sample size, disturbance such as wildfire, or possibly saturation. To investigate this anomaly, we plotted shrub change as the product of the full temperature range (Figure 4-2) as well as excluded the temperatures where shrub change dropped off precipitously (value = 11.5 C°). The plot (Figure 4-2) showed a strong non-linear relationship. Below 11.5 C° there was a strong positive relationship consistent with other Arctic and cold Arctic scene-pairs. Above 11.5 C° there was overall shrub loss, though the magnitude was low.

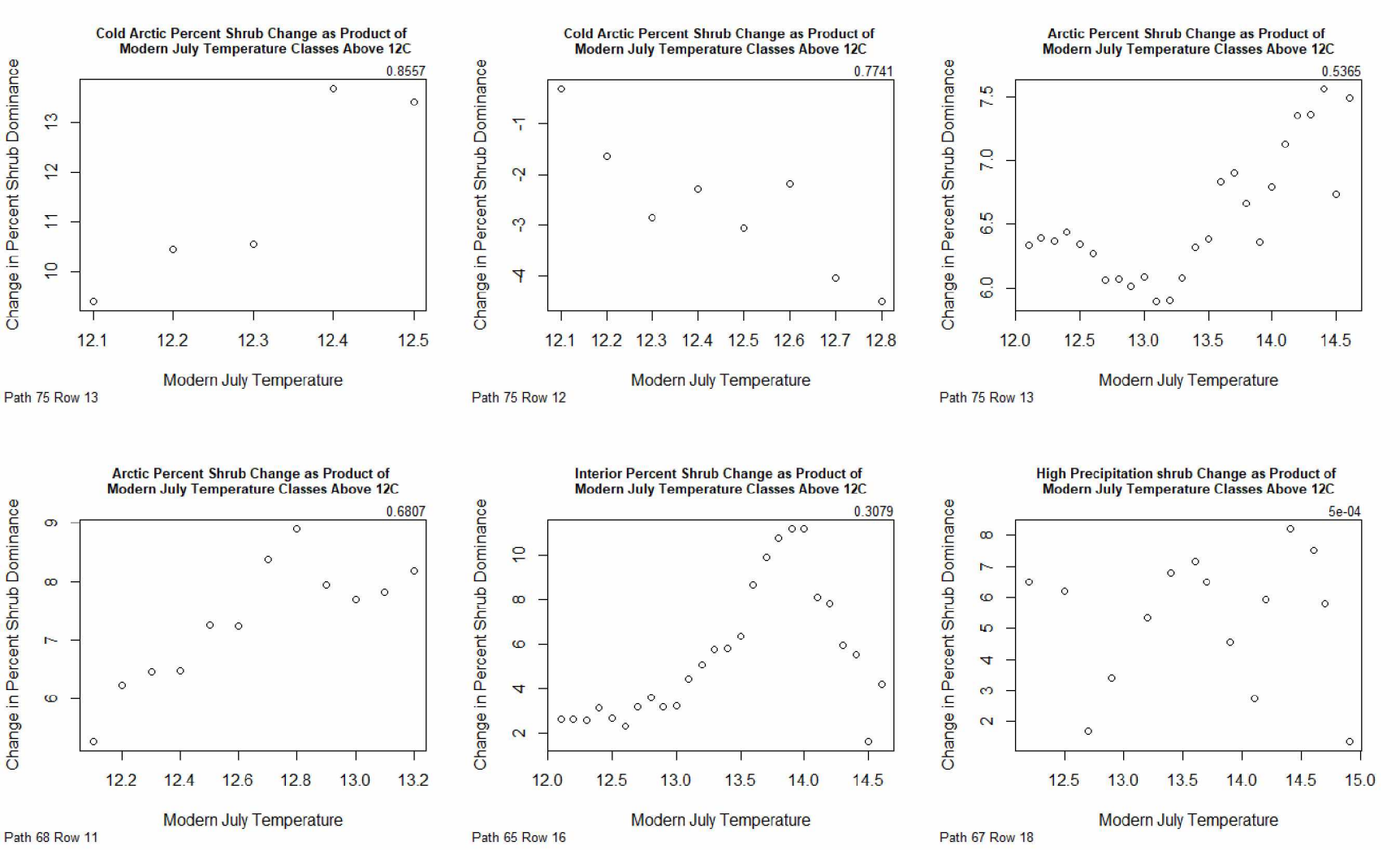


*Figure 4-1: Single-variate plots of percent shrub change as a product of temperatures for all scene-pairs. Relationships are strongest in the Arctic and cold Arctic classes, notably weaker in the interior climate class, and absent in the high precipitation climate class. Of note, path 75 row 12 of the cold Arctic climate class has a negative relationship with temperatures above 12 C°. This relationship is likely due to low sample size of pixels in the above limits growth class. $R^2$ for each regression is in the top right corner of its plot.*

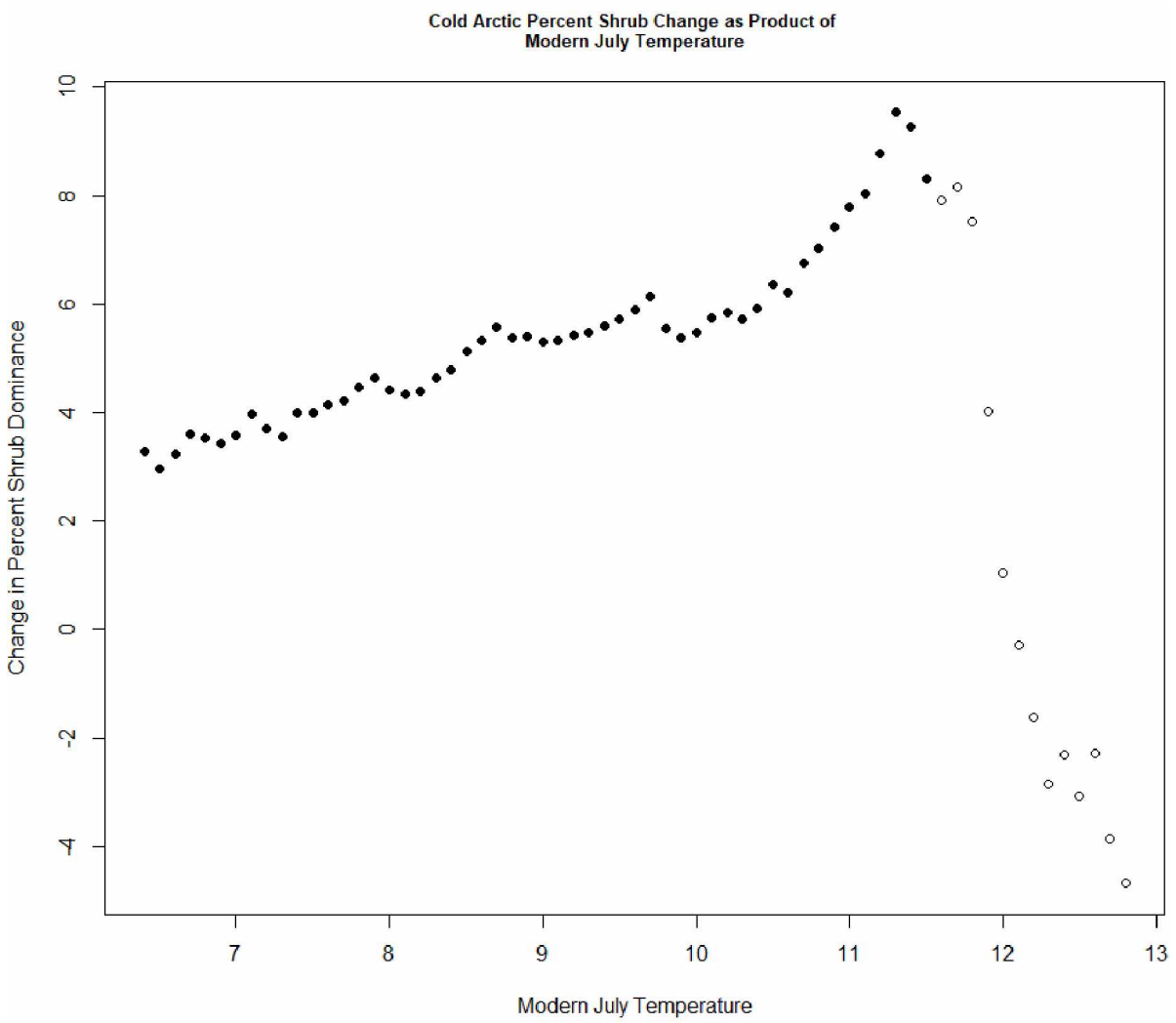


*Figure 4-2: Plot of percent shrub change as a product of temperature for path 75 row 12 of the cold Arctic climate class. Black points show shrub change for temperatures below 11.5 C°. Hollow points show shrub change for all available temperatures in the scene-pair. The strong relationship between temperature and percent shrub change below 11.5 C° is consistent with the relationship in other Arctic and cold Arctic scene-pairs, indicating the precipitous drop in shrub change warrants investigation.*

The area above growth limits was small comparable to other scene-pairs and climate classes. It is possible the low areal extent was not representative of the overarching patterns for the cold Arctic, as the alternate scene-pair (path 75 row 13) showed a strongly positive relationship between shrub change and temperature in its cold Arctic portion. Additionally, the climatic factors separating the cold Arctic and Arctic were limited (Appendix, pp 173 - 176) and both scene-pairs from the Arctic climate class showed a strongly positive relationship with shrub change at all temperatures in their range, including temperatures above 11.5 C°.

An examination of the relationship between vegetation and NDVI provides inference into what may be occurring. As vegetation densities increase within a given pixel, NDVI increases. However, the effect of vegetation on NDVI decreases as productive vegetation types become denser (Pettorelli et al 2005; Macander et al. 2015). Therefore, the shrub loss may not be loss, but rather a slowing response of NDVI to shrub densities that have been increasing over decades. It is possible that in some areas of the cold Arctic that are above 12 C° shrub expansion has occurred already occurred and, consequently rates of change reduced. The small magnitude of loss supports this argument.

### 4.2.3 Aspect

Shrub growth requires temperature minimums for expansion (Swanson 2015), but its spatial heterogeneity has been demonstrated as a product of local topography at lower latitudes (Ropars and Boudreau 2012). Local topography may also play a role in Arctic and cold Arctic climates. The topographic variable that differed notably between climate classes (but, importantly not between scene-pairs) was aspect. It should be noted elevation has a demonstrated relationship with shrub change that was collinear with temperature, which is why it was not explored as a topographic variable.

In the cold Arctic climate class the range of shrub change means was much wider (n ≈ 4.0 – 10.0%) compared to the Arctic climate class where the range was much more limited (n ≈ 6 – 7.5%).

Perhaps more importantly, the pattern of linear relationships differed. In the cold Arctic, change was highest on northern slopes and lowest on southern slopes. Whereas in the eastern Arctic (path 68 row 11), change was highest on the southern slopes and lower on the northern slopes. The central Arctic showed a similar pattern to the cold Arctic; however the range was considerably smaller, with north and northeastern slopes experiencing only 0.5% more shrub change. The northwestern and northern slopes experienced roughly 1-1.5% more shrub increase. Single-variate plots of percent shrub change as a product of temperature for north and south slopes showed mixed results (Figure 4-3). Results did not align by climate class or scene-pair. In the Arctic climate class, southern exposure appeared to have a positive impact on shrub growth for path 68 row 11 but not for path 75 row 13. In the cold Arctic climate class, southern exposure appeared to have a positive impact in path 75 row 13, but negative impact in path 75 row 12.

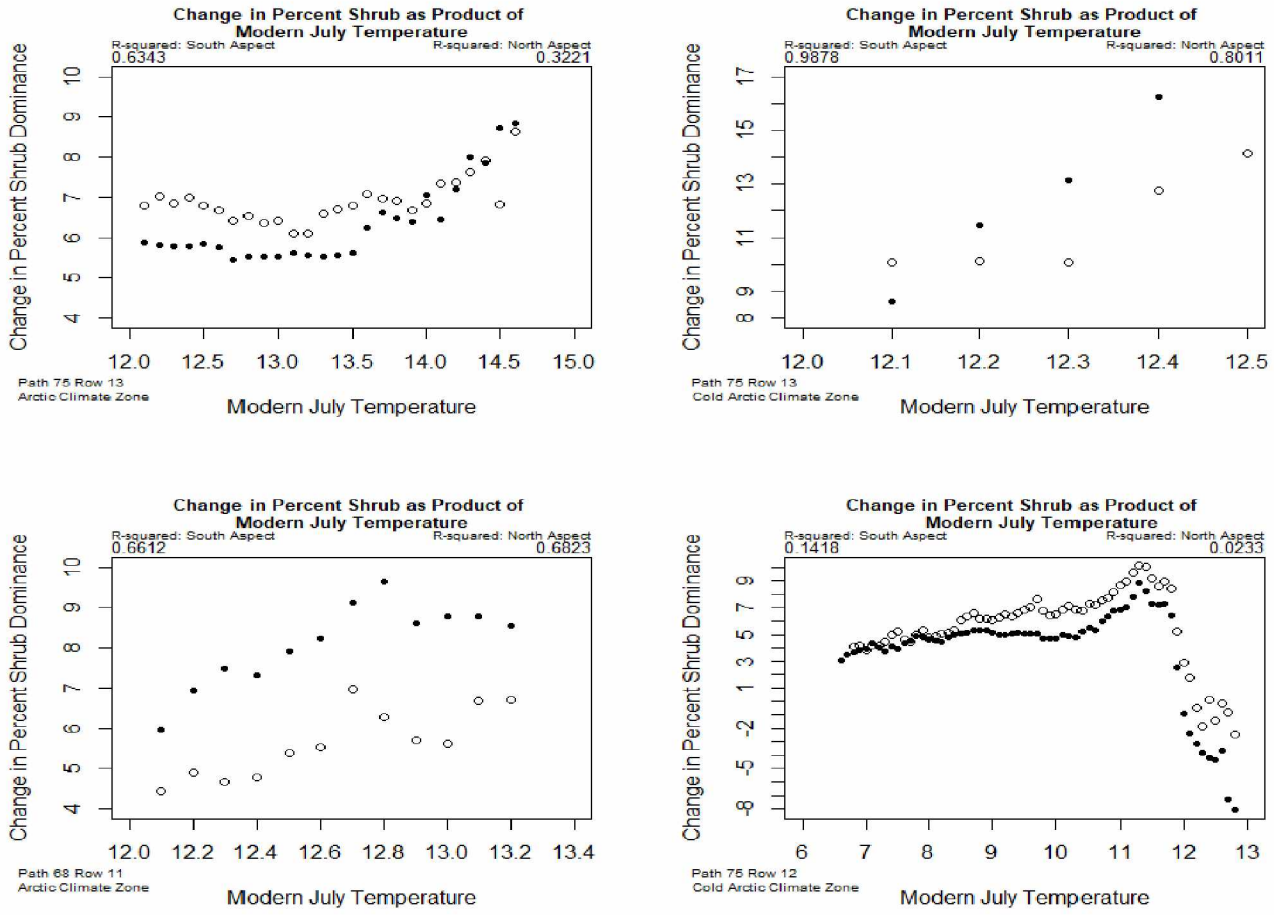


*Figure 4-3: Single-variate plots of percent shrub change as a product of temperature for northern (hollow points) and southern (black points) slopes for all scene-pairs in the Arctic and cold Arctic climate classes. $R^2$ for each regression is in the top left corner (southern slopes) or top right corner (northern slopes) of its plot.*

## 4.3 Warmer Growing Conditions: Interior Climate Class

### 4.3.1 Overview

Shrub change was highly correlated with modern July temperature when looking at the full range of July temperature in the interior climate class. As shrub change increased at higher temperatures, the acceleration of change appeared to slow. In the above limits growth class, correlation between modern July temperature and shrub change was relatively low (value = 0.31). The low correlation combined with a lack of relationships between the additional variables of length of growing season indicates that the drivers of shrub change at warmer temperatures may be predicated on localized conditions. This thinking coincides with research conducted in colder climates to assess risk of shrub expansion in the face of rising temperatures (Tape et al. 2012; Swanson 2015).

The interior climate class had a weak but evident linear relationship between percent shrub change and modern July temperature. All pixels of historic July temperature for path 65 row 16 contained values 11.5 C° or greater meaning that shrub growth was possible over the last several decades throughout the study area, so the overall increase in shrub over the same time period must include factors other than temperature.

### 4.3.2 Infilling

In areas where shrub expansion is occurring, canopy infilling is a primary mechanism by which shrub expansion occurs (Myers-Smith et al. 2011; Swanson 2015). The productive climate and comparably warmer growing season of the interior indicate infilling may be a mechanism here. Single-variate plots of climatic and terrain variables show high correlation between variables, complicating agents of causality. Global means of climatic factors for the interior climate class were limited in their ability to illuminate causality as the interior climate class did not have the highest global mean for any

variable. We explored the possibility that highly productive areas with minimal change in July temperature may be more prone to infilling than expansion across space.

While shrub expansion could occur in denser areas of shrub, it appears that denser areas are more prone to shrub loss than expansion (Figure 4-4.). Areas of moderate percent shrub dominance, however, show high increases in percent shrub dominance. As the relationship between historic percent shrub dominance and shrub change was negative, there is little inference into what factors are driving shrub expansion in the interior. We looked at aspect to compare its impact in the interior to the Arctic and cold Arctic climate classes.

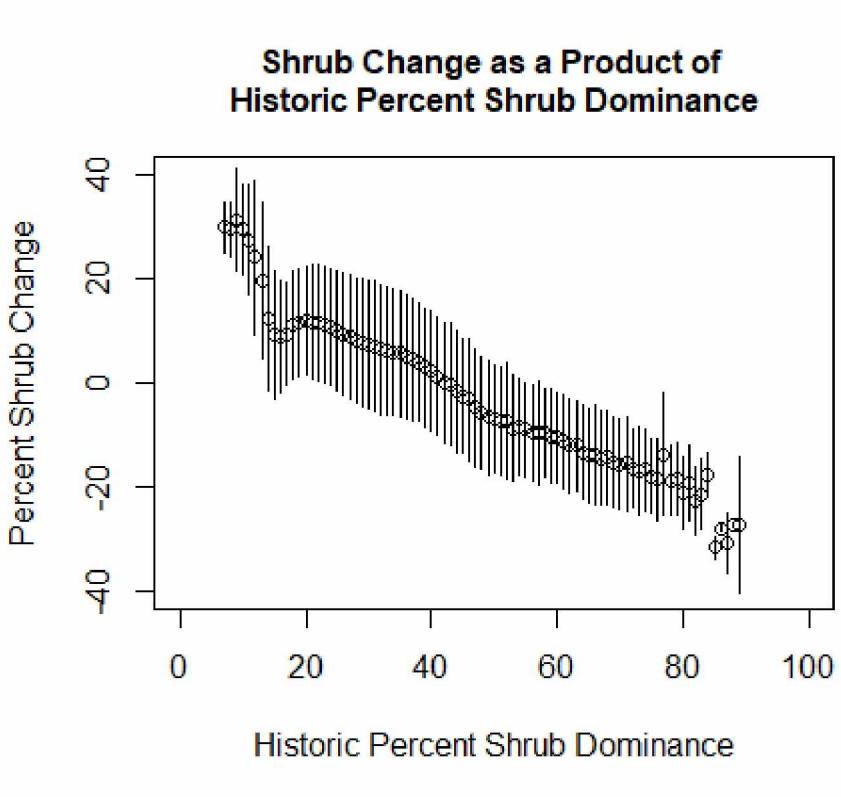


*Figure 4-4: Plot of shrub change as a product of historic percent shrub dominance. Used to aid in determining if shrub percent cover in the interior climate class, where mean July temperatures are above minimum July growing temperatures across both the modern and historic eras, plays a role in expansion.*

### 4.3.3 Disturbance

Boreal Alaska has experienced increases in fire intensity and number in response to climate change (Kasischke et al. 2006). Disturbances such as fire facilitate successional entrants such as shrubs (Swanson 2015). The spatial distribution of shrub loss in the interior climate zone indicates an event such as fire may have played a role in the loss. The interior climate class has the largest ratios of shrub loss pixels to shrub expansion pixels, indicating that disturbance may play a role in both the net change in shrub as well as the variability of shrub loss and expansion due to the variability of fire years. As such, research showing shrub expansion is greatest within inland climates of high latitudes (Verbyla and Kurkowski 2019) may be more indicative of gross productivity than net change on the landscape.

Incorporating fire data as an additional factor in the analysis of climate relationships would allow isolation and comparison of shrub expansion patches in disturbed and undisturbed areas.

### 4.3.4 Aspect

Landscape heterogeneity plays a prominent role in shrub growth and expansion (Ropars and Boudreau 2012; Tape et al. 2012). Despite the lower latitude of the interior climate class, aspect appears to play a strong role in the relationship between modern July temperature and shrub change (Figure 4-5). Southern slopes had a stronger relationship ($r^2 = 0.2941$) than the areas with northern exposure ($r^2 = 0.1165$). However, it should be noted that when slopes were analyzed separately, both areas had a weaker relationship compared to the average between slopes ($r^2 = 0.3097$), albeit negligible for southern slopes. While this difference may be due to sample size or chance, it warrants additional investigation as it could mean aspect may have less of an effect on the temperature/shrub change relationship than other climates.

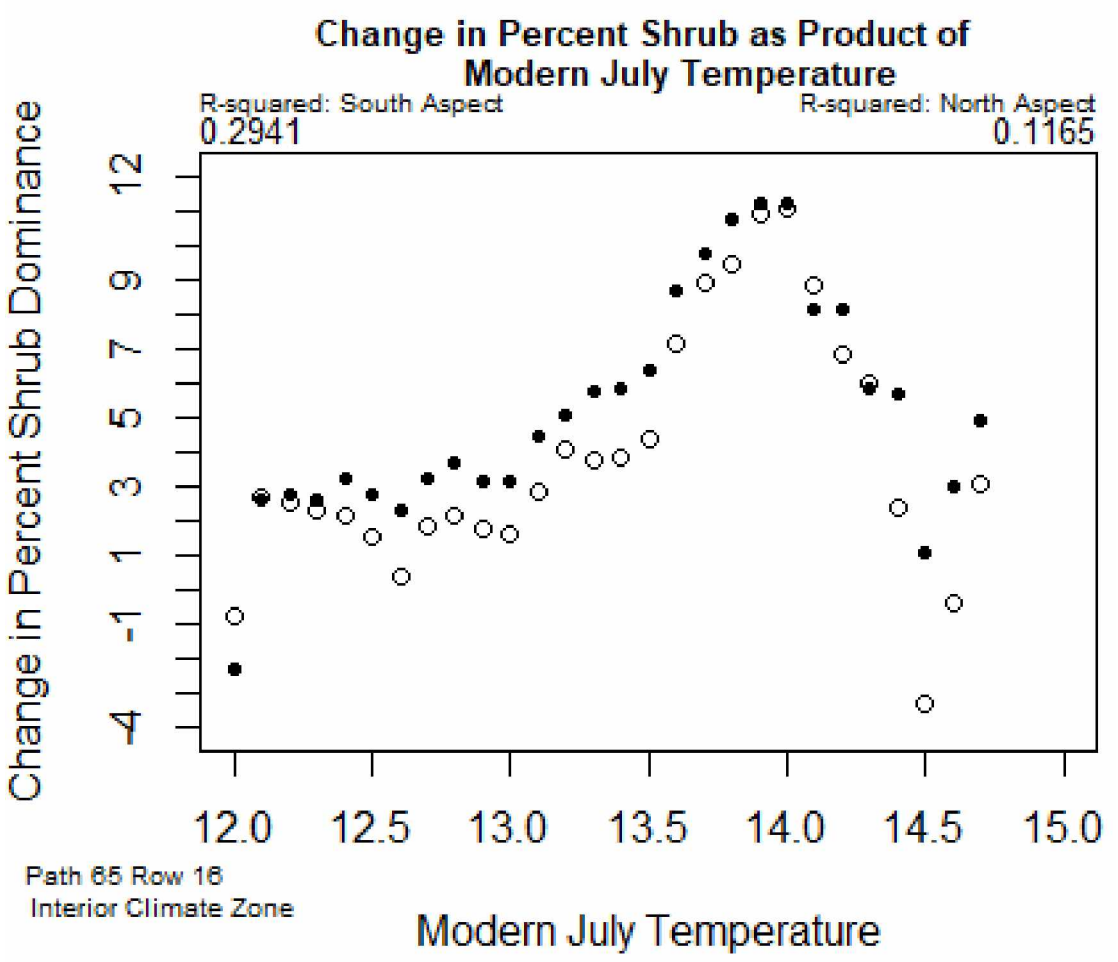


*Figure 4-5: Single-variate plot of percent shrub change as a product of temperature for northern (hollow points) and southern (black points) slopes for path 65 row 16 in the interior climate class. $R^2$ for each regression is in the top left corner (southern slopes) or top right corner (northern slopes) of its plot.*

### 4.3.5 Shrub Change Rates

Shrub expansion rates were relatively even between 12 and 13 C° (Figure 4-5). Rate of expansion increased between 13 and 14 C° prior to decreasing between 14 and 15 C°. Change in rate of shrub change could be indicative of a number of things: 1) succession 2) disturbance or 3) saturation.

In areas with mean July temperature near 12 C°, the only diamond leaf willow reached full canopy (≥ 0.5 m) (Swanson 2015). Alder reaches full canopy between 14 and 15 C°. It is possible that alder species may express a higher NDVI based on its leaf and canopy structure (Boelman et al 2011). This rationale may explain the increase in shrub change rate at higher temperatures: more productive species are taking over. The decline in shrub change rate above 14 C° may be indicative of coniferous species, with lower relative photosynthetic activity (Clark and Lister 1975), succeeding alders.

It is possible fire may only have a notable impact on shrub change at warmer temperatures in the interior. Decreases in shrub dominance above 14 C° due to fire would contribute to the shrub expansion rate when analyzing at a range-wide scale (Racine et al. 2004; Ju and Masek 2016). For example, a large patch of shrub lost to fire could strongly influence the overall rate of shrub change as burned soil has a NDVI value less than 0.2 and dense shrub patches are generally greater than 0.5, creating a substantial loss that could influence relatively slow, yet consistent, shrub expansion. This argument is supported by the patchy distribution of shrub change and modern shrub dominance.

Shrub saturation on the landscape may be occurring. The saturation may also be a perceived product of the vegetation index used. NDVI offers the most broadly used vegetative index and was the appropriate index for converting vegetation productivity to percent shrub dominance (Berner et al. 2018). However, the Enhanced Vegetation Index offers a superior alternative to NDVI for use in high density cover types (Pettorelli et al. 2005). A re-analysis of the study area's highly productive areas could help illuminate this further.

## 4.4 Warmer Growing Conditions: High Precipitation Climate Class

### 4.4.1 Precipitation

Mesic environments and shrub expansion have a demonstrated relationship (Ropars and Boudreau 2012; Ackerman et al. 2017) though site may render this relationship negligible (Ackerman et al. 2018). Interpolated precipitation data offers the most accessible inference into broadscale soil moisture levels and their potential impacts. The broadest range of annual precipitation occurred in the high precipitation class. The substantially smaller ranges of precipitation in the other climate classes limited the reliability of examining it as a driver in other classes. Within the high precipitation climate class, this relationship was strongly positive as a simple linear model, though the pattern of values indicates that, with more samples, the pattern may exhibit logistic growth rather than linear (Figure 4-6).

### 4.4.2 Aspect

Slopes with southern exposure showed a much stronger relationship with mean July temperature than their northern counterparts (Figure 4-6), which maintained an almost non-existent relationship with July temperature. Impacts of aspect on woody vegetation growth in mountain ranges in the high precipitation class have different documented impacts. Dial et al. (2007) used orthophotos to document an elevational increase in open woodland treeline on northern slopes, attributing these increases with the mesic state of these aspects. Despite a lack of elevational increase, woody vegetation became denser on southern slopes. The patterns are supported in Figure 4-6, where the relationship between temperature and shrub change is stronger on southern slopes, but the magnitude of shrub change is higher on northern slopes. The implied relationship between northern aspects and mesic state from Dial et al. (2007) also bolsters support for the relationship between precipitation and shrub change established here.

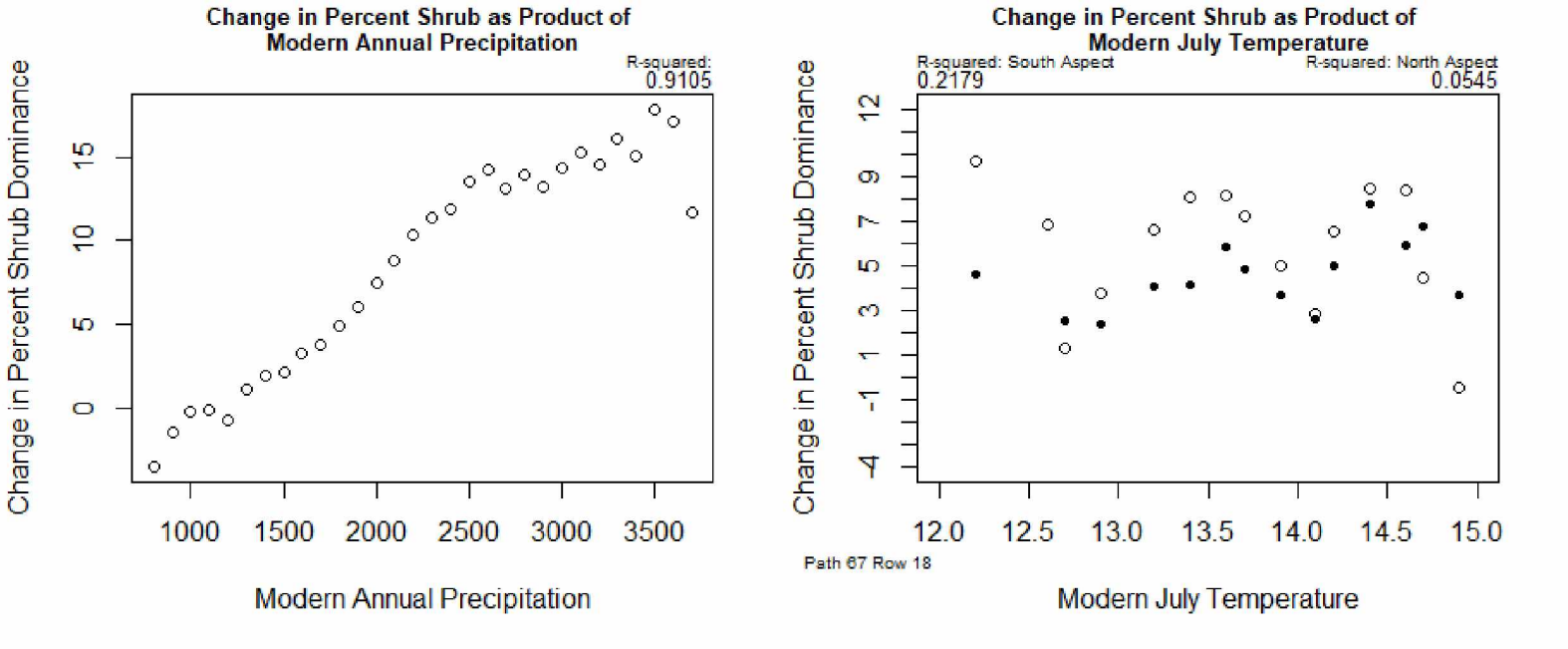


*Figure 4-6: Plots of shrub change as a product of modern annual precipitation (left) and as a product of temperature with aspect accounted for in the high precipitation climate class. Points with less than 50-pixel sample size were removed to limit error. In the right plot, solid black points indicate southern slopes, hollow points indicate northern slopes*

## 4.5 Implications for Dall's Sheep

Alaskan Dall's sheep populations have conflicting trends (Table 4-2) and the data surrounding populations estimates can be limited due to logistical constraints (ADF&G 2010; ADF&G and ABR, Inc. 2015). While a statewide decline has been suggested (2010), the regional trends vary with some populations functioning at stable or possibly increasing levels (ADF&G 2014).

The factors impacting these populations can be influenced by locality and regional climate (Arthur and Lohuis 2014; Downs et al. 2018). In the Arctic and cold Arctic climate classes, Dall's sheep populations are especially susceptible to precipitous declines in response to dramatic weather events and spring snow characteristics (van de Kerk et al. 2018b). A late spring in 2013 resulted in roughly 40 to 70% population declines in assessed areas of the Brooks Range and null recruitment (Rattenbury et al. 2018). Interior Dall's sheep populations showed a less dramatic decline in response to high snowfall between 1999 and 2000 (Mitchell et al. 2015). In a comparison of Dall's sheep mortality causes across regional climates, the Chugach mountains had high comparable rates of ewe and lamb deaths (n = 85%, 54%) caused by means other than predation, the primary cause in other mountain ranges (Arthur and Lohuis, 2014). Avalanche and disease were the primary causes of mortality in the Chugach mountains.

Impacts of shrub encroachment into the alpine is not well understood but likely mirrors shrub expansion elsewhere at high latitudes. Notable impacts could include 1) changes in nutritional content commensurate with vegetation shifts (Welker et al. 2005) 2) increased cover and distributions of other species, such as snowshoe hare (Zhou et al. 2017) and 3) increased snow depths as part of shrub feedback loops (Sturm et al. 2005).

Changes in nutritional availability may have mixed effects. Increases in more productive vegetation should translate to more nutritional forage. However, Dall's sheep prioritize open areas and

*Table 4-2: Population trends for Dall's sheep by alpine zone shown with average shrub change calculated from isolated pixel groups within growth classes.*

| Climate Class | Shrub Expansion | Alpine Zone | Population Trend |
|---|---|---|---|
| **Arctic** | 6.10 | Western Brooks Range South Slope | Decreasing |
| | | Central Brooks Range, South Slope | Decreasing |
| | | Eastern Brooks Range, South Slope | Decreasing |
| **Cold Arctic** | 3.02 | Western Brooks Range, North Slope | Decreasing |
| | | Central Brooks Range, North Slope | Decreasing |
| | | Eastern Brooks Range, North Slope | Decreasing |
| **High Precipitation** | 7.13 | Kenai Mountains | Decreasing |
| | | Alaska Range West, North Slope | Unknown |
| | | Alaska Range West, South Slope | Unknown |
| | | South Wrangell Mountains | Stable or Increasing |
| | | Chugach Mountains | Stable (at low levels) |
| | | Talkeetna Mountains | Stable (at low levels) |
| | | Alaska Range Central South Slope | Unknown |
| **Interior** | 6.01 | Alaska Range East, North Slope | Stable |
| | | Alaska Range East, South Slope | Stable |
| | | North Wrangell Mountains | Stable or Decreasing |
| | | Tanana Uplands | Stable |
| | | Alaska Range Central, North Slope | Unknown |

proximity to escape terrain in their resource selection (Roffler et al. 2016; Dertien et al. 2017). The potential improvement in nutritional content and availability may be negated by this preference. Further complicating impacts is how alternative wildlife species respond. Predation is the primary cause of mortality of ewes in the central Alaska range and eastern Brooks range and predator species is likely the product of predator composition (Arthur and Lohuis, 2015). Impacts to alternative prey species, such as snowshoe hare could both facilitate and limit Dall's sheep populations. Coyote predation on Dall's sheep increases during initial decline of cyclic hare populations (Arthur and Prugh 2010) however alternative data suggests lamb survival may increase during cyclic hare population peaks (Arthur and Lohuis, 2015).

Shrubs impact snowscapes in low precipitation climates by providing barriers for snow to accumulate and snow depths increases (Sturm et al. 2005). These increases in snow depths impact Dall's sheep winter movements are largely directed by snow density and depth combinations that allow for limited energy expenditure (Mahoney et al. 2018). Increased energy costs may also be exacerbated by increased rates of vigilance, as displayed by other prey species in response to increased shrub densities (Wheeler and Hik 2014). While species characteristics and spatial distribution of vegetation can impede avalanche risk (Gubler and Rychetnik 1991), alpine shrubline typically occurs in increasingly diffuse densities and would likely offer no decrease in avalanche risk for populations where avalanche is a primary mortality cause, such as the Chugach mountains.

Understanding how the aforementioned factors work in alpine systems may help illuminate the implications for Dall's sheep, though understanding their adaptive capacity may be more telling. Data is limited for Alaskan mountain ungulates. However, a study on plasticity of four mountain ungulate species found elevational range shifts occurred in response to warming (Büntgen et al. 2017). Such a shift, if it occurs, would likely be heterogenous throughout their range further complicating the response and differences between populations.

## 4.6 Conclusions

Through this study, we provide the broadest investigation of how regional climates impact shrub change in Alaska. We found rates of shrub change are highest in warmer, wetter climates such as the Kenai and Chugach mountains. In areas approaching temperature growth limits of shrubs, including many areas throughout the Brooks Range, temperature is the dominant driver of shrub growth and expansion. In areas above temperature growth limits, a combination of temperature and precipitation drive shrub growth and expansion. Aspect consistently impacts alpine microclimates, facilitating increased responsivity of shrub growth and expansion to temperatures on southern slopes when compared with northern slopes. Local heterogeneity of microclimatic factors likely determines the ability and scale of shrub growth and expansion within the regional temperature and precipitation ranges.

Implications for Dall's sheep are not well understood, but the landscape impacts they face as a response may mirror similar vegetation shifts at high latitude. Success of their response will vary locally and regionally as risks to population health change across their range.

## 4.7 Recommendations

There are three main ways to improve the study: 1) composite Landsat scenes across time and space in determining percent shrub dominance for the historic and modern eras 2) incorporate climatic variables on a higher native resolution and 3) incorporate field-based methods on a broadscale to account for important factors that cannot be remotely sensed.

To eliminate influence of interannual variability, methods from Berner et al. 2018 or Macander et al. 2015 applied to either Landsat TM or a Landsat TM/OLI combination would develop shrub change

rasters for almost the entire area of interest (limits based on cloud cover, similar to this study). Compositing would limit interannual variability in NDVI and thus variability in percent shrub dominance.

We used the best combination of resolution and swath available for climatic data in our study area. Improvements are needed in development and availability of SNAP rasters to meet recommendation two, but we mention it here as higher resolution would be beneficial for pixel-by-pixel analysis.

Implementing field approaches similar to Swanson (2015) across samples from different climate classes would help identify local factors important in shrub growth and expansion. This approach would be especially helpful in the interior climate class that has displayed browning trends over the same historic period and does not show strong relationship between temperature and shrub growth.

Field-based methods could improve future studies in two ways: 1) incorporation of metrics of factors related to shrub growth that are difficult to remotely sense, such as depth of active layer and 2) apply metrics focusing on Dall's sheep to help illuminate implications for population health in response to vegetative shifts throughout their range.

## Literature Cited


Ackerman, D., Griffin, D., Hobbie, S. E., & Finlay, J. C. (2017). Arctic shrub growth trajectories differ across soil moisture levels. *Global Change Biology*, *23*(10), 4294–4302. https://doi.org/10.1111/gcb.13677

Ackerman, D. E., Griffin, D., Hobbie, S. E., Popham, K., Jones, E., & Finlay, J. C. (2018). Uniform shrub growth response to June temperature across the North Slope of Alaska. *Environmental Research Letters*, *13*(4). https://doi.org/10.1088/1748-9326/aab326

Alaska Department of Fish and Game. (2011). *Dall's sheep management report of survey-inventory activities, 1 July 2007-30 June 2010. Division of Wildlife Conservation, Wildlife Management Report*.

Alaska Department of Fish and Game. (2014). *Trends in Alaska Sheep Populations, Hunting, and Harvests*.

Alaska Department of Fish and Game, & ABR, I.-E. R. and S. (2015). *Dall ' s Sheep Distribution and Abundance, Study Plan Setion 10.7, Study Completion Report*. Anchorage.

Alatalo, J. M., Jagerbrand, A. K., & Molau, U. (2016). Impacts of different climate change regimes and extreme climatic events on an alpine meadow community. *Scientific Reports*, *6*(February), 1–12. https://doi.org/10.1038/srep21720

Arthur, S. M., & Lohuis, T. D. (2014). Rate and Causes of Mortality of Dall's Sheep in Alaska: A Comparison Among Mountain Ranges. In *Proceedings of the Biennial Symposium of the Northern Wild Sheep and Goat Council* (p. 85). Fort Collins.

Arthur, S. M., & Prugh, L. R. (2010). Predator-Mediated Indirect Effects of Snowshoe Hares on Dall's Sheep in Alaska. *Journal of Wildlife Management*, *74*(8), 1709–1721. https://doi.org/10.2193/2009-322

Beck, P. S. A., & Goetz, S. J. (2011). Satellite observations of high northern latitude vegetation productivity changes between 1982 and 2008: Ecological variability and regional differences. *Environmental Research Letters*, *7*(2). https://doi.org/10.1088/1748-9326/7/2/029501

Berner, L. T., Jantz, P., Tape, K. D., & Goetz, S. J. (2018). Tundra plant above-ground biomass and shrub dominance mapped across the North Slope of Alaska. *Environmental Research Letters*, *13*(3). https://doi.org/10.1088/1748-9326/aaaa9a

Boelman, N. T., Gough, L., McLaren, J. R., & Greaves, H. (2011). Does NDVI reflect variation in the structural attributes associated with increasing shrub dominance in arctic tundra? *Environmental Research Letters*, *6*(3). https://doi.org/10.1088/1748-9326/6/3/035501

Boelman, N. T., Gough, L., Wingfield, J., Goetz, S., Asmus, A., Chmura, H. E., … Guay, K. C. (2015). Greater shrub dominance alters breeding habitat and food resources for migratory songbirds in Alaskan arctic tundra. *Global Change Biology*, *21*(4), 1508–1520. https://doi.org/10.1111/gcb.12761

Bonfils, C. J. W., Phillips, T. J., Lawrence, D. M., Cameron-Smith, P., Riley, W. J., & Subin, Z. M. (2012). On the influence of shrub height and expansion on northern high latitude climate. *Environmental Research Letters*, *7*(1). https://doi.org/10.1088/1748-9326/7/1/015503

Büntgen, U., Greuter, L., Bollmann, K., Jenny, H., Liebhold, A., Galván, J. D., … Mysterud, A. (2017). Elevational range shifts in four mountain ungulate species from the Swiss Alps. *Ecosphere*, *8*(4). https://doi.org/10.1002/ecs2.1761

Chander, G., Markham, B. L., & Helder, D. L. (2009). Summary of current radiometric calibration coefficients for Landsat MSS, TM, ETM+, and EO-1 ALI sensors. *Remote Sensing of Environment*, *113*(5), 893–903. https://doi.org/10.1016/j.rse.2009.01.007

Chapin, F. S., Sturm, M., Serreze, M. C., McFadden, J. P., Key, J. R., Lloyd, A. H., … Welker, J. M. (2005). Role of land-surface changes in arctic summer warming. *Science*, *310*(5748), 657–660. https://doi.org/10.1126/science.1117368

Chen, X., Vierling, L., & Deering, D. (2005). A simple and effective radiometric correction method to improve landscape change detection across sensors and across time. *Remote Sensing of Environment*, *98*(1), 63–79. https://doi.org/10.1016/j.rse.2005.05.021

Clark, J. B., & Lister, G. R. (1975). Photosynthetic Action Spectra of Trees. *Plant Physiology*, *55*(2), 407–413. https://doi.org/10.1104/pp.55.2.407

Dertien, J. S., Doherty, P. F., Bagley, C. F., Haddix, J. A., Brinkman, A. R., & Neipert, E. S. (2017). Evaluating Dall's sheep habitat use via camera traps. *Journal of Wildlife Management*, *81*(8), 1457–1467. https://doi.org/10.1002/jwmg.21308

Dial, R. J., Berg, E. E., Timm, K., McMahon, A., & Geek, J. (2007). Changes in the alpine forest-tundra ecotone commensurate with recent warming in southcentral Alaska: Evidence from Orthophotos and field plots. *Journal of Geophysical Research: Biogeosciences*, *112*(4), 1–15. https://doi.org/10.1029/2007JG000453

Dial, R. J., Scott Smeltz, T., Sullivan, P. F., Rinas, C. L., Timm, K., Geck, J. E., … Berg, E. C. (2016). Shrubline but not treeline advance matches climate velocity in montane ecosystems of south-central Alaska. *Global Change Biology*, *22*(5), 1841–1856. https://doi.org/10.1111/gcb.13207

Downs, C. J., Boan, B. V., Lohuis, T. D., & Stewart, K. M. (2018). Investigating Relationships between Reproduction, Immune Defenses, and Cortisol in Dall Sheep. *Frontiers in Immunology*, *9*(JAN), 1–11. https://doi.org/10.3389/fimmu.2018.00105

Elmendorf, S. C., Henry, G. H. R., Hollister, R. D., Björk, R. G., Boulanger-Lapointe, N., Cooper, E. J., … Wipf, S. (2012). Plot-scale evidence of tundra vegetation change and links to recent summer warming. *Nature Climate Change*, *2*(6), 453–457. https://doi.org/10.1038/nclimate1465

Fraser, R. H., Lantz, T. C., Olthof, I., Kokelj, S. V., & Sims, R. A. (2014). Warming-Induced Shrub Expansion and Lichen Decline in the Western Canadian Arctic. *Ecosystems*, *17*(7), 1151–1168. https://doi.org/10.1007/s10021-014-9783-3

Frost, G. V., Epstein, H. E., & Walker, D. A. (2014). Regional and landscape-scale variability of Landsat-observed vegetation dynamics in northwest Siberian tundra. *Environmental Research Letters*, *9*(2). https://doi.org/10.1088/1748-9326/9/2/025004

Gallant, A. L., Binnian, E. F., Omernik, J. M., & Shasby, M. B. (1995). *Ecoregions of Alaska - U.S. Geological Survey Professional Paper 1567*. https://doi.org/0160482909\r0607010010

Gao, B. C., & Li, R. R. (2000). Quantitative improvement in the estimates of NDVI values from remotely sensed data by correcting thin cirrus scattering effects. *Remote Sensing of Environment*, *74*(3), 494–502. https://doi.org/10.1016/S0034-4257(00)00141-3

Gubler, H., & Rychetnik, J. (1991). Effects of forests near the timberline on avalanche formation. *IAHS Publication (International Association of Hydrological Sciences)*, (205), 19–38.

Hallinger, M., Manthey, M., & Wilmking, M. (2010). Establishing a missing link: warm summers and winter snow cover promote shrub expansion into alpine tundra in Scandinavia. *New Phytologist*, *186*(4), 890–899. https://doi.org/10.1111/j.1469-8137.2010.03223.x

Harris, I., Jones, P. D., Osborn, T. J., & Lister, D. H. (2014). Updated high-resolution grids of monthly climatic observations - the CRU TS3.10 Dataset. *International Journal of Climatology*, *34*(3), 623–642. https://doi.org/10.1002/joc.3711

Harsch, M. A., Hulme, P. E., McGlone, M. S., & Duncan, R. P. (2009). Are treelines advancing? A global meta-analysis of treeline response to climate warming. *Ecology Letters*, *12*(10), 1040–1049. https://doi.org/10.1111/j.1461-0248.2009.01355.x

Hudson, J. M. G., Henry, G. H. R., & Cornwell, W. K. (2011). Taller and larger: Shifts in Arctic tundra leaf traits after 16 years of experimental warming. *Global Change Biology*, *17*(2), 1013–1021. https://doi.org/10.1111/j.1365-2486.2010.02294.x

Irons, J. R., Dwyer, J. L., & Barsi, J. A. (2012). The next Landsat satellite: The Landsat Data Continuity Mission. *Remote Sensing of Environment*, *122*, 11–21. https://doi.org/10.1016/j.rse.2011.08.026

Jex, B. A., Ayotte, J. B., Bleich, V. C., Brewer, C. E., Bruning, D. L., Larter, N. C., … Wagner, M. W. (2016). *Thinhorn sheep: conservation challenges and management strategies for the 21st century*. Boise, Idaho, USA.

Jia, G. J., Epstein, H. E., & Walker, D. A. (2004). Controls over intra-seasonal dynamics of AVHRR NDVI for the Arctic tundra in northern Alaska. *International Journal of Remote Sensing*, *25*(9), 1547–1564. https://doi.org/10.1080/0143116021000023925

Ju, J., & Masek, J. G. (2016). The vegetation greenness trend in Canada and US Alaska from 1984-2012 Landsat data. *Remote Sensing of Environment*, *176*, 1–16. https://doi.org/10.1016/j.rse.2016.01.001

Juszak, I., Erb, A. M., Maximov, T. C., & Schaepman-Strub, G. (2014). Arctic shrub effects on NDVI, summer albedo and soil shading. *Remote Sensing of Environment*, *153*, 79–89. https://doi.org/10.1016/j.rse.2014.07.021

Kasischke, E. S., Verbyla, D. L., Rupp, T. S., Mcguire, A. D., Murphy, K. A., Jandt, R., … Turetsky, M. R. (2010). Alaska ' s changing fire regime - implications for the vulnerability of its boreal forests. *The Canadian Journal of Forest Research*, *40*, 1313–1324. https://doi.org/10.1139/X10-098

Knipling, E. (1970). Physical and Physiological Basis for Reflectance of Visible and Near-Infrared Radiation from Vegetation. *Remote Sensing of Environment*, *1*, 155–159. https://doi.org/10.3171/2017.4.PEDS17159.

Ling, F., & Zhang, T. (2007). Modeled impacts of changes in tundra snow thickness on ground thermal regime and heat flow to the atmosphere in Northernmost Alaska. *Global and Planetary Change*, *57*(3–4), 235–246. https://doi.org/10.1016/j.gloplacha.2006.11.009

Macander, M. J., Frost, G. V., Nelson, P. R., & Swingley, C. S. (2017). Regional quantitative cover mapping of tundra plant functional types in Arctic Alaska. *Remote Sensing*, *9*(10), 1–26. https://doi.org/10.3390/rs9101024

Mahoney, P. J., Liston, G. E., LaPoint, S., Gurarie, E., Mangipane, B., Wells, A. G., … Prugh, L. R. (2018). Navigating snowscapes: scale-dependent responses of mountain sheep to snowpack properties. *Ecological Applications*, *28*(7), 1715–1729. https://doi.org/10.1002/eap.1773

Marcot, B. G., Jorgenson, M. T., Lawler, J. P., Handel, C. M., & DeGange, A. R. (2015). Projected changes in wildlife habitats in Arctic natural areas of northwest Alaska. *Climatic Change*, *130*(2), 145–154. https://doi.org/10.1007/s10584-015-1354-x

McCullough, D. R. (1999). Density dependence and life-history strategies of ungulates. *Journal of Mammology*, *80*(4), 1130–1146.

Melesse, A. M., Weng, Q., Thenkabail, P. S., & Senay, G. B. (2007). Remote Sensing Sensors and Applications in Environmental Resources Mapping and Modelling. *Sensors*, (7), 3209–3241. https://doi.org/10.3390/s7123209

Mitchell, C. D., Chaney, R., Aho, K., Kie, J. G., & Bowyer, R. T. (2015). Population density of Dall's sheep in Alaska: effects of predator harvest? *Mammal Research*, *60*(1), 21–28. https://doi.org/10.1007/s13364-014-0199-4

Myers-Smith, I. H., Forbes, B. C., Wilmking, M., Hallinger, M., Lantz, T., Blok, D., … Hik, D. S. (2011). Shrub expansion in tundra ecosystems: Dynamics, impacts and research priorities. *Environmental Research Letters*, *6*(4). https://doi.org/10.1088/1748-9326/6/4/045509

Olthof, I. A. N., Pouliot, D., Latifovic, R., & Chen, W. (2008). Recent ( 1986-2006 ) Vegetation-Specific NDVI Trends in Northern Canada from Satellite Data. *Arctic Institute of North America*, *61*(4), 381–394. Retrieved from https://www.jstor.org/stable/40513225

Parent, M. B., & Verbyla, D. (2010). The browning of Alaska's boreal forest. *Remote Sensing*, *2*(12), 2729–2747. https://doi.org/10.3390/rs2122729

Peñuelas, J., & Filella, L. (1998). Technical focus: Visible and near-infrared reflectance techniques for diagnosing plant physiological status. *Trends in Plant Science*, *3*(4), 151–156. https://doi.org/10.1016/S1360-1385(98)01213-8

Pettorelli, N., Vik, J. O., Mysterud, A., Gaillard, J. M., Tucker, C. J., & Stenseth, N. C. (2005). Using the satellite-derived NDVI to assess ecological responses to environmental change. *Trends in Ecology and Evolution*, *20*(9), 503–510. https://doi.org/10.1016/j.tree.2005.05.011

Pozzanghera, C. B., Sivy, K. J., Lindberg, M. S., & Prugh, L. R. (2016). Variable effects of snow conditions across boreal mesocarnivore species. *Canadian Journal of Zoology*, *94*(10), 697–705. https://doi.org/10.1139/cjz-2016-0050

Rachlow, J. L., & Terry Bowyer, R. (1998). Habitat selection by Dall's sheep (Ovis Dall'si): Maternal trade-offs. *Journal of Zoology*, *245*(4), 457–465. https://doi.org/10.1017/S0952836998008097

Racine, C., Janet, R., Meyers, C., & Dennis, J. (2004). Tundra Fire and Vegetation Change along a Hillslope on the Seward Peninsula, Alaska, U.S.A. *Arctic, Antarctic, and Alpine Research*, *36*(1), 1–10. https://doi.org/10.1657/1523-0430(2004)036[0001:tfavca]2.0.co;2

Rattenbury, K. L., Schmidt, J. H., Swanson, D. K., Borg, B. L., Mangipane, B. A., & Sousanes, P. J. (2018). Delayed spring onset drives declines in abundance and recruitment in a mountain ungulate. *Ecosphere*, *9*(11), 1–15. https://doi.org/10.1002/ecs2.2513

Raynolds, M. K., Walker, D. A., Verbyla, D., & Munger, C. A. (2013). Patterns of Change within a Tundra Landscape: 22-year Landsat NDVI Trends in an Area of the Northern Foothills of the Brooks Range, Alaska. *Arctic, Antarctic, and Alpine Research*, *45*(2), 249–260. https://doi.org/10.1657/1938-4246-45.2.249

Roffler, G. H., Adams, L. G., & Hebblewhite, M. (2016). Summer habitat selection by Dall's sheep in Wrangell-St. Elias National Park and Preserve, Alaska. *Journal of Mammalogy*, *98*(1), gyw135. https://doi.org/10.1093/jmammal/gyw135

Ropars, P., & Boudreau, S. (2012). Shrub expansion at the forest-tundra ecotone: Spatial heterogeneity linked to local topography. *Environmental Research Letters*, *7*(1). https://doi.org/10.1088/1748-9326/7/1/015501

Scenarios Network for Alaska and Arctic Planning, University of Alaska. (2019) *SNAP Data*. Retrieved January 14th, 2019 from http://ckan.snap.uaf.edu/dataset.

Sharratt, B. S. (1992). Growing Season Trends in the Alaskan Climate Record. *Arctic Institute of North America*, *45*(2), 124–127.

Song, C., Woodcock, C. E., Seto, K. C., Lenney, M. P., & Macomber, S. A. (2001). Classification and Change Detection Using Landsat TM Data. *Remote Sensing of Environment*, *75*(2), 230–244. https://doi.org/10.1016/s0034-4257(00)00169-3

Stafford, J. M., Wendler, G., & Curtis, J. (2000). Temperature and precipitation of Alaska: 50 year trend analysis. *Theoretical and Applied Climatology*, *67*(1–2), 33–44. https://doi.org/10.1007/s007040070014

Sturm, M., McFadden, J. P., Liston, G. E., Stuart Chapin, F., Racine, C. H., & Holmgren, J. (2001). Snow-shrub interactions in Arctic Tundra: A hypothesis with climatic implications. *Journal of Climate*, *14*(3), 336–344. https://doi.org/10.1175/1520-0442(2001)014<0336:SSIIAT>2.0.CO;2

Sturm, M., Schimel, J., Michaelson, G. J., Welker, J. M., Oberbauer, S. F., Liston, G. E., … Romanovsky, V. E. (2005). Winter biological processes could help convert arctic tundra to shrubland. *BioScience*, *55*(1), 17–26. https://doi.org/10.1641/0006-3568(2005)055[0017:WBPCHC]2.0.CO;2

Swann, A. L., Fung, I. Y., Levis, S., Bonan, G. B., & Doney, S. C. (2010). Changes in Arctic vegetation amplify high-latitude warming through the greenhouse effect. *Proceedings of the National Academy of Sciences of the United States of America*, *107*(4), 1295–1300. https://doi.org/10.1073/pnas.0913846107

Swanson, D. K. (2015). Environmental limits of tall shrubs in Alaska's Arctic national parks. *PLoS ONE*, *10*(9), 1–34. https://doi.org/10.1371/journal.pone.0138387

Tape, K. D., Sturm, M., & Racine, C. H. (2006). The evidence for shrub expansion in Northern Alaska and the Pan-Arctic. *Global Change Biology*, *12*, 686–702. https://doi.org/10.1111/j.1365-2486.2006.01128.x

Tape, K. D., Hallinger, M., Welker, J. M., & Ruess, R. W. (2012). Landscape Heterogeneity of Shrub Expansion in Arctic Alaska. *Ecosystems*, *15*(5), 711–724. https://doi.org/10.1007/s10021-012-9540-4

Tape, K. D., Gustine, D. D., Ruess, R. W., Adams, L. G., & Clark, J. A. (2016). Range expansion of moose in Arctic Alaska linked to warming and increased shrub habitat. *PLoS ONE*, *11*(7), 1–12. https://doi.org/10.1371/journal.pone.0160049

Tømmervik, H., Johansen, B., Riseth, J. Å., Karlsen, S. R., Solberg, B., & Høgda, K. A. (2009). Above ground biomass changes in the mountain birch forests and mountain heaths of Finnmarksvidda, northern Norway, in the period 1957-2006. *Forest Ecology and Management*, *257*(1), 244–257. https://doi.org/10.1016/j.foreco.2008.08.038

Tucker, C. J., Slayback, D. A., Pinzon, J. E., Ranga, S. O. L., & Taylor, M. G. (2001). Higher northern latitude normalized difference vegetation index, *7*, 184–190.

van de Kerk, M., D. Verbyla, A.W. Nolin, K.J. Sivy, and L.R. Prugh. (2018a). ABoVE: Dall Sheep Lamb Recruitment and Climate Data, Alaska and NW Canada, 2000-2015. ORNL DAAC, Oak Ridge, Tennessee, USA. https://doi.org/10.3334/ORNLDAAC/1640

van de Kerk, M., Verbyla, D., Nolin, A. W., Sivy, K. J., & Prugh, L. R. (2018b). Range-wide variation in the effect of spring snow phenology on Dall sheep population dynamics. *Environmental Research Letters*, *13*(7). https://doi.org/10.1088/1748-9326/aace64

Verbyla, D. (2008). The greening and browning of Alaska based on 1982-2003 satellite data. *Global Ecology and Biogeography*, *17*(4), 547–555. https://doi.org/10.1111/j.1466-8238.2008.00396.x

Verbyla, D. (2018) ABoVE: MODIS-derived Maximum NDVI, Northern Alaska and Yukon Territory for 2002-2017. ORNL DAAC, Oak Ridge, Tennessee, USA. https://doi.org/10.3334/ORNLDAAC/1614

Verbyla, D., & Kurkowski, T. A. (2019). NDVI–Climate relationships in high-latitude mountains of Alaska and Yukon Territory. *Arctic, Antarctic, and Alpine Research*, *51*(1), 397–411. https://doi.org/10.1080/15230430.2019.1650542

Walker, K. M., & Zenone, C. (1988). Multitemporal Landsat multispectral scanner and thematic mapper data of the Hubbard Glacier region, southeast Alaska. *Photogrammetric Engineering & Remote Sensing*, *54*(3), 373–376.

Weier, J., & Herring, D. (2000). Measuring Vegetation (NDVI & EVI). Retrieved from http://earthobservatory.nasa.gov/Features/MeasuringVegetation/measuring_vegetation_1.php

Welker, J. M., Fahnestock, J. T., Sullivan, P. F., & Chimner, R. A. (2005). Leaf mineral nutrition of Arctic plants in response to warming and deeper snow in northern Alaska. *Oikos*, *109*(1), 167–177. https://doi.org/10.1111/j.0030-1299.2005.13264.x

Wheeler, H. C., & Hik, D. S. (2014). Giving-up densities and foraging behavior indicate possible effects of shrub encroachment on arctic ground squirrels. *Animal Behaviour*, *95*, 1–8. https://doi.org/10.1016/j.anbehav.2014.06.005

Worley, K., Strobeck, C., Arthur, S., Carey, J., Schwantje, H., Veitch, A., & Coltman, D. W. (2004). Population genetic structure of North American thinhorn sheep (Ovis dalli). *Molecular Ecology*, *13*(9), 2545–2556. https://doi.org/10.1111/j.1365-294X.2004.02248.x

Zhou, J., Prugh, L., Kielland, K., Kofinas, G., & D. Tape, K. (2017). The Role of Vegetation Structure in Controlling Distributions of Vertebrate Herbivores in Arctic Alaska. *Arctic, Antarctic, and Alpine Research*, *49*(2), 291–304. https://doi.org/10.1657/aaar0016-058

# Appendix

All single-variate plots were developed by binning the climatic variable of interest and extracting the mean value for the shrub variable of interest. Shrub variables are 1) change in percent shrub dominance or 2) modern percent shrub dominance. All pairwise comparisons that examine collinearity between independent variables were developed by binning the shrub variable of interest and extracting the mean value for the climatic variables. The scene comparisons plots show global means for each scene-pair of the shrub variable and climatic variable of interest.

Arctic | Path 68 Row 11

Single-Variate Plots of Change in Percent Shrub Dominance As a Product of Modern Climatic Factors

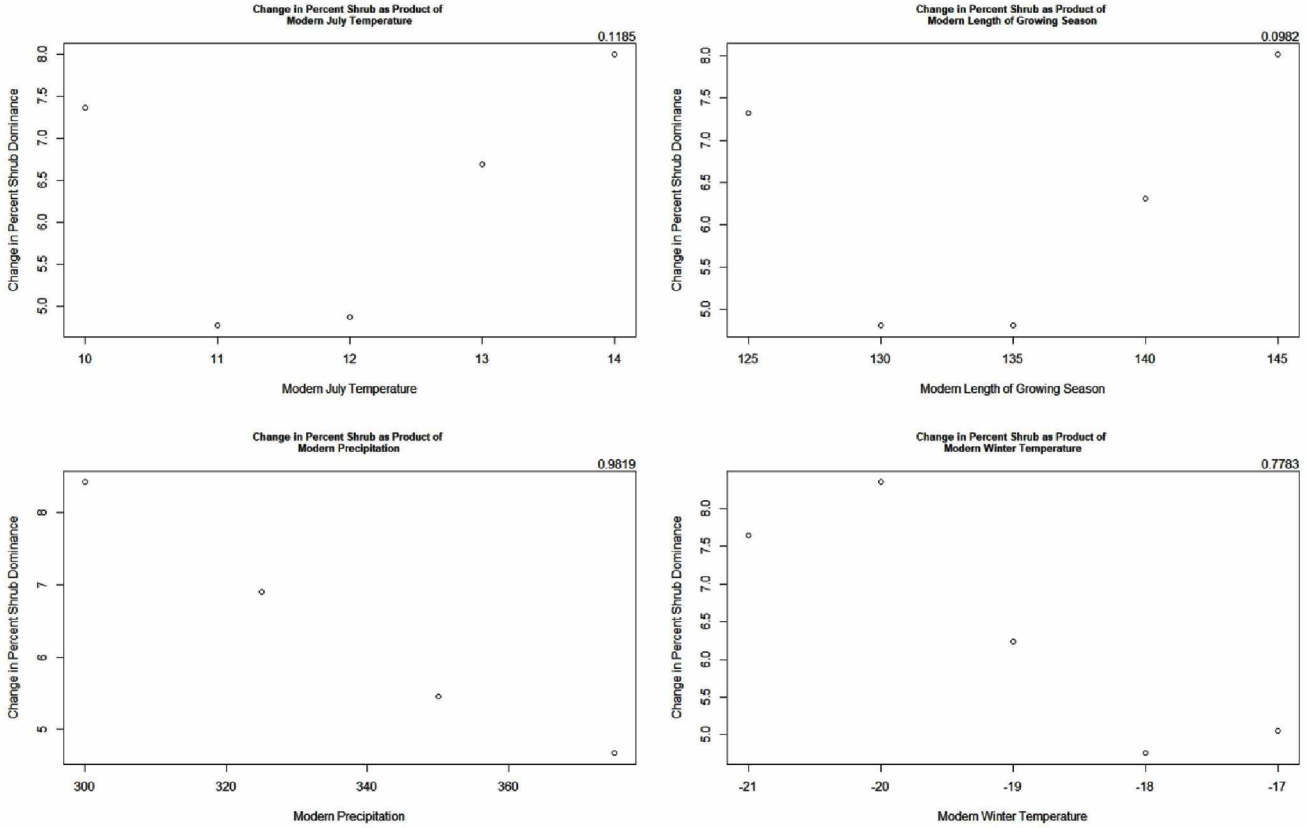

Arctic | Path 68 Row 11

Single-Variate Plots of Change in Percent Shrub Dominance As a Product of Modern Climatic Factors

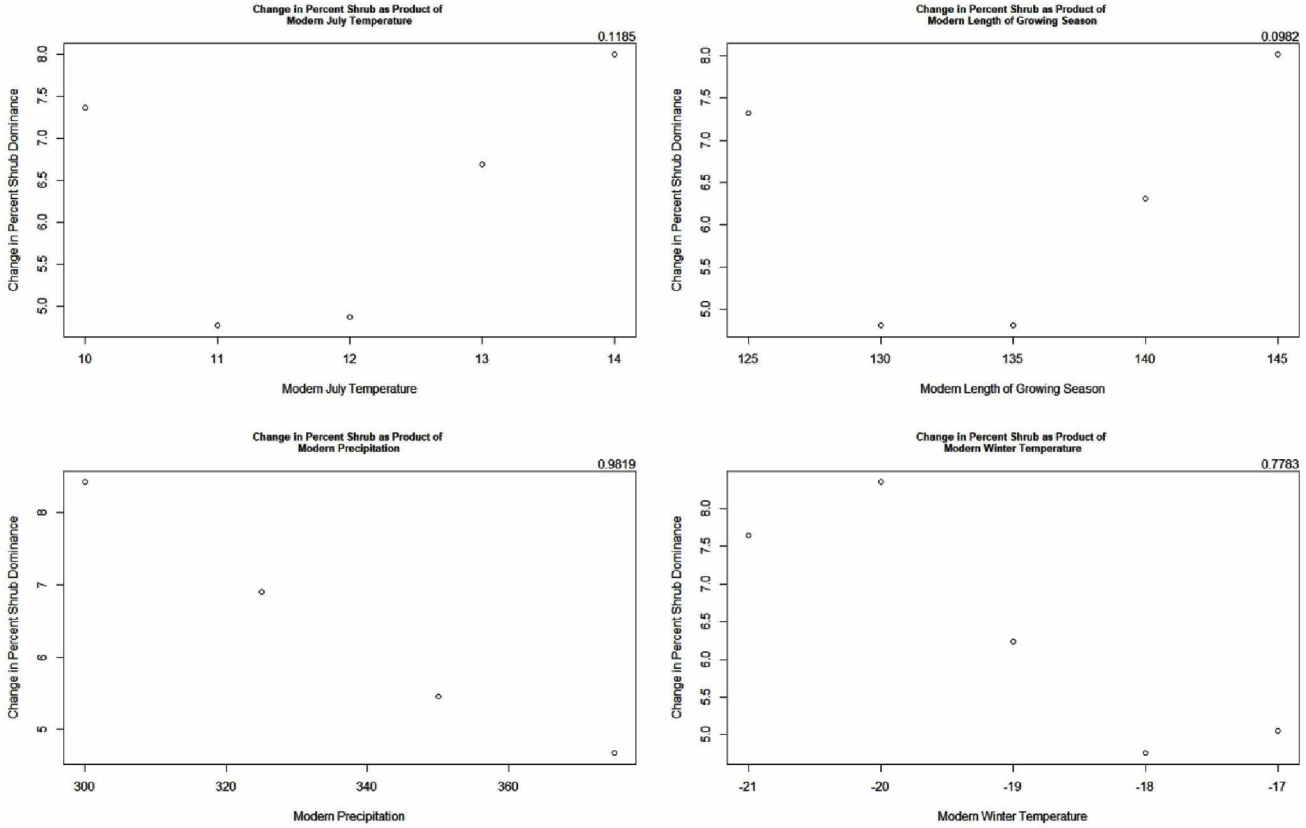

Cold Arctic | Path 75 Row 12

Single-Variate Plots of Change in Percent Shrub Dominance As a Product of Change in Climatic Factors

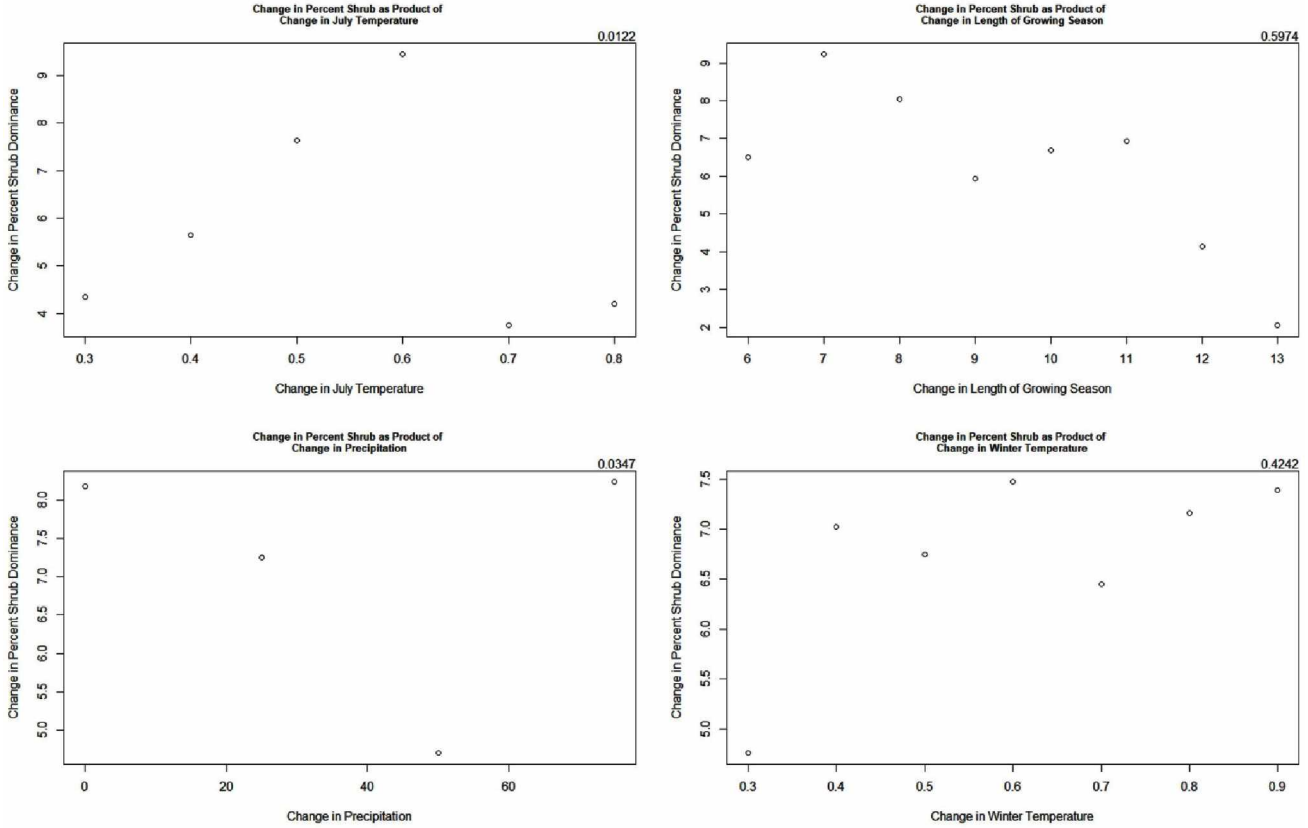

Cold Arctic | Path 75 Row 12

Single-Variate Plots of Change in Percent Shrub Dominance As a Product of Modern Climatic Factors

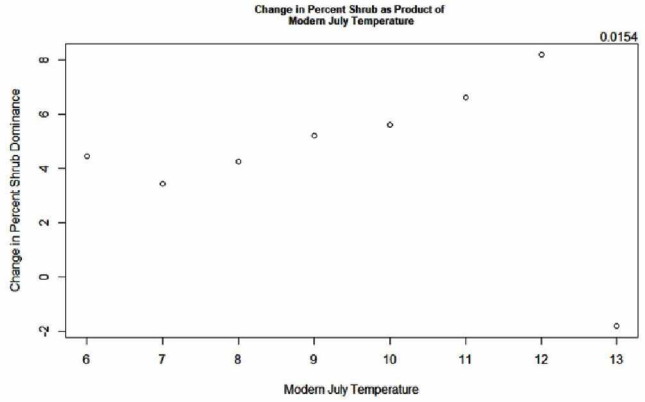


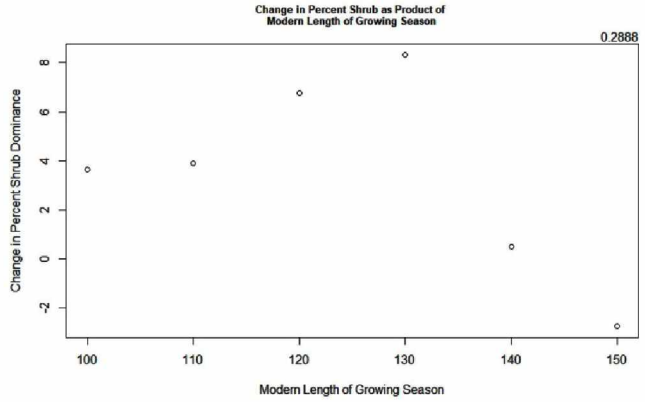


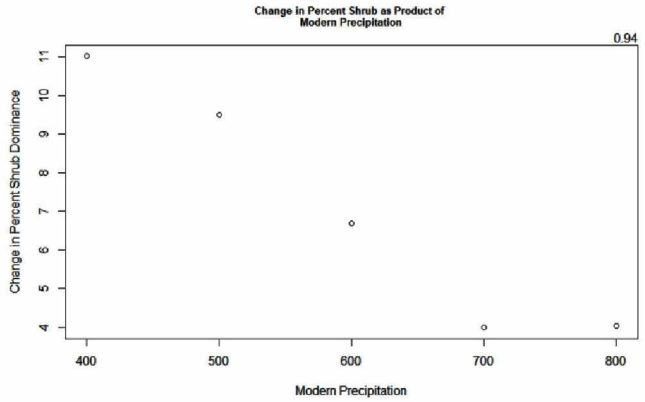


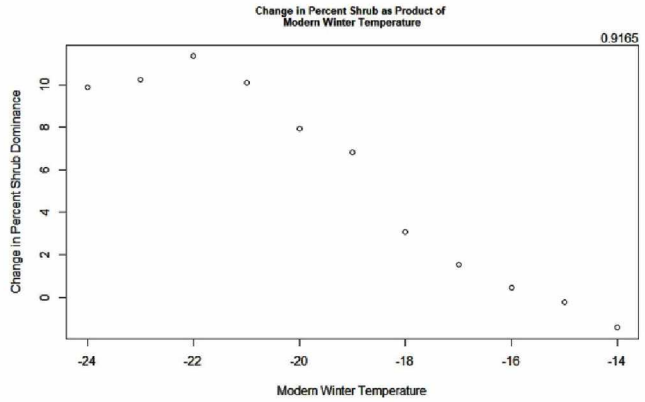

Cold Arctic | Path 75 Row 12

Single-Variate Plots of Change in Percent Shrub Dominance As a Product of Terrain Factors

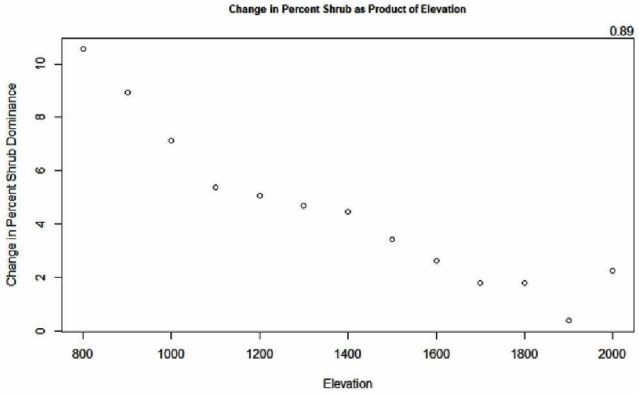


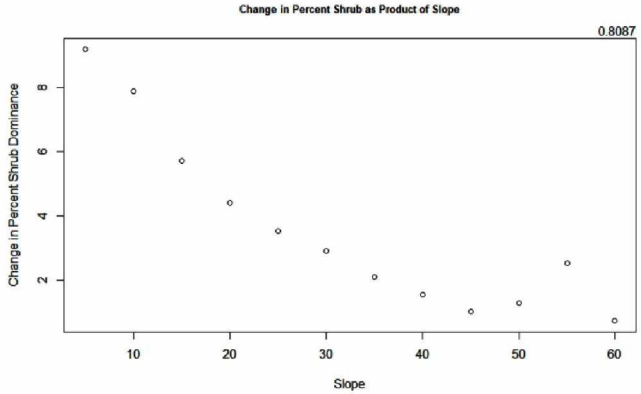


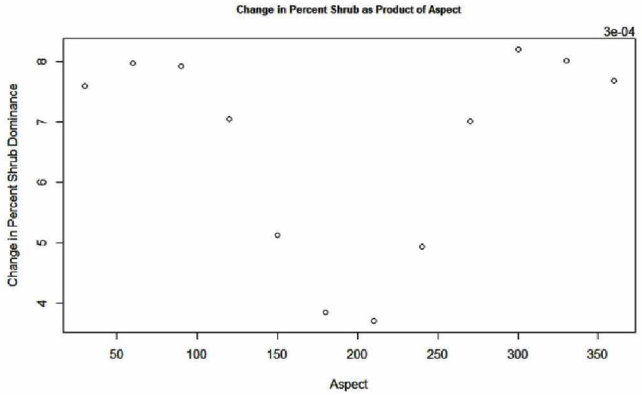

Cold Arctic | Path 75 Row 12

Single-Variate Plots of Modern Percent Shrub Dominance As a Product of Modern Climatic Factors

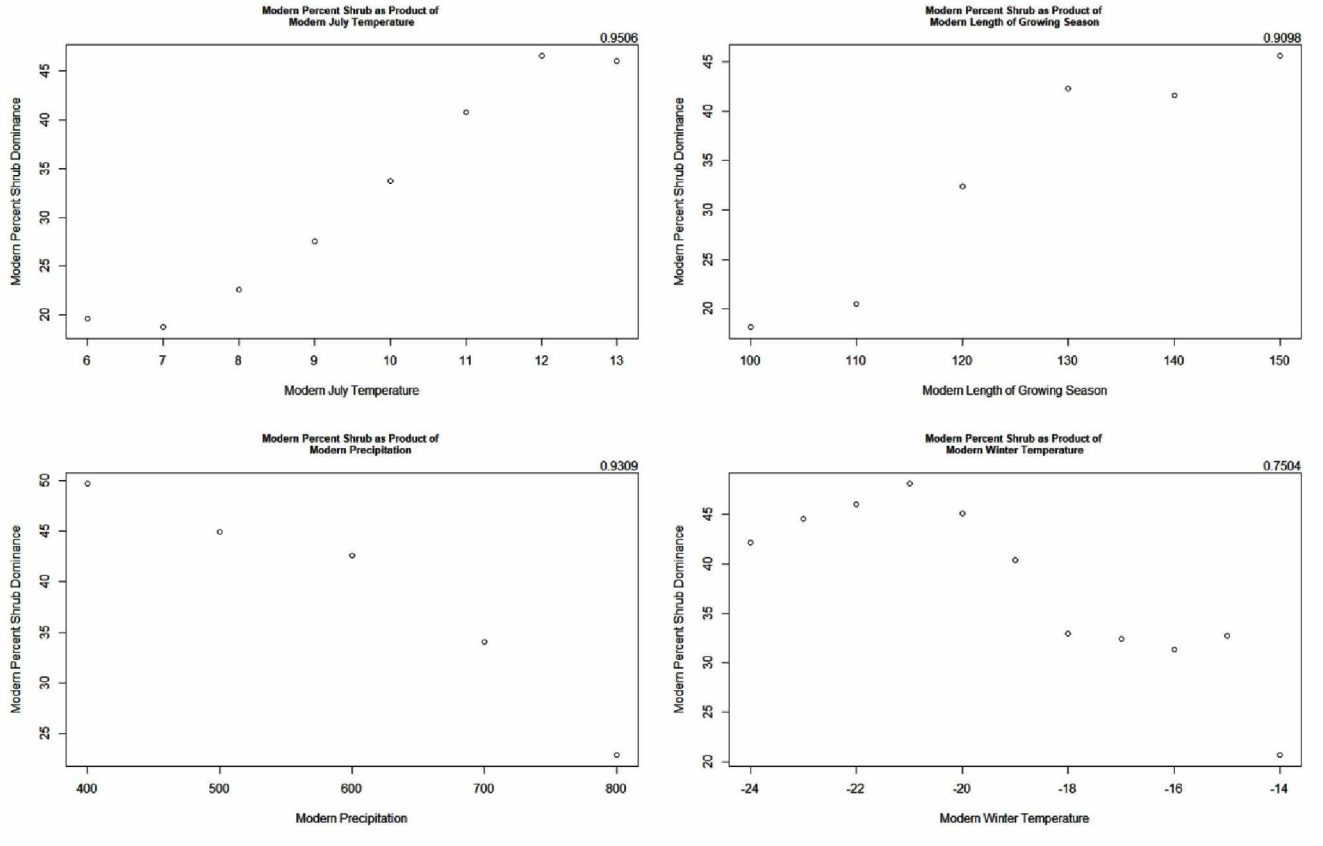

Cold Arctic | Path 75 Row 12

Single-Variate Plots of Modern Percent Shrub Dominance As a Product of Change in Climatic Factors

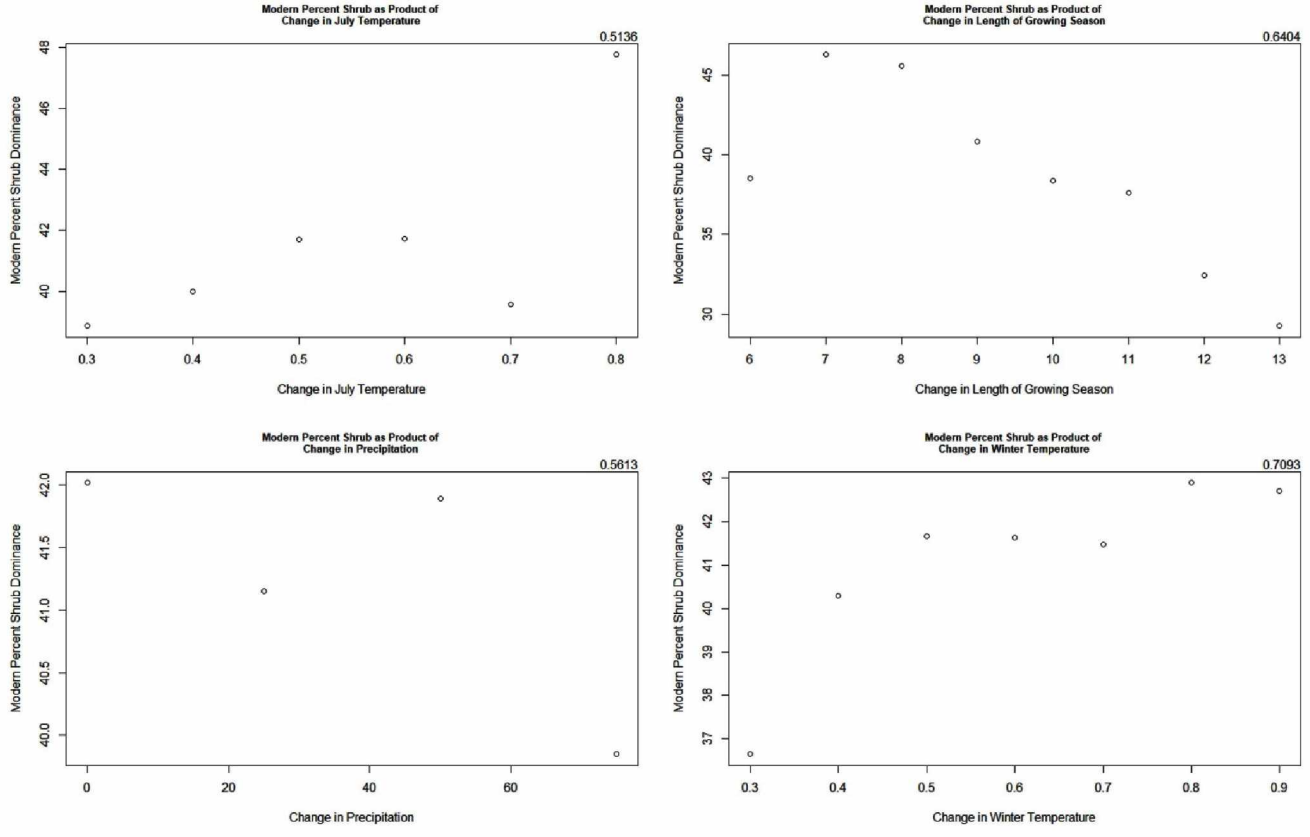

Cold Arctic | Path 75 Row 12

Single-Variate Plots of Modern Percent Shrub Dominance As a Product of Terrain Factors

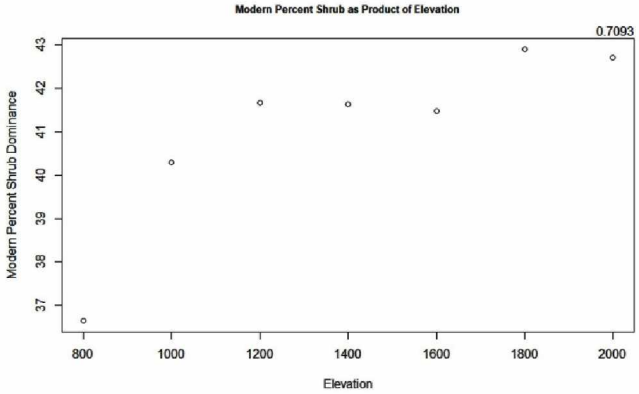


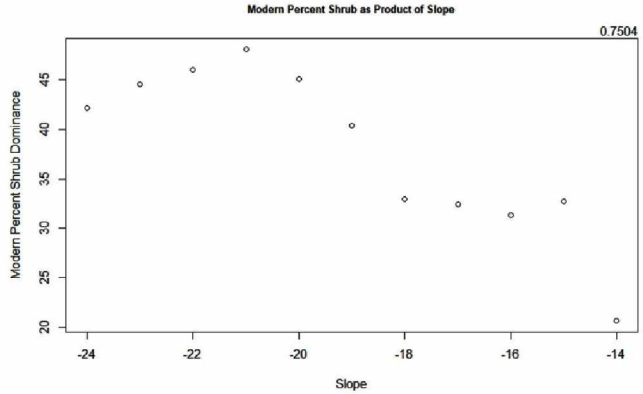


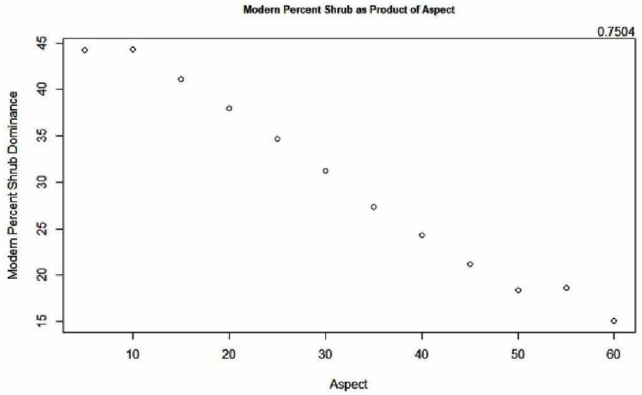

Cold Arctic | Path 75 Row 12

Pair Comparisons of Variables Using Change in Percent Shrub Dominance Bins

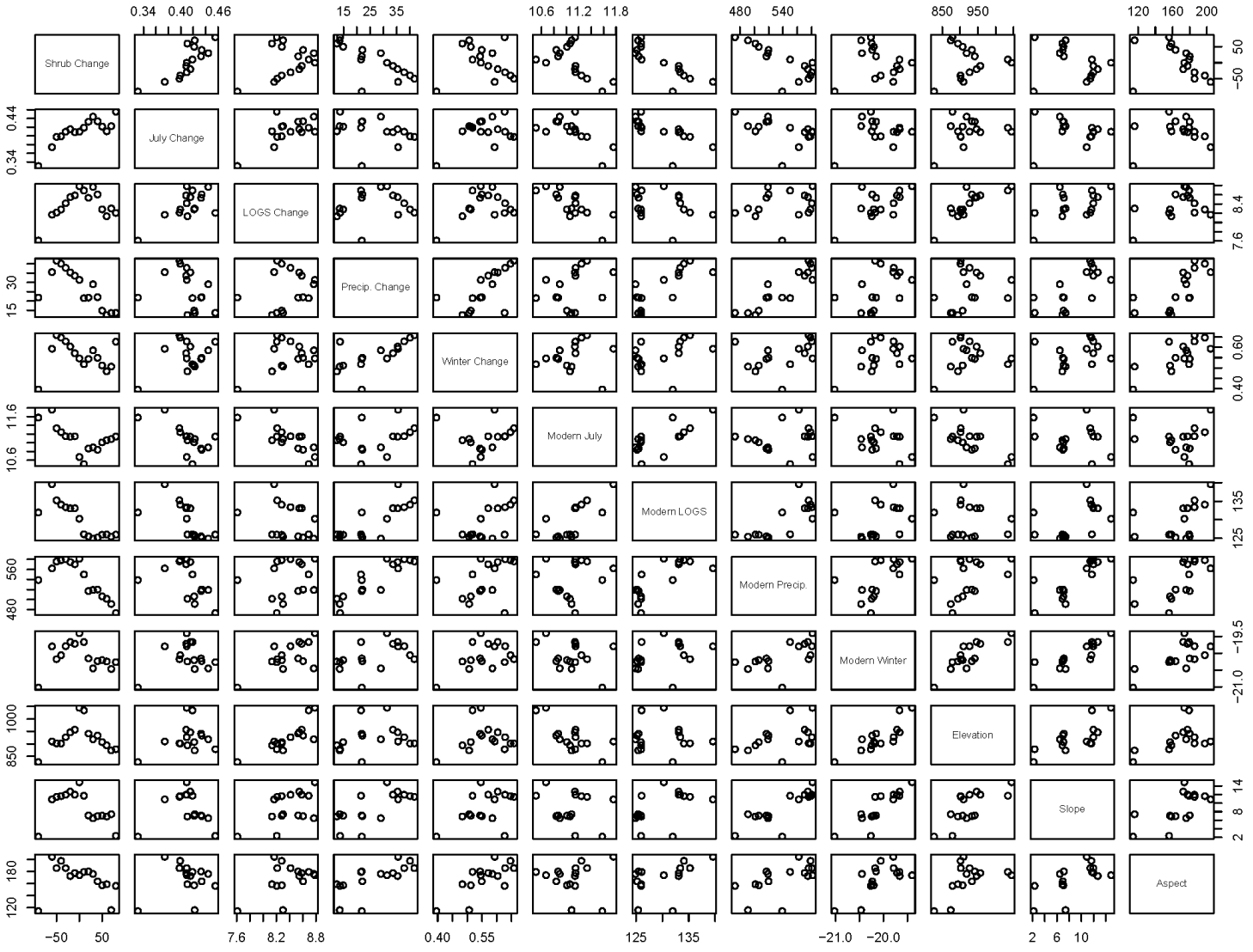

Cold Arctic | Path 75 Row 12

Pair Comparisons of Variables Using Modern Percent Shrub Dominance Bins

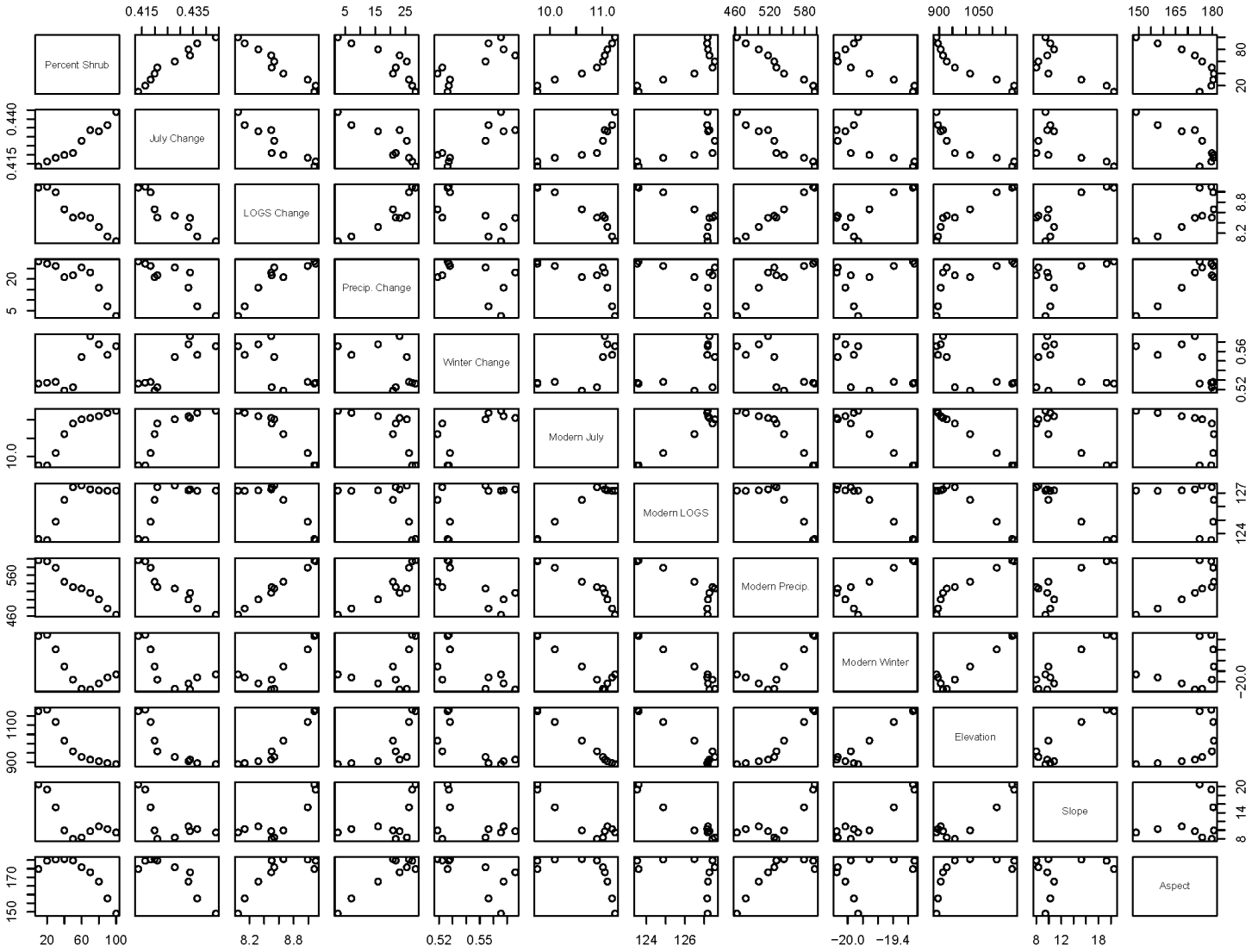

Cold Arctic | Path 75 Row 13

Single-Variate Plots of Change in Percent Shrub Dominance As a Product of Change in Climatic Factors

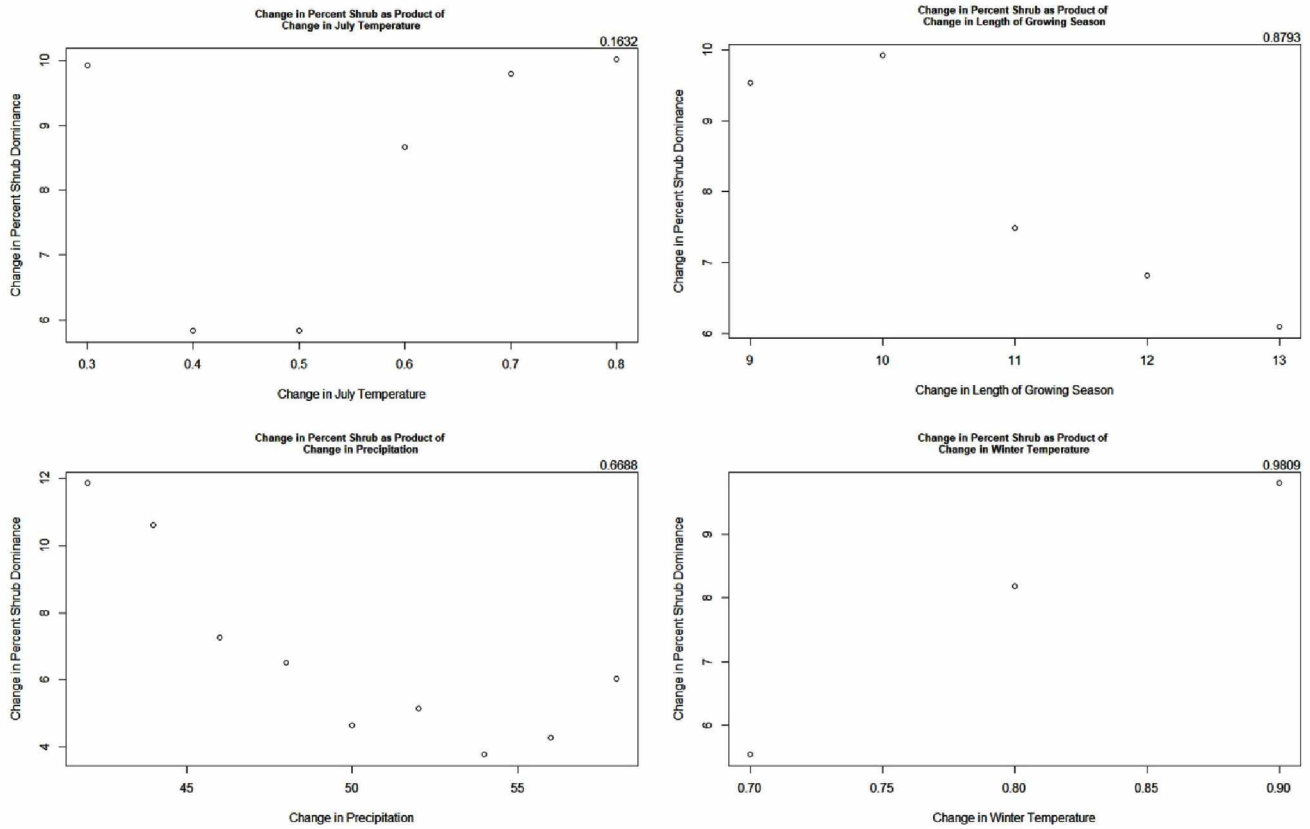

Cold Arctic | Path 75 Row 13

Single-Variate Plots of Change in Percent Shrub Dominance As a Product of Modern Climatic Factors

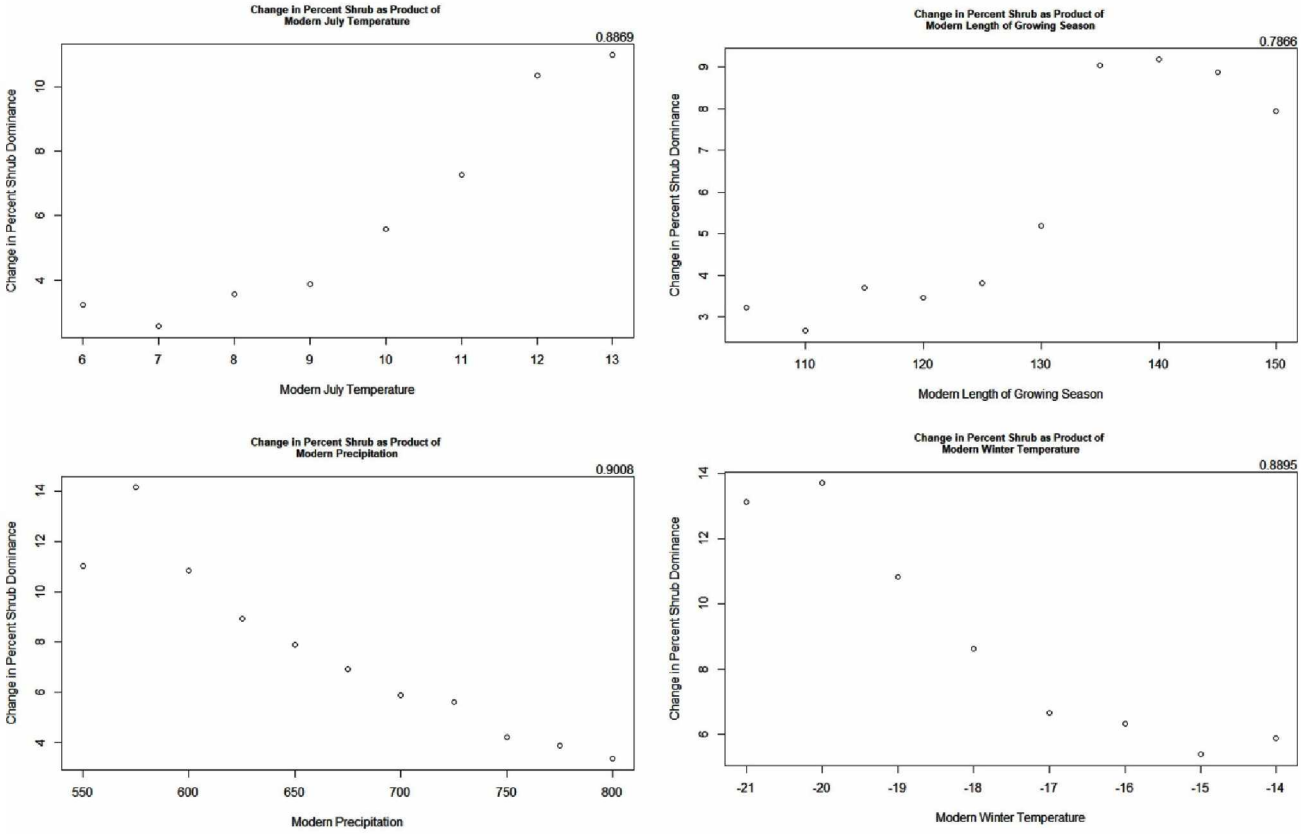

Cold Arctic | Path 75 Row 13

Single-Variate Plots of Change in Percent Shrub Dominance As a Product of Terrain Factors

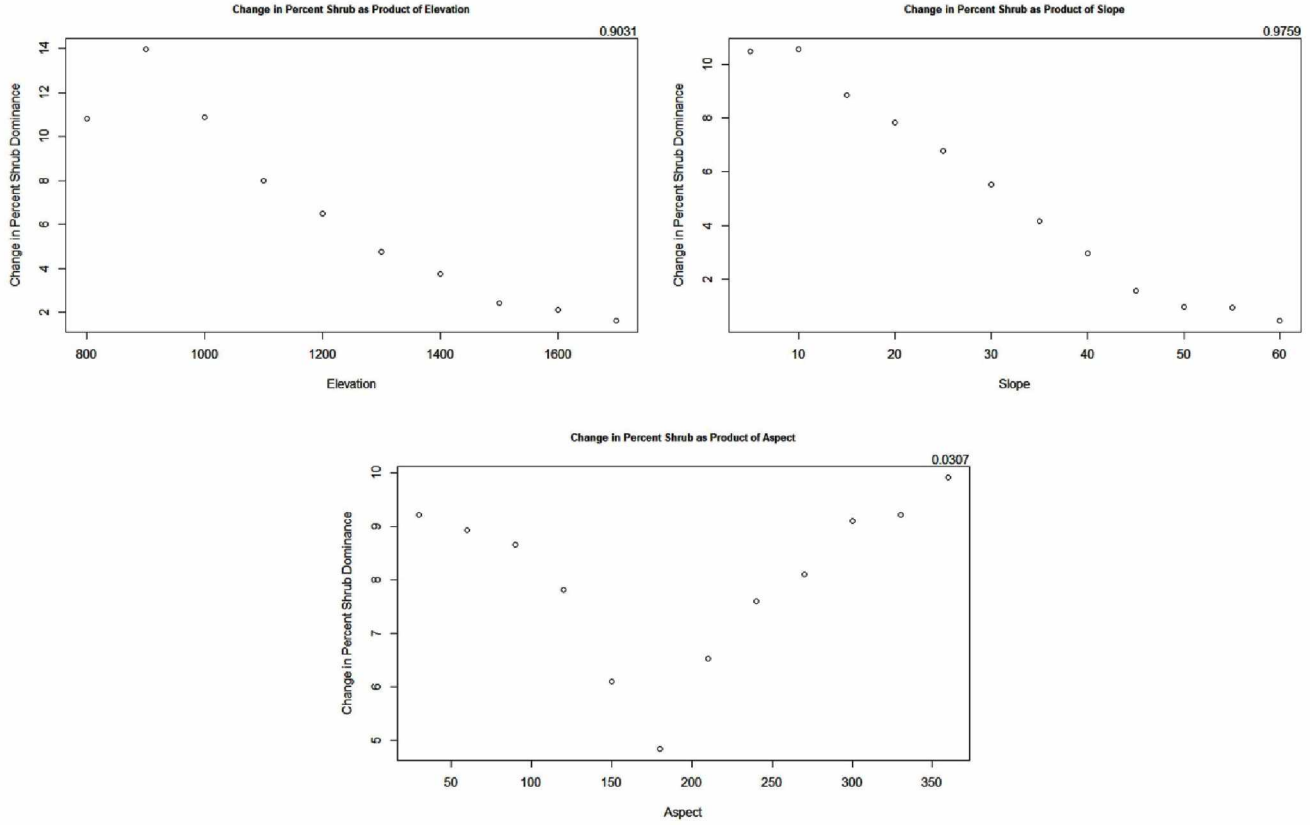

Cold Arctic | Path 75 Row 13

Single-Variate Plots of Modern Percent Shrub Dominance As a Product of Modern Climatic Factors

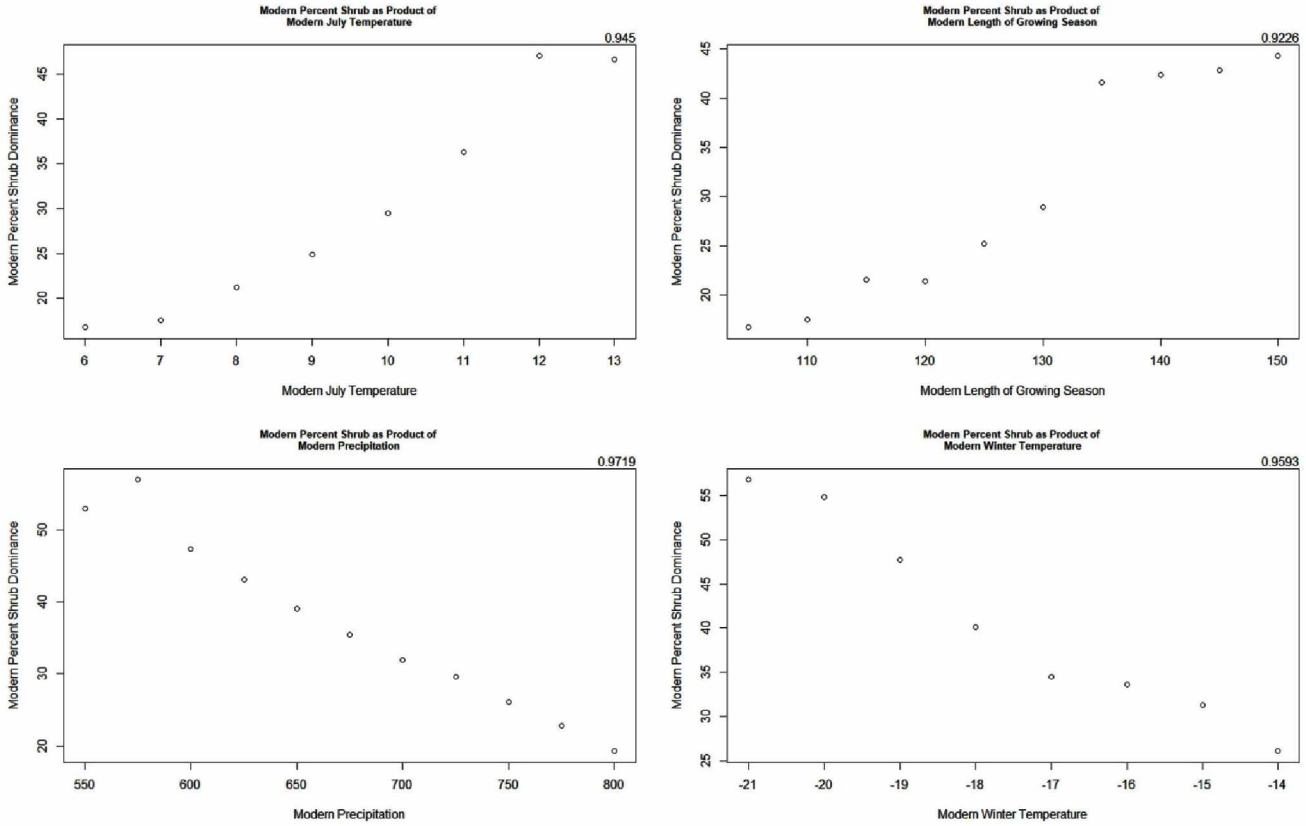

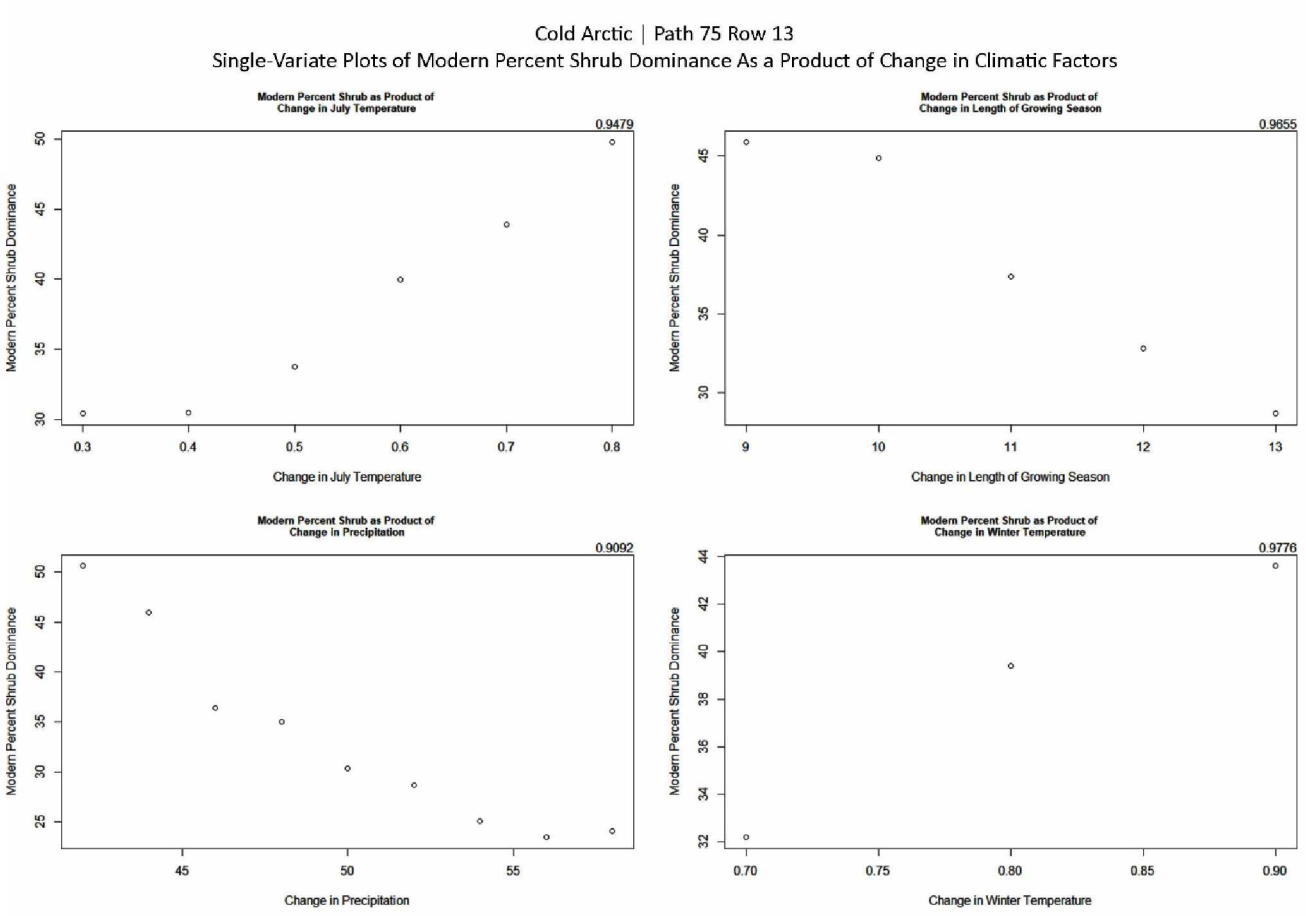
Cold Arctic | Path 75 Row 13
Single-Variate Plots of Modern Percent Shrub Dominance As a Product of Change in Climatic Factors
Modern Percent Shrub as Product of Change in July Temperature
0.9479
Modern Percent Shrub Dominance
Change in July Temperature
Modern Percent Shrub as Product of Change in Length of Growing Season
0.9655
Modern Percent Shrub Dominance
Change in Length of Growing Season
Modern Percent Shrub as Product of Change in Precipitation
0.9092
Modern Percent Shrub Dominance
Change in Precipitation
Modern Percent Shrub as Product of Change in Winter Temperature
0.9776
Modern Percent Shrub Dominance
Change in Winter Temperature

Cold Arctic | Path 75 Row 13

Single-Variate Plots of Modern Percent Shrub Dominance As a Product of Terrain Factors

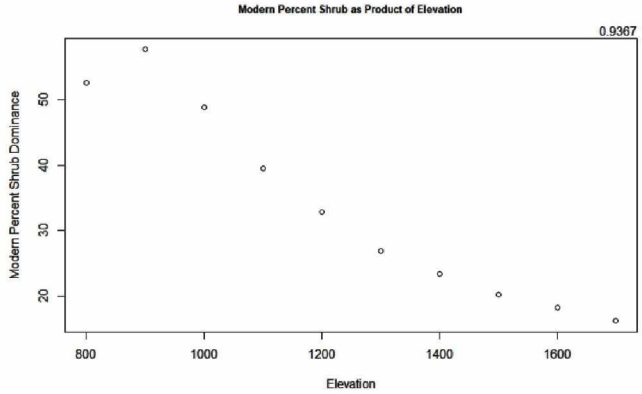


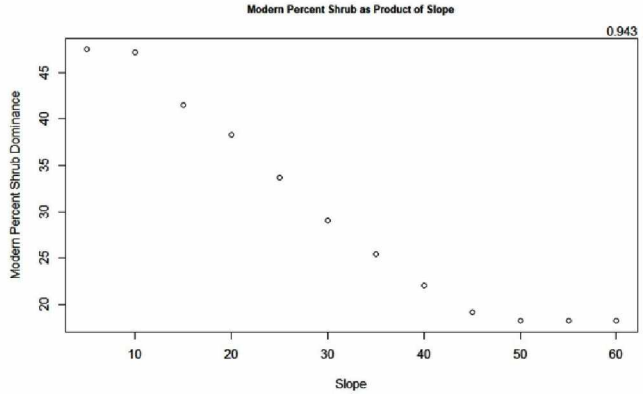


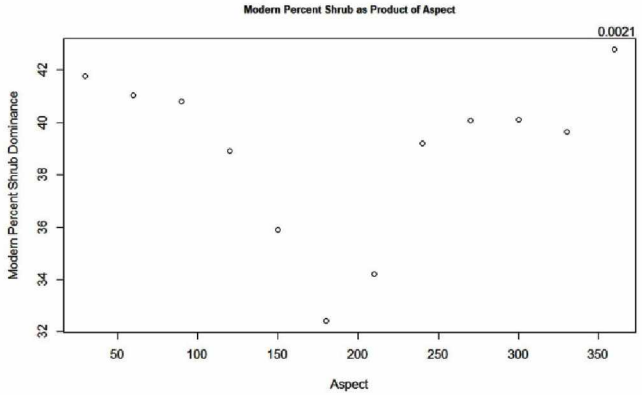

Cold Arctic | Path 75 Row 13

Pair Comparisons of Variables Using Change in Percent Shrub Dominance Bins

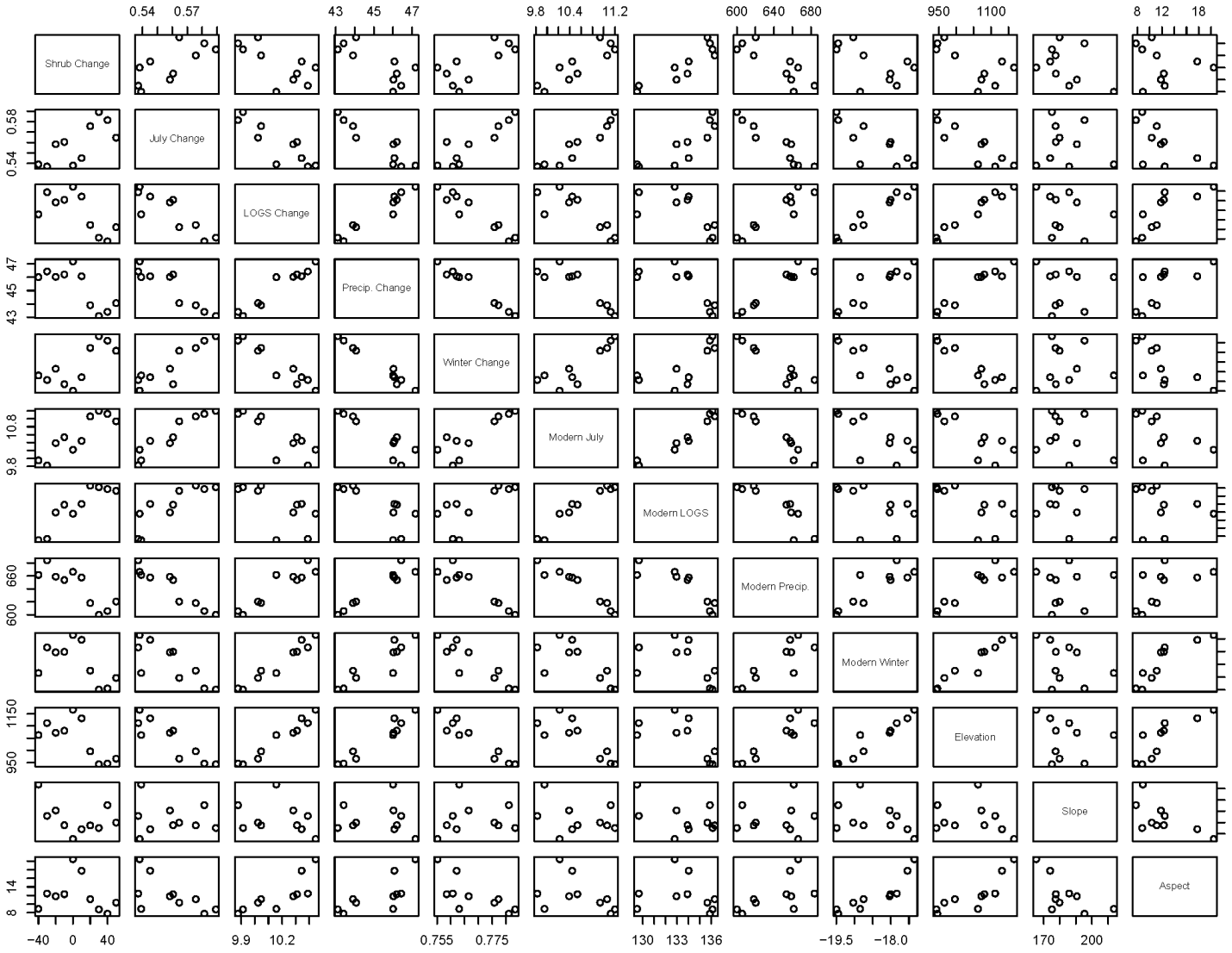

Cold Arctic | Path 75 Row 13

Pair Comparisons of Variables Using Modern Percent Shrub Dominance Bins

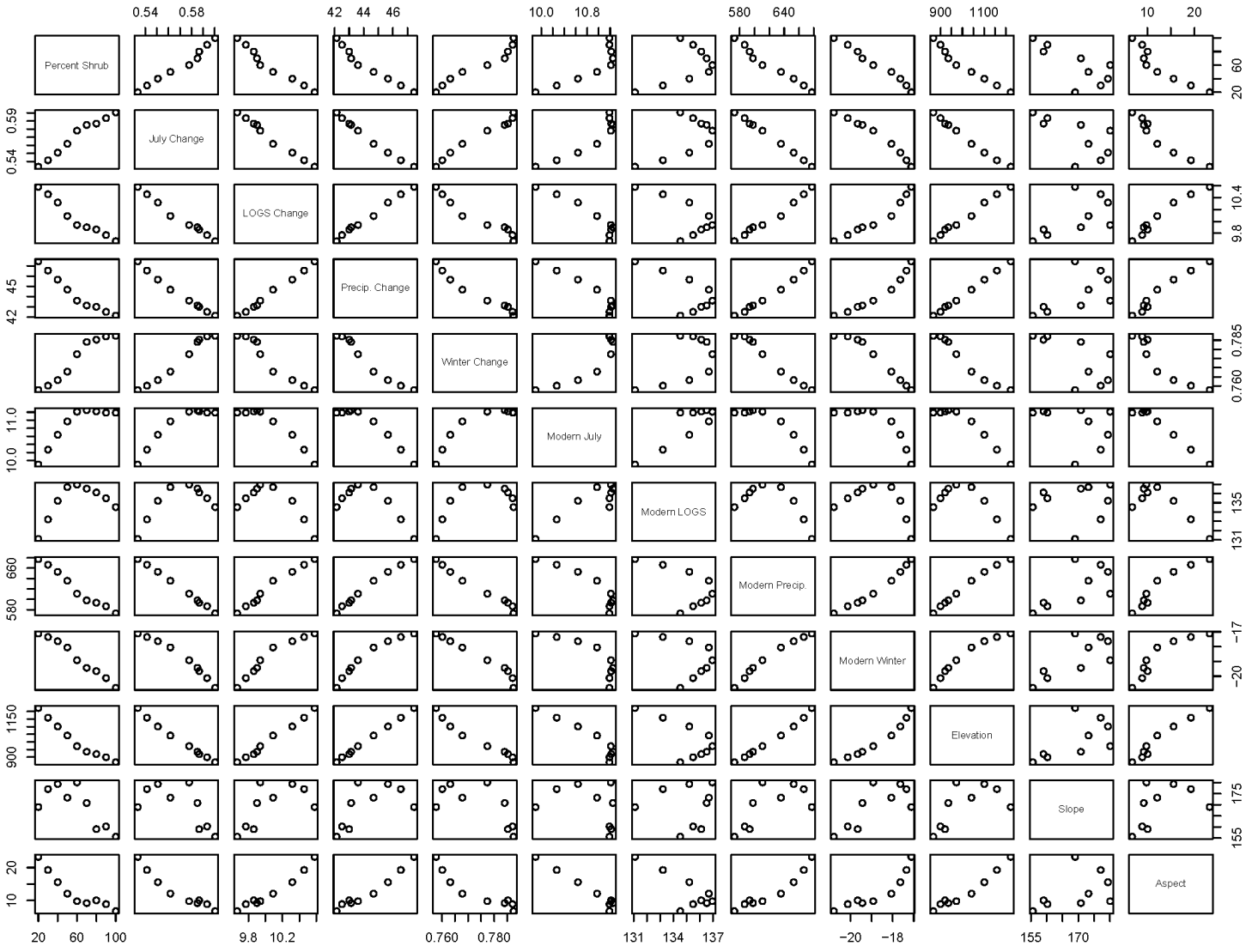

Arctic | Path 75 Row 13

Single-Variate Plots of Change in Percent Shrub Dominance As a Product of Change in Climatic Factors

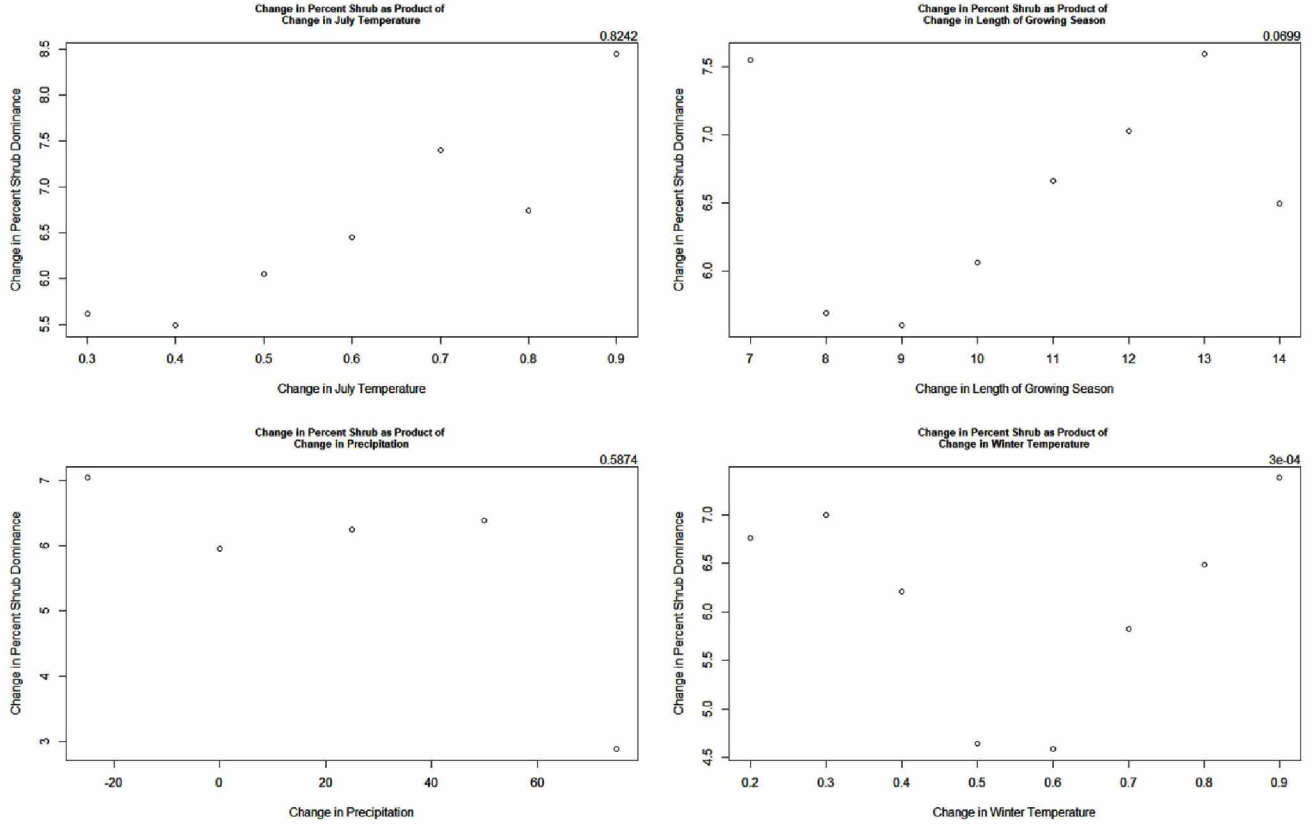

Arctic | Path 75 Row 13

Single-Variate Plots of Change in Percent Shrub Dominance As a Product of Modern Climatic Factors

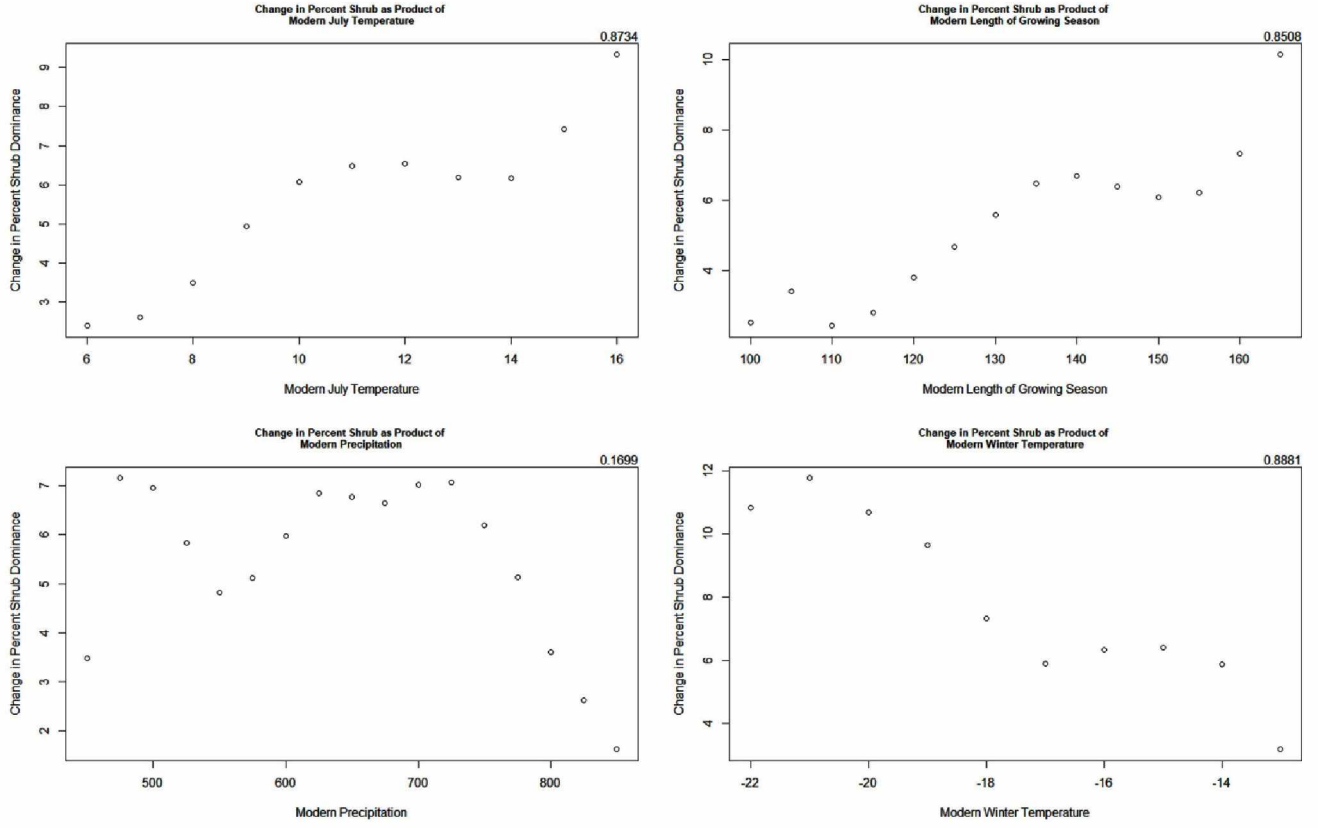

Arctic | Path 75 Row 13

Single-Variate Plots of Change in Percent Shrub Dominance As a Product of Terrain Factors

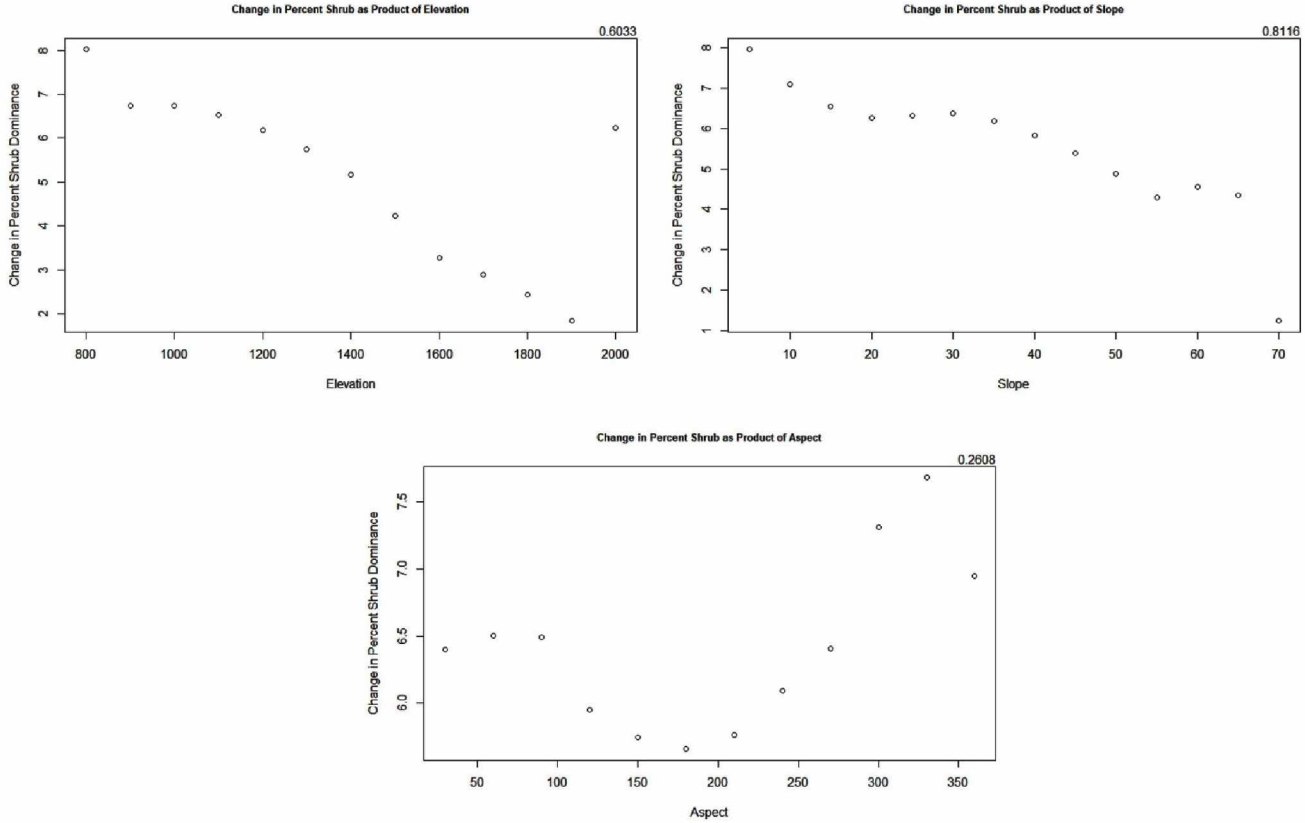

Arctic | Path 75 Row 13

Single-Variate Plots of Modern Percent Shrub Dominance As a Product of Change in Climatic Factors

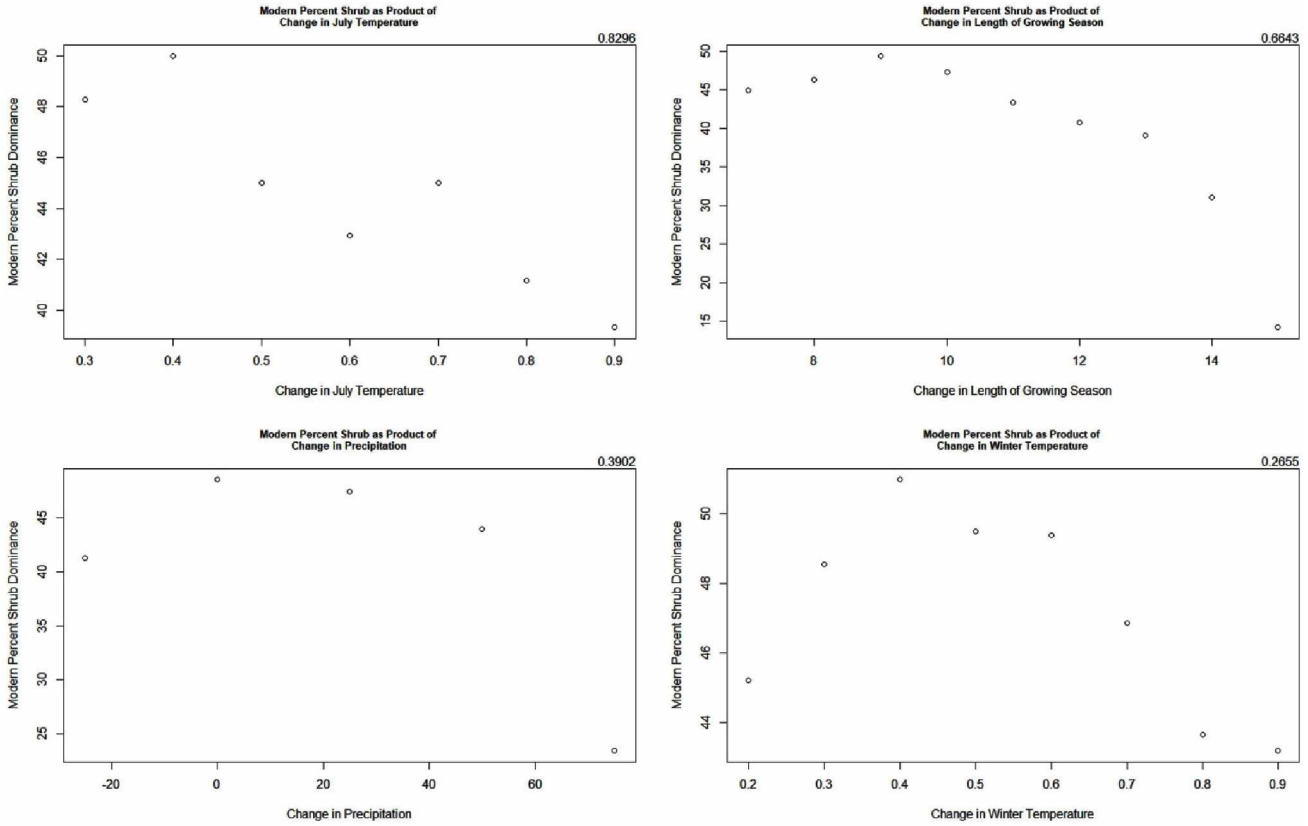

Arctic | Path 75 Row 13

Single-Variate Plots of Modern Percent Shrub Dominance As a Product of Modern Climatic Factors

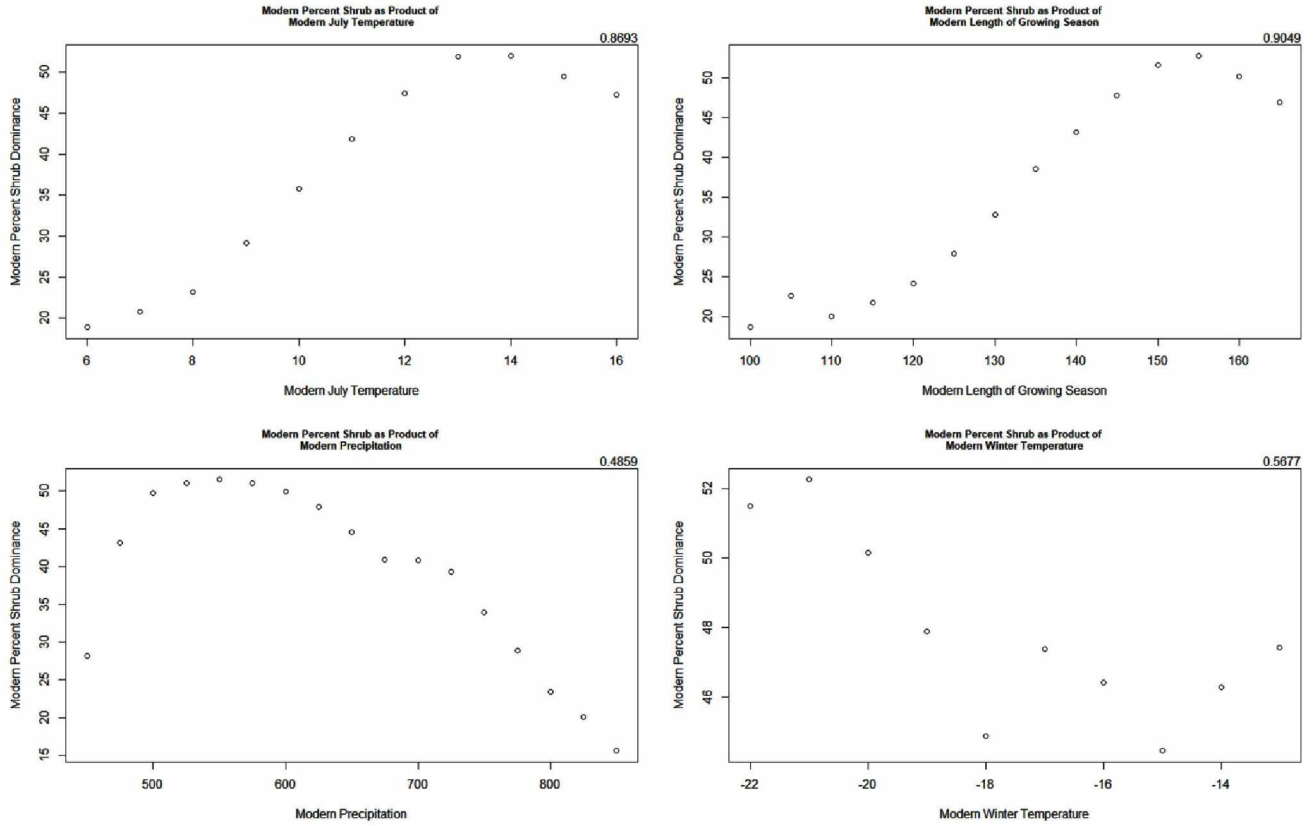

Arctic | Path 75 Row 13

Single-Variate Plots of Modern Percent Shrub Dominance As a Product of Terrain Factors

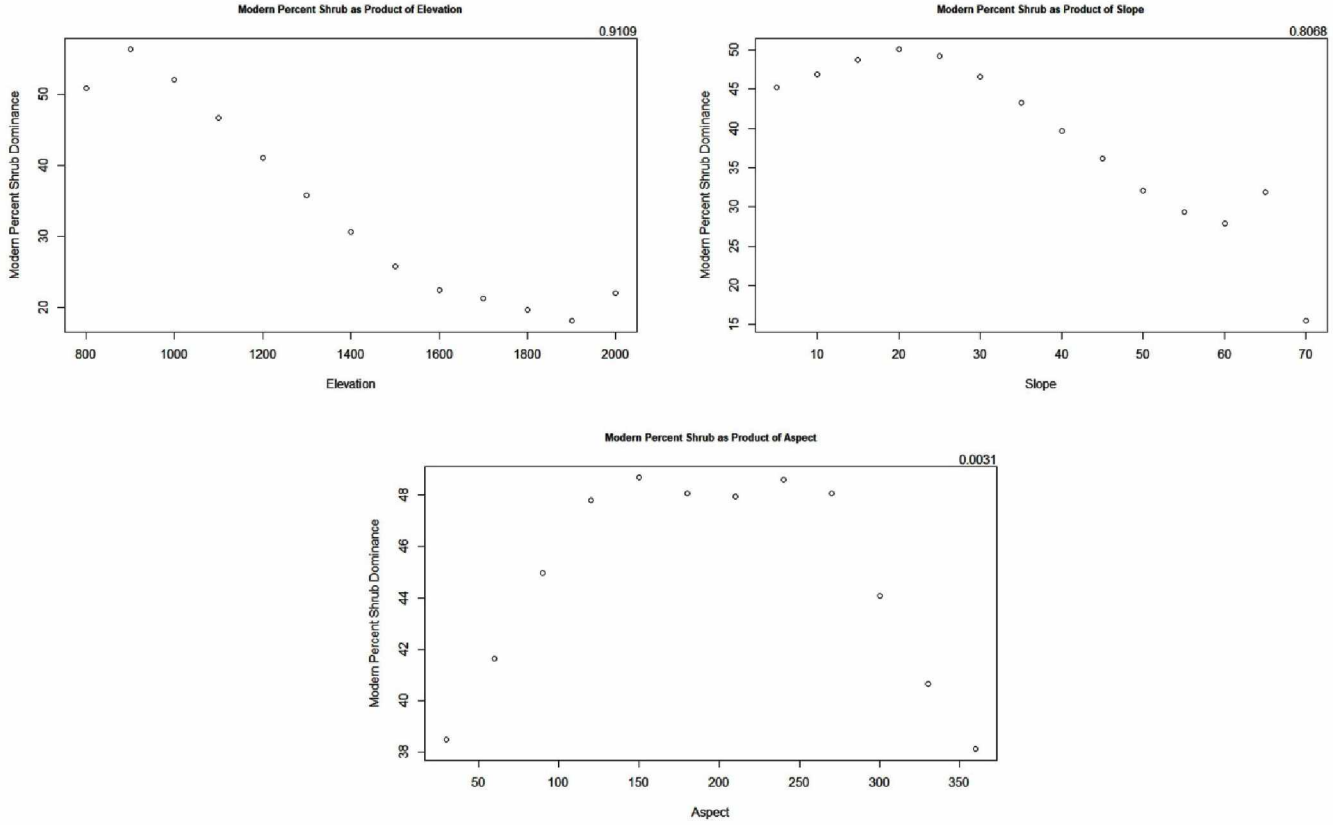

Arctic | Path 75 Row 13

Pair Comparisons of Variables Using Change in Percent Shrub Dominance Bins

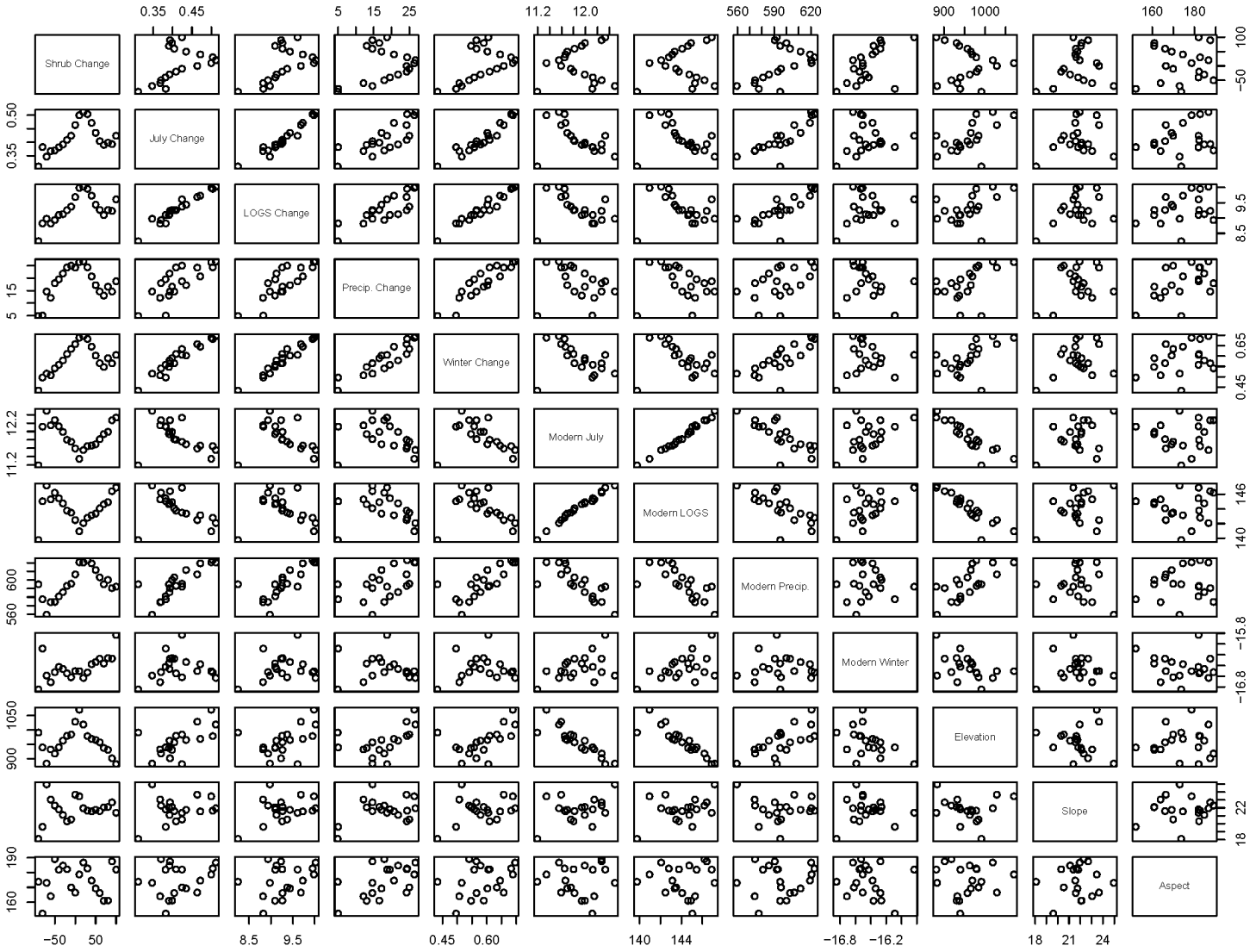

Arctic | Path 75 Row 13

Pair Comparisons of Variables Using Modern Percent Shrub Dominance Bins

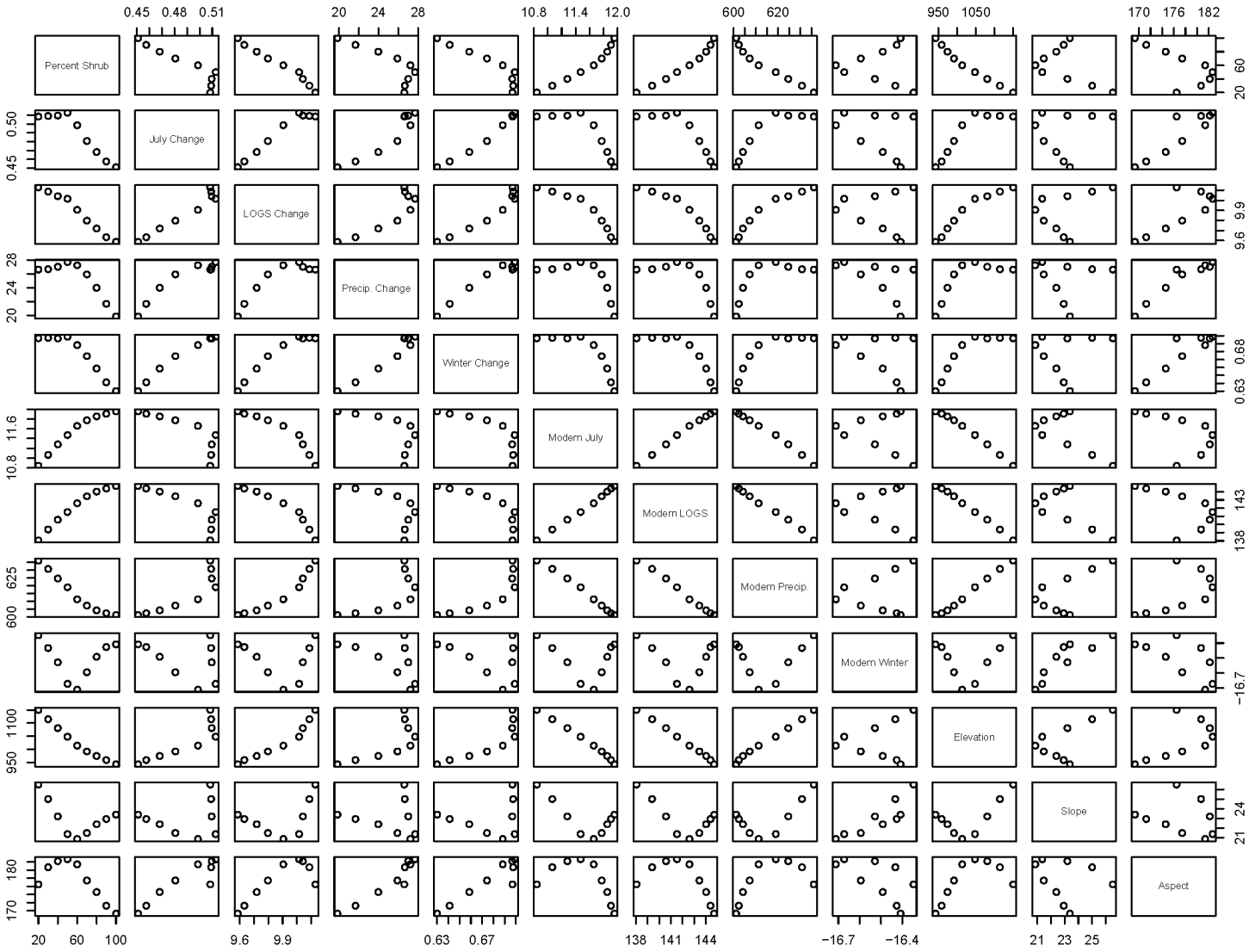

Arctic | Path 68 Row 11

Single-Variate Plots of Change in Percent Shrub Dominance As a Product of Change in Climatic Factors

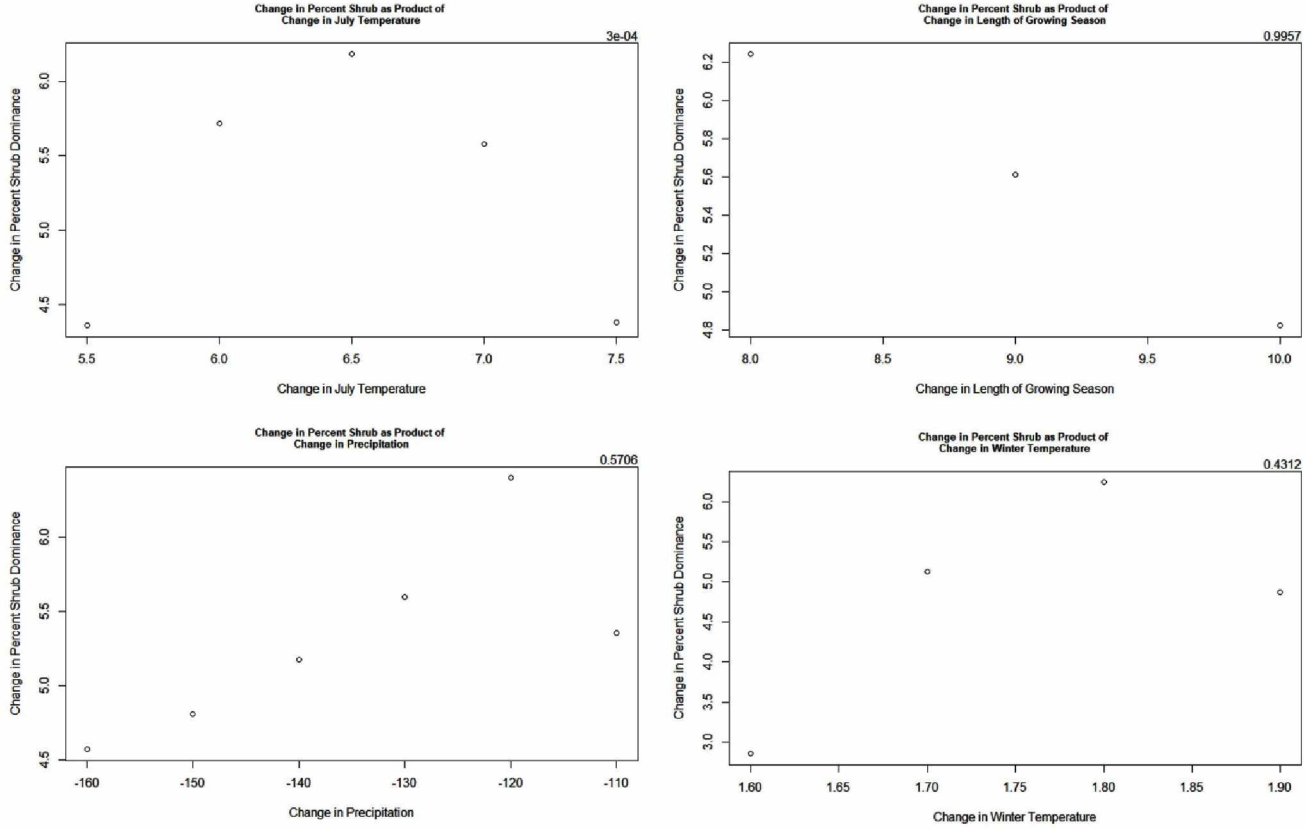

Arctic | Path 68 Row 11

Single-Variate Plots of Change in Percent Shrub Dominance As a Product of Modern Climatic Factors

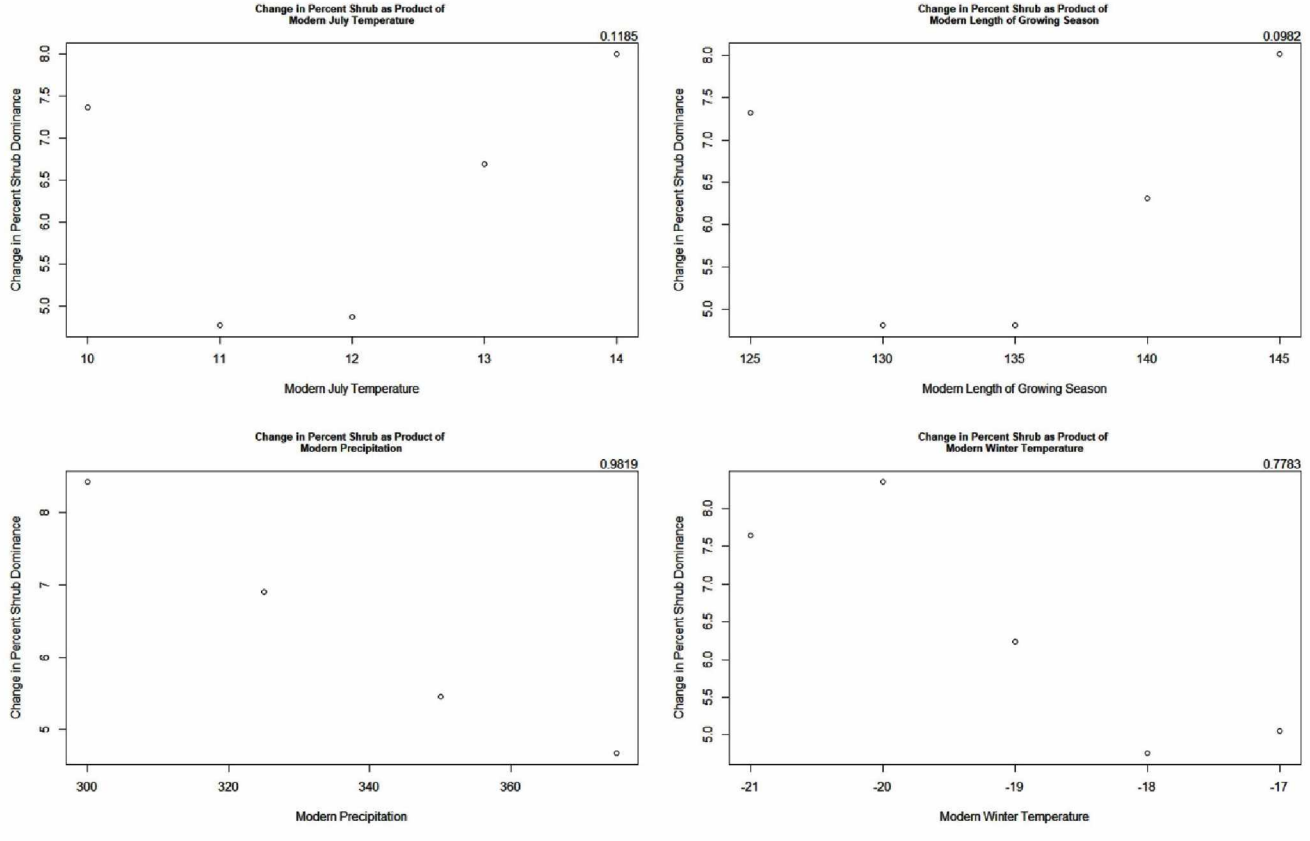

Arctic | Path 68 Row 11

Single-Variate Plots of Change in Percent Shrub Dominance As a Product of Terrain Factors

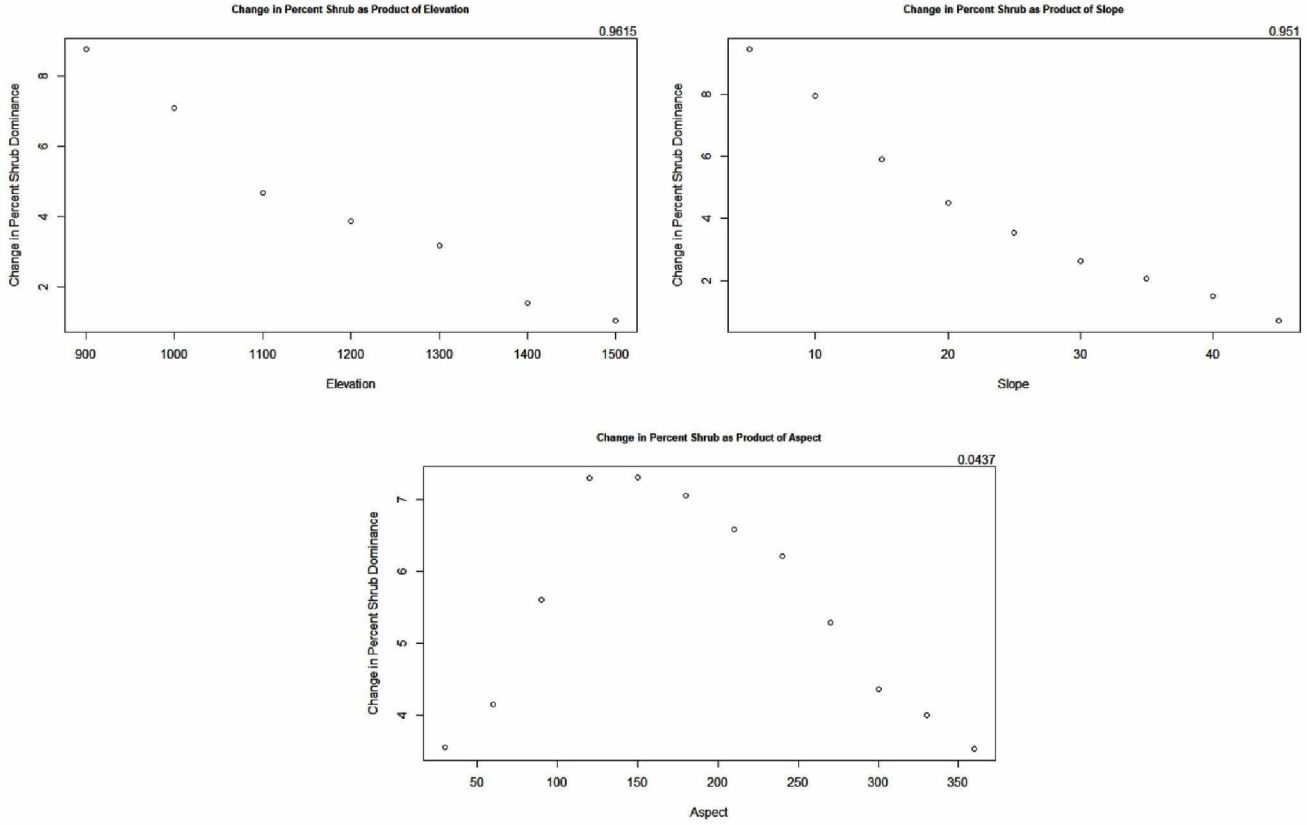

Arctic | Path 68 Row 11

Single-Variate Plots of Modern Percent Shrub Dominance As a Product of Change in Climatic Factors

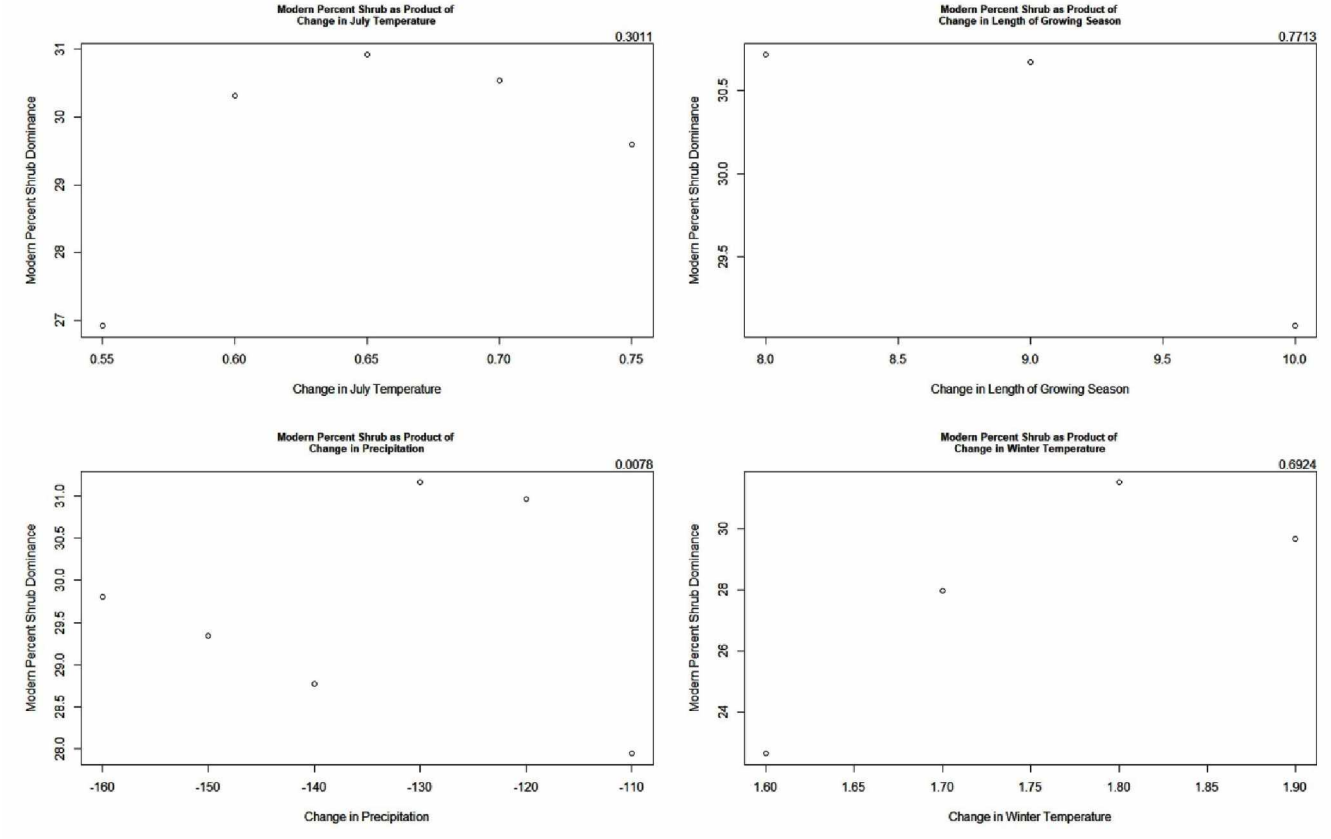

Arctic | Path 68 Row 11

Single-Variate Plots of Modern Percent Shrub Dominance As a Product of Modern Climatic Factors

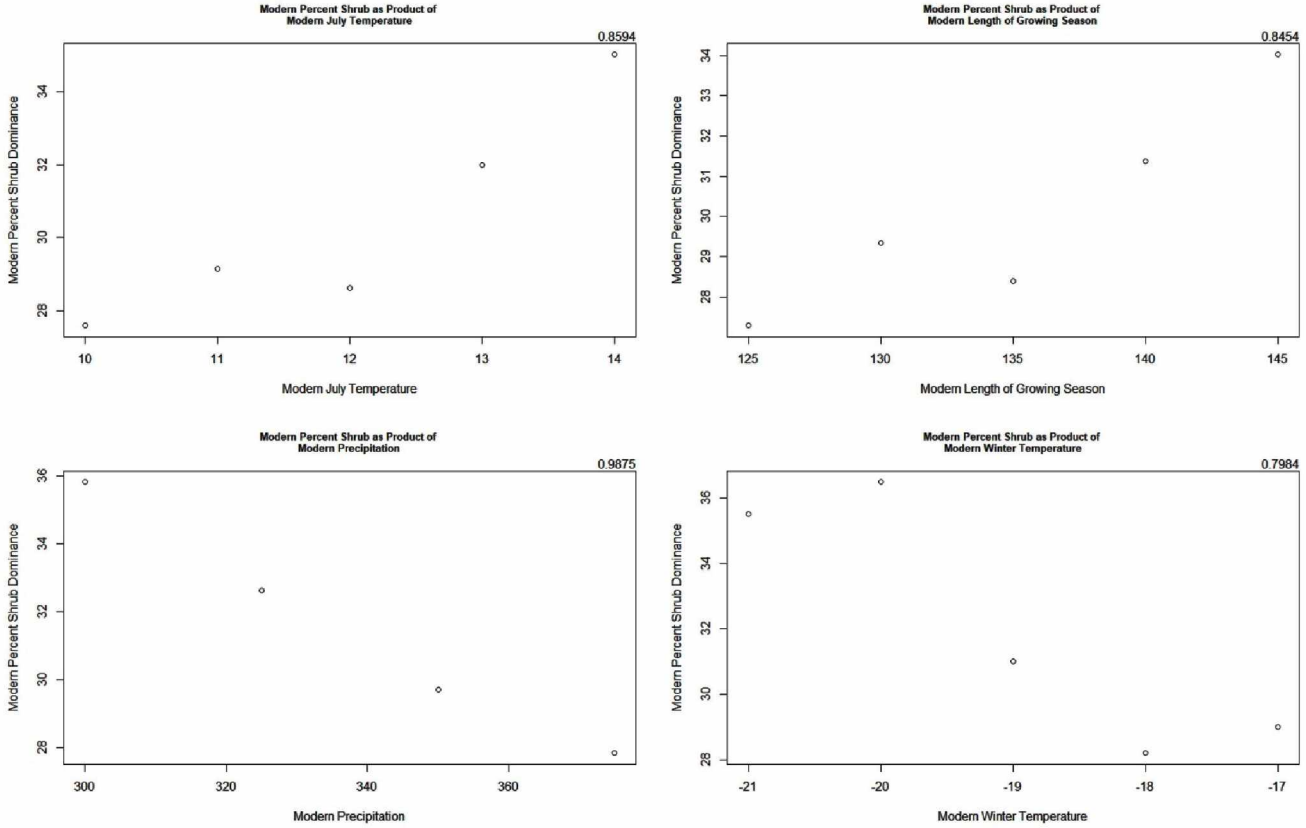

Arctic | Path 68 Row 11

Single-Variate Plots of Modern Percent Shrub Dominance As a Product of Terrain Factors

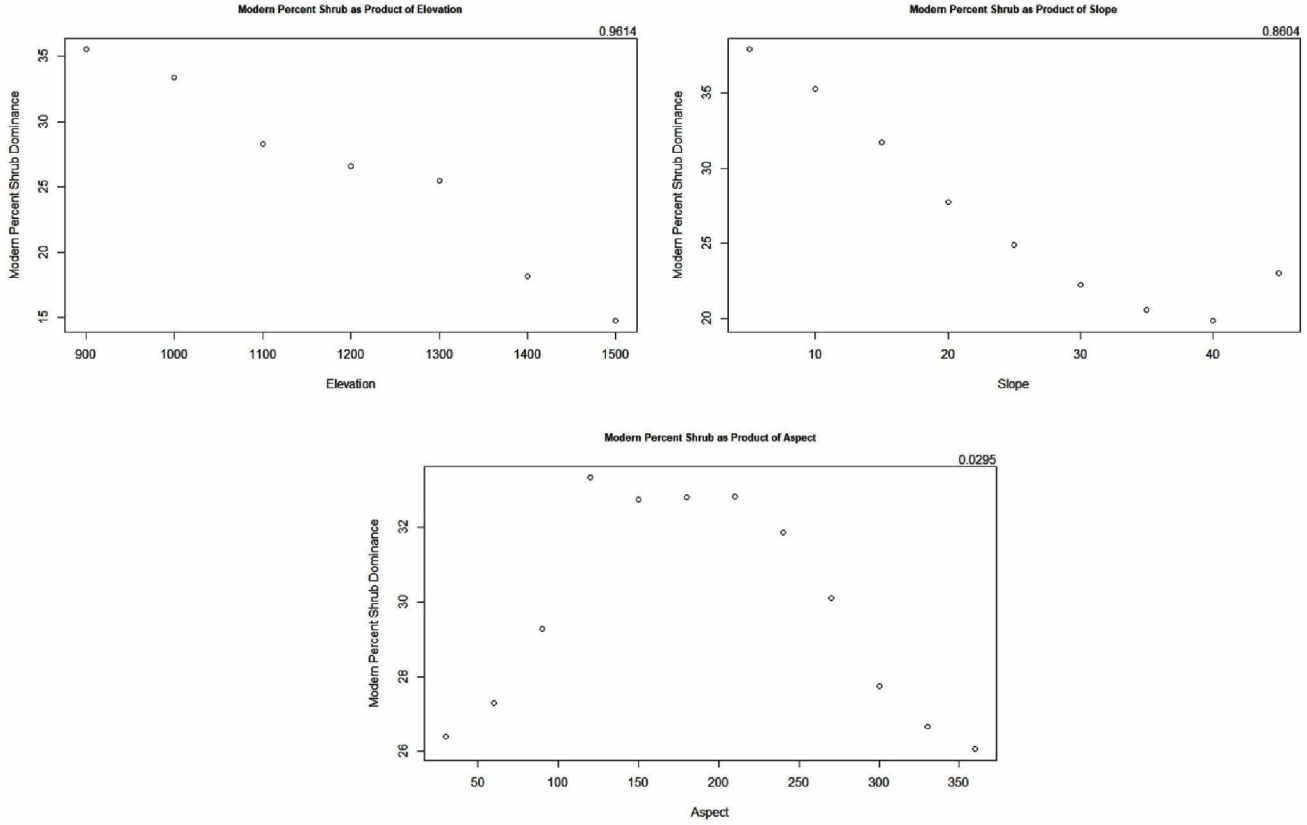

Arctic | Path 68 Row 11

Pair Comparisons of Variables Using Change in Percent Shrub Dominance Bins

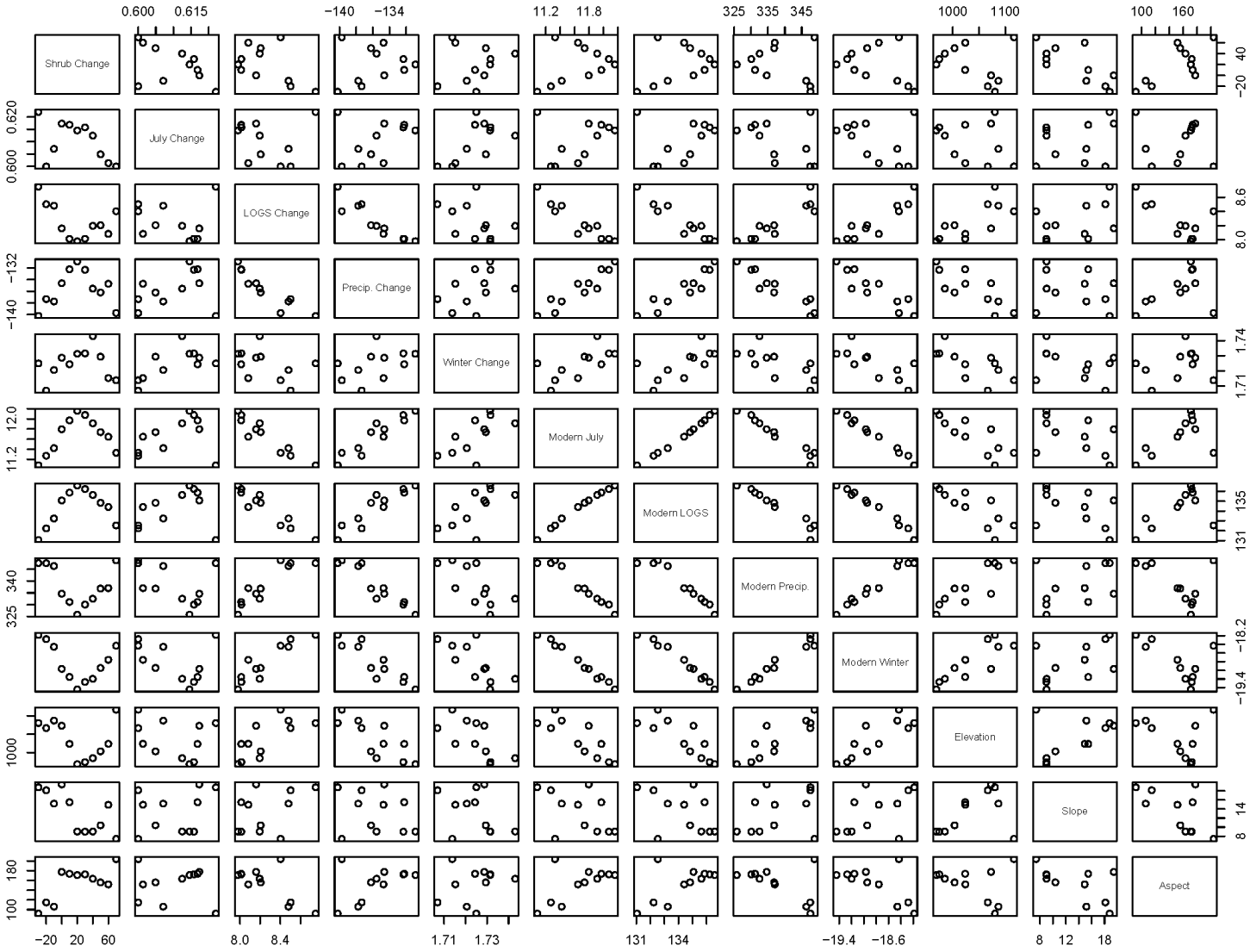

Arctic | Path 68 Row 11

Pair Comparisons of Variables Using Modern Percent Shrub Dominance Bins

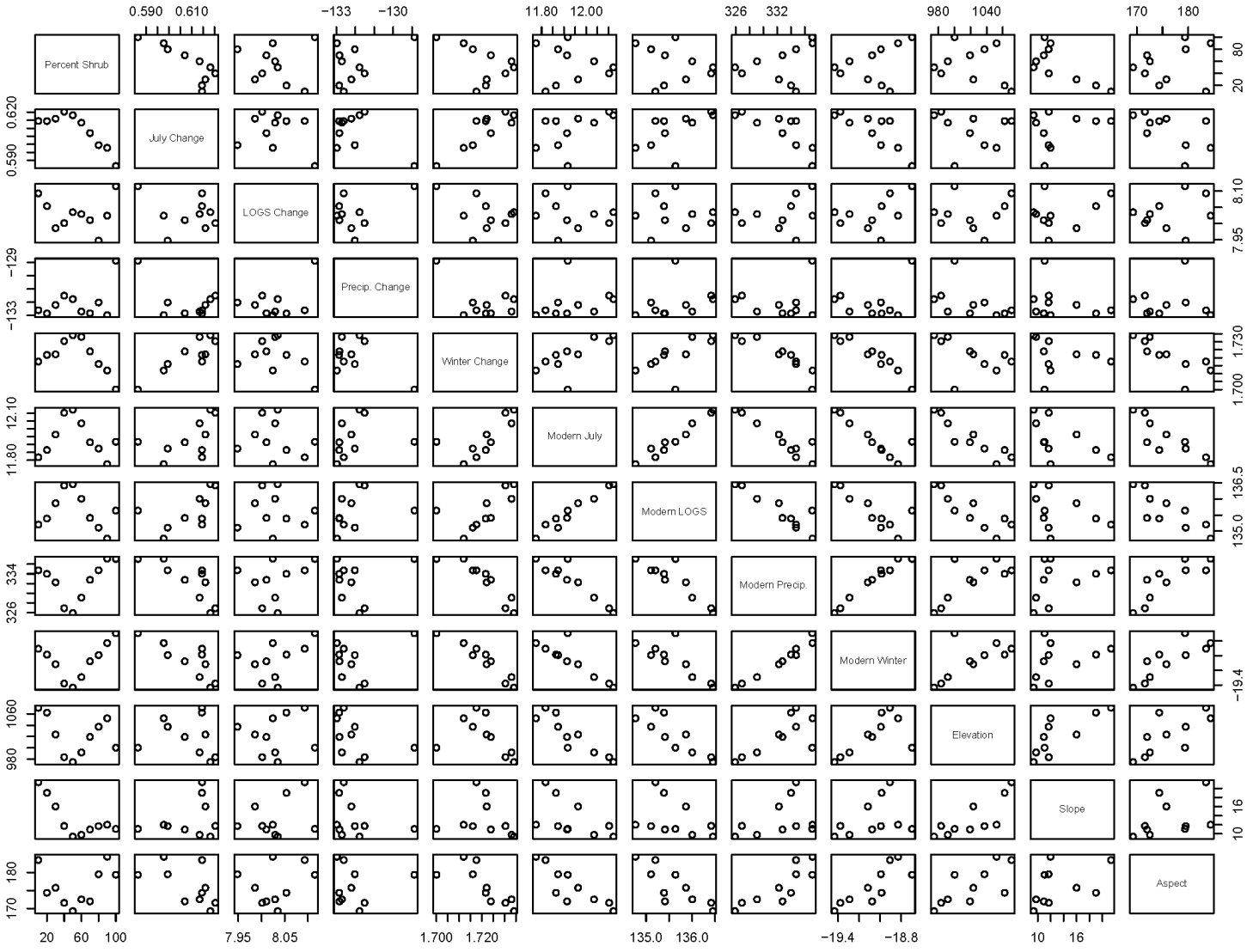

Interior | Path 65 Row 16

Single-Variate Plots of Change in Percent Shrub Dominance As a Product of Change in Climatic Factors

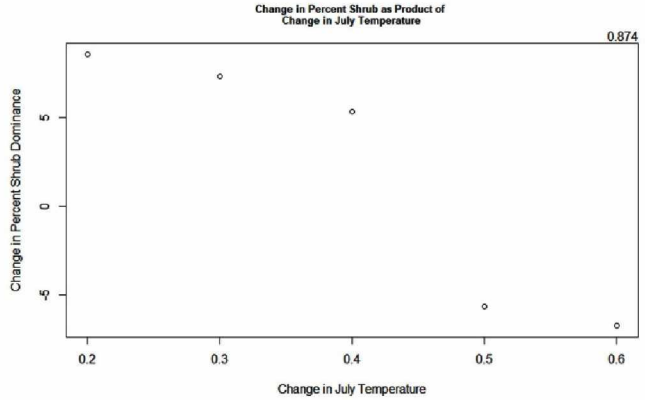


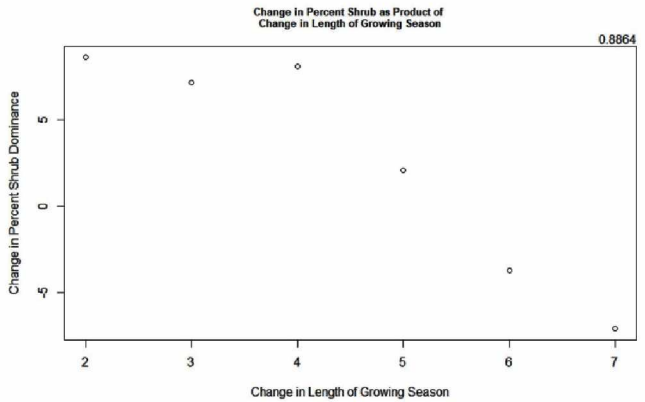


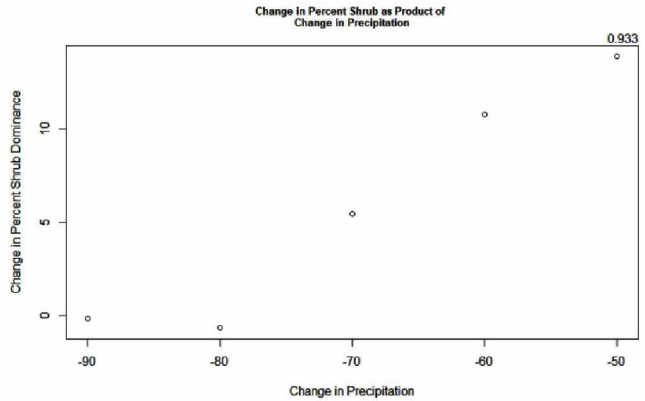


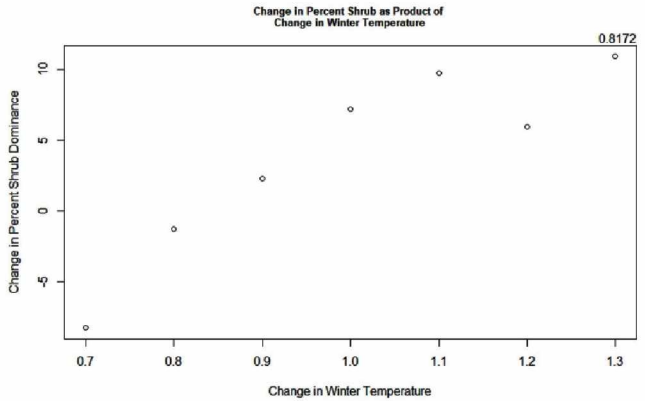

Interior | Path 65 Row 16

Single-Variate Plots of Change in Percent Shrub Dominance As a Product of Modern Climatic Factors

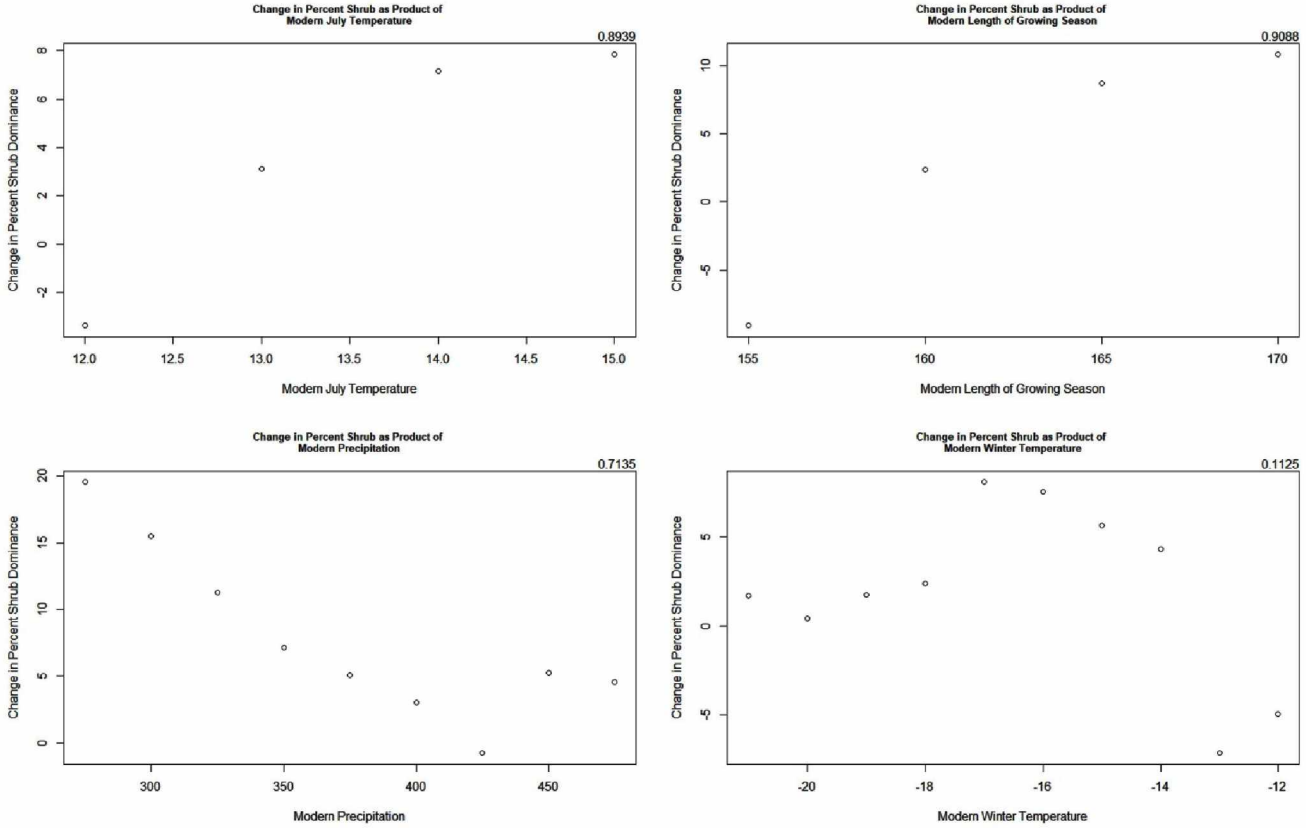

Interior | Path 65 Row 16

Single-Variate Plots of Change in Percent Shrub Dominance As a Product of Terrain Factors

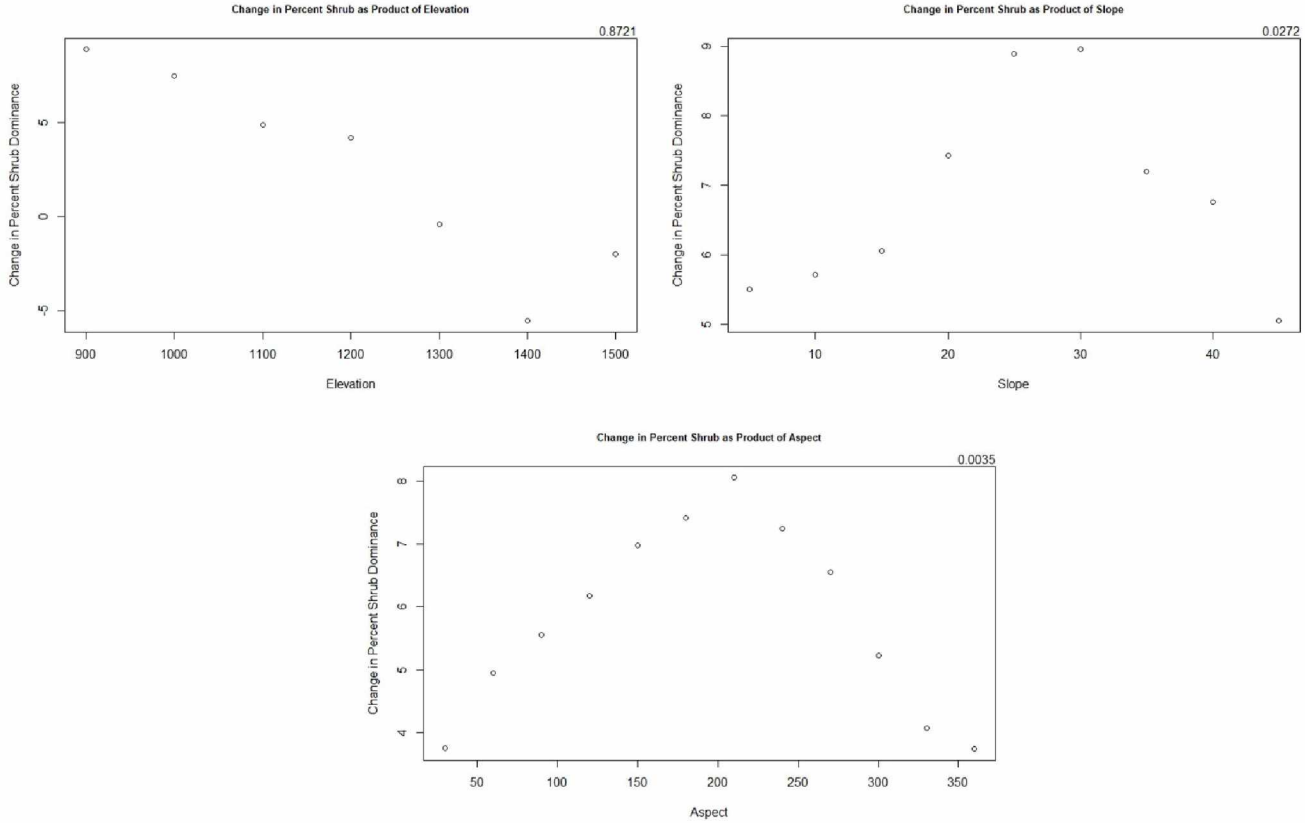

Interior | Path 65 Row 16

Single-Variate Plots of Modern Percent Shrub Dominance As a Product of Change in Climatic Factors

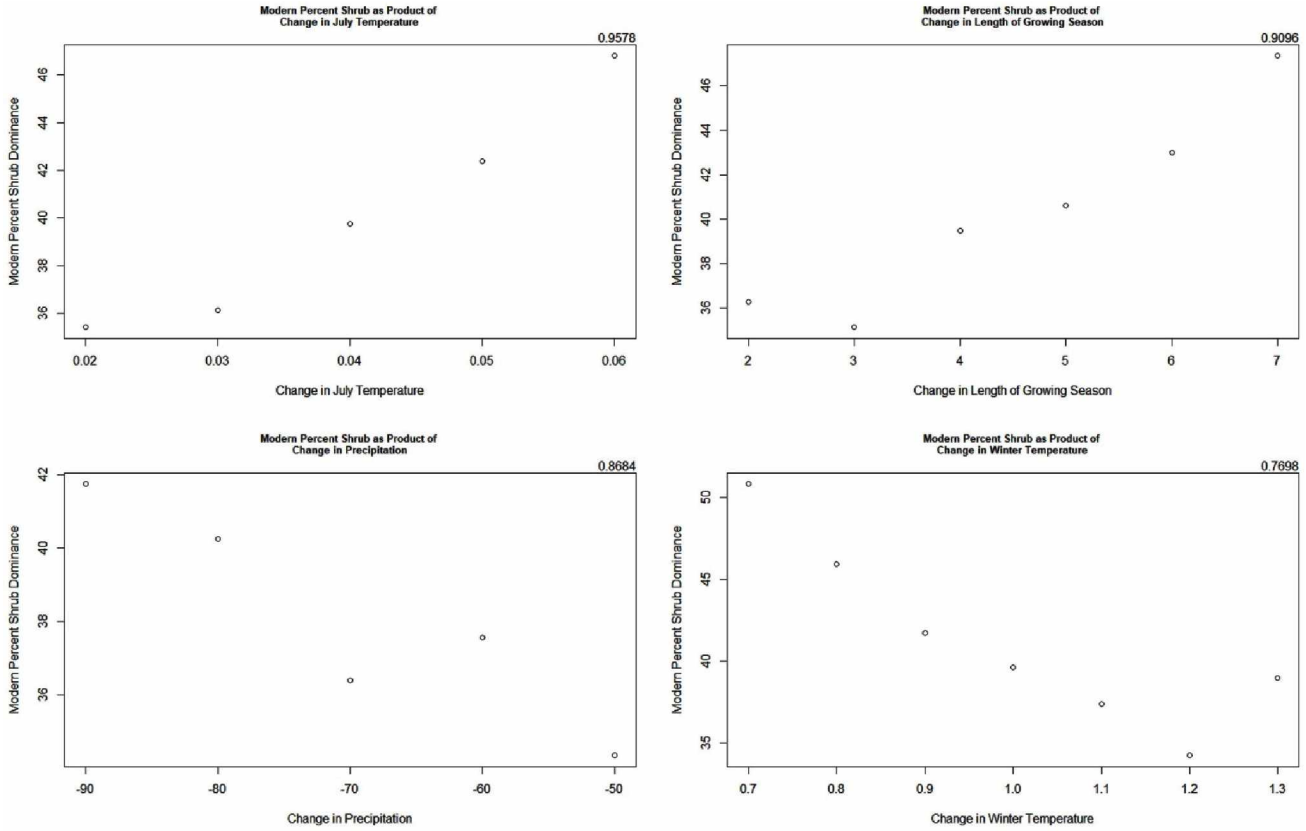

Interior | Path 65 Row 16

Single-Variate Plots of Modern Percent Shrub Dominance As a Product of Modern Climatic Factors

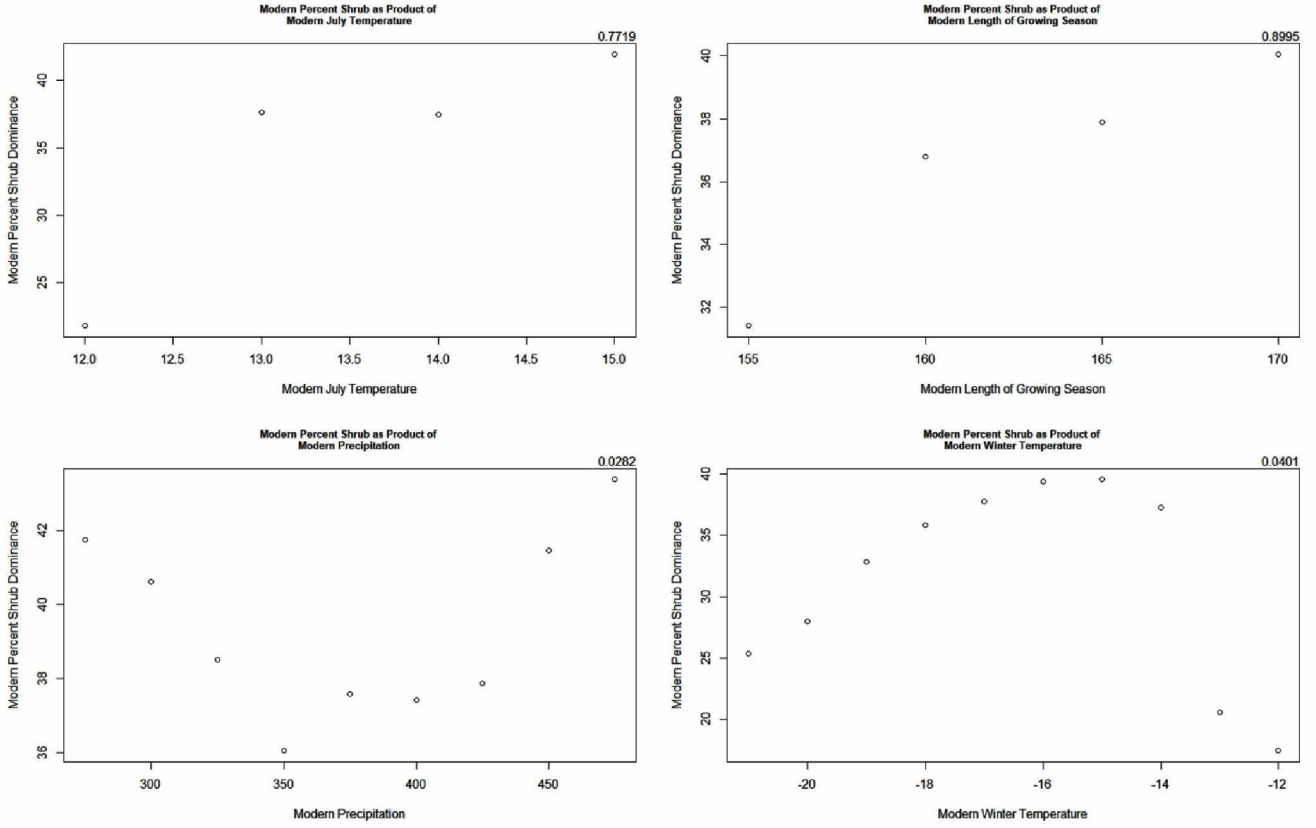

Interior | Path 65 Row 16

Single-Variate Plots of Change in Percent Shrub Dominance As a Product of Terrain Factors

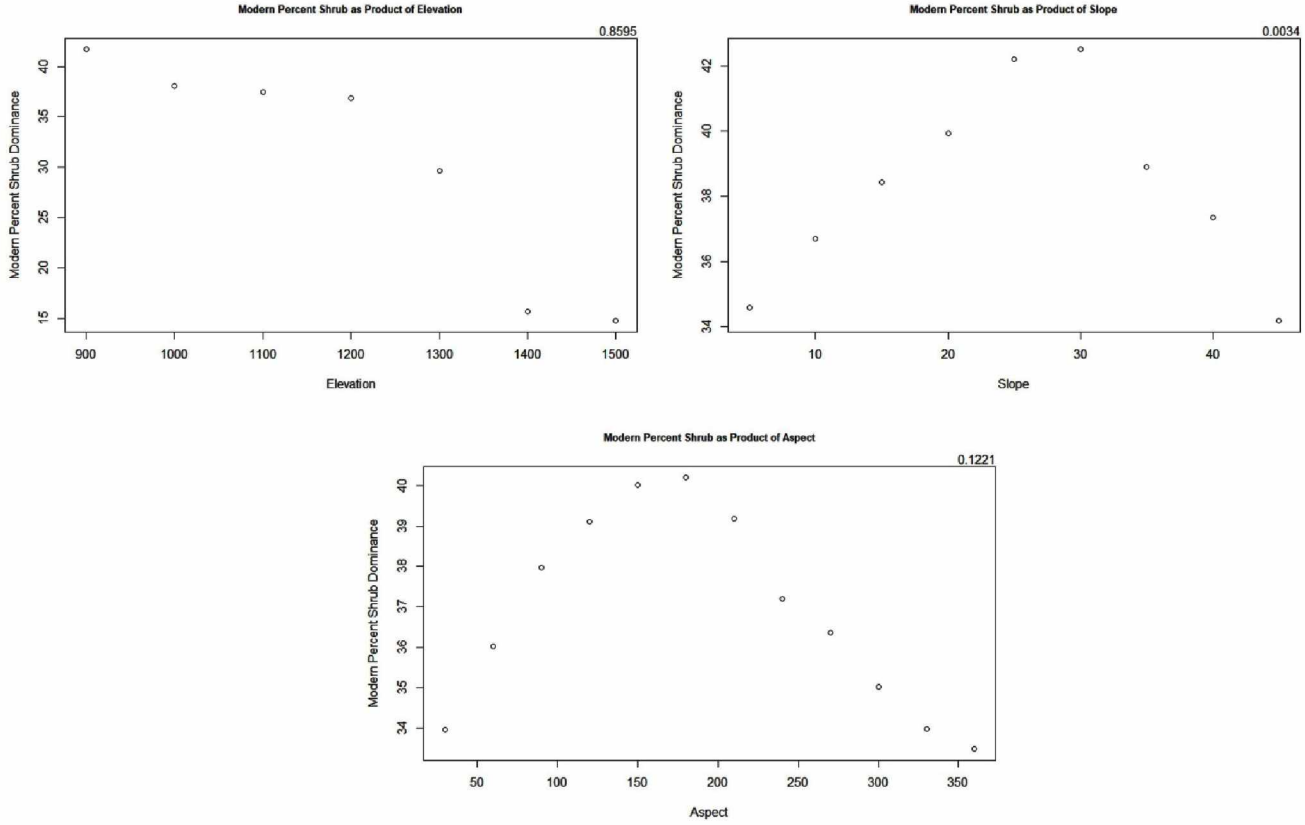

Interior | Path 65 Row 16

Pair Comparisons of Variables Using Change in Percent Shrub Dominance Bins

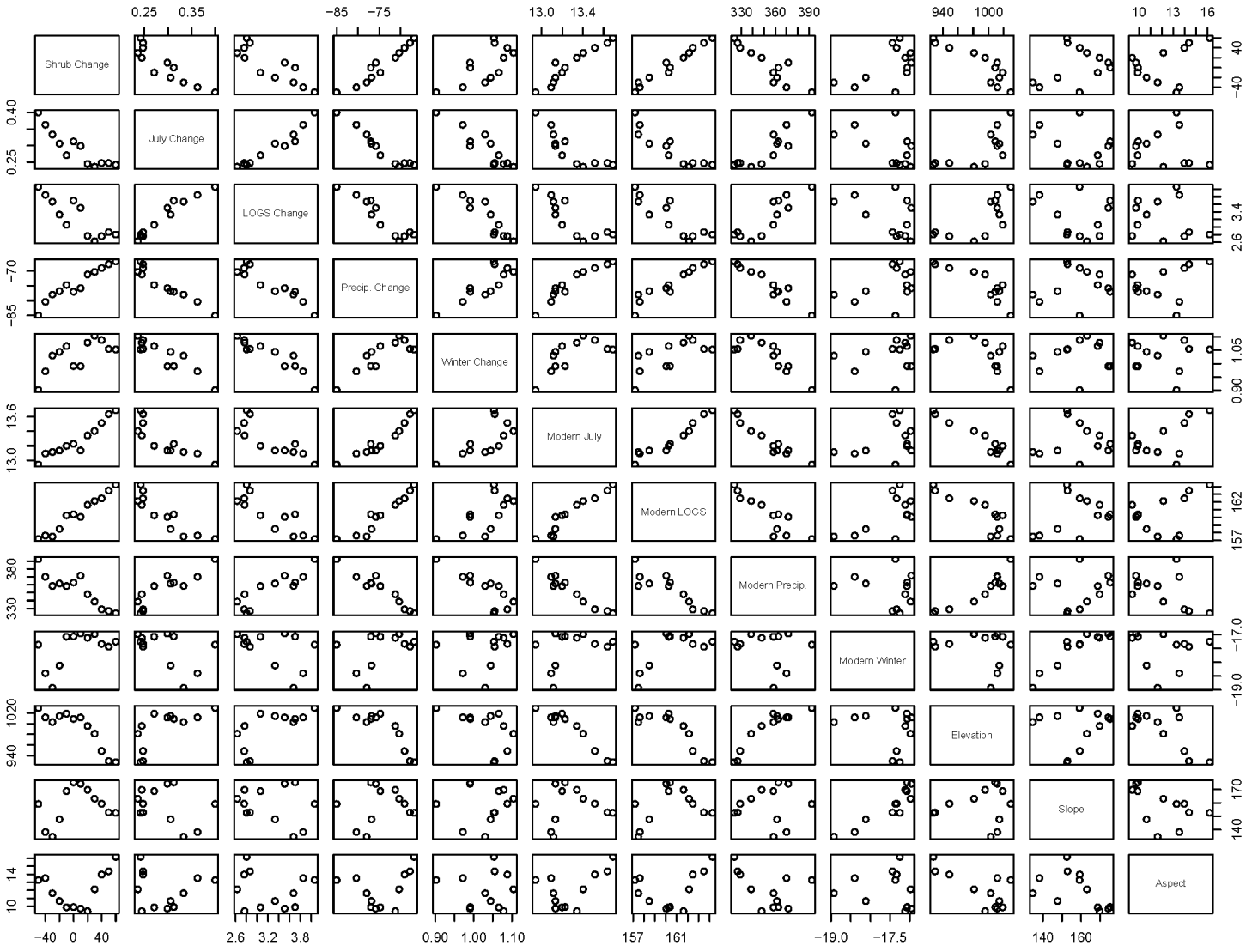

Interior | Path 65 Row 16

Pair Comparisons of Variables Using Modern Percent Shrub Dominance Bins

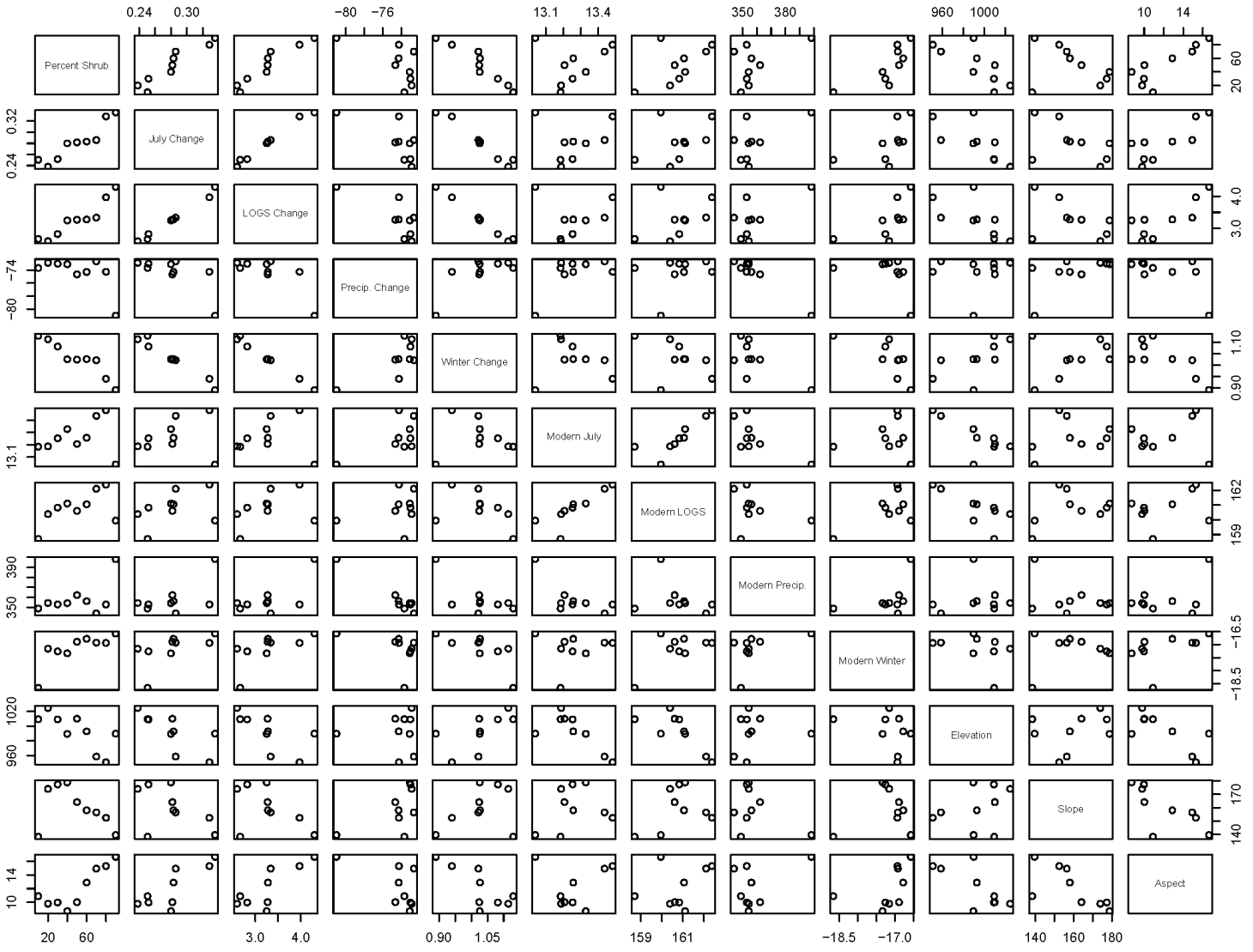

High Precipitation | Path 67 Row 18

Single-Variate Plots of Change in Percent Shrub Dominance As a Product of Change in Climatic Factors

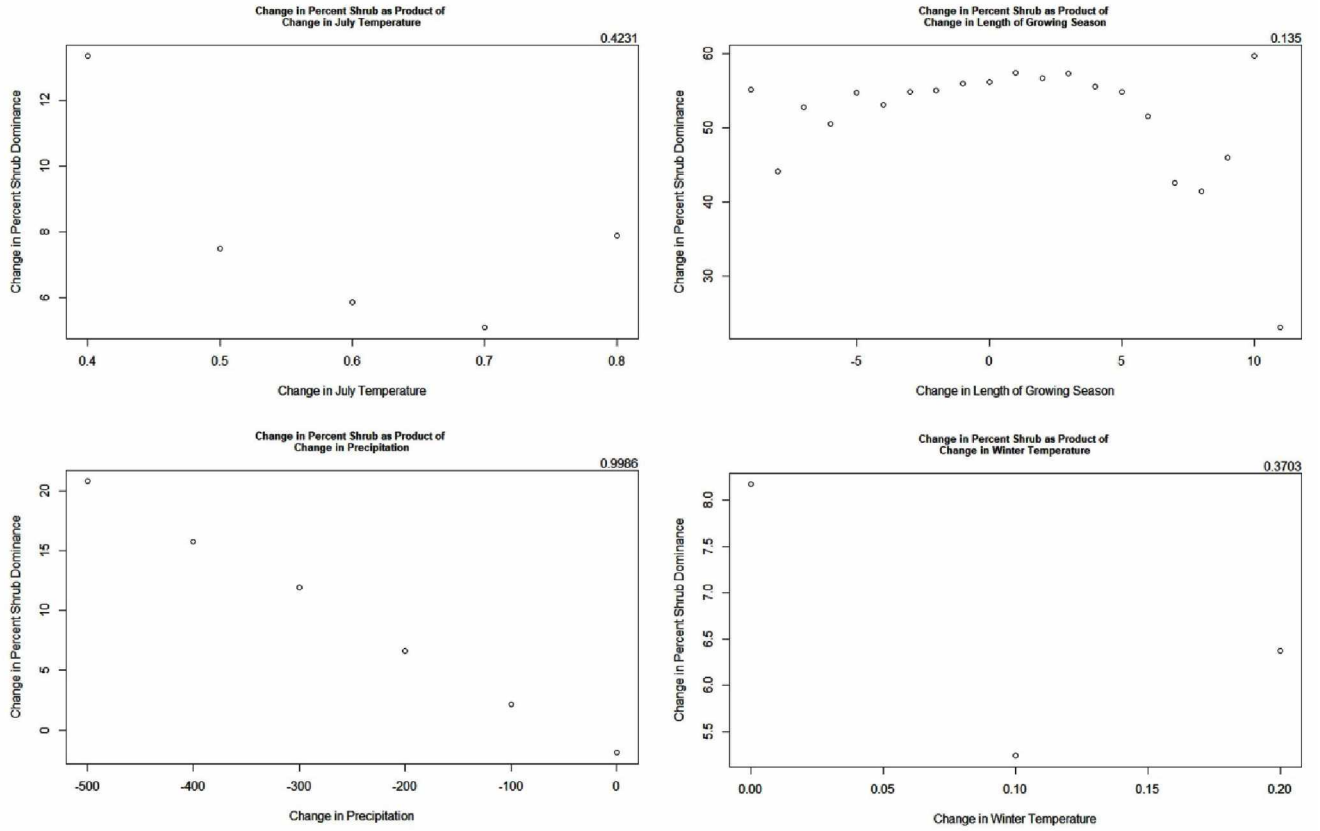

High Precipitation | Path 67 Row 18

Single-Variate Plots of Change in Percent Shrub Dominance As a Product of Modern Climatic Factors

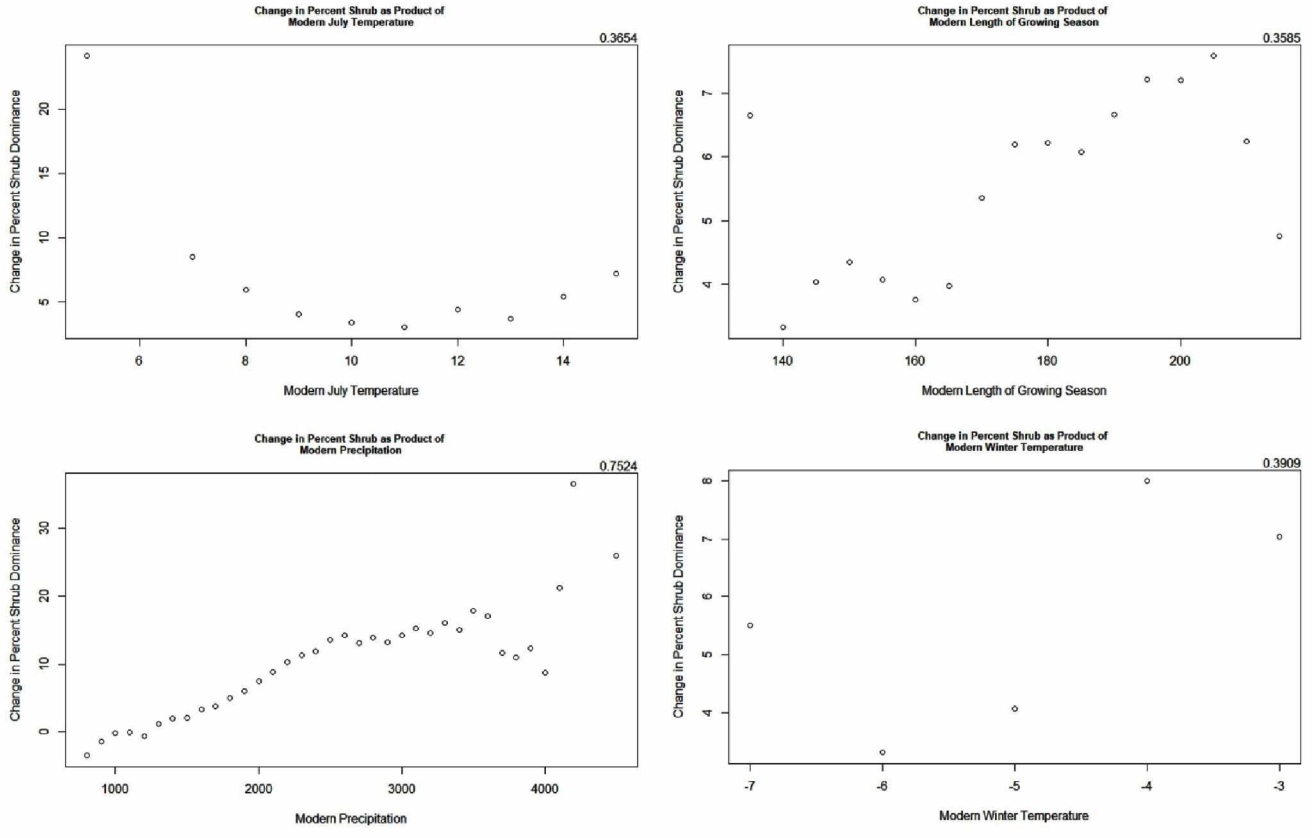

High Precipitation | Path 67 Row 18

Single-Variate Plots of Change in Percent Shrub Dominance As a Product of Terrain Factors

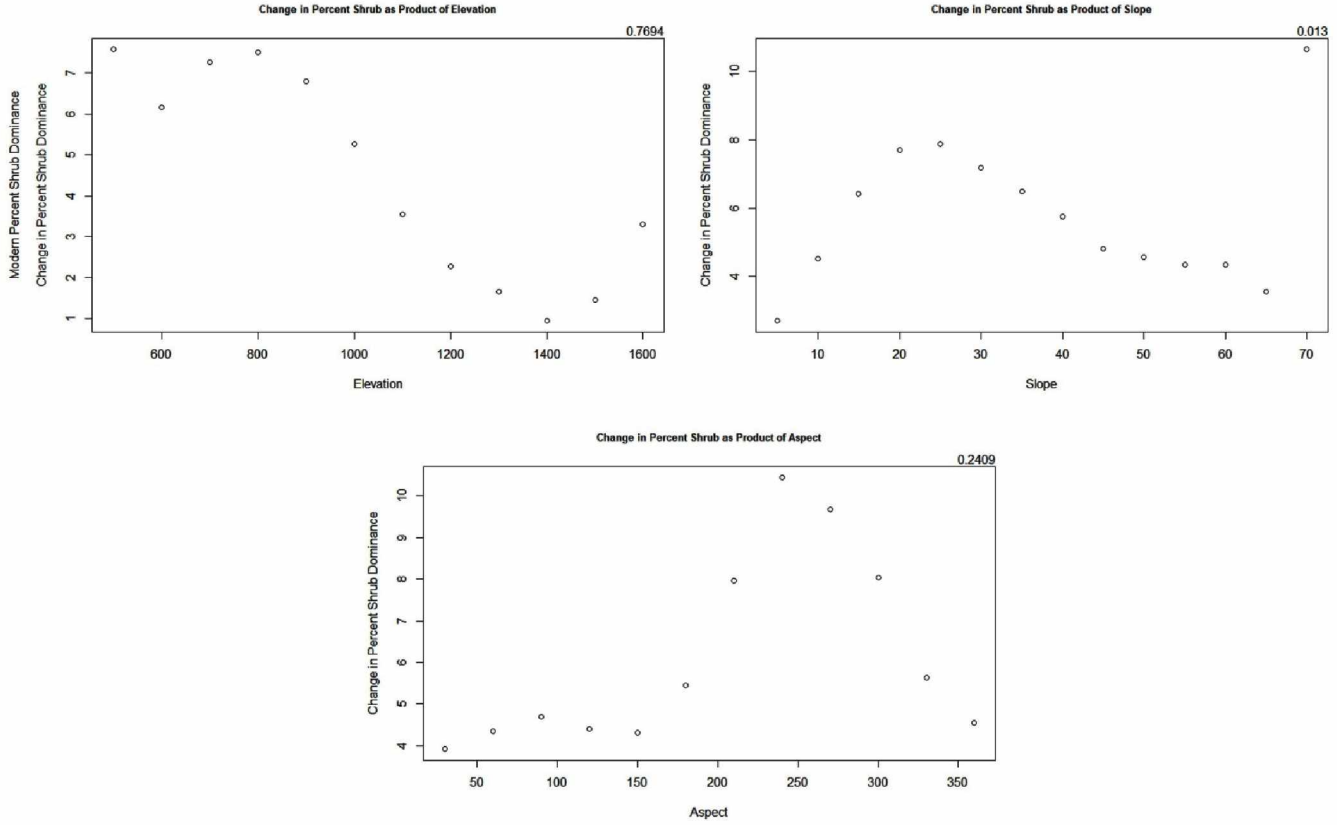

High Precipitation | Path 67 Row 18

Single-Variate Plots of Modern Percent Shrub Dominance As a Product of Change in Climatic Factors

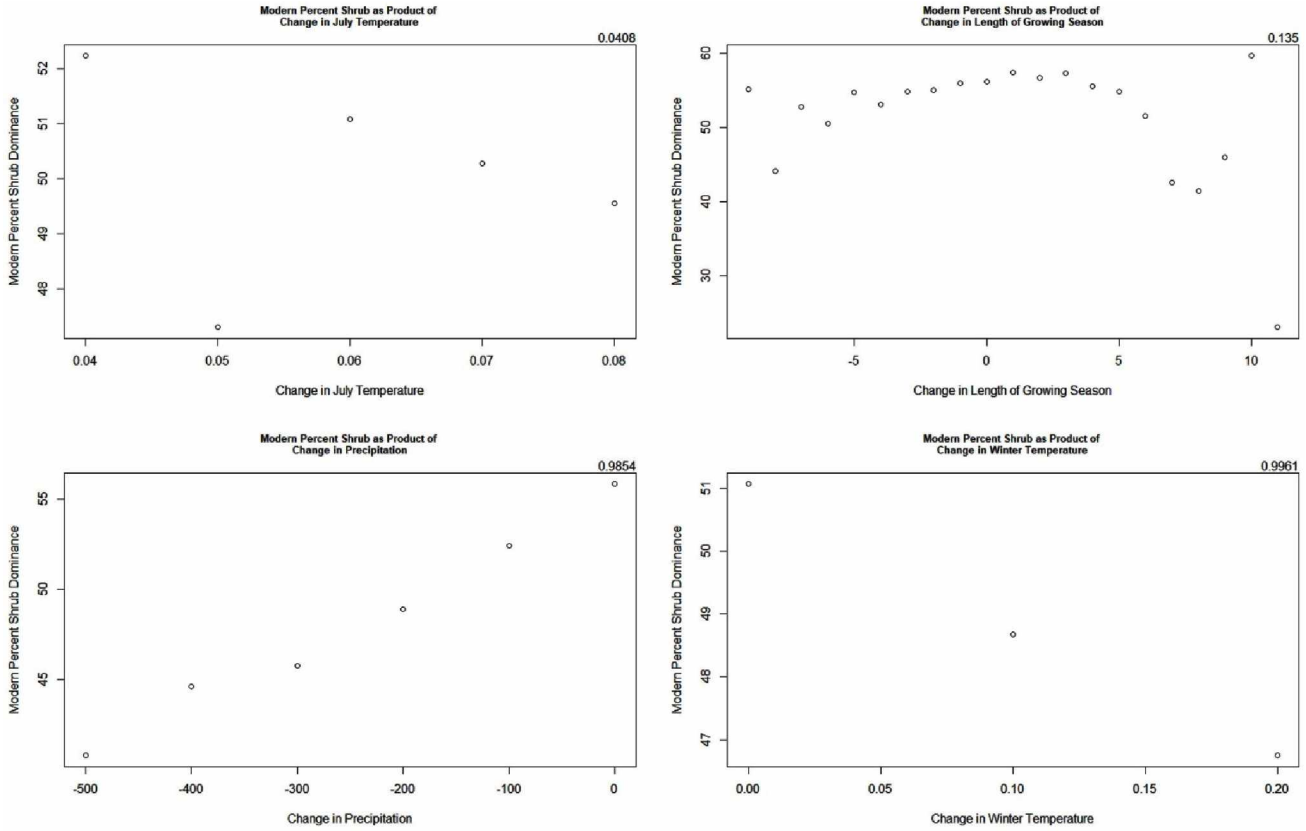

High Precipitation | Path 67 Row 18

Single-Variate Plots of Modern Percent Shrub Dominance As a Product of Modern Climatic Factors

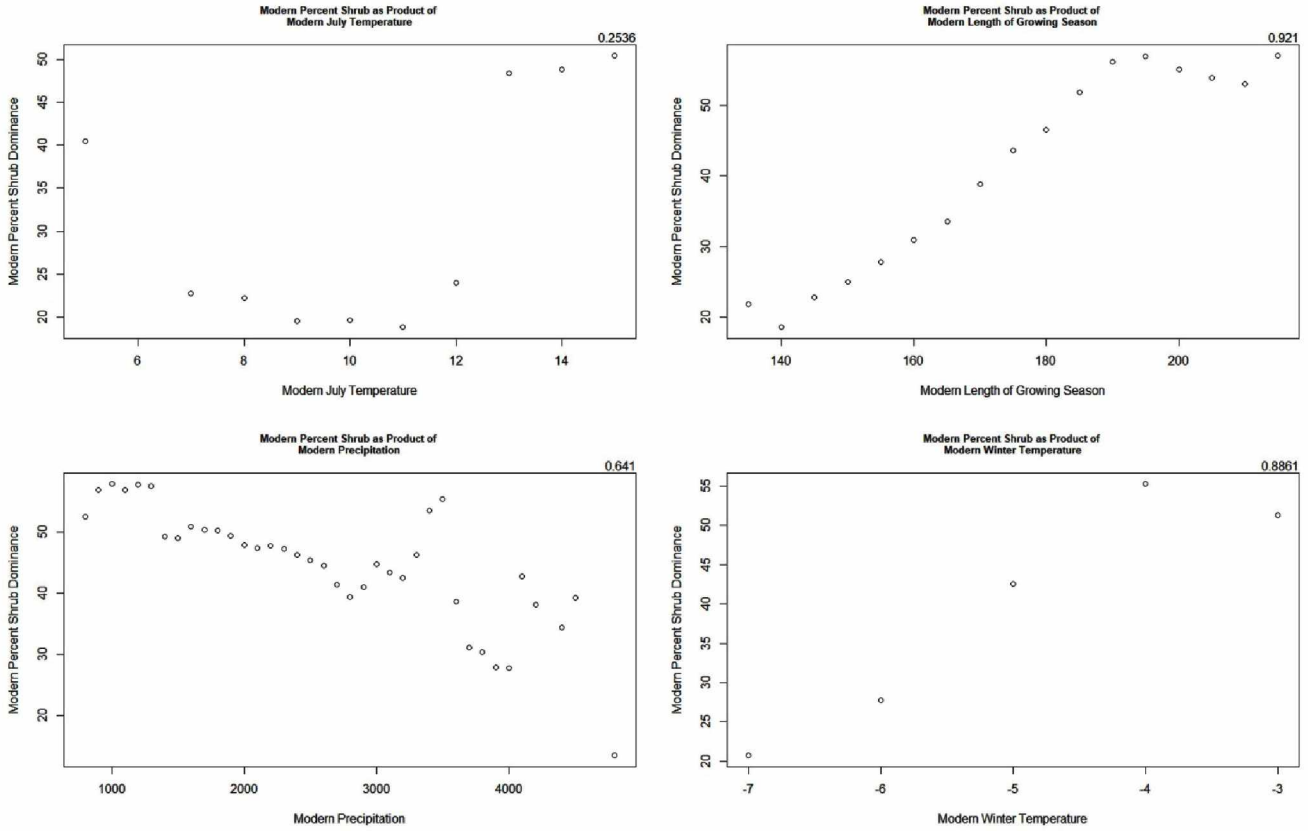

High Precipitation | Path 67 Row 18

Single-Variate Plots of Modern Percent Shrub Dominance As a Product of Terrain Factors

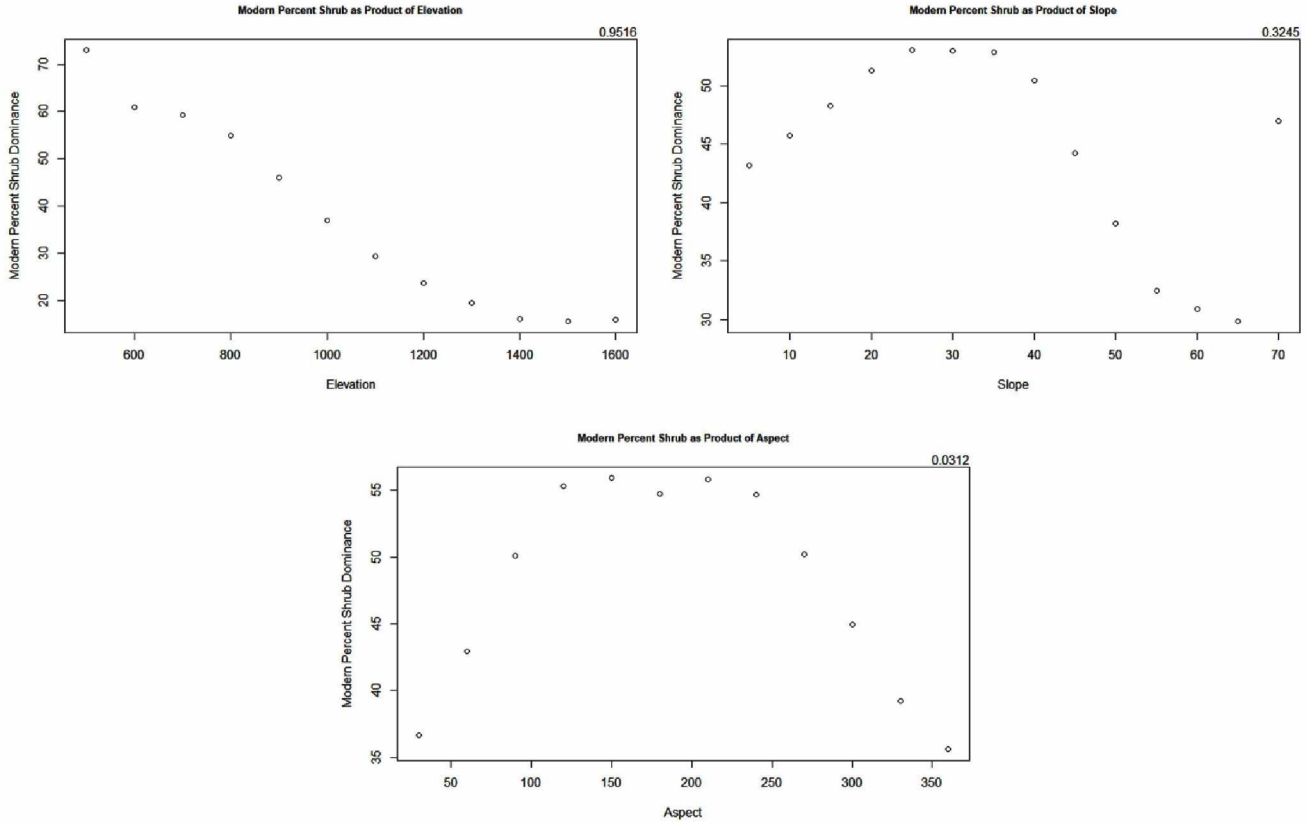

High Precipitation | Path 67 Row 18

Pair Comparisons of Variables Using Change in Percent Shrub Dominance Bins

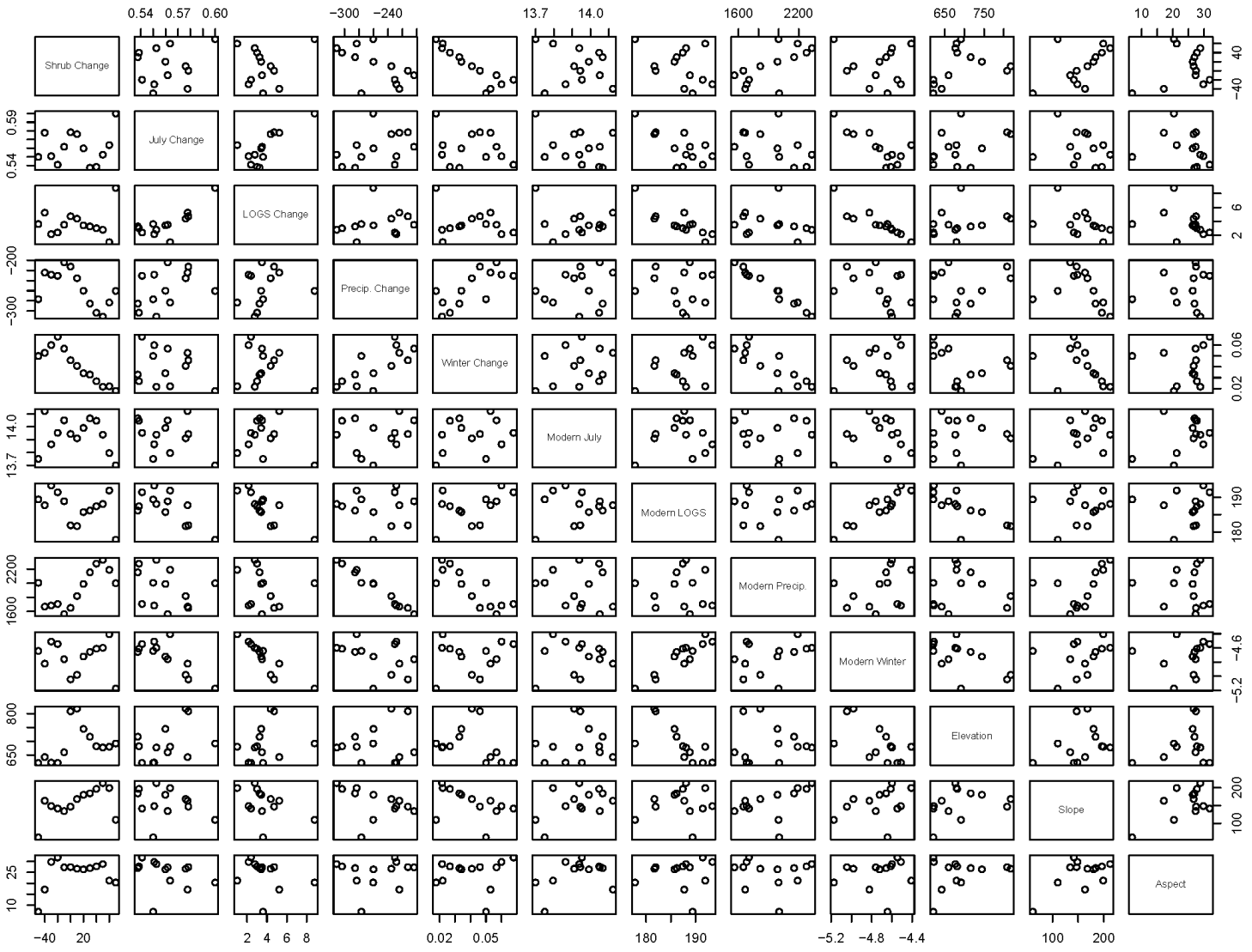

High Precipitation | Path 67 Row 18

Pair Comparisons of Variables Using Modern Percent Shrub Dominance Bins

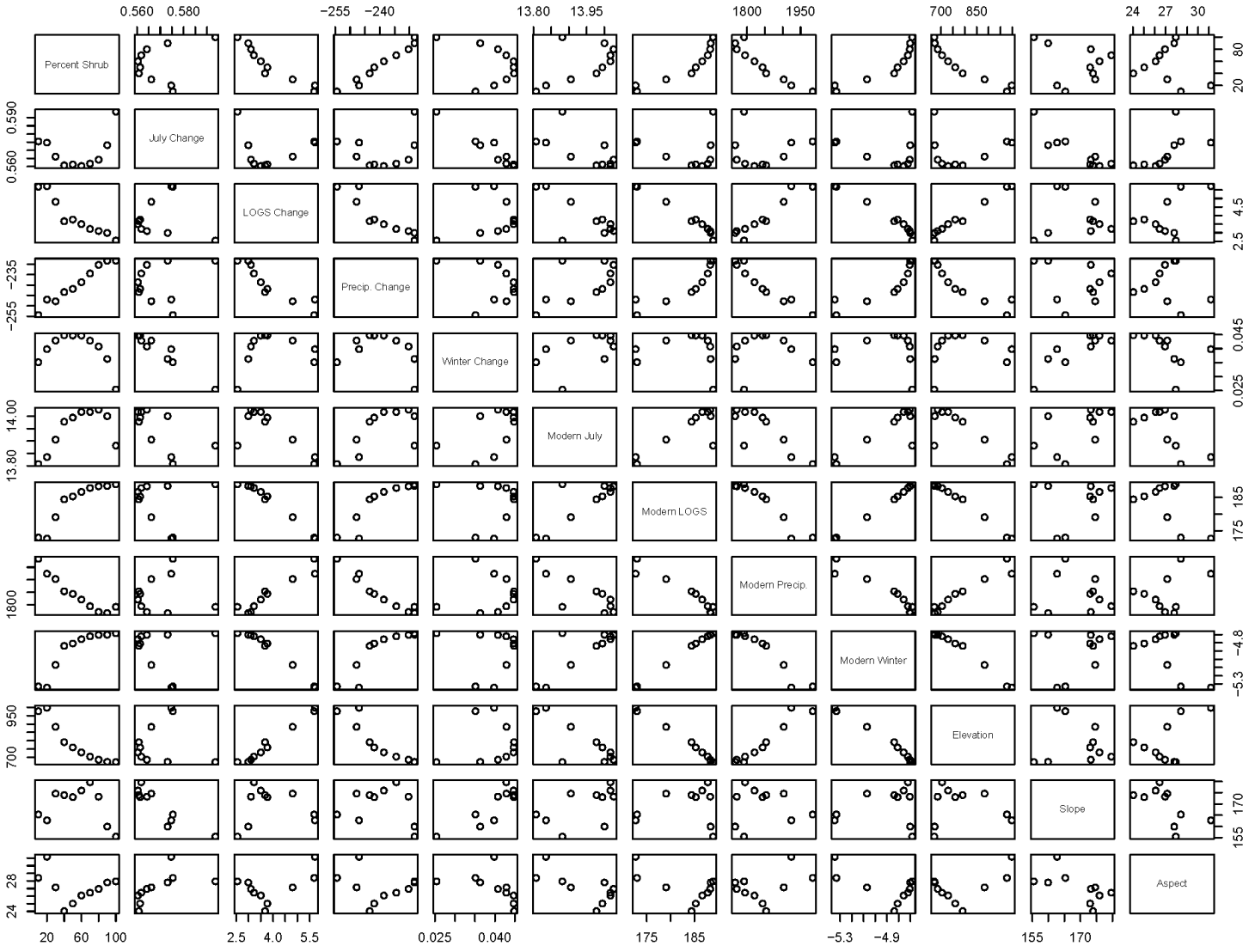

Scene Comparisons of Mean July Temperature

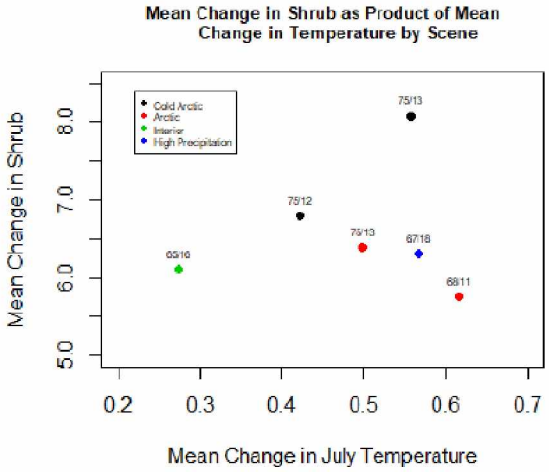


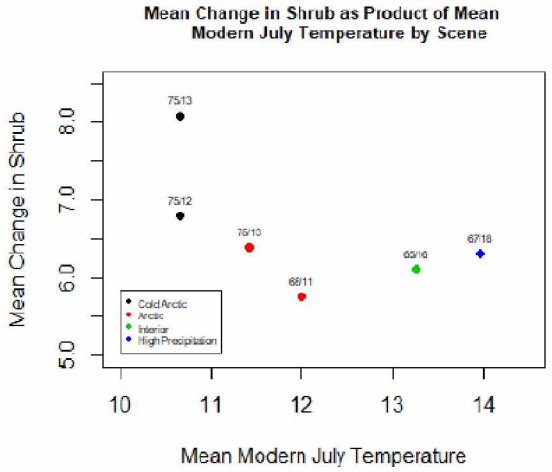


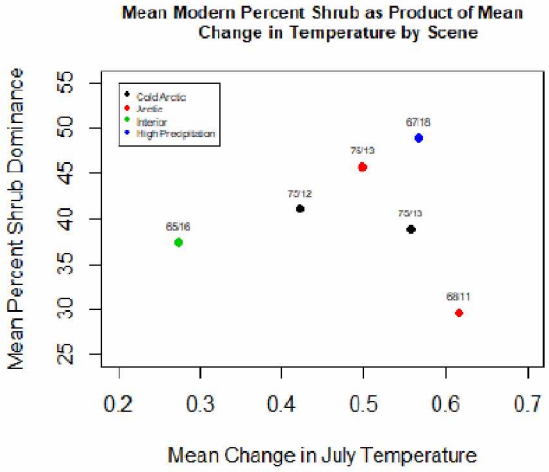


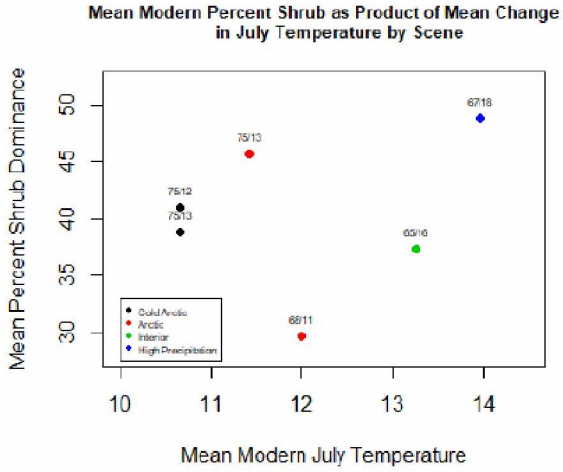

Scene Comparisons of Mean Length of Growing Season

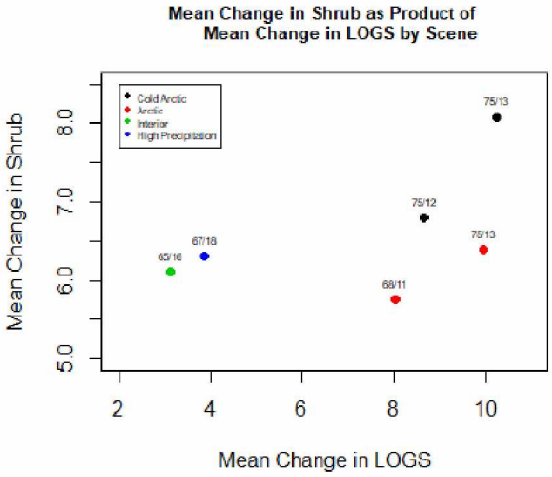


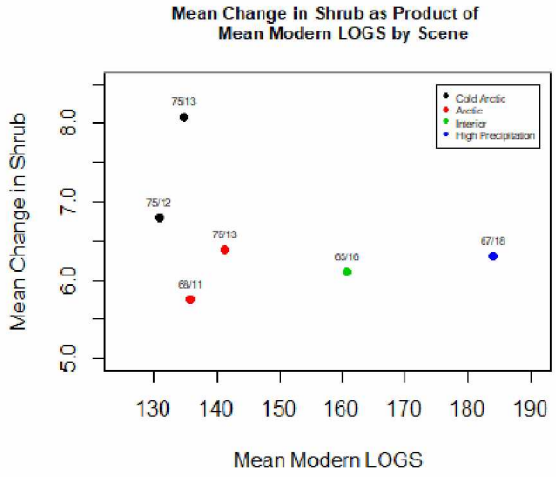


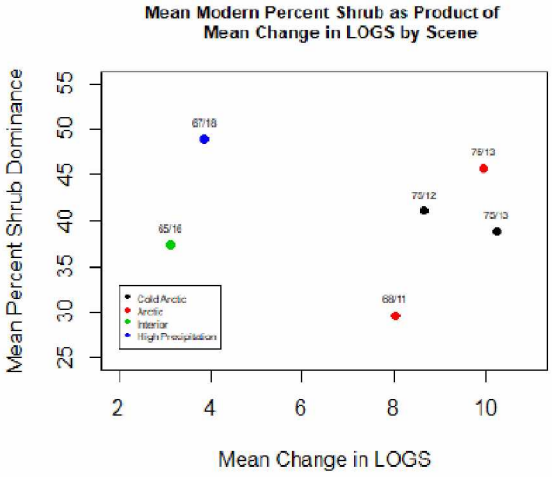


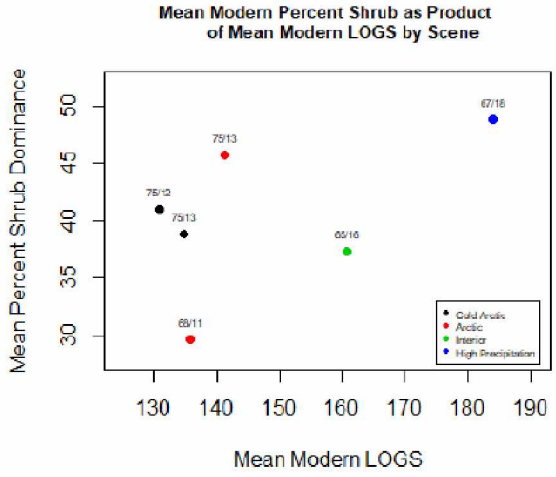

Scene Comparisons of Mean Precipitation

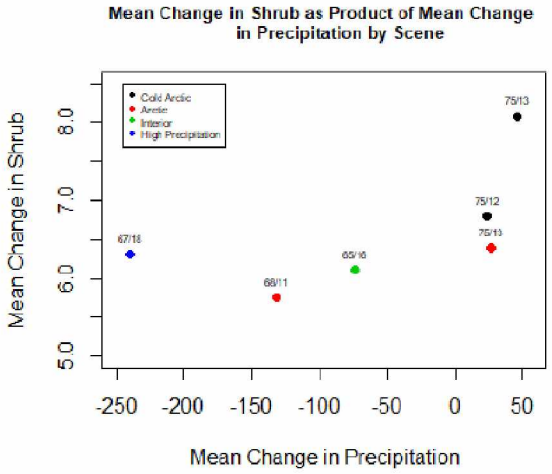


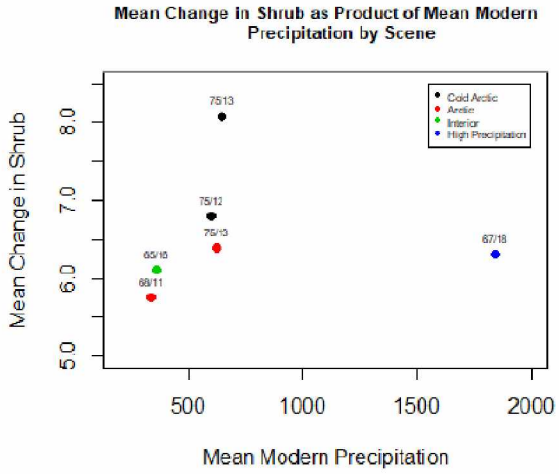


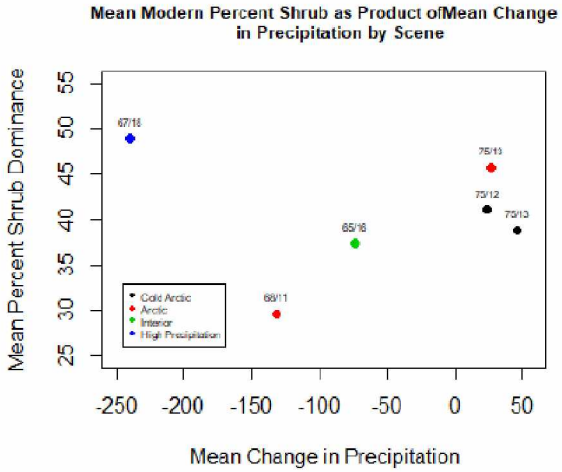


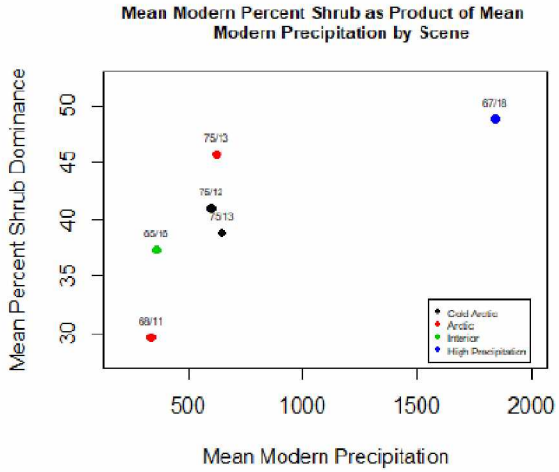

Scene Comparisons of Mean Winter Temperature

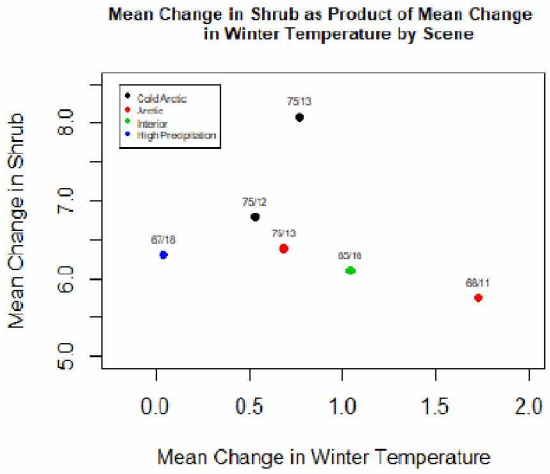


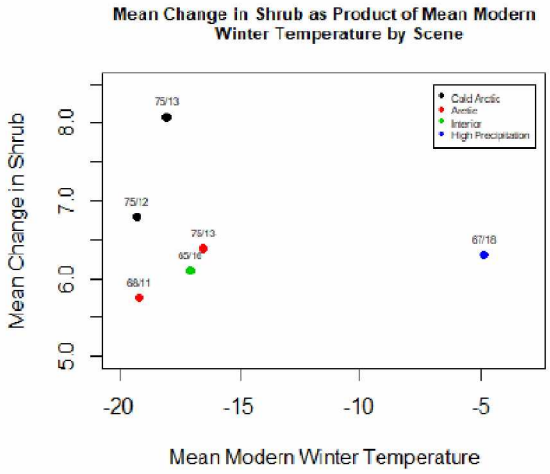


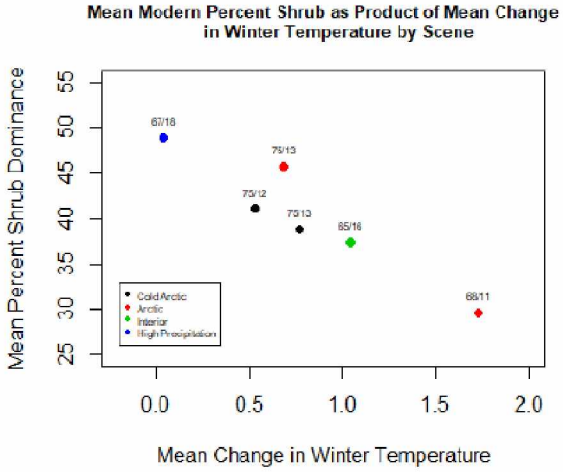


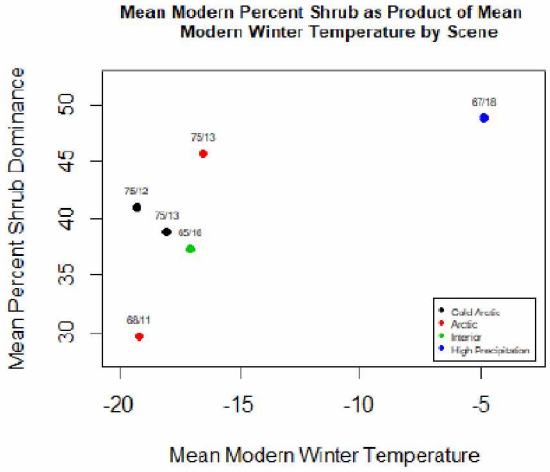

Scene Comparisons of Mean Elevation and Slope